Università degli Studi di Cagliari

Ph.D. DEGREE

EARTH AND ENVIRONMENTAL SCIENCES AND TECHNOLOGIES

Cycle XXXIV

DEEP-SEATED GRAVITATIONAL SLOPE DEFORMATION: INSIGHTS INTO THE GEOMORPHOLOGICAL AND KINEMATIC EVOLUTION. (EASTERN CENTRAL SARDINIA - WESTERN MEDITERRANEAN SEA).

GEO-04

Ph.D. Student: Demurtas Valentino

Supervisor: Prof. Paolo E. Orrù
Prof. Giacomo Deiana

Final exam. Academic Year 2020/2021

Thesis defence: April 2022 Session

1 Sommario

PREFACE

In this preface we introduce the PhD Thesis on Deep-Seated Gravitative Slope Deformation (DGSD) entitled "DEEP-SEATED GRAVITATIONAL SLOPE DEFORMATION: INSIGHTS INTO THE GEOMORPHOLOGICAL AND KINEMATIC EVOLUTION. (EASTERN CENTRAL SARDINIA - WESTERN MEDITERRANEAN SEA)". DGSD deserved a large interest in international literature in the last decades. The literature on this matter shows a markedly interdisciplinary approach, with contributions from different fields, such as geomorphology, engineering geology, rock mechanics, remote sensing. The subject is of high interest for many practical and scientific reasons. In fact, this phenomenon represents an important geo-hazard in relation to the deformation of large infrastructures and secondary collateral landslides. Although DGSDs play an important role in slope evolution and geo-hydrological risk. DGSDs are characterized by slow movements that can suddenly accelerate and cause catastrophic collapse of the deformed slopes.

With the aim of contributing in studying of DGSDs and collateral landslide in Eastern Sardinia, we highlight different aspects through geomorphological analysis with both field surveys and remote sensing techniques.

These phenomena represent highly critical, as they are located near the inhabited centers of Jerzu, Ulassai, Osini and Gairo. This area is characterized by a high risk linked to the manifestation of superficial collateral landslides that could have a close correlation with the DGSDs.

DGSDs, considered halfway between the common surface landslides and tectonic phenomena, are little known in Sardinia. A detailed study of the DGSDs was therefore carried out for the first time in order to understand their geo-structural characteristics and their temporal evolution. These have been related to the stratigraphic, structural and geomorphological setting of the area, framing them in the complex geodynamic context of the Western Mediterranean.

A preliminary basic study of the vast area dominated by the Pardu Valley and Quirra Valley and the carbonate plateaus called "Tacco di Ulassai" and "Tacco di Tertenia" through an important field surveys was carried out. In particular, the methodology was based on:

- Large scale geological and geomorphological field surveys and mapping;
- High detail geomorphological and structural surveys based on Uncrewed Aerial Vehicle Digital Photogrammetry (UAV-DP);
- Morphotectonic analysis;
- Large scale DGSDs analysis in relation on fluvial evolution in particular whit river capture;
- Multi-source and multi scale Monitoring of active DGSDs.

The manuscript was structured in four different but complementary papers. The papers are briefly introduced, examining their contribution in understanding of the DGSDs in Sardinia as follows.

The first paper "***Deep-seated gravitational slope deformations in central Sardinia: insights into the geomorphological evolution***" published on ***Taylor & Francis – Journal of Maps*** describes characteristics of the main DGSDs in central Eastern Sardinia, in the right slope of Pardu Valley.

The paper highlight the occurrence of DGSDs associated with the evolution of river slope in the uplift setting with in the low seismic and low tectonic activity regions of Sardinia. Using Geological and geomorphological analysis was possible to identify different evolutionary stages of DGSDs, focusing on the probable and catastrophic evolution of these processes in an urban setting. The paper is associate at the geomorphological map comprising all different paleo and active geomorphological process of the area.

Valentino Demurtas, Paolo E. Orrù & Giacomo Deiana (2021) Deep-seated gravitational slope deformations in central Sardinia: insights into the geomorphological evolution, Journal of Maps, 17:2, 594-607, ***Published October 2021*** *https://doi.org/10.1080/17445647.2021.1986157*

The second paper "***Evolution of Deep-Seated Gravitational Slope Deformations in Relation with Uplift and Fluvial Capture Processes in Central Eastern Sardinia (Italy)***" published on ***MDPI-Land*** present an innovative approach for analyse relations of DGSDs and fluvial dynamics by using morphotectonic, morphostratigraphic, geomorphic and In- SAR data in the Pardu and Quirra rivers. The paper presents a methodology that allowed to identify different active DGSDs with both lateral spread and sackung characteristics in a sector of Sardinia historically affected by hydrogeological instability. The multidisciplinary and multi-scale analysis made it possible to understand that in this contest the DGSDs have an important role in the evolution of the slopes and in the triggering of collateral landslides.

Demurtas, V.; Orrù, P.E.; Deiana, G. Evolution of Deep-Seated Gravitational Slope Deformations in Relation with Uplift and Fluvial Capture Processes in Central Eastern Sardinia (Italy). Land 2021, 10, 1193. ***Publisced November 2021 https://doi.org/10.3390/land10111193***

The third paper "***Preliminary results from active lateral spreads monitoring using Multi-source and multi-scale monitoring system in East-Central Sardinia***" Submitted on ***Taylor & Francis - European Journal of Remote Sensing*** focused on the DGSD and the collateral landslides in Ulassai village. Active Lateral spread processes and large toppling in an urban and tourist contest were highlighted. The work aims to present a methodology that integrates remote-sensing techniques, field

mapping, and monitoring systems to support a civil protection plan based on the Early warning system.

Valentino Demurtas, Paolo E. Orrù & Giacomo Deiana (2022) Preliminary results from active lateral spreads monitoring using Multi-source and multi-scale monitoring system in East-Central Sardinia, Eur. J. Remote Sens. ***Submitted December 2021***

Finally, the correlations with DGSDs in different geological, geodynamic and climatic context have been made. Paleo and active DGSDs and large landslides were analyzed in an emerged and submerged sector in southern Sardinia. These processes are correlated with the post Last Glacial Maximum sea level rise phases.

Deiana, G.; Lecca, L.; Melis, R.T.; Soldati, M.; Demurtas, V.; Orrù, P.E. Submarine Geomorphology of the Southwestern Sardinian Continental Shelf (Mediterranean Sea): Insights into the Last Glacial Maximum Sea-Level Changes and Related Environments. Water 2021, 13, 155. ***Publisced January 2021 https://doi.org/10.3390/w13020155***

During the research period carried out in Trondheim in Norway, in collaboration with the Norwegian Geological Survey (NGU) and the University Center in Svalbard, the DGSDs in the Svalbard Islands were studied as part of the "*Mapping of deep seated gravitational slope deformations (DGSDs) on Svalbard (Svalbard-dgsds)*" project. The first results are summarized in the paper "*Evidence of Deep-seated Gravitational Slope Deformation on Nordenskjold Land (Western Svalbard)"* ***under preparation paper.*** The work is based on remote sensing mapping and database creation of the geomorphological elements related to potential DGSDs in the Svalbard Islands. The survey and the geomorphological description/mapping is carried out through DEM and aerial photographs together. The work allowed the identification of large areas affected by DGSDs in the slopes of glacial valleys and in the coasts of the fjords in a sector of the archipelago.

1 *DEEP- SEATED GRAVITATIONAL SLOPE DEFORMATION: a review*

Deep-Seated Gravitational Slope Deformation - DGSD is a complex type of landslide and represent a very important geomorphological element, both from the scientific point of view and for the possible implications in terms of social and economic impact (*Záruba & Mencl, 1969; Dramis & Sorriso-Valvo, 1994; Pánek & Klimeš, 2016; Martino et al., 2020*). The DGSD are placed in an intermediate position between tectonics and superficial landslides（*Pánek & Klimeš, 2016, Discenza & Esposito 2021*）.

These are processes that generally follow a mechanical behavior called *gravitational creep* in the initial and intermediate stage (*"Creep evolution", Coltorti et al., 1984*). This mechanism is characterized by very slow deformations speed and is develop on materials with more or less plastic rheological behavior. The speeds are very slow, from a few mm/year to cm/year but can increase following extreme meteoric events or seismic events *(Dramis et al., 2002, Jibson et al., 2004; Tibaldi et al., 2015, Delchiaro et al., 2019; Francioni et al., 2019*).

These phenomena are indicated with various terms in the international literature:

- Slope Tectonics *(Jaboyedoff et al., 2011*),
- Mass Rock Creep (*Radbruch-Hall, 1978; Chigira, 1992*)
- Deep-seated gravitational slope deformation (DSGSD) (*Terzaghi K., 1962*),
- Deep-seated continuous creep (*Hutchinson J.N., 1988*),
- Sackung (*Zischinsky U., 1966; 1969*),
- Rock Slope Deformation (*Hungr et al., 2014; Jarman & Harrison, 2019*).
- Deformazione gravitativa profonda di versante (DGPV) in Italy (*Dramis F., 1984; Sorriso-Valvo M., 1988*).

The DGSD are defined as complex type of rock slope failure characterized by large dimensions generated in stone rocks (*Dramis et al., 2002*). They are characterized by a very slow and long-term deformation with deformations on a very large surface of the slope and with the triggering of secondary collateral gravitational phenomena. A fundamental aspect that determines the danger of DGSDs is that, under certain conditions, the slow movements typical of these mass movements can suddenly accelerate and give rise to catastrophic collapses of entire slopes (*Radbruch-Hall, 1978; Nemčok A., 1982; Onida M, 2001; Crosta & Agliardi, 2003*).

Distinctive element among superficial landslides and DGSDs is both the lack of a continuous sliding surface or basal shear zone (*Dramis & Sorriso-Valvo, 1994*) and the absence of continuous and well-defined external boundaries (*Agliardi et al., 2001; Jarman, 2006; Agliardi et al., 2012; Crosta et al., 2013; Jarman & Harrison, 2019*).

From the tectonic processes, they are distinguished by the lower rock volume involved and by the triggering factors. In the tectonic processes the stress effects are directly linked to deep deformations of the earth's crust while in the DGSDs to the stresses linked to the relief morphological and geological parameters (*Dramis et al 2002, Discenza & Esposito 2021*).

1.1 Geomorphological evidence

The most particular geomorphological evidences of the slopes affected by DGSDs vary along the slope (Figure 1). In the top slope there are usually extensional features such as double-crested, ridges, trenches, synthetic and antithetic (uphill-facing) scarps, tension cracks. Swellings, rotations of blocks, compressive cutting surfaces and landslides characterize the medium-low portions of the slopes. More information on superficial and deep structures of DGSD s are reported in the papers by *Chigira (1992), Agliardi et al. (2001, 2012)* and *Jaboyedoff et al. (2013)*, and the references therein.

In general, the following common characteristics can be distinguished in the DGSD:

- The area involve are comparable up to the entire slope (*Agliardi et al., 2001*); the volumes involved are generally variable between 10^6 m^3 (*Jarman, 2006; Discenza et al., 2011*) and 10^9 m^3 (*Tibaldi et al., 2015; Agliardi et al., 2019; ; Drouillas et al., 2020*), although locally they can reach 10^{10}- 10^{11} m^3 (*Baroň et al., 2013*). Many DS GSD s are included in this range, with volumes varying between 10^7 and 10^8 m^3 (*Nichol et al., 2002; Hürlimann et al., 2006; Jarman, 2006; Gutiérrez et al., 2008; Ghirotti et al., 2011; Oppikofer et al., 2017; Glueer et al., 2019; Martino et al., 2020*). The rock thickness involved varies from a few tens to hundreds of meters (*Pánek & Klimeš, 2016*)and the extensions in width can reach the order of kilometers (*Kojan & Hutchinson, 1978; Radbruch-Hall et al., 1976; Agnesi et al., 1978; Carraro et al., 1979*).

- The speed displacement is very slow in the order of mm/y (*Agliardi et al., 2001*). The temporal behavior is variable according to various factors: some phenomena evolve at a constant speed (*Chigira M., 1985*), while others evolve according to phases of reactivation and acceleration

following heavy rain or seismic events (*Dramis & Sorriso-Valvo, 1994; Varnes et al., 1990; Agliardi et al., 2001; Ambrosi & Crosta, 2006; Agliardi et al., 2012; Jaboyedoff et al., 2013; Pánek & Klimeš, 2016; Della Seta et al., 2017*). In particular cases, the DGSD can evolve in a catastrophic way, giving rise to collateral mega-slides. (*Radbruch-Hall, 1978; Dramis & Sorriso-Valvo, 1994; Panek et al., 2009*, *Hungr & Evans, 2004; Pánek & Klimeš, 2016*) One of the most important features is the presence of minor collateral landslides around the DGSDs (*Agliardi et al., 2001*). The deep gravitational phenomenon plays the role of predisposing and triggering the secondary phenomenon.

- The deformation type is characterized in the initial and advanced stage by a mechanical behavior called *gravitational creep*, characterized by very slow deformations evolution, whose speed is controlled by the plastic rheological behavior of the rock (*Genevois & Tecca, 1984; Genevois & Prestininzi, 1979; Martino et al., 2017; Discenza et al., 2020*). In the final stages, preceding the collapse, the velocities increase (*Muller, 1968*), thus passing to an accelerated creep that precedes the rupture.

- DGSDs are identifiable through characteristic morphostructures such as ridge-top splits, escarpments, counter-scarps, trenches, tension cracks (*Jahn, 1964; Zischinsky, 1966; 1969; Ter-Stepanian, 1966; Beck, 1968; Patton & Hendron, 1974; Tabor, 1971; Radbruch-Hall et al., 1977; Mahr, 1977; Bovis, 1982 ; Agliardi et al., 2001, 2012*). Most frequently structures, well descripted in this thesis, are the extensional trenches, depressions similar to narrow grabens, constituting a system of escarpments and counter escapes set on high-angle cutting planes (*Demurtas et al. 2021a*).

- One of the most important features is the presence of minor collateral landslides around the DGSDs (*Agliardi et al., 2001*). The deep gravitational phenomenon plays the role of predisposing and triggering the secondary phenomenon (*Demurtas et al 2021*).

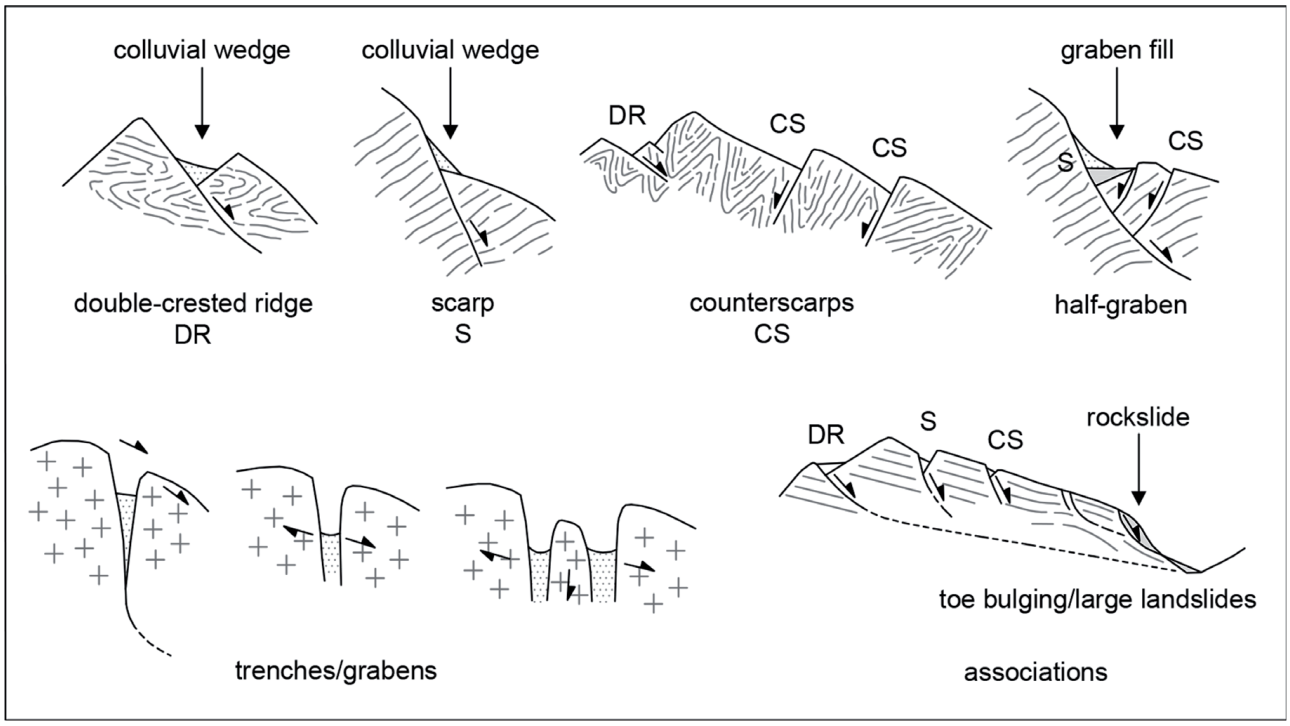

Figure 1 - Morpho-structural features characteristic of DGSD phenomena, related kinematic significance, and typical associations. From Discenza & Esposito 2021 redrawn after Agliardi et al., 2012

1.2 Classification

Over the years, many terms and definitions were used by several authors to describe the phenomena acting on large space-time scales, which can be considered as complex, or sometimes multiple, processes deriving from the mutual interaction of many mechanisms of movement (Cancelli & Casagli, 1995 Discenza & Esposito 2021). DGSDs are commonly classified into three types (*Dramis and Sorriso Valvo, 1994; Dramis et al., 2002*): sackung or rock-flow, lateral spreads, and deep seated block slide.

The sackung (*Zischinsky, 1966, 1969*), is a term later translated in English into "rock flow" (*Varnes, 1978*). These are rock volumes of varying sizes, from the slope scale to that mountain ridge scale, which move on large sliding surfaces that are difficult to identify.

Mainly involve schistose metamorphic rocks. Are characterized by very slow creep movements along a series of shear micro-planes or by a slow plastic deformation of the rock mass. These phenomena present a complex system of brittle fractures, especially in the upper and lower part of the slope, where the stress is lower and the rock mass have more rigid behavior.

The deformation is manifested by the profile of the slope characterized by a concave top slope and a convex foot slope (*Bisci etal.,1996; Rad- bruch-Hall, 1978; Radbruch-Hall etal.,1976; Zischinsky, 1966, 1969*).

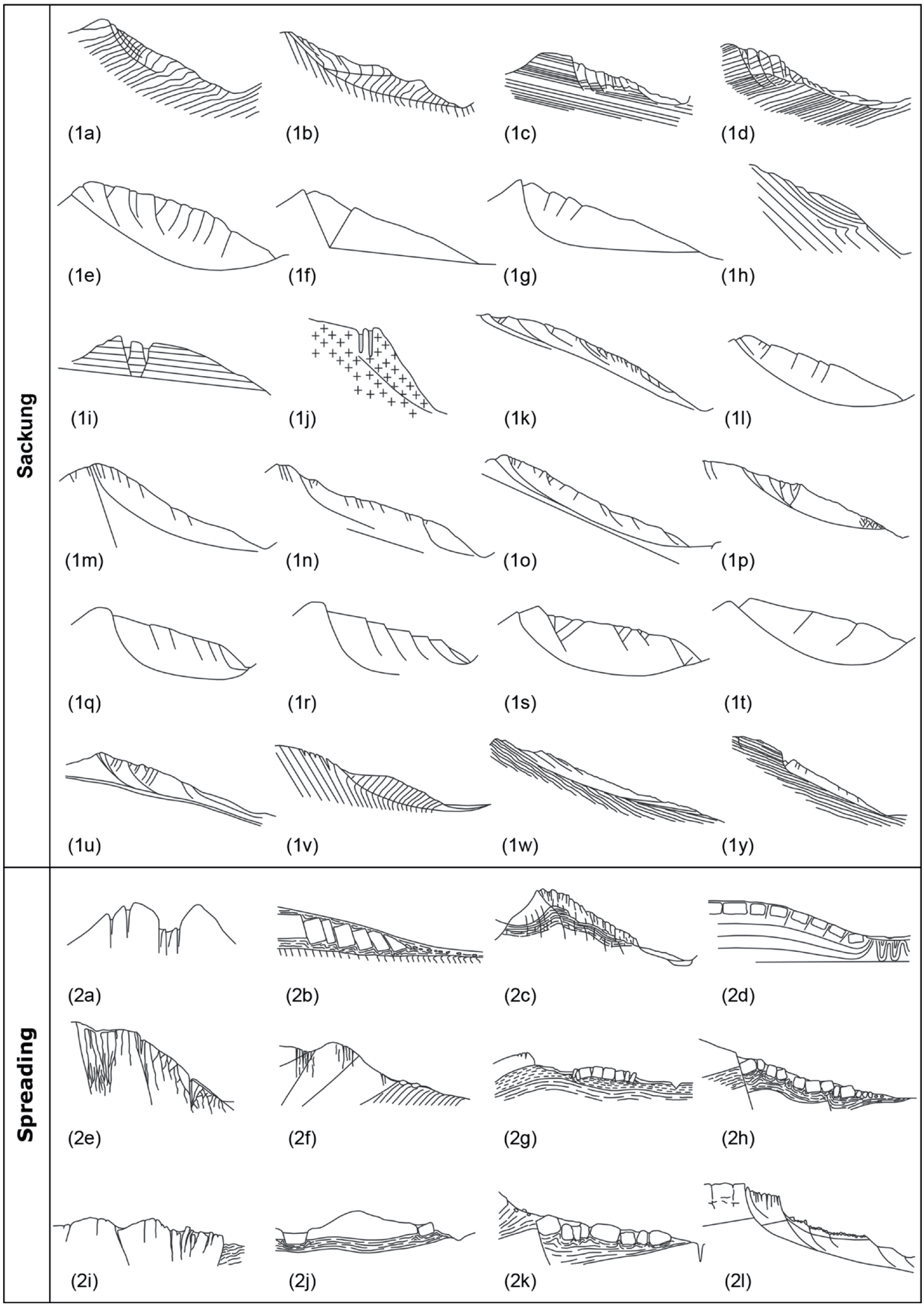

Figure 2 Examples of DGSDs proposed in the literature, divided on the basis of general typology (sackung and spreading) and ordered on the basis of year of publications (Discenza & Espostito 2021, modified after Agliardi et al., 2012). Sackung: (1a), (1b) Zischinsky (1966); (1c), (1d) Nemčok (1972); (1e) Mahr (1977); (1f), (1g) Hutchinson

(1988); (1h), (1i), (1j) Chigira (1992); (1k) Agliardi et al. (2001); (1l), (1m), (1n), (1o) Ambrosi & Crosta (2006); (1p) Apuani et al. (2007); (1q), (1r), (1s), (1t) Bois et al. (2008)*; (1u) Agliardi et al. (2009); (1v) Martino et al. (2020); (1w), (1y) Vick et al. (2020). Spreading: (2a) Jahn (1964); (2b) Záruba & Mencl (1969); (2c) Nemčok (1982); (2d) Hutchinson (1988); (2e) Martino et al. (2004); (2f) Esposito et al. (2007); (2g), (2h), (2i), (2j), (2k) Di Maggio et al. (2014); (2l) Pánek & Klimeš (2016)*

Lateral spread refers to the sub-horizontal movement of rigid rock blocks above a more ductile substrate (such as limestone, massive sandstone, or volcanic rock overlying clayey rocks) (*Varnes, 1978; Dramis et al., 2002; Cru-den &Varnes,1996; Jahn, 1964; Pasuto &Soldati, 1996*). Lateral spread tend to be associated with structural arrangements such as anticline folds or emergence of thrust fronts (*Dramis & Soriso-Valvo, 1994*). The movements are very slow, discontinuous, but can be greatly accelerated by earthquakes.

The block slide is the sliding for relatively short distances of large rocky blocks, which can involve an entire slope, reaching, in these cases, dimensions greater than those normally found in the other two types of DGSDs (*Voight, 1973; Záruba & Mencl, 1982*). This phenomenon, especially in Italian literature, is also referred to rock block slide (Esposito et al., 2007).

Often these phenomena involve large rock masses characterized by a generally translational motion, along one or more well-defined shear zones (*Varnes, 1978*). On the upper part, graben-like depressions are formed similar to those described for sackung.

Despite the similarity of the phenomena, the difference with the lateral spreads consists, in addition to the different deformation modality, in the height-length ratio of the deformed mass. In the Block slide, the rigid rocks affected by structural discontinuities are not reduced into metric or decametric blocks, as occurs in the lateral spread. Also this deformation type is characterized by a long creep phase which can eventually, but less frequently than sackung, evolve to the final accelerated creep phase and collapse.

Compared to other types of gravitational deformations, a decisive role in triggering this phenomenon is played by the presence of tectonic fractures and faults subjected to regional tectonic stress or affected by seismic activity.

1.3 Deformative models

The DS GSD s produce significant deformations within the rock masses and soils involved in the instability, of both brittle and ductile nature (Chigira, 1992; Jaboyedoff et al., 2013, Discenza & Esposito 2021). As regards the deep structural geometries *Chigira M., (1992)* he states that, under the action of the gravity, both brittle and ductile rock structures are similar to those of tectonic origin.

According to *Dramis et al., (2002)* the shear planes do not continue in depth due to the high pressures resulting in areas of ductile deformation. In this cases, in the inner portion of slope, creep processes determine the progressively decreasing of deformations with depth (*Jahn,1964; Zischinsky, 1966; Mencl, 1968; Nemčok, 1972; Mahr & Nemčok, 1977; Varnes, 1978; Nemčok, 1982; Dramis & Sorriso-Valvo, 1994; Cruden & Varnes, 1996; Martino et al., 2004; Esposito et al., 2007; Discenza et al., 2011; Martinotti et al., 2011; Di Maggio et al., 2014; Della Seta et al., 2017*), without the development of a continuous sliding plane or basal shear zone. The basal shear zone generally present thickness between few meters and some ten of meters and is composed by cataclastic breccias with abundant fine matrix (*Crosta & Zanchi, 2000; Madritsch & Millen, 2007; Crosta et al., 2013*).

Analyzing DGSDs, the rock mass must be considered as a discontinuous volume formed by rigid blocks separated by planar joints whit various extension and spacing (*Beck 1968*). This model is quite applicable to the study of lateral spreads and block slides.

While for the Sackungs the most suitable deformation model is that associated with plastic and viscous deformations (*Onida, 2001*).

Zischinsky 1966; 1969 propose for the first time a geomechanical model based on the concept of DGSDs interpreting as rocks mass affected by plastic-viscous deformations.

However, the most accredited model is that of *Mencl (1968)*, which derives from the works of *Zischinsky (1966; 1969)*. He postulates that in the central part of the slope, where the confinement pressure is high and therefore the deviatoric stresses are too low to generate shear deformation, the rock mass behaves like a viscous fluid. This model was well schematized by *Mahr, 1977* through the construction of geological sections (Figure 3). On the other hand, in the upper and lower parts of the slope involved by DGSDs, where the confinement pressures are lower, the deviatoric stresses can generate brittle deformations. These surfaces they manifest on the ground in the form of morphostructures. More recently, a Sackung model has been introduced by Savage and Varnes

(*Savage & Varnes, 1987; Varnes et al., 1989*) according to which the shear stress acting in depth would give rise to a plastic flow along a continuous sliding basal surface.

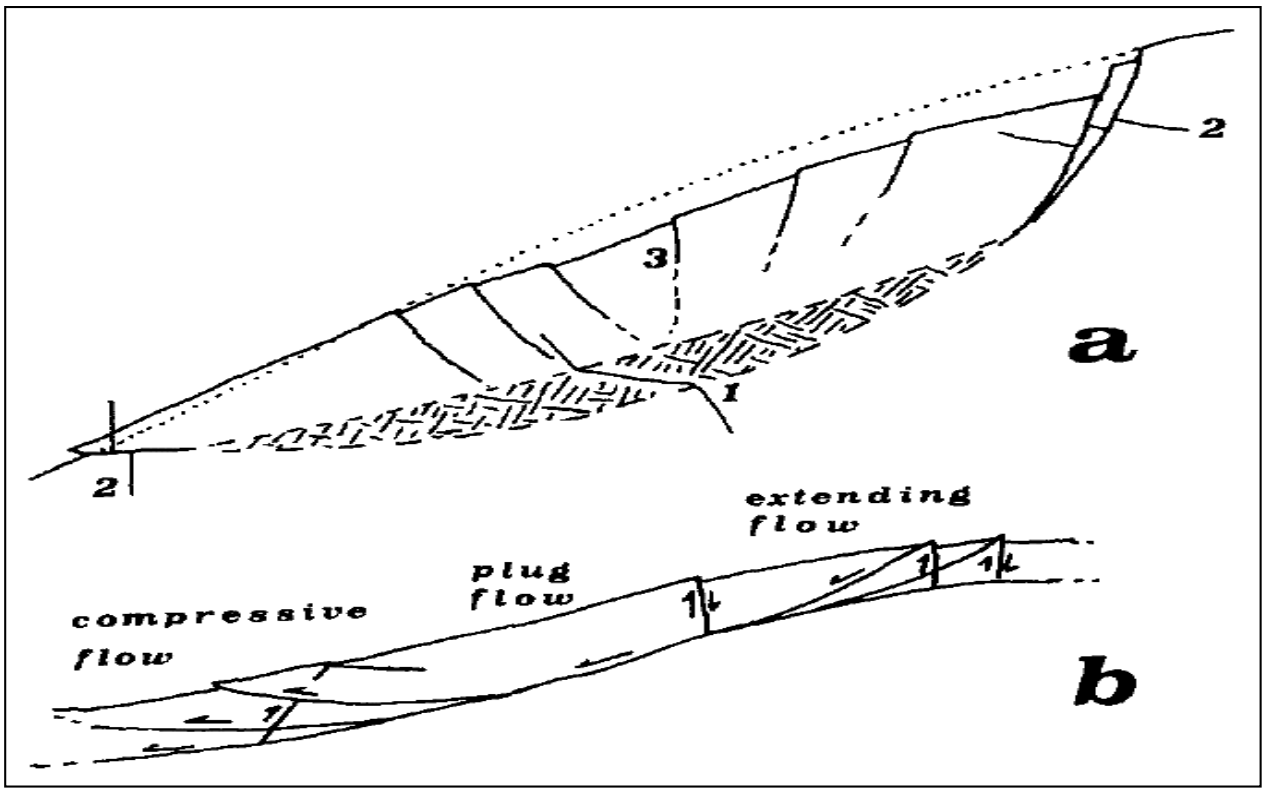

Figure 3 - Deformation models mainly applicable to the Sackungs taken from (Dramis & Sorriso-Valvo, 1994). a) from Mahr, 1977 modeling on the basis of Mencl's theory (1968); b) from Savage and Varnes, 1987. LEGEND. 1) Viscous deformation zone; 2) shear breakage zone; 3) shear zone in the fragile, shallow zone.

1.4 Control factors

DGSDs are controlled by various control factors related to the interaction between the geodynamic activity and the geo-structural setting of the involved slope (*Dramis, 1984*). The main factors can be summarized in the following points:

- The relief energy, that is the difference in height between the upper part and the lower part of the slope, represents the decisive morphological element in the triggering of the DGSDs. This must be high enough to allow the destabilization of large volumes and masses of rock (*Onida, 2001, Crosta et al. 2013*). *Mortara & Sorzana (1987)* in the western Alps, 50% of the DGSDs occur on slopes with relief energy between 500 and 1000 m.
- The slope does not seem to be such a fundamental factor in triggering DGSDs. However, the slope instability tends to grow with the slope, although many works show that the DGSDs involve slopes with inclinations typically between 18 ° and 50 ° (*Sorriso-Valvo, 1984*). For

lower slope values there are generally no favorable conditions for the development of Deep Gravitational phenomena, while for higher values, the modeling of the slope tends to evolve through more rapid and superficial gravitational processes such as landslides (*Mortara & Sorzana, 1987*).

- The lithological and structural characteristics, play a central role in triggering the DGSD. These processes occur where the geological structure makes the slope less subject to superficial landslides with faster kinematics. Therefore, the apparent paradox arises that it is precisely the most coherent rocks that are most favorable for the development of larger deep gravitational phenomena (*Dramis, 198*4). A large number of lithologies are affected by deep gravitational deformations, from metamorphic to sedimentary rocks, but sometimes also plutonic ones. When the slopes are set on shale, the DGSD tend to manifest themselves in the form of Sackung; on the other hand, in the case of slopes characterized by the overlapping of massive sedimentary units (limestone, sandstone, dolomite or conglomerate) on more tender units (shale, siltstone or marl), the lateral spread typically develops; finally, slopes made up of igneous rocks generally show block slide phenomena (*Nemčok, 1972*). A more important role than lithology, however, is played by the structural setting of the rock mass, understood as schistosity or foliation, stratification and fracture/faults network. (*Mortara & Sorzana, 1987; Massironi et al., 2003, 2010*).
- Another important trigger factor is the slope tectonic history. The tectonic events suffered by a slope can persist in the form of residual stresses that are reactivated when they are no longer compensated in the direction normal to the slope by a neighboring pressure. The relationship between tectonic activity and slope movements can be direct or indirect (*Onida, 2001*). We speak of a direct relationship when the regional stress field, producing tectonic deformations (faults, folds, thrusts, etc.), modifies the slope geometric structure, thus determining conditions of instability and the development of DGSDs. Passive influence, on the other hand, is established in cases of tectonic lifting (Uplift). The vertical movements of the earth's crust produce topographical differences in height to which increases in the activity of erosive processes and in the deepening of the local hydrographic network. This processes more rapid depending on the climatic and morphological conditions. The two conditions can easily coexist. The association between DGSDs and seismic activity is documented by several authors (*Dramis et al 1984, 2002*). Strong earthquakes can be accompanied by slope deformations, caused both by the tectonic movements that caused the earthquake and by gravitational readjustments (*Onida, 2001*). Seismic tremors act in different ways on the slopes: disconnecting the rock masses; reducing the cohesion; by varying the interstitial

pressures of the waters, causing the collapse of the rock mass shear resistance (*Solonenko, 1977; 1979*).

- Finally, morphoclimatic factors also affect the triggering of gravitational deformations of the slope, although there are greater knowledge gaps on this factor than the others. Favorable conditions are created by the deep alteration processes by groundwater (*Genevois & Perstininzi, 1979*) and by extreme meteoric events (*Starkel, 1976*). Effects of instability of the valley slopes can also develop following the rapid retreat of glaciers following changes in the climate (*Panizza, 1973*).

2 STUDY AREA

Central eastern Sardinia (Gerrei, Barbagia, Ogliastra, Sarcidano) is characterized by the presence of carbonate plateaus called "Tacchi" or "Tonneri" which give the sector the name of "Area dei Tacchi". This landscape is represented by a series of Mesozoic carbonate plateaus that cover in discordance Paleozoic metamorphites and granites. The "Tacchi" are the result of a complex geological evolution and derive from a single and extensive Mesozoic limestone and dolostone coverage; divided into various fragments following tertiary tectonic movements from which it was fractured, uplifted or down lifted and subsequently eroded and isolated by fluvial, gravitational and meteoric processes.
The study area is located on the eastern border of the *Tacchi* area and covers part of the territory of the municipalities of Ulassai, Osini, Jerzu, Gairo and Tertenia.

2.1 Geological setting

Sardinia can be divided into main geological complexes for approximately equivalent extensions: the Paleozoic metamorphic basement, the late Paleozoic intrusive complex and the late Paleozoic and Meso-Cenozoic volcano-sedimentary covers. The study area is mainly made up of Paleozoic metamorphites, Mesozoic deposits and Quaternary continental coverings. The most ancient rocks of Sardinia, which have an age ranging from a probable Precambrian to the Upper Paleozoic, show a variable metamorphism from anchizone to a high degree. Igneous rocks emerge extensively, making up almost a third of the island; it is essentially linked to the intrusive complex with a basically calcalkaline affinity, which took place in the Upper-Permian Carboniferous (Figure 4).
The post-varisic coverings are represented by sedimentary and volcanic rocks weakly deformed during the Alpine orogenesis phases in particular during the opening of the Balearic Basin and the Tyrrhenian Sea. (*Carmignani et al., 2001*).

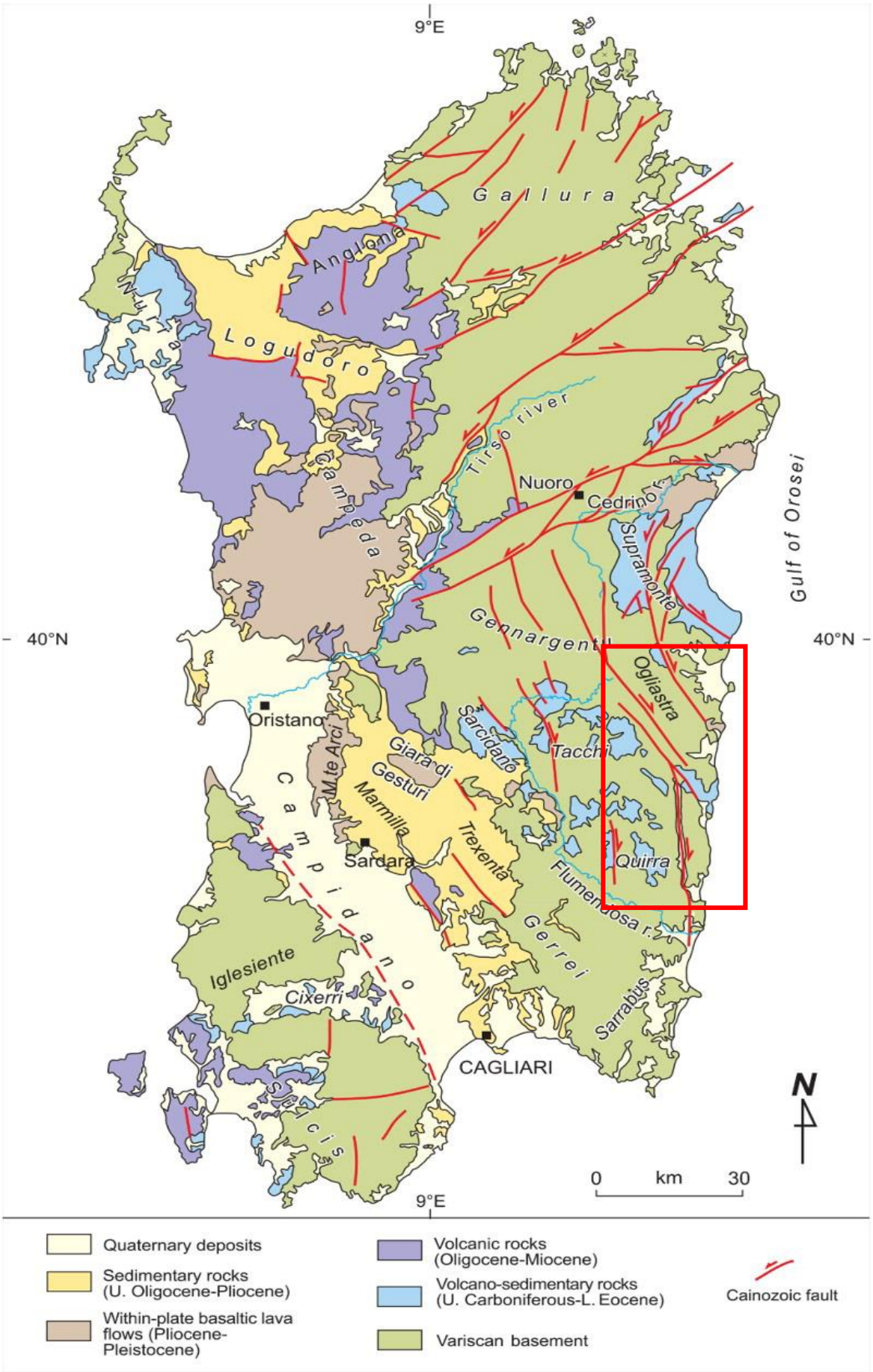

Figure 4 Main geological complexes of Sardinia (Carmignani et al.. 2016).

2.1.1 *Paleozoic basement*

The fundamental features of the Paleozoic basement derives from tectonic events of the Hercynian (Carboniferous) orogenesis, which produced deformations, metamorphism and an important magmatism.

The basement shows a tectonic-metamorphic zoning typical of collisional orogenetic chains with a NE-SW trend (Figure 5) (*Carmignani et al., 1994; 2001, 2016*).

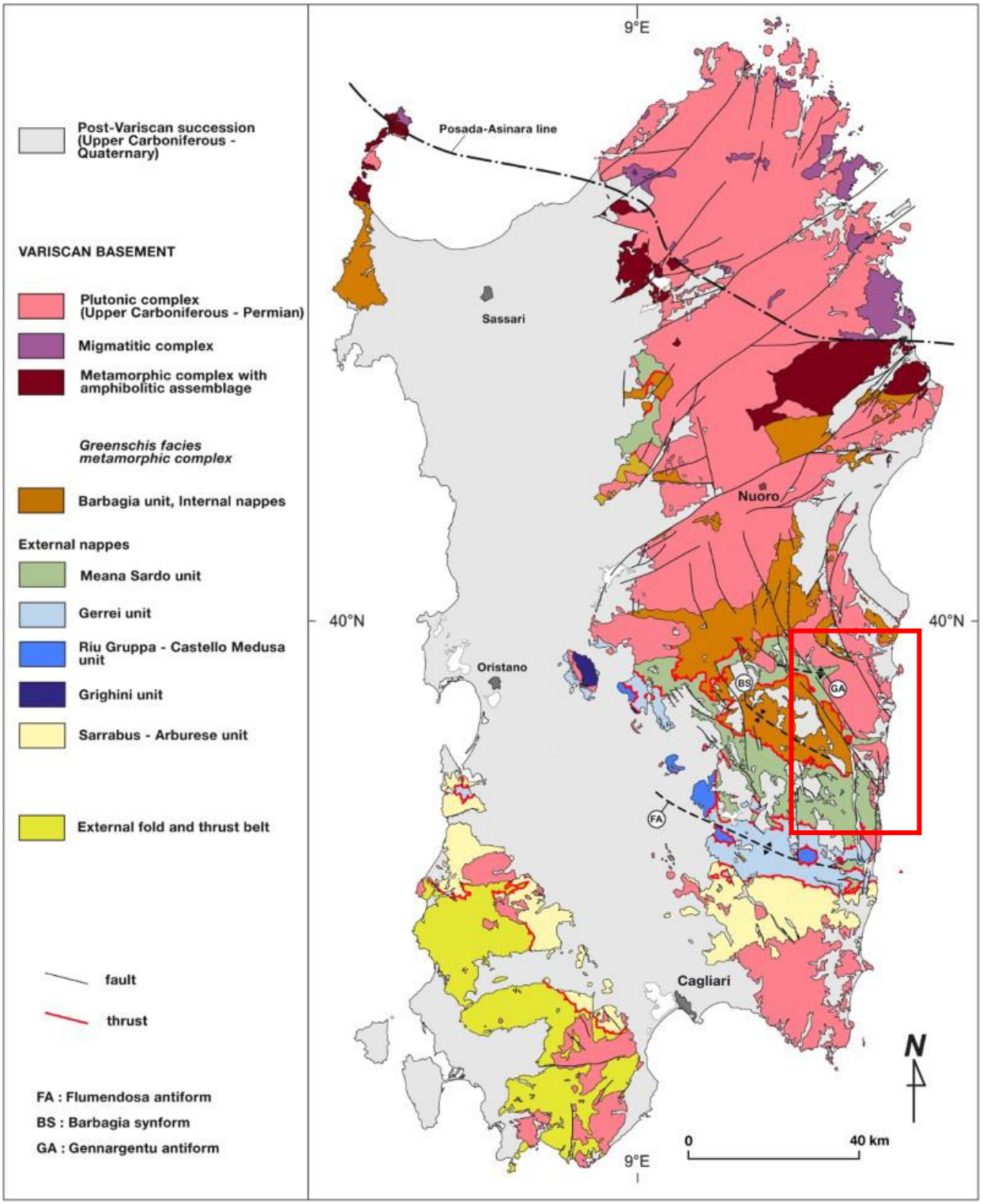

Figure 5 Main structural elements of the Sardinian Hercynian base. (Carmignani et al.. 2016).

The Varisic basement of Sardinia has been divided into four metamorphic zones (Elter et al., 2004; 2010) which show an increase in the metamorphic degree towards the NE (Franceschelli et al., 2005).

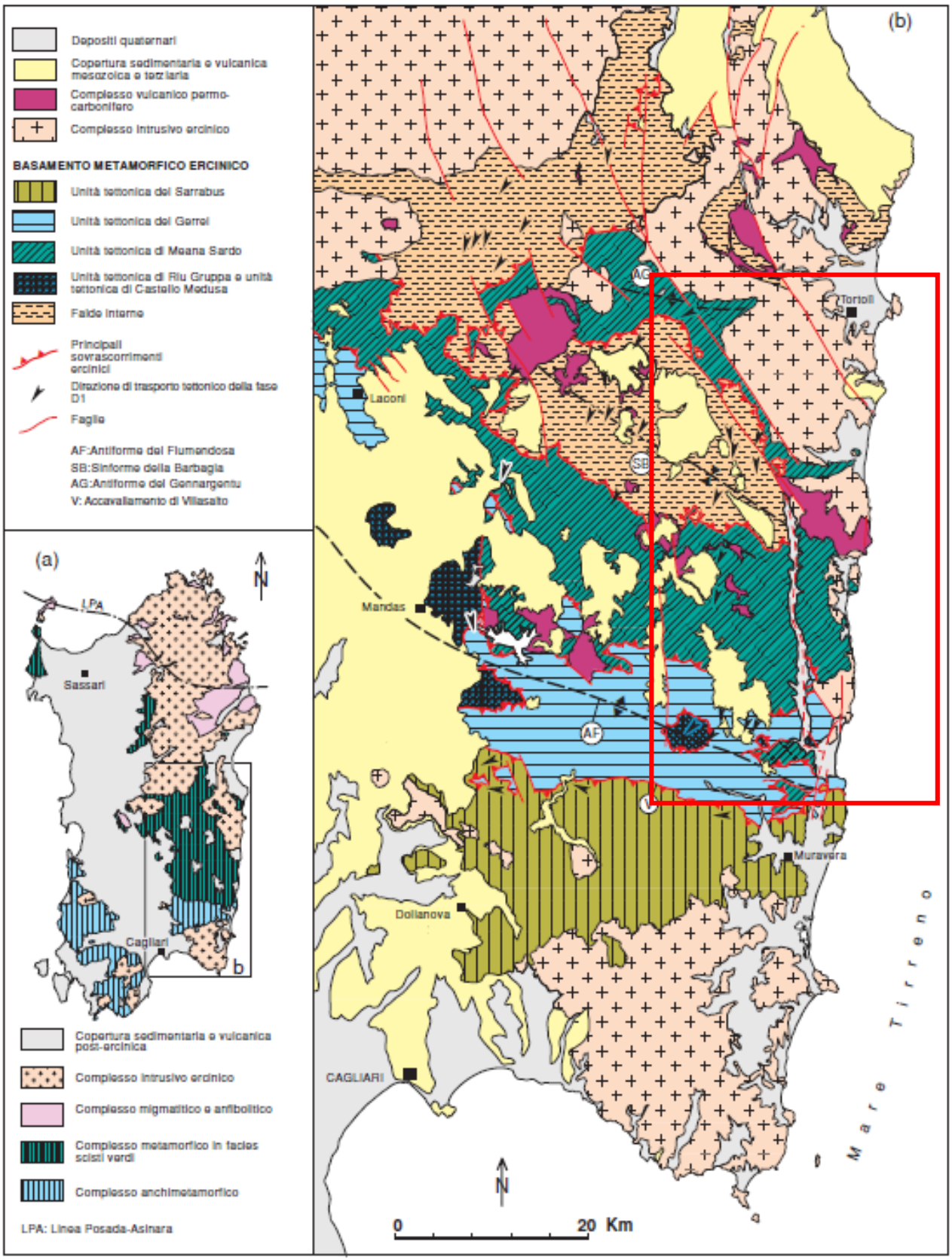

Figure 6 - Tectonic scheme of the Paleozoic basement of South-Eastern Sardinia (Carmignani et al., 2001).

During the Upper-Carboniferous and the Permian, an important post-collisional distensive tectonics overlaps these structures, resulting the exhumation of metamorphites and the intrusion of a granite complex (*Conti et al., 1995*). The metamorphic basement of the study area consists by low grade metamorphic complex consisting of a predominantly terrigenous succession and metavolcanites. Towards the sea, the outcrops of the granite area increase (Figure 6) (*Vai & Cocozza, 1974*).

2.1.2 Late paleozoic and meso-cenozoic covers

Above the Variscan basement (Figure 7) lies a thick Mesozoic–Cenozoic volcano-sedimentary succession containing different sedimentary and volcano-sedimentary complexes (*Salvador, 1994; Costamagna 2015, 2017*) linked to the evolution of the present-day western Mediterranean Sea.

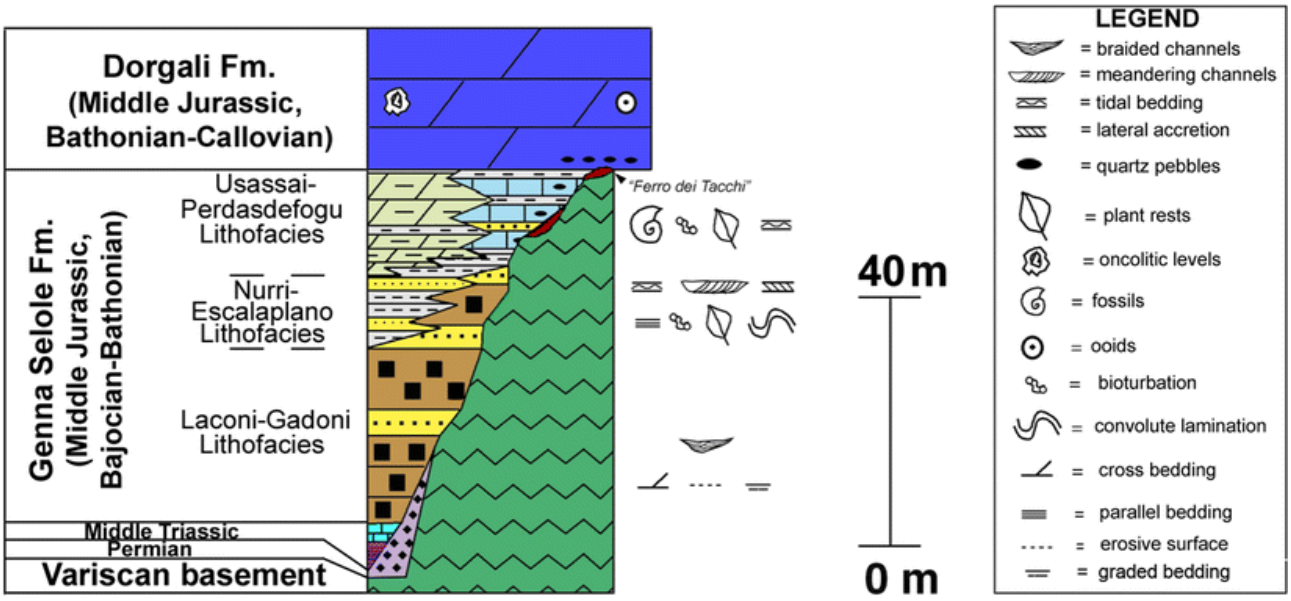

Figure 7 General stratigraphic composition of the Genna Selole Formation (modified after Costamagna 2015, 2017)

The extensional regime, which began with the collapse of the Hercynian chain in the upper Carboniferous, continued during the Permian and Triassic, identifying a long period of intracratonic evolution. During this geological period developed an intense and general peneplanation. The continently context helped by climatic factors, allowed favorable conditions for the formation of anthracitiferous lake basins (Seui, Seulo and Perdasdefogu) and the residual iron concentrations of Ogliastra (Ferro dei Tacchi). (*Marini, 1984*). In the South of Ogliastra, these continental conditions persist until the Middle Jurassic, during which the Mesozoic transgression manifest by transitional environments by carbonate platform. (*Carmignani et al. 2001, Costamagna & Barca, 2004*).

The Jurassic succession at the base is characterized by a discontinuous unit, whose thickness does not exceed a few tens of meters, with a silicoclastic-carbonatic constitution, of a continental to transitional environment, which takes the name of Genna Selole Formation (Bajociano-Bathonian) (*Dieni et al.,*

1983). This formation passes above a dolomitic platform succession called the Dorgali Dolomite Formation (Bathoniano-Kimmeridgiano) (*Amadesi et al., 1960; Costamagna & Lecca, 2002*).

Following the Cretaceous marine regression, Sardinia was affected by low tectonic processes. The major morpho-structural features of Sardinia derive from compressive (mainly Oligocene) and distensive (Miocene and Plio-Quaternary) deformations respectively connected with the collisional margin of north-eastern Corsica, with the opening of the Balearic Basin and with that of the Tyrrhenian Sea (Figure 8) (*Carmignani et al., 2001*).

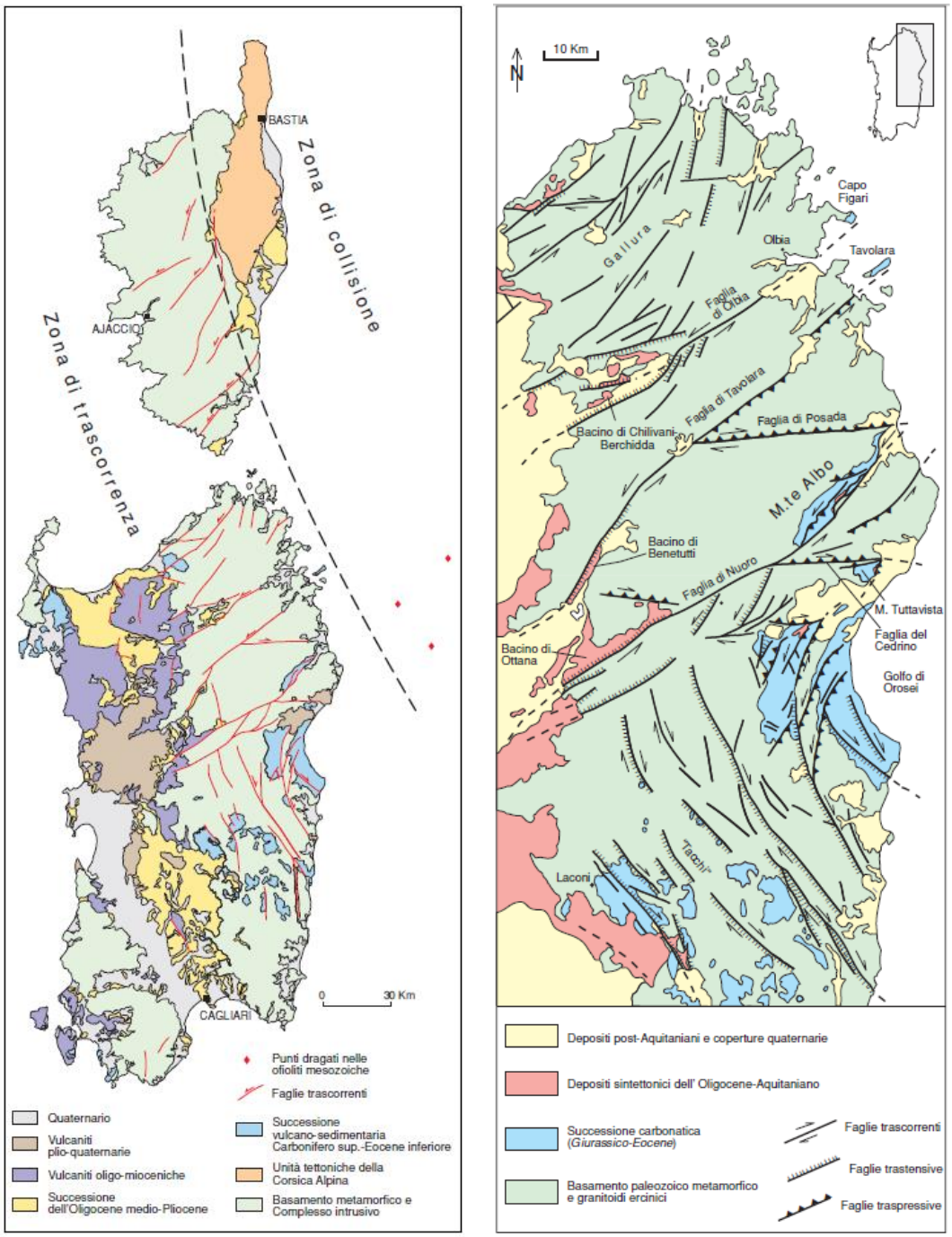

Figure 8 Structural sketch showing the main features of Tertiary transcurrent tectonics in Sardinia and Corsica (Carmignani et al., 2001).

The morpho-structural features determined by the NE-SW transcurrent faults of central-northern Sardinia give the most direct physiographic expression of compressive tectonics (Aquitanian-Lower Burdigalian).

In the study area, the major tectonic features are represented by a system of transcurrent faults with extensional components, oriented NW-SE.

In the upper Burdigalian the deformation regime changes completely becoming extensional, this occurs with the formation of deep basins which are later filled by various transgressive cycles. In this period, the "Tacchi" area does not register marine deposits as it results in a high morpho-structural (*Carmignani et al., 2001*).

In the Pliocene, the relaxing components continue to act associated with the opening of the Tyrrhenian Basin which lead to the formation of the Campidano graben and the lifting of the lateral horst, resulting in a reliefs rejuvenation. This phenomenon is associated with widespread basaltic magmatism. In the Ogliastra sector, these phenomena manifest themselves with the Barisardo basaltic flow of the Plio-Pleistocene age and with geomorphological evidence that indicates an important recent up-lift caused by the reactivation of the faults in a relaxing regime (*Carmignani et al. 2001*).

2.2 Geodynamic setting

Sardinia is located in the center of the western Mediterranean between two Neogenic ocean basins: the Liguro-Provencal Basin to the West, open between 30 and 15 Ma (*Cherchi & Montadert, 1982*), and the Tyrrhenian Basin to the East, still evolving for about 10 Ma (*Kastens et al., 1988; Sartori R., 1989*). The island is closely linked, in its Cenozoic evolution, to Corsica and together they constitute the Sardinian-Corsican block. This is an extensive fragment of continental lithosphere consisting mainly of intrusive igneous and Paleozoic metamorphic lithologies. The central-western Mediterranean is constituted by sets of chains and basins (Figure 9). The geodynamic evolution of the whole area was controlled by the interaction between two major plates, Africa and Europe, originally separated by the Tethys basin (*McKenzie D, 1972; Amodio Morelli et al., 1976; Dewey et al., 1989; Ziegler , 1988*) and from minor plates: Iberia (corresponding to Spain) and Adria (referable to the lithospheric basement of the Italian peninsula and the Adriatic Sea; *Oldow et al., 2002*).

The main phases of this tectonic cycle are:

- Ocean opening (Middle - Upper Jurassic);
- Transition (Lower Cretaceous);
- convergence oceanic (Upper Cretaceous-Middle Eocene);
- Continental collision (upper Eocene - present day).

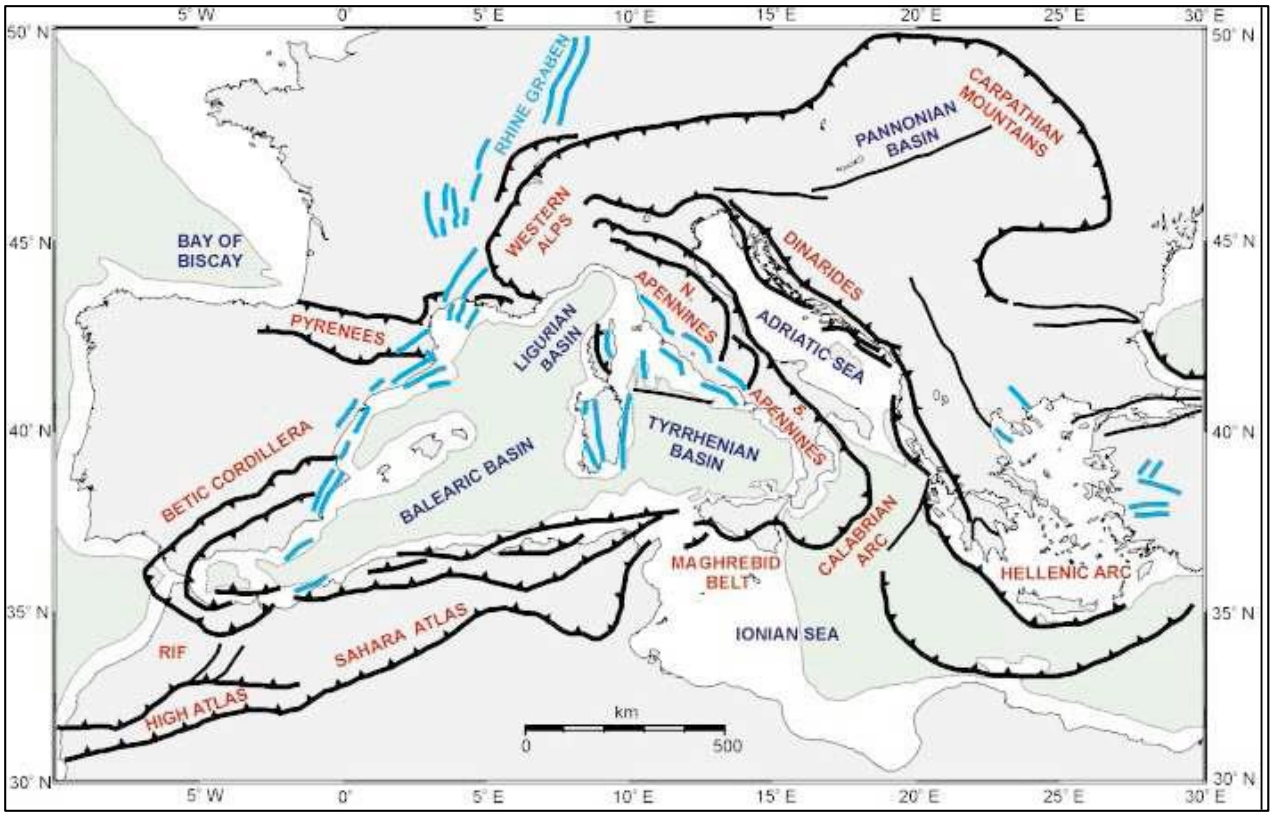

Figure 9 - Tectonic structure of the Mediterranean region (from Oldow et al. 2002). Compression faults (black lines with indentations on the upper plate). Transcurrent faults (simple black lines) Extensional faults (blue lines).

The Apennine orogeny is the current result of this last collisional context and develops according to an extensional basins-chains system starting from the Tyrrhenian Basin and with a general vergence towards the NE in southern Italy and south in Sicily. (*Boccaletti et al., 1990; Lentini et al., 1996; 2006*).

In this context, the Sardinian-Corsican block represents a fragment of continental lithosphere at the center of Neogenic oceanic lithosphere (*Mazzella M.E., 2010*). The Sardinian-Corsican block represents a detached and rotated sector of the Alpine foreland that includes a small fragment of the western Alps in northern Corsica (*Alvarez w., 1972; Montigny et al., 1981; Vigliotti and Langenheim, 1995*). The collision of the block with the Adriatic margin occurs in the Middle Miocene (*Patacca et al., 1990*). Since then, an extensional tectonics linked to the rifting of the Tyrrhenian has dominated in Sardinia and Corsica (*Assorgia et al., 1997; Casula et al., 2001*). In the last phases a translation-rotation of the Sardinian-Corsican block, the "*Fossa Sarda*" was formed, consisting of a series of basins arranged in a N-S direction, distributed from the Gulf of Cagliari to the Gulf of Asinara. Ogliastra belongs to the great horst of Eastern Sardinia.

The "Fossa Sarda", corresponding to a sedimentation basin, was formed by a marked tectonic type of relaxation (connected to the translation of the Sardinian-Corsican block) which favored an intense volcanic activity, as demonstrated by the vast distribution in this sector of the Sardinia of volcanic materials, interspersed in sedimentary rocks.

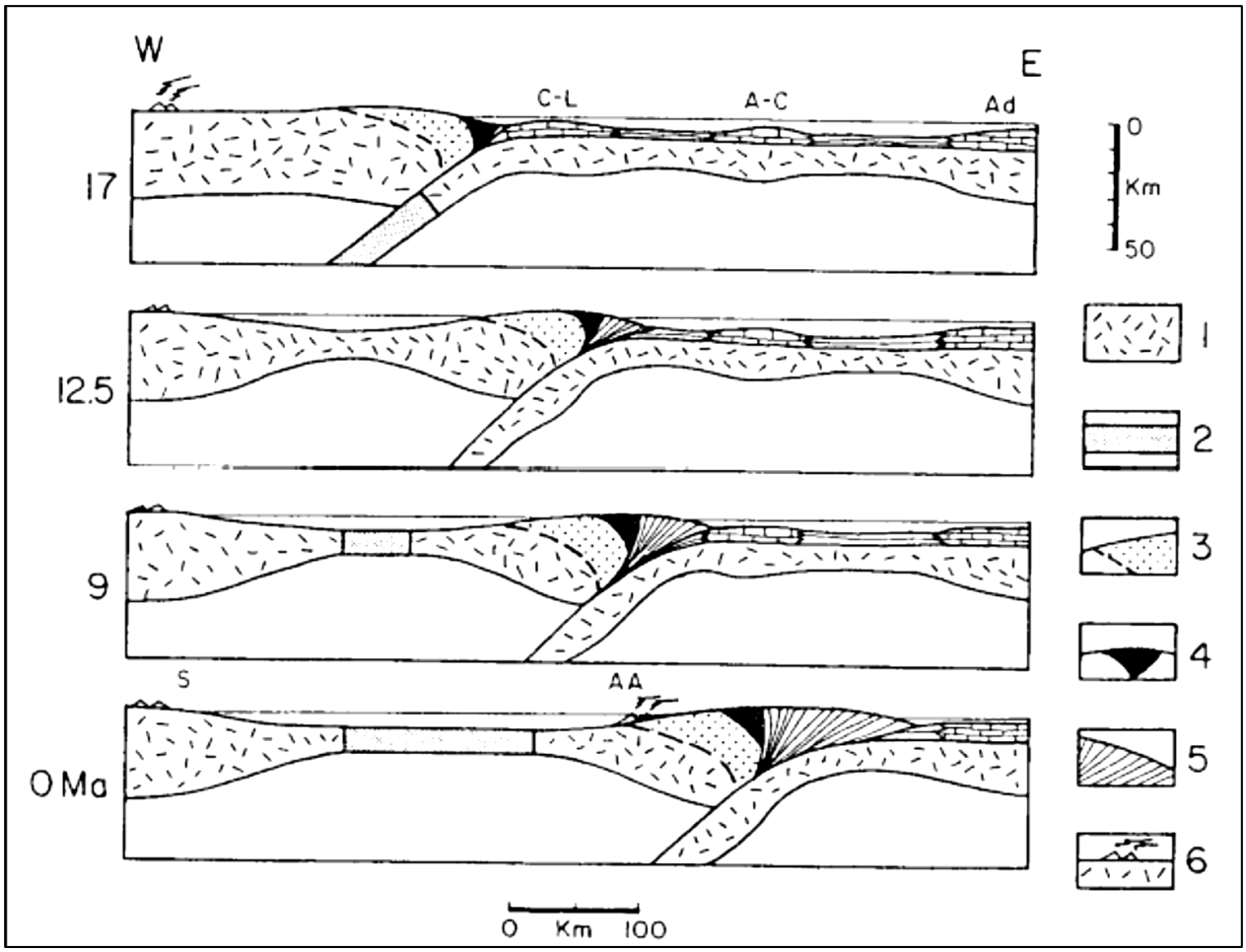

Figure 10 Evolution of the Tyrrhenian - Apennine system along an E-W section. 1: continental crust; 2: oceanic crust; 3: Alpine units of Calabria; 4: oceanic units innermost of the Apennines; 5: Apennine accretionary wedge; 6: active calcalcaline volcanoes. C-L: Campania-Lucanian platform; A-C: Abruzzo-Campania platform; Ad: Adriatic block; S: Sardinia; AA: arch of the Aeolian Islands. (Malinverno and Ryan, 1986). From Mazzella M.E., 2010)

In the Plio-Quaternary (approximately between 5 and 2 Ma), a new rift valley is formed between the Gulf of Cagliari and the Gulf of Oristano known as Graben del Campidano, exploiting the structures that generated the Fossa Sarda.

The Graben is bordered to the west by normal faults oriented NW-SE and plunging towards the depression (Figure 11). In Ogliastra, located in the eastern horst, a series normal faults were formed. These are set on the previous Oligo-Myocene transcurrent faults (Casula et al., 2001).

Based on preliminary geodetic data from the PTGA network, *Ferranti et al., (2008)* found the presence of a weak but present internal deformation in the Campidano graben area. The velocities, respect to Cagliari, of the sites east and west of the basin define a right lateral movement astride the graben which would occur between 3 and 7 mm/a (Figure 11) (*Mazzella et al., 2010*).

Despite the stability of this area, the residual speeds of the GPS sites compared to Cagliari are still appreciable. The TEUL and RUIN sites move away from CAGL at about 1.5 mm/y thus suggesting, due to their proximity to the fixed site, a possible activity of the synthetic faults and the faults bordering the Campidano to the west (eg Sarroch Fault).

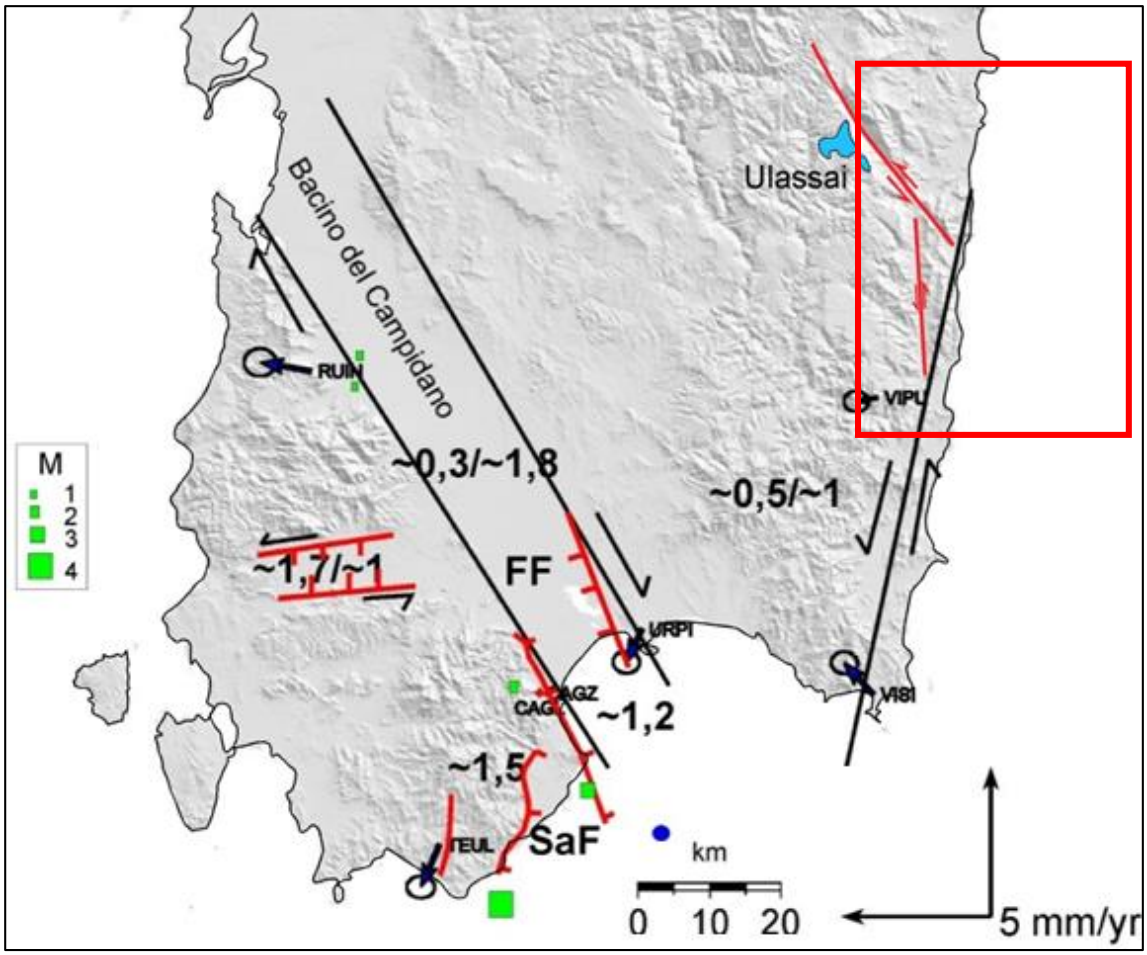

Figure 11 PTGA speed field in southern Sardinia referred to the stable site of CAGL. In blue the rotation pole, in green the recent seismicity. The numbers show the extension/traverse components in mm/y. FF: Fangario Fault; SaF: Sarroch Fault. (Mazzella et al. 2010) (Faults from Casula et al., 2001 and from Carmignani L., 1996). The sector in blue represents the Ulassai plateau while continuous lines represent the Quirra fault and the Genna and Crexia fault. Red square represent the study area.

To the east of the basin, the URPI site has a residual velocity approaching the CAGL of 1.2 ± 0.2 mm/y which would suggest the presence of an active tectonic structure between the two sites very close to each other. Between the URPI and TEUL sites, the velocity differential is 0.3 ± 0.2 mm/y in divergence, in a direction perpendicular to the NW-SE development direction of the basin, the same as that recorded between URPI and RUIN, plus north. These latter sites also diverge from each other with a lateral component of right-side movement which, along the direction of the border faults of the basin, is 1.8 ± 0.3 mm/a. To the west of the basin, the relative speed between the TEUL and RUIN sites defines an oblique divergence of 1.7 ± 0.3 mm/a in the N-S direction and 1 ± 0.3 mm / a in the perpendicular direction in the interposed area. Although historical and instrumental seismicity fails to give information on local active structures (*Boschi et al., 2000*), the PTGA speeds suggest a widespread but consistent pattern of deformation that currently occurs asismically. It is therefore possible that the Campidano border faults, where the main strain is accumulate, have a creep-type kinematic. The fact that the entire Sardinia block is no longer affected by intense tectonic activity is

the reason for its current low seismicity. The earthquakes that are observed from time to time are generally linked to the mild activity of the faults bordering the Sardinian-Corsican block on the various sides, especially on the eastern and southern sides. Looking at the INGV instrumental catalog (*http://terremoti.ingv.it*), we can observe the distribution of earthquakes since 1985 (Figure 12). There are a few dozen and only in 4 cases magnitude 4 has been exceeded: in the north east there were the 2 earthquakes of April 26, 2000 (magnitude 4.2 13:28; magnitude 4.7 at 13 : 37) and the earthquake of magnitude 4.3 of 18 December 2004. In the south of Sardinia there was the earthquake of magnitude 4.1 of 24 March 2006. The most recent low-magnitude earthquake events in the astudy area were ML1.8 (Escalaplano, 4 April 2019) and ML1.6 (Perdasdefogu, 14 October 2020) (*INGV, 2021*).

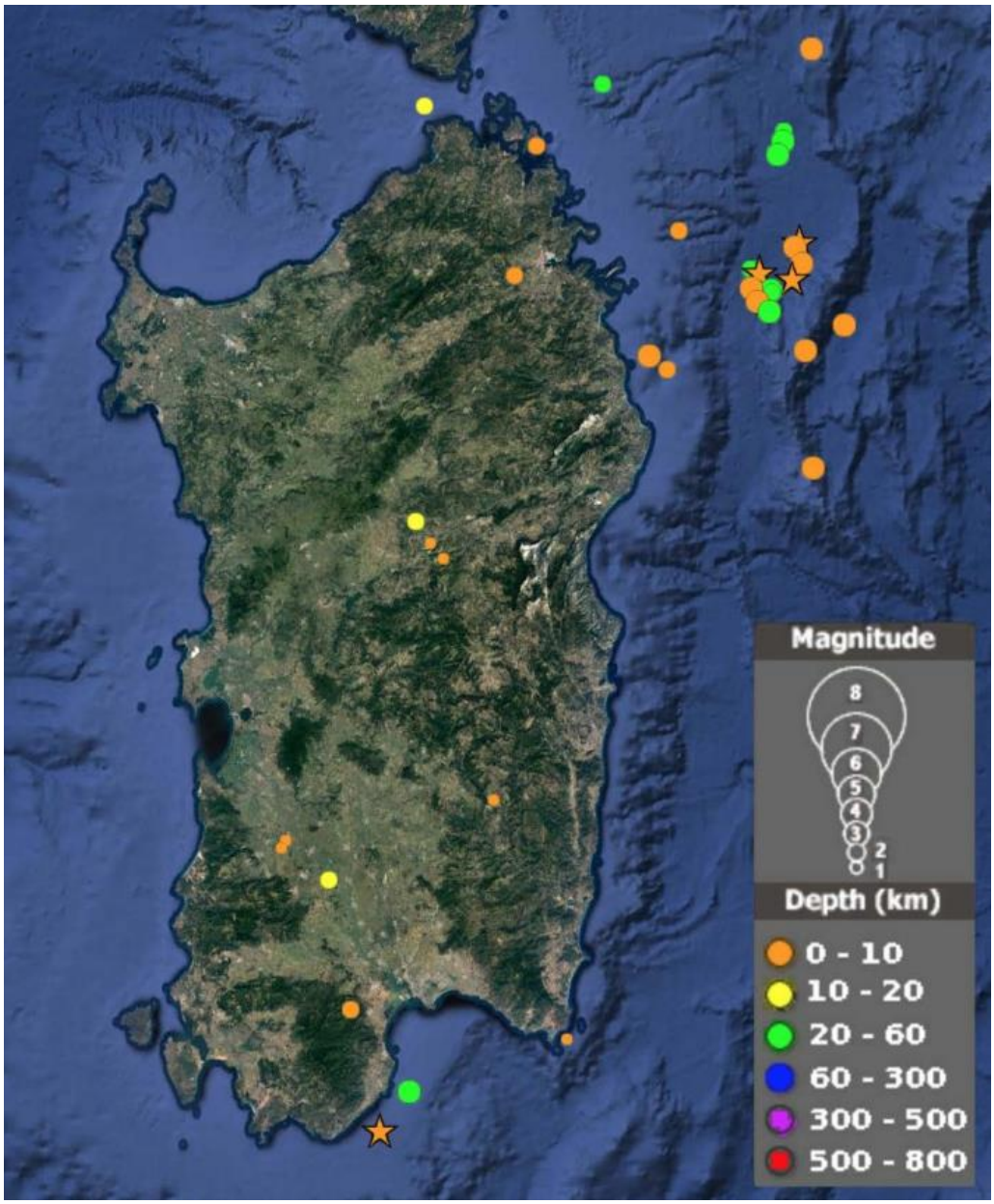

Figure 12 Recent seismicity in Sardinia (1st January 1985 – 14th April 2020) according the instrumental catalog compiled by INGV (http://terremoti.ingv.it).

3 CHAPTER I

Deep-seated gravitational slope deformations in central Sardinia: insights into the geomorphological evolution

Valentino Demurtas, Paolo E. Orrù & Giacomo Deiana (2021) Deep-seated gravitational slope deformations in central Sardinia: insights into the geomorphological evolution, Journal of Maps, 17:2, 594-607, ***Published October 2021*** *https://doi.org/10.1080/17445647.2021.1986157*

ABSTRACT

In this study, we analyse deep-seated gravitational slope deformations (DGSDs) in central Sardinia. The area is characterised by plateaus with a prominent limestone scarp overlying metamorphites. A comprehensive mapping of structural, karst, fluvial, and slope morphologies in Pardu and Ulassai valleys is presented herein. The uplift linked to the Plio-Pleistocene tectonic activity leads to high-slope topography, which favours gravitational processes, such as DGSDs and rock-avalanches. Although DGSD is a common phenomenon in the relief of the central Mediterranean region, it has never been studied in Sardinia. We describe the kinematic models and geomorphological evolution of DGSD in Sardinia for the first time. The application of light detection and ranging, high-resolution unmanned aerial vehicle photogrammetry, and geological, structural, and geomorphological surveys enabled a depth morphometric analysis and the development of interpretative three-dimensional models. The geo-structural setting and high relief energy associated with recent upliftment are the major controlling factors of DGSDs.

KEYWORDS: Deep-seated gravitational slope deformation; tectonic geomorphology; morphostratigraphy; geomorphological mapping; rock avalanche; UAV.

3.1 Introduction

Deep-seated gravitational slope deformation (DGSD; *Dramis & Sorriso-Valvo, 1994*) is a complex type of rock slope failure characterised by large dimensions generated in stone rocks (*Dramis et al., 2002*). DGSDs are characterised by slow movements that can suddenly accelerate and cause catastrophic collapse of large sections of the deformed slopes (*Agliardi et al., 2020; Crosta & Agliardi, 2003; Nemčok, 1972; Ostermann & Sanders, 2017; Radbruch-Hall, 1978*). Therefore, this phenomenon represents a major geological hazard associated with the deformation of large infrastructures and the generation of secondary landslides. Although DGSDs represent a major geological hazard, information about them is scarce so far (*Soldati, 2013*). Advanced technologies in both remote sensing (e.g. satellite data and space-borne interferometric synthetic aperture radar) (*Frattini et al., 2018; Mantovani et al., 2016; Novellino et al., 2021*) and proximal sensing such as unmanned aerial vehicle (UAV); (*Deiana et al., 2021; Devoto et al., 2020; Eker & Aydın, 2021*) and light detection and ranging (LiDAR) have enabled a better understanding of these processes. They are characterised by extremely slow deformation rates (*Cruden & Varnes, 1996*) and landform assemblages such as double-crested ridges, trenches, synthetic and antithetic (uphill-facing) scarps, tension cracks, and convex (bulged toes) and deep basal shear zones (*Agliardi et al., 2001; Chigira, 1992; Crosta et al., 2013; Mariani & Zerboni, 2020; Panek & Klimeš, 2016*). Shear zones exhibit the characteristics of cataclastic breccias with abundant fine matrix (*Crosta & Zanchi, 2000*) and thicknesses up to tens of metres (*Ostermann & Sanders, 2017*).

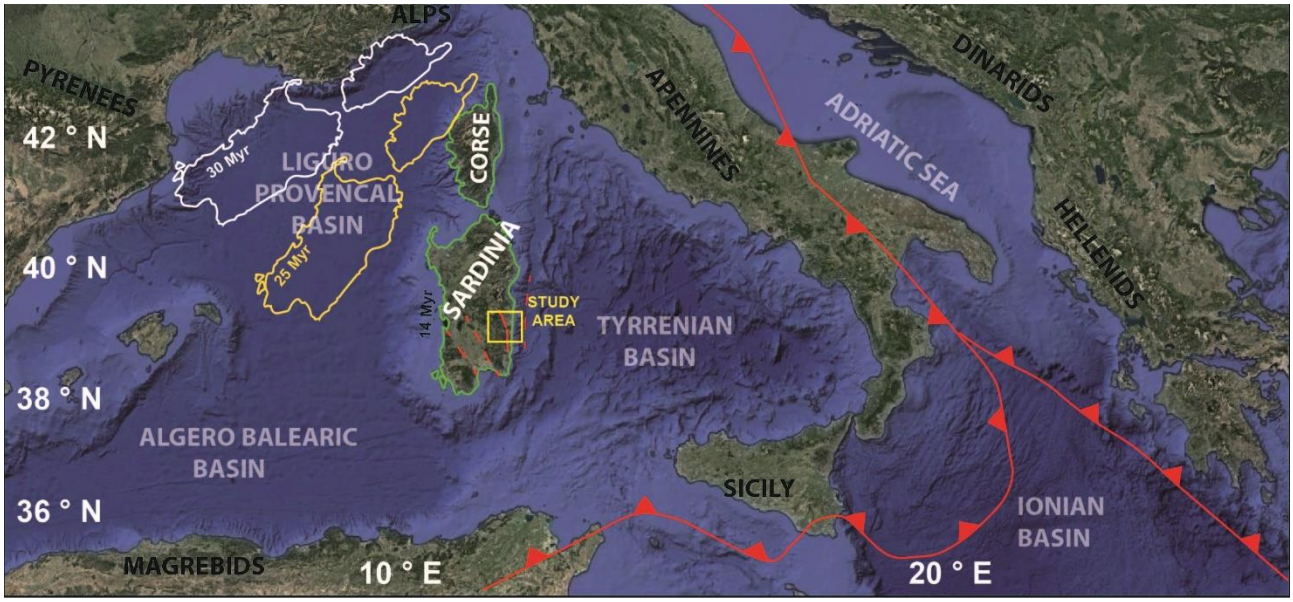

Figure 13 Geographical location and structural features of the study area modified after Deiana et al. (2021): red lines represent thrust fronts; white lines are the Sardinian–Corse Block translation 30 Ma; yellow line represents the Sardinian–Corse Block translation 25 Ma (modified after Carminati & Doglioni, 2005); green line represents the Sardinian–Corse Block translation 14 Ma (Gattacceca et al., 2007).

In this study, we present three cases of DGSDs in Sardinia. The study area is located in Ogliastra (central-east Sardinia) in the Pardu River Valley (Figure 13). The area is characterised by wide plateaus, called Tacchi, with a prominent Jurassic limestone scarp overlying Palaeozoic metamorphites (*Carmignani et al., 2016; Pertusati et al., 2002*).

The major evidence of DGSDs in the Pardu River Valley is the presence of large prismatic blocks of dolomitic Mesozoic slab displaced up to tens of metres downstream from the initial altitude. The geomorphological features associated with DGSDs vary along the slope. A set of ridge-top trenches, with widths up to 50 m, lengths of hundreds of metres, and depths of >50 m is present in the plateau edge. The middle slopes are characterised by tilted blocks, shear zones, and rockfall deposits. Large block deposits with rock avalanche features in the foot-slope are associated with the final-collapse phases of the DGSDs.

For the first time in this setting, we delineated long-term deformations, such as gravitational slides *(Zaruba & Mencl, 1982*) with lateral spreading (*Cruden & Varnes, 1996; Jahn, 1964; Pasuto & Soldati, 1996*) and sackung kinematics (*Bisci et al., 1996; Radbruch-Hall, 1978; Radbruch-Hall et al., 1976; Zischinsky, 1966, 1969*), which involve giant carbonate blocks, and the underlying foliated metamorphites. Geomorphological and geological analyses enabled the identification of various evolutionary stages as follows: (I) early stage represented by the spreading at the plateau edges, (II) second stage of the old DGSDs located in the middle slope, and (III) third stage corresponding to the final evolution of the deformation process developed through collapse.

We highlight the occurrence of DGSDs associated with the evolution of river slope in the uplift setting within the low seismic and low tectonic activity regions of Sardinia. Thus, we analysed the geomorphological evolution of the slope, particularly focusing on the probable and catastrophic evolution of these processes in an urban setting.

A geomorphological map at a scale of 1:10.000 was generated showing: (i) the karst morphology on carbonate plateaus; (ii) the gravity feature on the edge plateau linked to the extensional trenches and tilted blocks; (iii) different landslide deposits on the slopes (rockfalls, palaeo-DGSDs, slope debris, and rock avalanches); and (iv) hydrographic elements (e.g. creeks, canals, and fluvial elbows).

3.2 Geological setting

East-central Sardinia (Italy) is characterised by a Jurassic dolomitic plateau (Tacchi) overlying a metamorphic Palaeozoic basement, primarily comprising metasandstone, quartzites, and phyllites (Figure 14) (*Carmignani et al., 2016; Pertusati et al., 2002*).

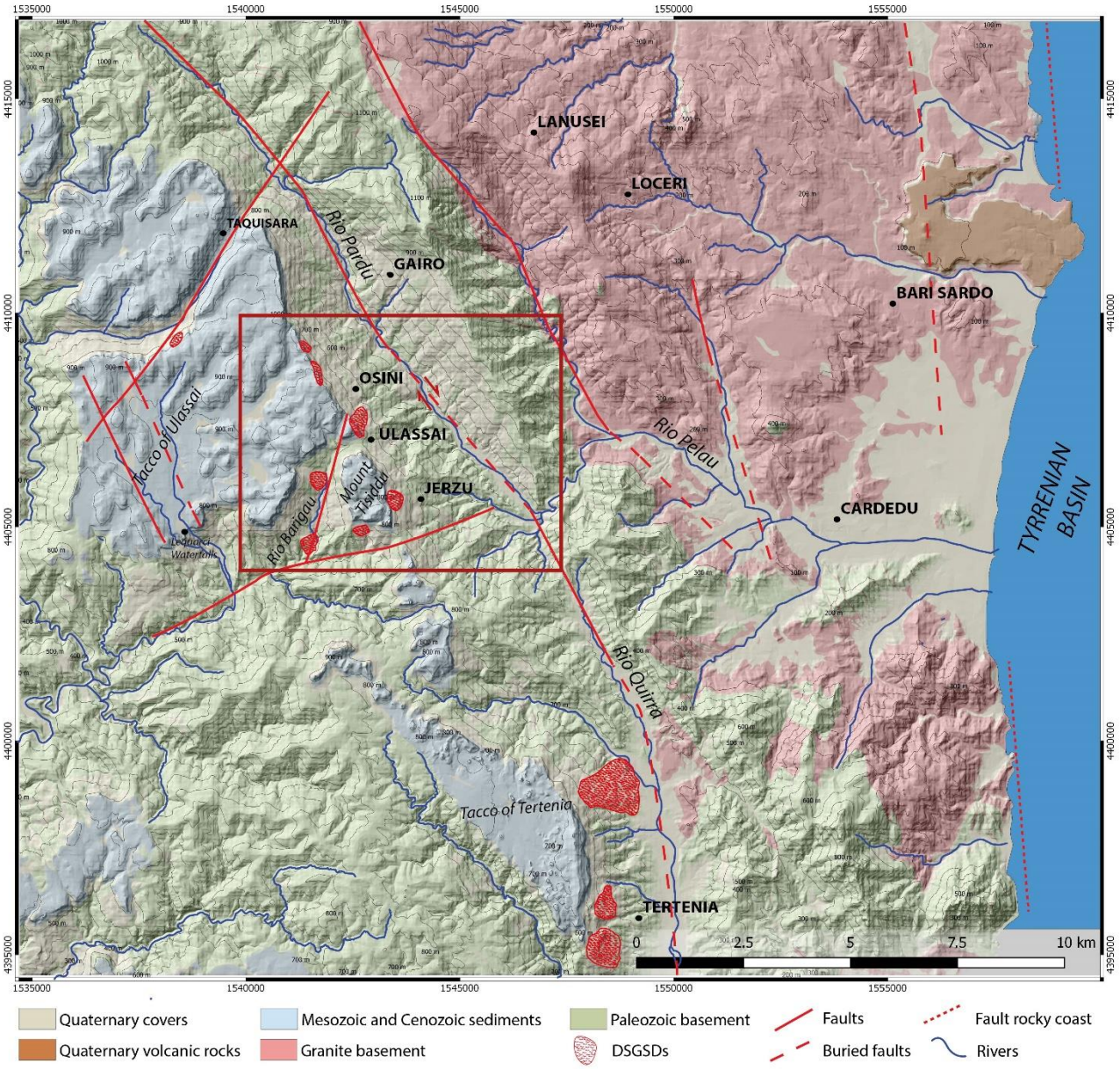

Figure 14 - Geolithological sketch map of the study area based on geological data of Autonomous Region of Sardinia. The red boxes indicate the location of the main map that covers Pardu Valley and the east side of Tacco of Ulassai.

The area is characterised by the Pardu River Valley in the east and the Barigau River Valley in the south-west; the central and north-western sectors include extensive dolomitic plateau called Tacco of Ulassai. The geological basement comprises Palaeozoic metamorphites affected by complex plicative structures and regional low-grade metamorphism (*Carmignani et al., 2001, 1994; Elter et al., 2004, 2010*). The major Palaeozoic units are the Filladi Grigie del Gennargentu Formation and Monte Santa Vittoria Formation, which constitute metarenites, quartzites, shales, and metavolcanites (Middle Cambrian–Middle Ordovician) (*Meloni et al., 2017; Pertusati et al., 2002; Vai & Cocozza, 1974*). The metamorphic basement summit has suffered chemical alteration associated with

a warm humid climate during the Permian and Triassic periods (*Costamagna & Barca, 2004; Marini, 1984*).

An angular unconformity of Mesozoic sedimentary succession rests on the metamorphic basement. Basal layers are primarily fluvial sediments of the Genna Selole Formation (Middle Jurassic), which are overlain by dolomitic limestones of the Dorgali Formation (Middle–Upper Jurassic). (*Costamagna et al., 2018; Costamagna & Barca, 2004; Dieni et al., 1983; Pertusati et al., 2002*). These Mesozoic deposits are extensive and decipherable from their plateau morphology. The Genna Selole Formation (*Costamagna, 2015; Dieni et al., 1983*) represents a mixed succession of siliciclastic to siliciclastic–carbonate deposits. The Dorgali Formation is represented by dolomitic sequences with thickness up to tens of metres. The lower part, with a thickness of approximately 30 m, is affected by marl intercalations, whereas the upper part is typically massive. Mesozoic units are sub-horizontal strata with an attitude of approximately N90/0–5°, and the plateau edges can reach a dip amount of up to 40° and direction parallel to the slope owing to the DGSD.

Quaternary covers, represented by continental deposits, are primarily colluvial and alluvial deposits. The most extensive outcrops represent landslide deposits, including rockfalls, toppling, and collapsed DGSDs at the foot-slope of the Tacchi, abundant on the right slopes of the Pardu and Barigau rivers. Moreover, terraced alluvial deposits have also been identified in the downslope.

The rockfalls and toppling landslides have been characterised by different sedimentological features based on age. These deposits are associated with rockfalls affecting the plateau edge wall and the collapse of some parts of the DGSDs.

3.3 Tectonic and geodynamic settings

The geodynamic setting is associated with the collisional dynamics between the African and European plates (Figure 13). The structural setting is associated with the Alpine cycle, which first appeared with a strike-slip fault in the Oligo–Miocene and in the Pliocene and Quaternary with an extensional component (*Carmignani et al., 2001, 2016; Carminati & Doglioni, 2005; Cherchi & Montadert, 1982; Gattacceca et al., 2007; Gueguen et al., 1997; Oggiano et al., 2009; Ulzega et al., 2002*).

The major features in the study area are the NW–SE faults on which the Pardu Valley is engraved, and the secondary fault directions include ENE–WSW and NNE–SSW (*Pertusati et al., 2002*).

The Plio-Quaternary tectonic phase is associated with conspicuous N–S faults (*Casula et al., 2001*). These rectilinear and normal faults are also evident in the continental margin and control its morphology (Figure 14). In the continental region, these N–S faults are associated with alkaline basalts with an age of approximately 3.9 Ma (*Lustrino et al., 2007*). Quirra River follows this N–S

direction from the south of the Pardu River capturing elbows and flows in a straight line for approximately 30 km (Figure 15).

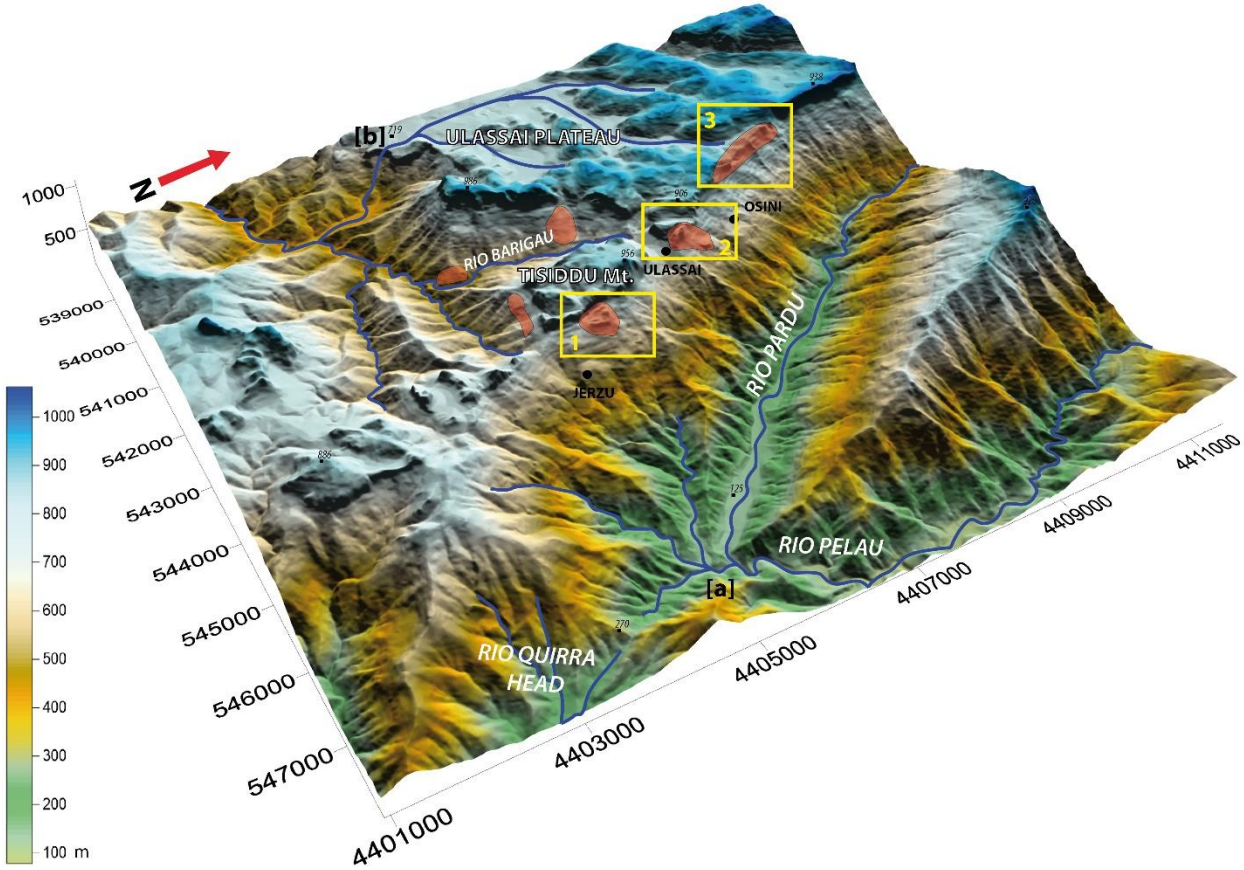

Figure 15 Three-dimensional (3D) model of Pardu River (Rio Pardu) Valley and Ulassai Plateau. Blue lines represent major hydrographic features, and red areas represent the major DGSDs. (a) Fluvial capture elbow; (b) Lequarci waterfall. (1) Tisiddu Mountain DGSD; (2) Bruncu Pranedda DGSD; (3) Scala San Giorgio DGSD.

Based on preliminary geodetic data from the Peri-Tyrrhenian Geodetic Array network, *Ferranti et al. (2008)* revealed the presence of low internal deformation in Sardinia. In Sardinia, seismicity is typically scattered and sporadic, except for the dozen tremors detected following the ML4.7 earthquake of 7 July 2011 in the Corsican Sea, which primarily characterises the edges of the continental lithosphere block. Significant seismic events also occurred in the eastern sector, in particular, three events with a magnitude > 4 (26 April 2000, magnitude ML 4.2 and 4.7, and 18 December 2004, magnitude ML 4.3) located in the central Tyrrhenian Sea approximately 60 km east of Olbia in the Comino depression (*Cimini et al., 2016*). The most recent low-magnitude earthquake events were ML 1.8 (Escalaplano, 4 April 2019) and ML 1.6 (Perdasdefogu, 14 October 2020) (INGV, 2021).

3.4 Geomorphological setting

The landscape is characterised by sub-horizontal carbonate plateaus, separated by deep rectilinear valleys engraved in the Palaeozoic basement for several hundreds of meters (*Maxia et al., 1973; Ulzega & Marini, 1973*). Erosion primarily acted on the Oligo–Miocene strike-slip faults with an increase in the erosive rate during the Plio-Pleistocene uplift phases (*Marini & Ulzega, 1977*). A significant karstic process has acted on plateau surfaces, comprising ancient palaeoforms and currently hypogeal and superficial morphologies (*De Waele et al., 2005, 2012*). Karst palaeoforms represented by complex cockpit doline types have been characterised in the area in a humid and warm morphoclimatic setting (*Fleurant et al., 2008; Liang & Xu, 2014; Waltham, 2008*). These dolines are separated by residual reliefs called Fengcong, sorted along the major structural features. The hypogean karst enabled the development of sinkholes, karst springs, cavities, and caves (e.g. Su Marmuri Cave and Is lianas Cave). The combined action of karst, uplift, river erosion, and gravity has led to the formation and evolution of numerous hanging valleys on the plateau surface (*Ulzega & Marini, 1973*).

The presence of major regional faults has influenced the watercourses, which maintain a prevalent N–S direction in the Pardu River (set on the main fault), toward the western side of the map, corresponding with the secondary faults. Considering the descriptive parameters, geometrical conditions, and longitudinal profile, the evolutionary conditions of the Pardu Valley are associated with a cycle of underdeveloped fluvial erosion, suggesting a relatively young age of engraving (*Marini & Ulzega, 1977; Maxia et al., 1973; Ulzega & Marini, 1973*).

The evolution of Pardu River is closely associated with that of Quirra River (*Palomba & Ulazega, 1984; Pertusati et al., 2002*). Pardu River flows from the NW toward the SE and then abruptly changes direction toward the NE. At this point, a capture elbow adjacent to the present head of the Quirra River is well developed. The upstream part of Quirra River flows at an altitude of approximately 200 m higher than the Pardu River.

It also presents an over-sized and over-flooded valley with respect to the upstream catchment area. Moreover, there are various orders of terraces and deposits in the Pleistocene. This setting indicates that the Pardu River, previously flowing south along with the Quirra River, was captured by Pelau River (*De Waele et al., 2012; Palomba & Ulzega, 1984*).

Gravity-related mass movements occur along carbonate cornices with rockfalls and toppling. We have focused on the DGSDs in this study, as they are important in the morphological evolution of the carbonate plateau.

3.5 Methods

Geological and geomorphological analyses were performed and a 1:10.000 geomorphological map was generated in accordance with cartographic models in the literature related to geomorphological mapping (*GNGFG, 1994; ISPRA 2007; ISPRA & AIGEO, 2018; Miccadei et al., 2012; Smith et al., 2011*). A remote sensing survey, accompanied by the interpretation of aerial photos and digital terrain models (LiDAR data of 1-m cell size, by Autonomous Region of Sardinia acquired in 2008), and field surveys were performed to analyse vast areas, including the Tacco di Ulassai and the Pardu River and Barigau River valleys.

The main map was created using the ESRI ArcGIS/ArcMap using the Regional Technical Cartography of the Autonomous Region of Sardinia at 1:10.000 scale. We comprehensively analysed three areas with specifically interesting DGSD process: Bruncu pranedda, Scala San Giorgio, and Tisiddu Mountain (Figure 15).

To analyse the DGSDs at the local scale, we used high-resolution digital elevation models (DEMs) acquired via structure for motion from a UAV. Structural and geomorphological field mapping surveys were performed at a 1:200 scale for each landslide, thereby enabling the creation of a geological 3D model of the slope deformations (*Clapuyt et al., 2016; Eker & Aydın, 2021; Peternal et al., 2017; Valkaniotis et al., 2018*). Briefly, 100 structural survey stations were set in the metamorphic basement and in the Mesozoic units using geological compass. Structural data were processed using Rocscince Dips.

The aerial surveys were performed using UAVs (DJI Phantom 4) flying at altitudes of 50–60 m above ground level. The acquired images were analysed and processed using photogrammetric Agisoft MetaShape software and constrained by 10–12 ground control points using GEODETIC LEICA GNSS for each area. The resulting orthorectified mosaic and DEM (WGS 84 datum and UTM 32N projection) had a cell size of 5 cm/pixel and were considered sufficiently precise to be used for the geomorphological analysis. 3D high-resolution UAV models were used to develop interpretative superficial models using geomorphological evidence and stratigraphic and structural data of the DGSDs. Geological interpretative cross-sections of geologic features crossing the major DGSDs were also generated to define the movement kinematics, deformative style, and deep geometries of the DGSDs.

3.6 Results

3.6.1 Geomorphological map

The cartographic synthesis was based on the lithologies on which landforms were highlighted, with distinct morphogenetic processes and relative chronological positions.

Geomorphological map shows the lithology from the Palaeozoic basement to the continental Quaternary covers (Figure 16).

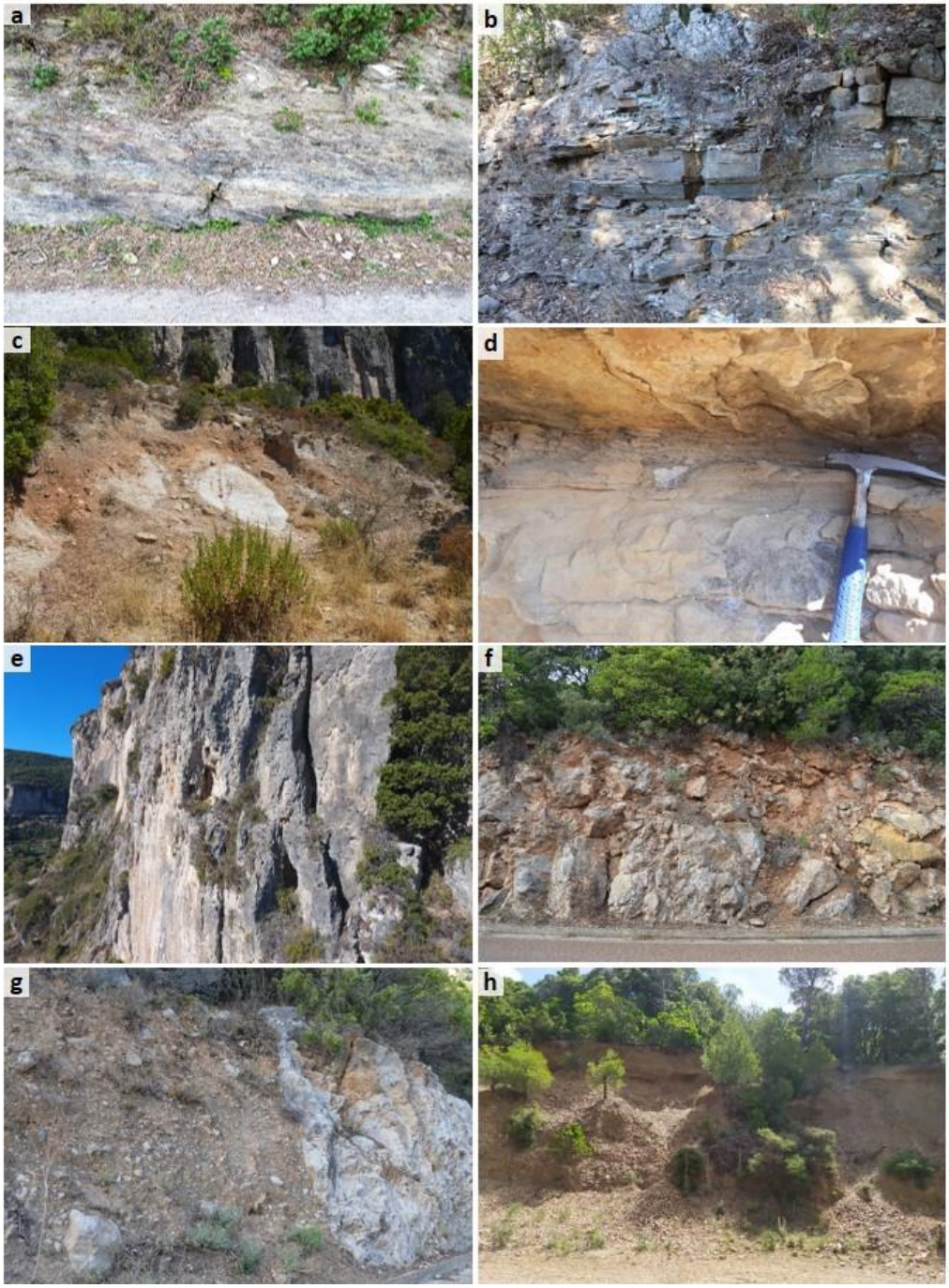

Figure 16 - Major geological units presented in the main map: Metamorphic basement: (a) altered phyllites; (b) Fractured metasandstone and quartzites. Transitional and marine Mesozoic succession: (c) Genna Selole Formation (siliciclastic–carbonate deposits and clays); (d) Basal facies of Dorgali Formation (layered dolostone and marls); (e) Dolostone of massive Dorgali Formation. Rockfall deposits: (f) Cemented; (g) Quiescent; (h) Slope deposits.

The major physiographic units presented in the geomorphological map are the Tacco of Ulassai, Tisiddu Mountain, and the two main valleys, namely Pardu River and Barigau River valleys. The Ulassai Plateau, which comprises Mesozoic dolomitic lithologies, is affected by various superficial and underground karst morphologies (*De Waele et al., 2012*). A karst palaeo-landscape with a sub-tropical climate consisting of cockpit and Fengcong was detected (*Fleurant et al., 2008*). The latter, characterised by gentle relief, is aligned in the direction of the Oligo–Miocene faults. These formations are the major pathways of underground waterflows, on which sinkholes have developed. The plateau surface is affected by extensive polje-type dolines, which defines an extensive hydrography. The catchment area of the plateau flows out of the Santa Barbara area, which flows into the Ulassai stream after an 80-m hydraulic jump (Lequarci waterfall) (Figure 15).

The edge of the plateau was affected by gravitational processes at different scales. Moreover, there widespread rockfalls and toppling of various magnitudes were present. Three orders of landslide deposits were identified, namely cemented, quiescent, and active.

The valley floor of the Pardu River in the upper part is characterised by a bed set on rock with major erosive features, whereas in the downstream part near the capture elbow, alluvial deposits exist with two orders of terraces. Downstream of the capture, the river resumes the erosive character with the valley floor set on the rock.

The legend signifying geomorphology in this study was conceived to effectively represent the features of the study area. We highlighted outcropping bedrock lithology, tectonic features, superficial deposits, and the distribution of structural, gravitational, and karst landforms.

3.6.2 Morphostructural setting of DGSDs

Various areas affected by DGSDs located at the edges of the carbonate plateau were identified, with the major ones located on the east side of Tacco di Ulassai and Tisiddu Mountain. The main structures that indicate the deep gravity phenomenon were large and deep extensional trenches which are evident in the carbonate lithotypes. A complex structural setting was deciphered based on the analysis of faults, foliation, and tectonic-gravitational structures (Figure 17). Trenches had lengths of several hundreds of metres and a decametric opening and depth (Figure 18).

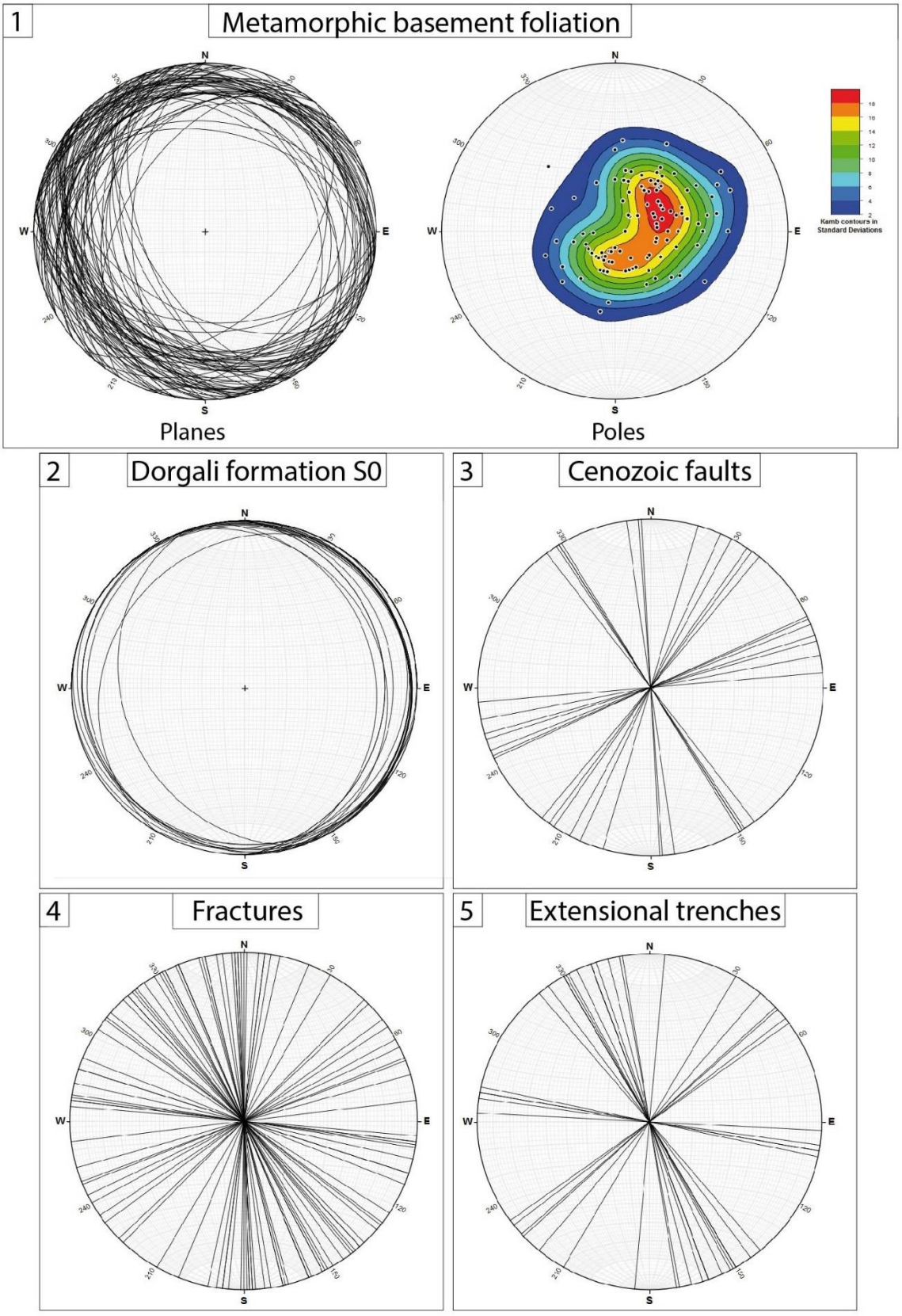

Figure 17 - Stereographic projections of tectonic and gravitational structures. (1) Low-angle dip schistosity in the metamorphic basement; (2) Dorgali Formation layering. The larger angles indicate the blocks of the DGSD; (3) Primary Cenozoic faults, NW–SE and secondary sub-vertical faults; (4) Vertical fractures in the Mesozoic units associated with the tectonic structures; (5) Extensional trenches.

Figure 18 UAV images of the DGSD showing the major geomorphological and structural features. The white dashed lines represent the major extensional trenches. (A1). Panoramic view of the Ulassai Village. (A2) Bruncu Pranedda DGSD. (A3) Top slope sector. (A4) Middle slope sector. (B) San Giorgio DGSD. (C) Tisiddu Mountain DGSD. (D) Evidence of collapse deposits of rock avalanches. Recent collapse near Ulassai Village. (D1, D2) Palaeo-collapses of mega-blocks, 20–40 m for each side.

The Bruncu Pranedda DGSD depicted two regions with different settings located in the top and middle slopes. In the top slope toward the east of the largest extensional trenches called Pranedda Canyon (Figure 18 (A1–A3);Figure 19 (A,A1,D)), the rock mass fracturing increased, and the attitude of the Dorgali Formation is toward the east, with a dip amount of up to 40°. In this area, both facies of the Dorgali Formation were visible, with the summit comprising dolomitic banks and the lower part characterised by an alternation of well-stratified dolomites and marls. This subdivision was not observed in the middle slope (Figure 18 (A4)), where basal marly levels do not appear on the surface. This indicates that the basal facies (approximately 30 m) were partially covered by slope deposits; however, they also sank a few metres inside the fractured and altered Palaeozoic metamorphic basement. This can be correlated with the field observations at the same altitude, with the basement and the massive facies of the Dorgali Formation.

The Scala San Giorgio DGSD is located north of Osini Village (Figure 18 (B) and Figure 19 (C)) and is characterised by two major extensional trenches parallel to the slope that affect the Dorgali Formation with dip amount up to 20°. All the sequences of the Dorgali Formation are exposed; however, the Genna Selole Formation is covered by rockfall deposits.

The Tisiddu Mountain DGSD in the south of Ulassai Village is characterised by a highly fractured segment of the Dorgali Formation located tens of metres downstream. Only the top massive banks of dolostones are visible. The basal level was partially sinking in the metamorphic basement.

Shear zones are located in different geological units that represent structural weaknesses (Figure 20). (I) The top of the metamorphites was affected by sub-horizontal foliation (Figure 17) and advanced weathering, and the rock exhibited a reddish or whitish colour. This type of alteration could be linked to the pre-transgressive Mesozoic period (*Marini, 1984*); (II) Genna Selole Formation exhibited plastic clay layers; (III) basal levels of Dorgali Formation were characterised by the alternations of marl and dolomite.

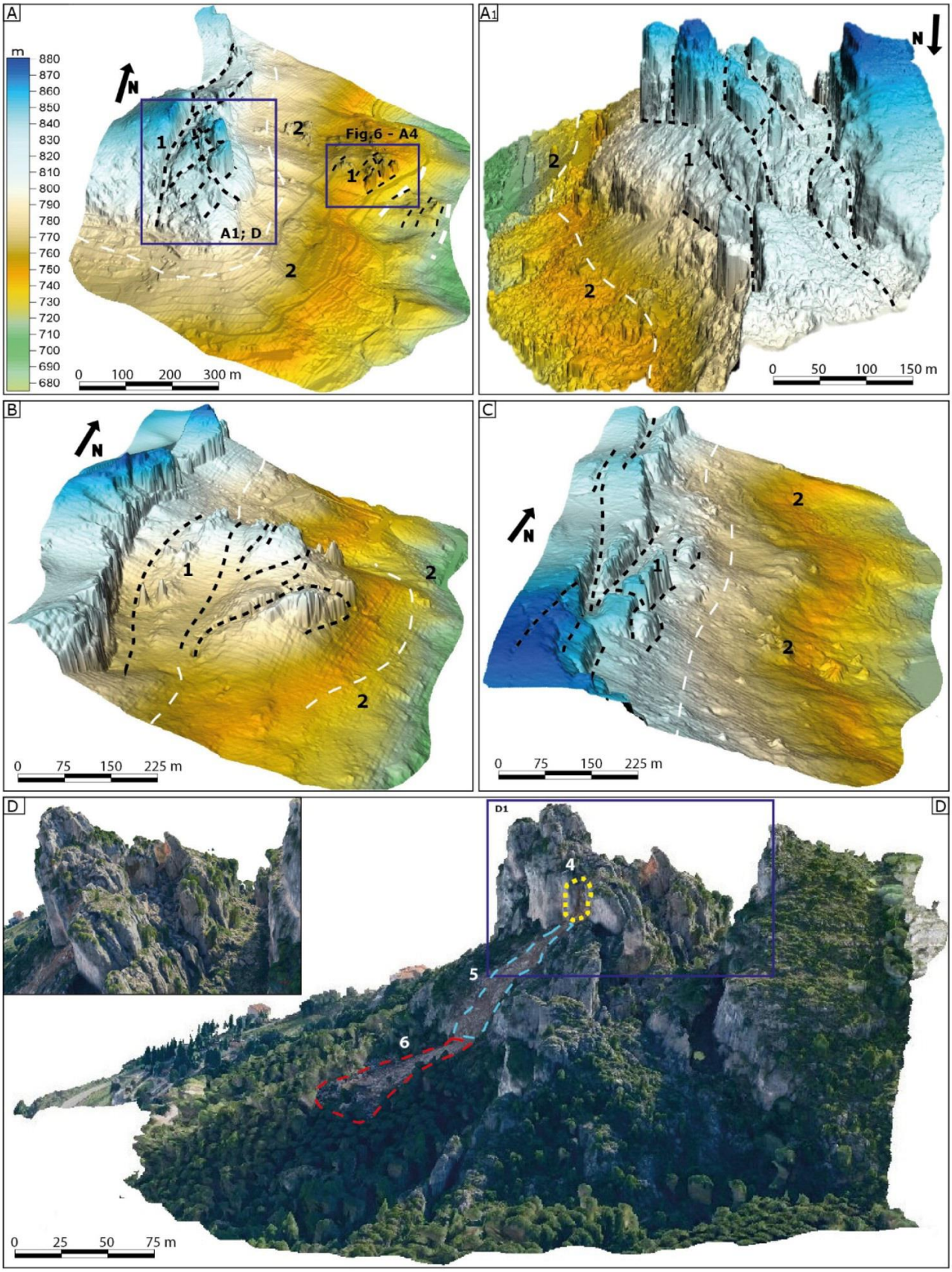

Figure 19 - LiDAR 3D model of the DGSD. (A1) Bruncu Pranedda. (B) Tisiddu Mountain. (C) Scala San Giorgio. (1) High fracturing area with active extensional trenches. (2) Collapse deposits of rock avalanches. The black dashed lines represent the major extensional trenches. White dashed lines represent the major stratigraphic discontinuity between marine Mesozoic sequence and the metamorphic basement. (D) UAV 3D model of Bruncu Pranedda. (4) Detachment niche. (5) Transit area. (6) Collapse deposits of rock avalanches.

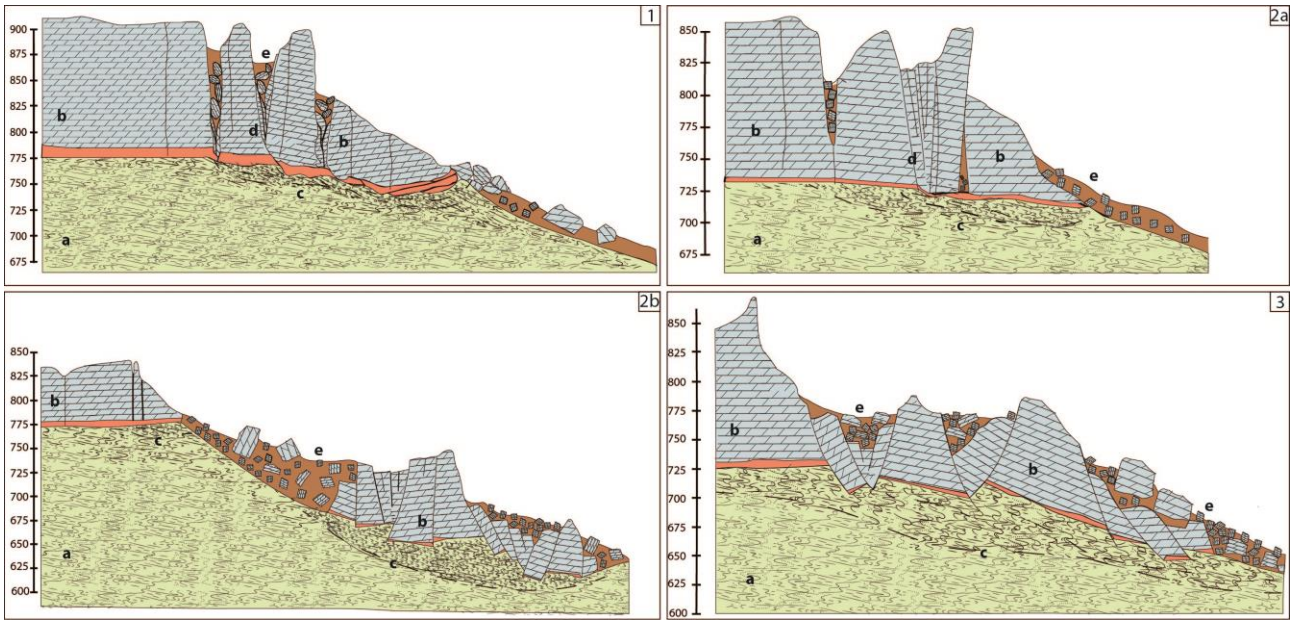

Figure 20 Interpretative geological cross-sections. (1) Scala San Giorgio, (2a) Bruncu Pranedda lateral spread; (2b) Bruncu Pranedda sackung; (3) Tisiddu Mountain sackung. (a) Metamorphic basement; Dorgali Formation over Genna Selole (orange). (c) Hypothetical shear zone, (d) active extensional trenches, (e) trench rockfall deposits.

Geomorphological evidence and stratigraphic and structural analyses enabled the identification of various DGSDs characterised by different kinematics. From the structural analysis (Figure 17), the major faults with NW–SE and NE–SW directions were in concordance with the main trenches. The secondary trenches and the joints did not exhibit a good correlation with the large-scale structures because they were associated with the features inside the deformation rock mass. Lateral spreads were developed at the plateau edge due to the sub-vertical pre-existing fractures (Figure 17). Consequently, there was a predominant horizontal movement associated with vertical fractures in the carbonate and a zone of ductile basal deformation that affected the Genna Selole Formation and the summit, which altered the metamorphites (Bruncu Pranedda top slope and San Giorgio DGSD). DGSDs with a higher vertical shift represented a more advanced stage with sackung features (Tisiddu Mountain and middle slope of Bruncu Pranedda). A large part of the deformation affected the Palaeozoic basement, which was evidenced by the sinking of the carbonate sequence in the metamorphites.

These DGSs were associated with numerous rockfalls and toppling landslides that affect carbonate walls. Dolomitic blocks with sizes up to 30 m on each side were identified, moving up to 900 m away from the detachment points, which were linked to mega-rockfall events with rock avalanche features (Figure 18 (D)). We also identified mega-blocks of Dorgali Formation in the downslope that were associated with collapsed palaeo-DGSD.

3.7 Discussion

Geomorphological data regarding the DGSD of Bruncu Pranedda, Scala San Giorgio, and Tisiddu Mountain were used to generate geological sections for reconstructing a hypothetical surface of basal rupture and deep geometries (Figure 20).

Geological and geomorphological analyses using high-resolution topographic data enabled the identification of different DGSD kinematic and evolutionary models. Based on the collected data, it was possible to identify three evolutionary stages.

The initial movement stage was characterised by lateral spread kinematics (*Delgado et al., 2011; Dramis & Sorriso-Valvo, 1994; Fioraso, 2017; Gutiérrez-Santolalla et al., 2005; Pánek & Klimeš, 2016; Taramelli & Melelli, 2008*) (Figure 20 (1,2a)), with a separation of the DGSD from the edge of the plateau. This occurred via horizontal movement without vertical sinking.

The stratigraphic setting is characteristic of the lateral spreads because the Dorgali Formation (hard formation) rests on the Genna Selole clays and on an altered and fractured schist basement (plastic formations). In the carbonate lithologies, the deformation is brittle and develops with a major fracture; however, in the basement, it is ductile with a sub-horizontal movement. The basal sub-horizontal shear zone is primarily located in the Genna Selole Formation and in the summit altered metamorphites.

The second stage (Figure 20 (2b,3)) is associated with the deformation pattern of the sackung type (*Ambrosi & Crosta, 2006, 2011; Audemard et al., 2010; Bovis & Evans, 1996; Coquin et al., 2015; McCalpin & Irvine, 1995; Oppikofer et al., 2017; Soldati et al., 2004*), which can be deduced from the partial sinking of the DGSD body inside the Palaeozoic basement. This stage is the observable downslope of the plateau edges located in the parts of the Dorgali Formation tens of metres away from the original stratigraphic altitude. They are separated from the plateau by an extensive transit area characterised by the presence of slope deposits with limited outcrops of the Palaeozoic basement. This is an advanced stage assimilable at a sackung landslide and is associated with a major basal deformation that allows the movement of the bodies even for several hundreds of metres. The shear zone is located in the metamorphic basement with a sub-circular shape.

The third stage is the consequence of the collapse of the peripheral margins of DGSDs and is manifested through rock avalanche deposits (Figure 19 (D)). These deposits, comprising blocks with a size of several thousands of cubic metres, cover the most recent slope deposits and represent one of the major evidence for present movements of the DGSDs. In fact, rock avalanche deposits have been found to exhibit sedimentological and geomorphological characteristics of a very recent event. The evidence of current activity is demonstrated by the detachment of a rock avalanche which occurred in November 2014, involving a total volume of rock more than 1500 m3.

The type and evolutionary characteristics of rockfalls and rock avalanches represent high risk factors in some sectors of the inhabited centre below; a monitoring network is being created based on satellite and geotechnical technologies with the aim of developing an early warning system.

3.8 Conclusions

A kinematic model and geomorphological evolution characteristics of DGSD in Sardinia were described for the first time in this study. The study highlighted an extremely young territory conformation, associated with the Neogene and Quaternary geodynamic events, implying a series of problems related to the slope process. The causes of the DGSDs are associated with the structural characteristics of the area and the Neogene and Quaternary geomorphological evolution of the river valley associated with the recent uplift. In the main map, a comprehensive mapping of structural, karst, fluvial, and slope morphologies in Pardu and Ulassai valleys is presented.

The predisposing factors of DGSDs can be identified in the following points:

- The tectonic history of the slope with a passive influence has been caused by a major uplift associated with the Neogene and Quaternary geodynamic events. The upliftment has increased the erosion rates, thereby leading to the deepening of the valleys and detente of the slopes. The energy of the relief of the slopes is the decisive morphological element which initiates the DGSDs; in the cases studied, it is higher than 650 m.
- Cenozoic tectonics have also conferred the structural conditions that predisposed the development of DGSD, particularly in the Dorgali Formation. In fact, the major DGSD trenches are evidently parallel to the major faults and primarily parallel to that of Pardu Valley in the NW–SE direction, on which the slope is also set
- The lithostratigraphic conditions are represented by the Mesozoic units on the foliated and altered metamorphic basement.

The initiation of rapid catastrophic processes such as rock avalanche is associated with the accelerations of DGSDs. These accelerations are linked to seismic activities and extreme rainfall events. The latter cause the hydration of the rocks in the shear zones, thereby decreasing the geomechanical characteristics.

High-resolution topographic data and geological and geomorphological field surveys enabled the identification of three evolutionary stages of DGSD.

- The first stage preceding the capture of the Rio Pardu by the Rio Pelau associated with the uplift and the Plio-Quaternary tectonics.

- The second phase associated with a major erosive activity following the capture of the Rio Pardu which triggered the oldest DGSDs with sackung features.
- The present evolution of plateau edges through lateral spread DGSDs and rock avalanches.

3.9 Software

The map was digitised using ESRI ArcGIS ® 10.6 software. UAV photogrammetry data were processed by Agisoft Metashape Professional ®. The digital terrain models were generated using the Global Mapper ® 21.0. Geological sections were created using Adobe Illustrator ® CC2015.

3.10 Main map

https://www.tandfonline.com/doi/suppl/10.1080/17445647.2021.1986157?scroll=top

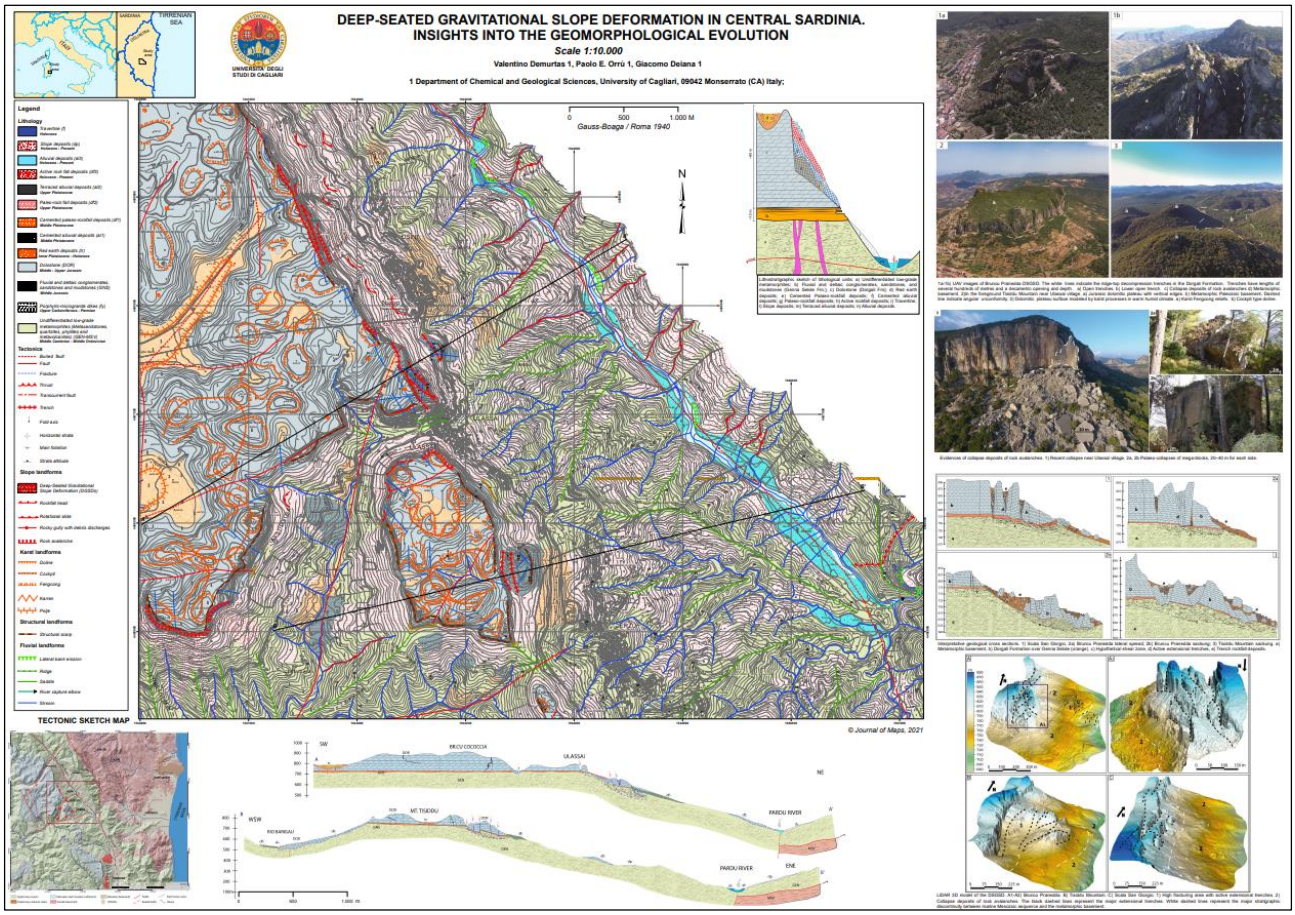

4 CHAPTER II

Evolution of Deep-Seated Gravitational Slope Deformations in Relation with Uplift and Fluvial Capture Processes in Central Eastern Sardinia (Italy)

Demurtas, V.; Orrù, P.E.; Deiana, G. Evolution of Deep-Seated Gravitational Slope Deformations in Relation with Uplift and Fluvial Capture Processes in Central Eastern Sardinia (Italy). Land 2021, 10, 1193. ***Publisced November 2021 https://doi.org/10.3390/land10111193***

ABSTRACT

Connections between Plio-Pleistocenic tectonic activity and geomorphological evolution were studied in the Pardu Valley and Quirra Valley (Ogliastra, East Sardinia). The intensive Quaternary tectonic activity in Sardinia linked to the opening of the Tyrrhenian Basin is known. In Eastern Sardinia, it manifests with an uplift that is recorded by geomorphological indicators, such as deep-seated gravitational slope deformation, fluvial captures, engraved valleys, waterfalls, and heterogeneous water drainage. The Pardu River flows from the NW toward the SE and then abruptly changes direction toward the NE. At this point, a capture elbow adjacent to the current head of the Quirra River is well developed. The Quirra River, in its upstream part, flows at altitudes approximately 200 m higher than the Pardu River. It also shows an oversized and over-flooded valley with respect to the catchment area upstream. This setting indicates that the Pardu River, which previously flowed south along the Quirra River, was captured by the Pelau River. We analyzed long-term landslides with lateral spreading and sackung characteristics, which involve giant carbonate blocks and underlying foliated metamorphites in both valleys. The use of LiDAR, high-resolution uncrewed aerial vehicle digital photogrammetry (UAV-DP), and geological, structural, and geomorphological surveys enabled a depth morphometric analysis and the creation of interpretative 3D models of DGSDs. Space-borne interferometric synthetic aperture radar (InSAR) data using ERS and Sentinel-1 satellites identified downslope movement of up to 20 mm per year in both Pardu Valley flanks. Multi-source and multi-scale data showed that the state of activity of the DGSDs is closely linked to the geomorphological evolution of the catchment areas of the Rio Pardu and Rio Quirra. The intense post-capture erosion acted in the Rio Pardu Valley, giving it morphometric characteristics that were favorable to the current evolution of the DGSDs, while the Rio Quirra Valley presents paleo-DGSDs that have been fossilized by pre-capture terraced alluvial deposits.

Keywords: morphotectonic; morphostratigraphy; DGSDs; river capture; fluvial terraces; Sardinia; Italy

4.1 Introduction

The Pliocene and Quaternary geodynamic processes related to the Tyrrhenian basin opening led an uplift in Sardinia (*Carmignani L. et al. 2001; Carminati & Doglioni, 2005; Cherchi A & Montardert 1982*). This is evidenced by a morphotectonic setting linked to fluvial and gravitative morphologies (*Maxia C, et al. 1973; Ulzega & Marini 1973*). Therefore, the hydrographic basins of the Rio Quirra and the Rio Pardu have been studied in detail in order to analyze their evolutionary scenarios in relation to a river capture.

Rio Pardu and Rio Quirra are two of the most important rivers in central eastern Sardinia. The two basins are separated by a river capture caused by the Rio Pelau, which isolated Rio Pardu, the catchment area of Rio Quirra. Rio Pardu flows from northwest to southeast and then flows towards the northeast through a river capture elbow with the name of Rio Pelau. Rio Quirra flows from the north to the south parallel to the coast and then abruptly bends towards the Tyrrhenian Sea near the mouth. The flow directions are closely related to the structural conditioning of the main alpine structural setting and are linked to the opening of the Tyrrhenian basin (*Demurtas, V. el al. 2021, De Waele, J. et al 2012*) (Figure 21).

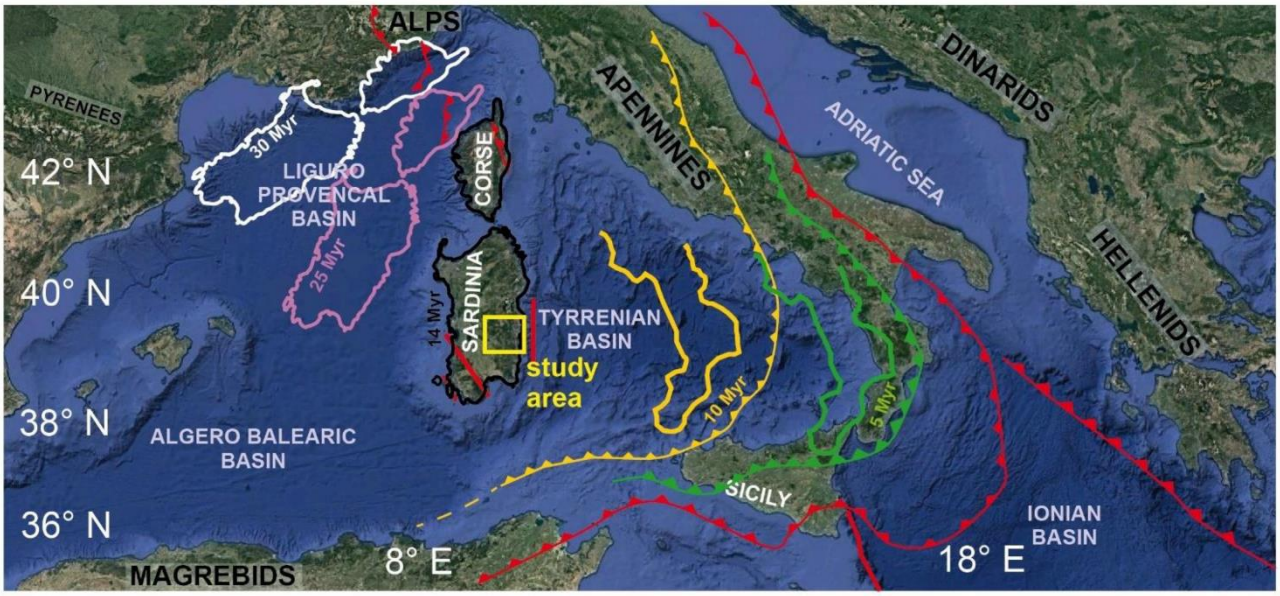

Figure 21- Geographical location and structural features of the study area, modified after (Deiana et al. 2021); red lines represent thrust fronts; white lines are the Sardinian–Corse Block translation at 30 Ma; the pink line represents the Sardinian–Corse Block translation at 25 Ma; the yellow line represents the Calabrian block translation at 10 Ma; the green line represents the Calabrian block translation at 5 Ma.

River drainage systems are very dynamic features of the landscape. Geological changes can cause fluvial captures, leading to abnormal large-scale river networks (*Suhail, H.A et al. 2020; Carabella et al, 2020; Fan, N et al 2018; Bishop P, 1995; Willett,S .D et al 2014; Whipple, K. 2017; Prince P 2011; Aslan A et al, 2014, De Waele 2012*). The main geological changes that cause river captures

are glaciation and tectonic movements associated with earthquakes and faults (*Shugar D 2017*). Tectonic movements, especially landscape uplift, are much slower than glacial processes. Therefore, the development of tectonic river capture normally requires hundreds of thousands of years, or even millions of years (*Bracciali et al. 2015; Anton D.2014*).

The particular evolutionary characteristics of the Pardu and Quirra valleys in relation to slope instability dynamics have been the subject of various studies (*Maxia et al., 1973; Ulzega & Marini, 1973, De Waele et al. 2012; Demurtas et al 2021*). This sector of Sardinia represents one of the most susceptible areas to landslides in the region. This high hazard is closely linked to the particular vulnerability to important weather events, especially rainstorms. Rainfall-induced landslides represent a relevant threat to the population, infrastructure, buildings, and cultural heritage (*Panek et al. 2011, Quesada- Roman et al. 2019 , Volpe et al. 2021, Shoe et al. 2021, Quesada-Roman et al. 2021*). Among the most important catastrophic geological events in Sardinia are those that occurred in the Rio Pardu valley, which involved the inhabited centers of Gairo, Osini, Ulassai, and Jerzu. Between 15 and 17 October, 1951, extreme rainfall of about 1000 mm involved this area, triggering mudflows and landslides. This catastrophic event caused abandonment of the villages of Osini and Gairo (*De waele,2012; Ulzega 1977, Demurtas et al 2021*). These settlements have been rebuilt at least in part, sometimes with transfer to another area on the same slope. However, these measures proved useless, as the new sites present the same geo-hydrological risks as the previous ones (*The AVI project - Landslide Database; Moretti A. 1953*). Landslides affected schistose Paleozoic metamorphites on the left slope, while on the right, there was also widespread rockfall. Recent studies have highlighted the presence of deep-seated gravitational slope deformations with sacking (*Zichinsky, 1966, 1969; Radbruch-Hall et al., 1976; Radbruch- Hall, 1978; Bisci et al., 1996)* and lateral spread (*Jahn, 1964; Cruden & Varnes, 1996; Pasuto & Soldati, 1996*) characteristics that affect the sub-horizontal carbonate succession and the underlying metamorphites (*Demurtas et al. 2021*).

Deep-seated gravitational slope deformation (DGSD, (*Dramis & Sorriso-Valvo, 1994*) is a complex type of rock slope failure characterized by large dimensions generated in stone rocks (*Dramis et al., 2002*). DGSDs are characterized by slow movements that can suddenly accelerate and cause catastrophic collapse of sections of the deformed slopes (*Agliardi et al., 2020; Crosta & Agliardi, 2003; Nemčok, 1972; Ostermann et al., 2017; Radbruch-Hall, 1978*). Therefore, this phenomenon represents an important geo-hazard in relation to the deformation of large infrastructures and secondary collateral landslides. Although DGSDs play an important role in slope evolution and geo-hydrological risk, knowledge about them was scarce for a long time (*Soldati, 2013*). They are characterized by very slow deformation rates (*Cruden & Varnes, 1996*), landform assemblages (such

as double-crested ridges, trenches, synthetic and antithetic scarps, tension cracks, and convex bulged toes), and deep basal shear zones (*Agliardi et al., 2001, Chigira, 1992; Crosta et al., 2013; Mariani & Zerboni, 2020; Panek et al., 2016*). Often, shear zones present characteristics of cataclastic breccias with an abundant fine matrix (*Crosta & Zanchi, 2000*) and thicknesses up to tens of meters (*Ostermann et al., 2017*). DGSD is a common phenomenon in the relief of the Mediterranean Sea in relation to the particular geodynamic context that characterizes the region and to the widespread orogenetic chains. In this context, DGSDs play an important role in slope relief evolution, showing at least geometric analogies with gravity-accommodated structural wedges. Often, DGSD phenomena are influenced by the scale structural context of the slope and use pre-existing tectonic structures (fault and thrust) to guide their evolution, which is also in relation to a reactivation linked to a slope stress field variation (*Gentili et al 1994, Iovine et al. 1998*).

In Sardinia, the studies and evidence of DGSDs are quite scarce, but the distensive tectonics and the Plio-Quaternary uplift could justify the favorable conditions for the development of DGSDs, which could also be due to local reactivation of Hercynian and Alpine tectonic structures. In this context, the slope evolutionary characteristics are analyzed in particular, the DGSDs and the evolution of watercourses in relation to the uplift. The aim is to correlate these different aspects through geomorphological analysis with both field surveys and remote sensing techniques. Furthermore, the choice to analyze these basins takes on a particular characteristic due to the economic and social repercussions that the conditions of instability of the slopes determine in the populations of the towns of Ulassai, Osini, Jerzu, and Gairo. In fact, as is well known, these inhabited centers are continually threatened by disasters. Different types of interventions were carried out to protect inhabited centers and infrastructures, but they were carried out without a global study of the problem and, therefore, without real knowledge of the evolutionary modalities of the valley and the real gravitational dynamics of the slopes. Understanding the kinematics and temporal behavior of DGSDs and landslides is important for designing monitoring systems based on strong process knowledge. In some cases, continuous monitoring is the only way to reduce risk (*Frigerio et al 2014, Sestras et al 2021, Zhang et al 2021 ,Bianchini et al 2021 , Demurtas et al 2021 b*).

We hypothesize that the Plio-Quaternary tectonics and uplift in the Ogliastra area are the main forcing mechanisms for sustaining the necessary gravitational forces of DGSDs.

Here, we present an innovative approach for analysis of DGSDs and fluvial dynamics by using morphotectonic, morphostratigraphic, and geomorphic data and time-series InSAR data in the Pardu and Quirra rivers. We also integrated stratigraphic and morphotectonic data of the drainage basin scale to support our observations and analyses about the relation between DGSD activity and fluvial capture.

4.2 Geological setting

East-central Sardinia (Italy) is characterized by widespread Jurassic dolomitic plateaus—called "Tacchi" in Sardinia overlying a Paleozoic basement (Figure 22 and Figure 23 a,b) (*Carmignani et al., 2016; Pertusati et al., 2002*).

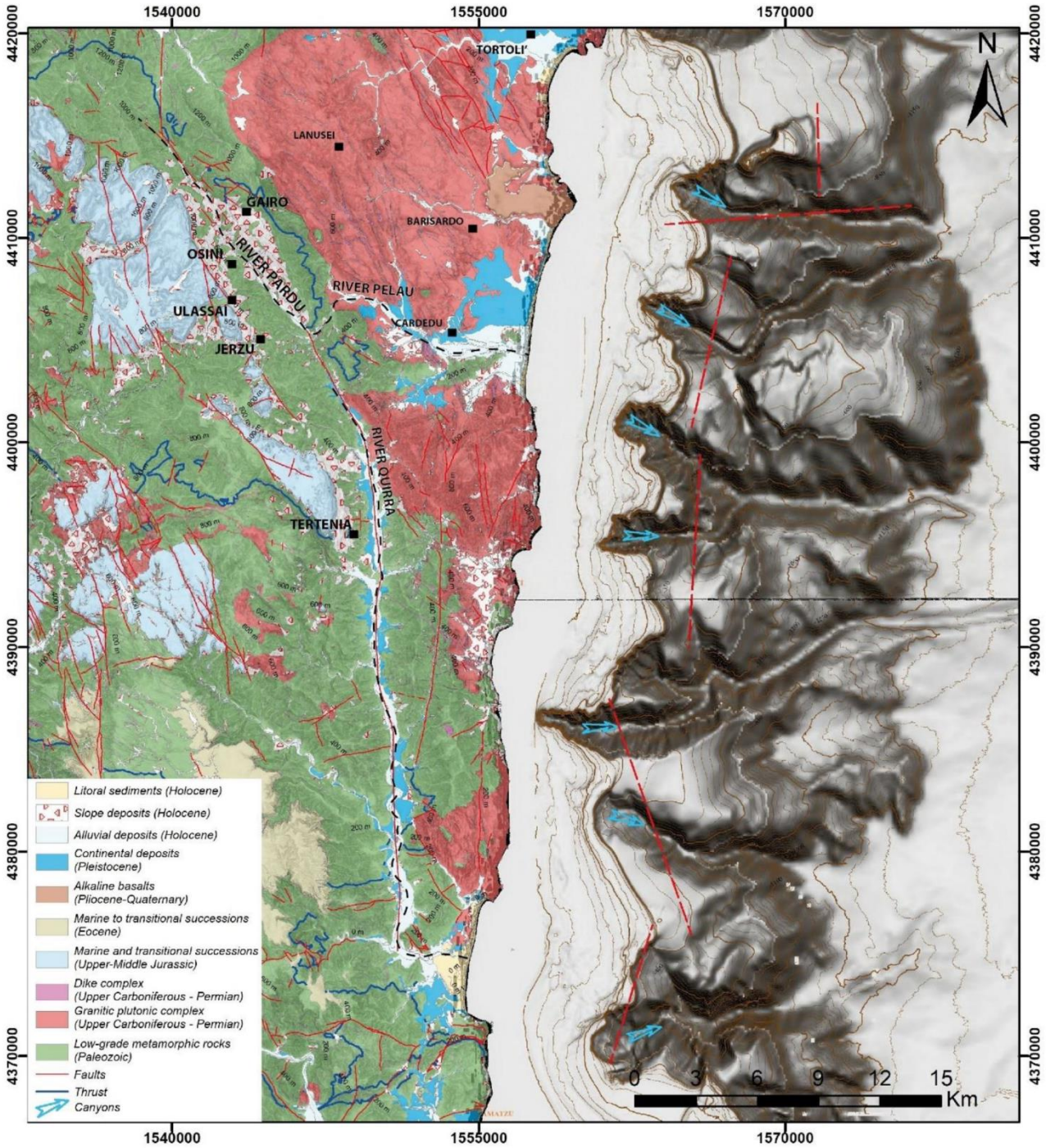

Figure 22 - Geolithological sketch map of the study area based on geological data of the Autonomous Region of Sardinia. Continental margin topography by (Chiocci et al. 2021). Black dashed lines show the analyzed rivers.

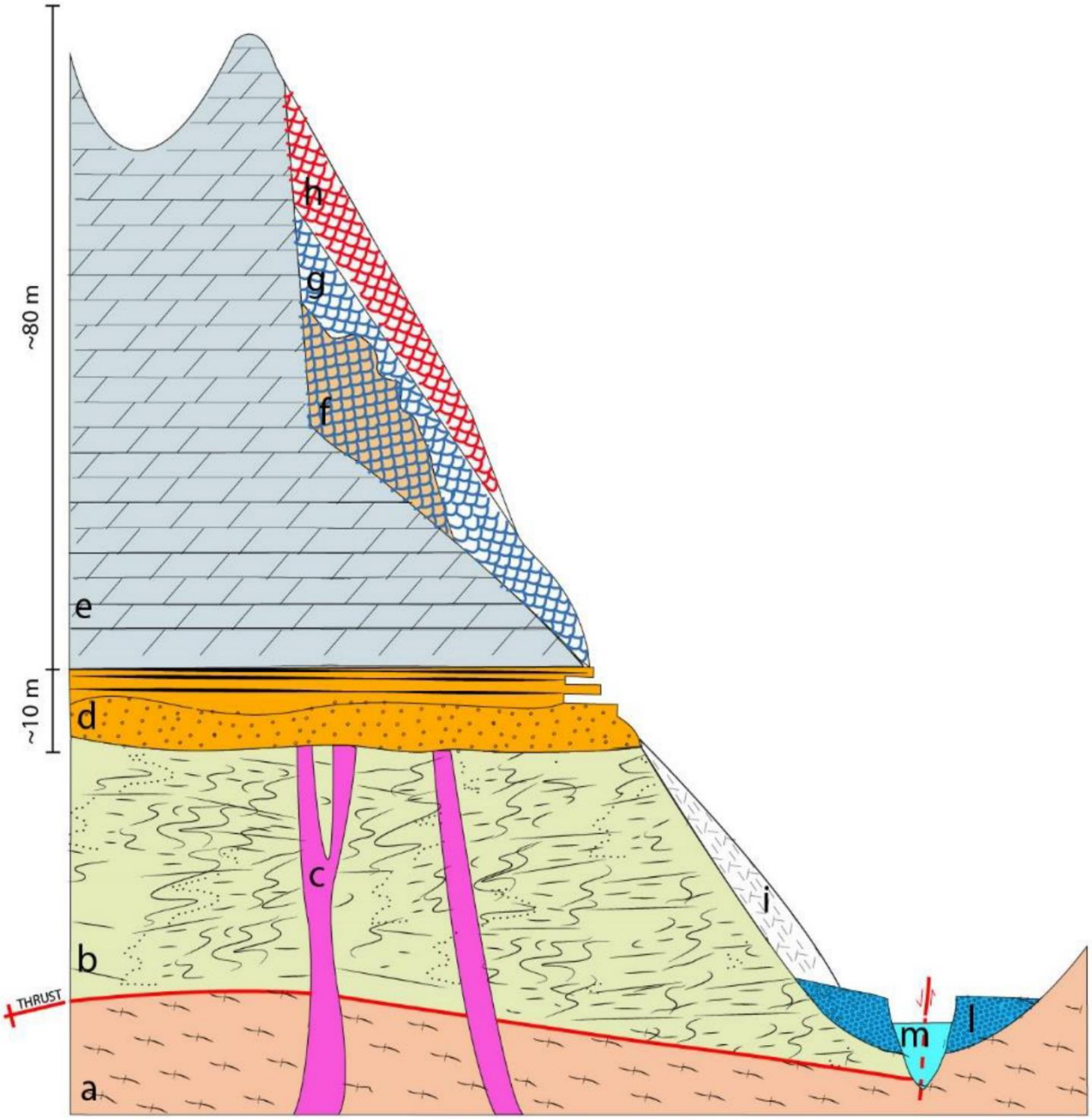

Figure 23 - Lithostratigraphic sketch of lithological units: Low-grade metamorphic rocks: (a) Monte Santa Vittoria Fm; (b) Filladi del Gennargentu Formation; (c) granitic plutonic complex and dikes; marine and transitional Mesozoic sedimentary succession; (d) gluvial and deltaic conglomerates, sandstones, and mudstones (Genna SeloleFormation); (e) dolostone (Dorgali Formation); (f) cemented paleo-rockfall deposits; (g) paleo-rockfall deposits; (h) active rockfall; (i) slope deposits; (l) terraced alluvial deposits; (m) alluvial deposits (modified after Demurtas et al.2021).

The area is characterized by the Pardu River Valley in the north, the Quirra River Valley in the south, and the Rio Pelau toward the east (Figure 24). The geological basement primarily comprises low-grade Paleozoic metamorphites affected by complex plicative structures, while in the coastal sector, there are widespread outcrops of carboniferous granites placed in the terminal phases of the Hercynian orogeny (*Carmignani et al., 2001, 1994; Elter et al., 2004, 2010*). The major metamorphic Paleozoic units are the Filladi del Gennargentu Formation and Monte Santa Vittoria Formation, which

are constituted by metasandstones, quartzites, phyllites, and metavolcanites (Middle Cambrian–Middle Ordovician) (*Meloni et al., 2017; Pertusati et al., 2002; Vai & Coccozza, 1974*). The summit of the metamorphic basement has suffered chemical alteration associated with a warm humid climate during the Permian and Triassic periods (*Costamagna & Barca, 2004; Marini, 1984*).

The marine and transitional Mesozoic sedimentary succession rests on the metamorphic basement in angular unconformity. These Mesozoic deposits are extensive and decipherable from their plateau morphology and are clearly visible along the right slope of the Rio Pardu and the Rio Quirra. The basal layers are primarily fluvial sediments of the Genna Selole Formation (Middle Jurassic) , which are overlain by dolomitic limestones of the Dorgali Formation (Middle–Upper Jurassic). (*Costamagna & Barca, 2004; Costamagna et al., 2018; Dieni et al., 1983; Pertusati et al., 2002*).

The Genna Selole Formation (Costamagna, 2015; Dieni et al., 1983) represents a mixed succession of siliciclastic to siliciclastic–carbonate deposits. The presence of clay layers is important as a predisposing factor for lateral spread. The Dorgali Formation is represented by dolomitic sequences with thicknesses of up to tens of meters. The lower part, with a thickness of approximately 30 m, is affected by marl intercalations, whereas the upper part is typically massive. The attitude of the strata of the Mesozoic units is sub-horizontal with a dip of approximately N90/0–5°, while at the plateau edges, it can reach a dip of up to 40° and a direction parallel to the slope owing to the DGSDs. Quaternary covers, which are represented by continental deposits, are primarily gravitative and alluvial deposits. The most extensive outcrops are represented by landslide deposits, including rockfalls, toppling, and collapsed DGSDs, and are abundant in the lower part on the right slopes of the Pardu Valley and Quirra Valley (eastern slope of Monte Arbu). Downslope, actual and terraced alluvial deposits have also been identified, and they are well developed and hierarchized in the Rio Quirra (*Petrusati 2002*).

The deposits of the rockfalls and toppling landslides have been characterized by their different sedimentological features based on age. These deposits are associated with rockfalls affecting the plateau edge wall and the collapse of some parts of the DGSDs (*Demurtas et al 2021*).

4.3 Geodynamic setting

The river networks' geometry and gravity processes show a young conformation of the landscape, which is typical of a recent tectonic setting. The geodynamic setting is associated with the collisional dynamics between the African and European plates (*Carminati & Doglioni, 2005*) (Figure 21). The structural setting is associated with the Alpine cycle, which first appeared with a strike-slip fault in the Oligo–Miocene, and then in the Pliocene and Quaternary with an extensional component

(*Carminati & Doglioni, 2005; Carmignani et al., 2001, 2016; Cherchi & Montadert, 1982; Gattaceca et al., 2007; Gueguen et al., 1997; Oggiano et al., 2009, Ulzega et al., 2002*).

The major features in the study area are the NW–SE and N–S faults on which, respectively, the Pardu Valley and Quirra River are engraved, and the secondary fault directions include ENE–WSW and NNE–SSW (*Pertusati et al., 2002*).

The Plio-Quaternary tectonic phase is associated with conspicuous N–S faults (*Casula et al., 2001*). These rectilinear and normal faults are also evident in the continental margin and control its morphology (Figure 22). In the continental region, these N–S faults are associated with alkaline basalts with an age of approximately 3.9 Ma—Pleistocene (*Lustrino et al., 2007*). Especially during the upper Pliocene, a general areal elevation occurred throughout the island, highlighted by the traces of the paleo-surfaces and by the numerous and superimposed paleo-hydrographies; moreover, the Neogenic sediments, which were already affected by Oligo-Miocene Tectonics, are currently also found at altitudes of 700 m, such as on the Tacco di Laconi, and are widely found above 500 m of altitude in various locations on the island. The reasons for these events are related to the more general distensive tectonics that affect the whole Tyrrhenian area (*Marini 1983*).

Based on preliminary geodetic data from the Peri-Tyrrhenian Geodetic Array network, Ferranti et al. (2008) revealed the presence of low internal deformation in Sardinia. In Sardinia, seismicity is typically scattered and sporadic, except for the dozen tremors detected following the ML4.7 earthquake of 7 July 2011 in the Corsican Sea, which primarily characterized the edges of the continental lithosphere block. Significant seismic events also occurred in the eastern sector—in particular, three events with a magnitude > 4 (26 April 2000, magnitudes ML 4.2 and 4.7, and 18 December 2004, magnitude ML 4.3)—located in the central Tyrrhenian Sea, approximately 60 km east of Olbia in the Comino depression (Cimini et al., 2016).The most recent low-magnitude earthquake events were ML 1.8 (Escalaplano, 4 April 2019) and ML 1.6 (Perdasdefogu, 14 October 2020) (*INGV, 2021*).

Along the Ogliastra coast, recent movements have acted by conditioning the trend of the hydrographic network and the morphological evolution. The basaltic plateau of the Teccu in Barisardo can be related to these movements along an N–S line.

The Sardinian continental margin started from around 9 Ma, following the opening of the Tyrrhenian Sea, which caused the thinning of the continental crust and the formation of tectonic depressions, which are now sites of deep intra-slope basins.

The continental margin off the Ogliastra is represented by the continental shelf, the continental slope, and the plain called the Ogliastra basin, which reaches the deepest point of the whole Sardinian

margin at 1750 m depth. The continental shelf is very narrow with less than 10 km of width, and it is indented by several submarine canyons (*Chiocci et al. 2021, Ulzega et al. 2002*).

4.4 Geomorphological setting

The landscape, which is characterized by sub-horizontal carbonate plateaus, represents the result of the paleogeographic evolution of the region. The current dolomitic plateaus represent the extensive carbonate sedimentation due to the Jurassic marine transgression on the peneplanated Paleozoic metamorphites during the Permian and the Triassic. The continental phase following the post-Mesozoic emergence determined the setting of a tectonic control hydrographic network represented by deep rectilinear valleys engraved in the Paleozoic basement for several hundreds of meters (*Maxia et al., 1973; Ulzega & Marini, 1973*) (Figure 24. Erosion primarily acted on the Oligo-Miocene strike-slip faults with an increase in the erosive rate during the Plio-Pleistocene uplift phases (*Marini & Ulzega, 1977*). The presence of major regional faults has influenced the watercourses, which maintain a prevalent N–S direction in the Pardu and Quirra Rivers (set on the main fault).

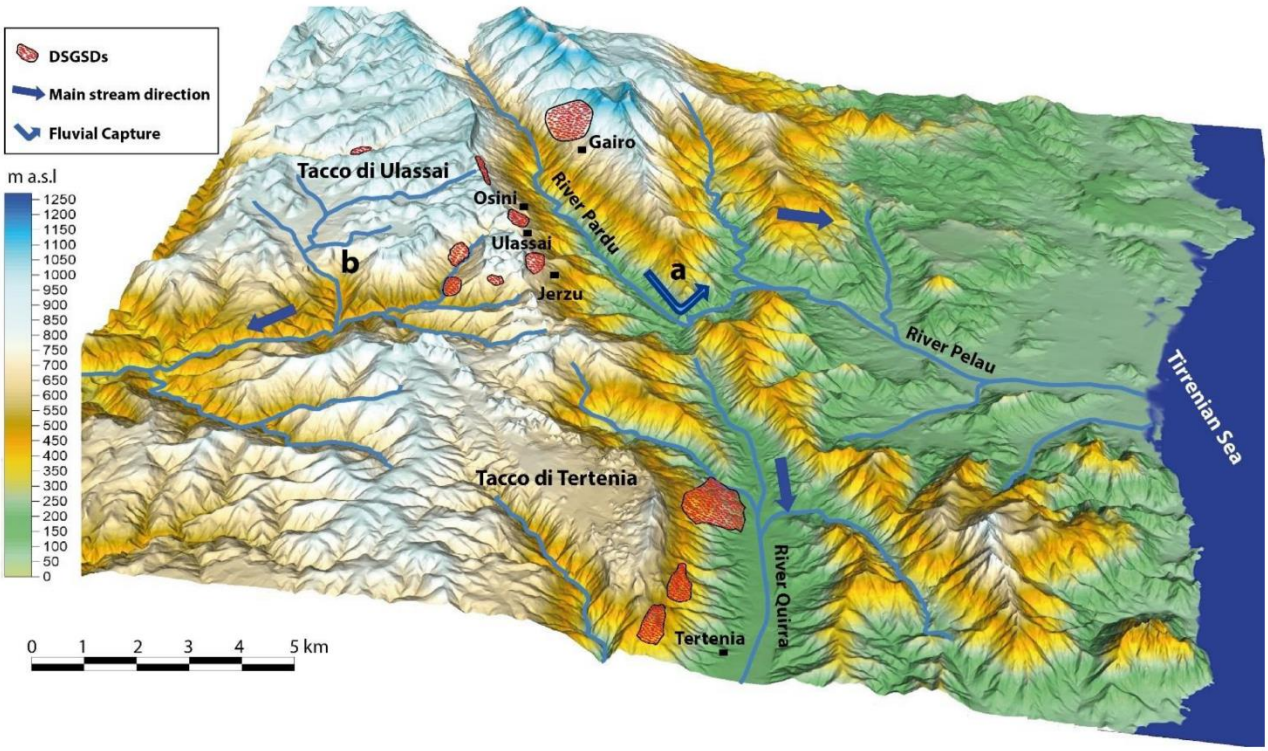

Figure 24 Three-dimensional (3D) model of the Pardu River and Quirra River. Blue lines represent major hydrographic features, and red areas represent the major DGSDs. (a) Fluvial capture elbow; (b) Lequarci waterfall.

The evolution of the Pardu River is closely associated with that of the Quirra River (*Palomba & Ulazega, 1984; Pertusati et al., 2002, De Waele 2012*). The Pardu River flows from the NW toward the SE and then abruptly changes direction toward the NE. At this point, a capture elbow adjacent to

the present head of the Quirra River is well developed. The upstream part of the Quirra River flows at an altitude of approximately 200 m higher than the Pardu River. It also presents an over-sized and over-flooded valley with respect to the upstream catchment area. Moreover, there are various orders of river terraces and slope deposits of the Pleistocene. This setting indicates that the Pardu River, previously flowing south along the Quirra River, was captured by the Pelau River (*De Waele et al., 2012; Palomba & Ulzega, 1984*). Considering the descriptive parameters, longitudinal profile, and the evolutionary conditions, the Pardu Valley is associated with a cycle of underdeveloped fluvial erosion, suggesting a relatively young age of engraving (*Marini & Ulzega, 1977; Maxia et al., 1973; Ulzega & Marini, 1973*).

DGSDs are present in both river basins and cause collateral landslides. In particular, rockfalls and toppling occur along carbonate cornices, while rotational slide occurs in the metamorphic rocks (*Demurtas et al 2021*). We focused on the DGSDs in this study, as they are important in the morphological evolution of the slopes.

A significant karstic process has acted on plateau surfaces, comprising ancient paleoforms and, currently, hypogeal and superficial morphologies (*De Waele et al., 2005, 2012, Demurtas et al. 2021*). Karst paleoforms represented by complex cockpit doline types have been characterized, and they belong in a humid and warm paleo-morphoclimatic setting (*Fleurant et al., 2008; Liang & Xu, 2014; Waltham, 2008*). These dolines are separated by residual reliefs called Fengcong, which are sorted among the major structural features. The hypogean karst enabled the development of sinkholes, karst springs, cavities, and caves (e.g., Su Marmuri Cave and Is lianas Cave). The combined action of karst, uplift, river erosion, and gravity has led to the formation and evolution of hanging valleys on the plateau surfaces (*Ulzega & Marini, 1973*). The geomorphological analysis of the continental margin off the coast shows that the area occupied by the shelf is rather narrow and is engraved with numerous submarine canyons (*Chiocci et al 2021, Gamberi et al 2021 ,Marani et al 2004*) (Figure 22). The structural lines coincide with those of the continental part that has emerged—mainly N–S, accompanied by normal tectonic lines in the E–W direction. The shelf break is about −130 m; however, locally, it is at about −60 m due to the erosion of retrogressive canyons. The submerged and emerged morphologies highlight the extremely young landscape conformation, which is associated with the Neogene and Quaternary geodynamic events, implying a series of problems related to the slope process. The control factors of the DGSDs are associated with the geo-structural characteristics and the Neogene and Quaternary geomorphological evolution of the river valley, which is associated with the recent uplift (*Demurtas et al. 2021*).

We can summarize the events that dominated the valleys' evolution (*Demurtas et al. 2021; Palomba et al. 1984; Maxia et al. 1973*):

- The first stage preceding the capture of the Rio Pardu by the Rio Pelau associated with the uplift and the Plio-Quaternary tectonics. This phase involves a general incision of the valleys and erosion of the slopes, and it led to a new hydrographic setting, causing river capture (Middle-Lower Pleistocene).
- The second phase was associated with major erosive activity in the Pardu Valley following the capture, which led to complete erosion of the valley (Upper Pleistocene).
- The present evolution of the slopes through widespread landslides and DGSDs.

4.5 Materials and methods

A morphotectonic analysis of the River Pardu and River Quirra was carried out based on an integrated approach that incorporated a cartographic and morphometric analysis (*ISPRA e AIGEO 2018, Miccadei E. et al. 2018; Carabella et al. 2020; Miccadei et al. 2021*). Remote sensing analysis and geological and geomorphological field mapping in slopes and the valley floor of the Rio Quirra and Rio Pardu were performed from the head to the mouth on a scale of 1:10,000. The field surveys were based on the interpretation of data from remote sensing on a large scale. Particular attention was paid to the study of morphologies related to river dynamics (fluvial and orographic terraces) and slope gravitational process (DGSDs and collateral landslides).

Multi-scale field surveys were carried out to analyze the geological and structural setting of the slopes in particular, the plateaus' edges and the left slope of the Pardu Valley (*Guzzetti et al. 1999, Dragićević et al. 2015, Shi et al. 2018 , Deiana et. al 2019, Melis et al. 2020*).

The DGSDs were surveyed in detail by reconstructing the structural setting and analyzing the relationships with the surrounding collateral landslide and alluvial deposits. The study areas were often not accessible due to their steep slopes; therefore, they required remote sensing survey systems to complete the field investigations. Uncrewed aerial vehicle digital photogrammetry (UAV-DP) is a robust methodology for the investigation of DGSDs and large landslides. In particular, it was used for the recognition of large lateral spreads in Malta and Tunisia (*Devoto et al. 2020, Gaidi et al. 2021*). We used UAV-DF and light detection and ranging (LiDAR) to extract high-resolution topographic 3D DGSD models and perform detailed morphometric analyses.

DGSD displacement and rate were evaluated using space-borne interferometric synthetic aperture radar (InSAR). Over the last 30 years, InSAR techniques have been widely used to investigate geological (e.g., volcano activity, earthquakes' ground effects, etc.) and geomorphological processes in particular, DGSD. In different geological and climatic contexts, this technique allows one to analyze extremely slow DGSDs and to identify displacements of about 1–2 mm in favorable

conditions (*Devoto et al 2020, Gaidi et al 2021,Delgado et al 211, Oliviera et al 2015Crosetto et al 2016, Mantovani et al 2016, Frattini et al 2018, Novellino et al 2021, Eker et al 2021*).

Based on previous studies on the fluvial deposits of Rio Quirra and Rio Pardu (*Ulzega 1973, Palomba 1984, Demurtas et al. 2021*), the geological analysis was implemented by using high-resolution topographies based on UAV-DP and LiDAR. Detail-scale field surveys were carried out in the alluvial quaternary deposits with the aim of the identification and mapping of various terraced orders and the reconstruction of the relative chronology among morphostratigraphy and sedimentological indicators. Stratigraphic profiles relating to the various orders of river terraces and landslide deposits were surveyed in the natural outcrops of the alluvial plains.

4.5.1 Aerial and Uncrewed Aerial Vehicle Remote Sensing

LiDAR and aerial photogrammetric data produced by the Autonomous Region of Sardinia were used to perform visual and morphometric analysis of DGSDs and fluvial morphologies. A detailed orthophoto dating from 2016 was used together with LiDAR data with a cell size of 1 × 1 m and vertical resolution of 30 cm.

The aerial surveys were performed using UAVs (DJI Phantom 4 and DJI Matrix 200) flying at altitudes of 50–60 m above ground level. The acquired images were analyzed and processed using the photogrammetric Agisoft MetaShape software and constrained by 10–12 ground control points using GEODETIC LEICA GNSS for each area. The resulting orthorectified mosaic and DEM (WGS 84 datum and UTM 32N projection) had a cell size of 5 cm/pixel and were considered sufficiently precise to be used for the geomorphological analysis.

To analyze the DGSDs at the local scale, we used high-resolution digital elevation models (DEMs) acquired via structure from motion from a UAV-DF (*Clapuyt et al., 2016; Eker & Aydın, 2021; Peternal et al., 2017; Valkaniotis et al., 2018*).

The 3D high-resolution UAV-DF models were used to develop interpretative superficial models by using geomorphological evidence and stratigraphic and structural data of the DGSDs. Geological interpretative cross-sections of geologic features crossing the major DGSDs were also generated to define the movement kinematics, deformative style, and deep geometries of the DGSDs.

The DTMs were used to analyze the morphometric parameters of the hydrographic basins under analysis. The longitudinal and transversal profiles of the valleys were extracted in such a way as to highlight different erosive structures in relation to river capture and to analyze the different altitudes of the various river terraces.

4.5.2 InSAR Analysis

Space-borne interferometric synthetic aperture radar (InSAR) data were used to analyze the slope deformation (*Ietto et al. 2015, Mateos et al. 2018, Moretto et al. 2021,Mondini et al. 2021*). Interferometric permanent scatters (PSs) are used to investigate the temporal and spatial superficial slope deformation. To detect ground displacement, we used only high-PS coherence (0.6–1) located on built dolomitic blocks and the metamorphic rock outcrops. Low-coherence PSs, which are not useful, are located on rockfall deposits and in vegetated areas. We used the Sentinel-1 and European Remote Sensing (ERS) satellites (Table 1) and took into account the line-of-sight (LOS) velocities. We used a dataset from 1992 to 2000 from the ERS satellite and a dataset from 2014 to 2020 from Sentinel 1. The processed data from ERS and Sentinel 1 were provided, respectively, by Ministero dell'Ambiente e della Tutela del Territorio e del Mare (Italy) and the Geological Survey of Norway. The total area analyzed covered the entire Pardu Valley and Quirra Valley. Four focus areas (Table 1) that showed interesting results were analyzed by using time series of PSs to understand the landslides' temporal evolution.

Table 1 Parameters of the InSAR data on the sectors in focus.

Area	Satellite	Acquisition Geometry	Acquisition Interval	TrackAngle	Inc Angle
Ulassai	Sentinel 1	Ascending	Oct 2014–Feb 2020	−9.6	42.4
Osini	Sentinel 1	Ascending	Oct 2014–Feb 2020	−9.6	42.4
San Giorgio	Sentinel 1	Ascending	Oct 2014–Feb 2020	−9.6	42.4
Gairo	Sentinel 1 ERS	Descending	Oct 2014–Feb 2020May 1992–Dec 2000	−169.6 - - - - -	36.3 - - - - -

4.6 Results

4.6.1 InSAR, PS, and Time Series Analysis

The results of the large-scale InSAR analysis showed that most PSs were located in stable areas, while high deformation rates were recorded in the slopes of Pardu Valley, where slope-failure processes in particular, rockfalls and DGSDs were widespread. All four focus areas were analyzed in detail with the Sentinel 1 data (from 2014 to 2020). For the left flank of Rio Pardu, the ERS data (from 1992 to 2000) were also used in descending order of acquisition. The data from the periods 1992–2000 and 2014–2020 indicated areas with large slopes that were identified as DGSDs that were active in Pardu Valley. We used only PSs with high coherence (0.6–1) that were located in the rocky outcrops and in the urban structures, while low-coherence points located in rockfall deposits and in vegetated areas were not considered. The PS analysis allowed the recognition of active DGSDs and the measurement of their movement rates, which turned out to be extremely slow, ranging from 6 to 20 mm/year (Figure 25 and Figure 26. We identified a downslope movement of up to 1 cm/y in the right slope of the Pardu

Valley and a movement of up to 2 cm/y in the left slope. Continuous movements that did not change over years with both linear and seasonal trends were observed. The InSAR analysis showed no perceptible movements on the slopes of Rio Quirra.

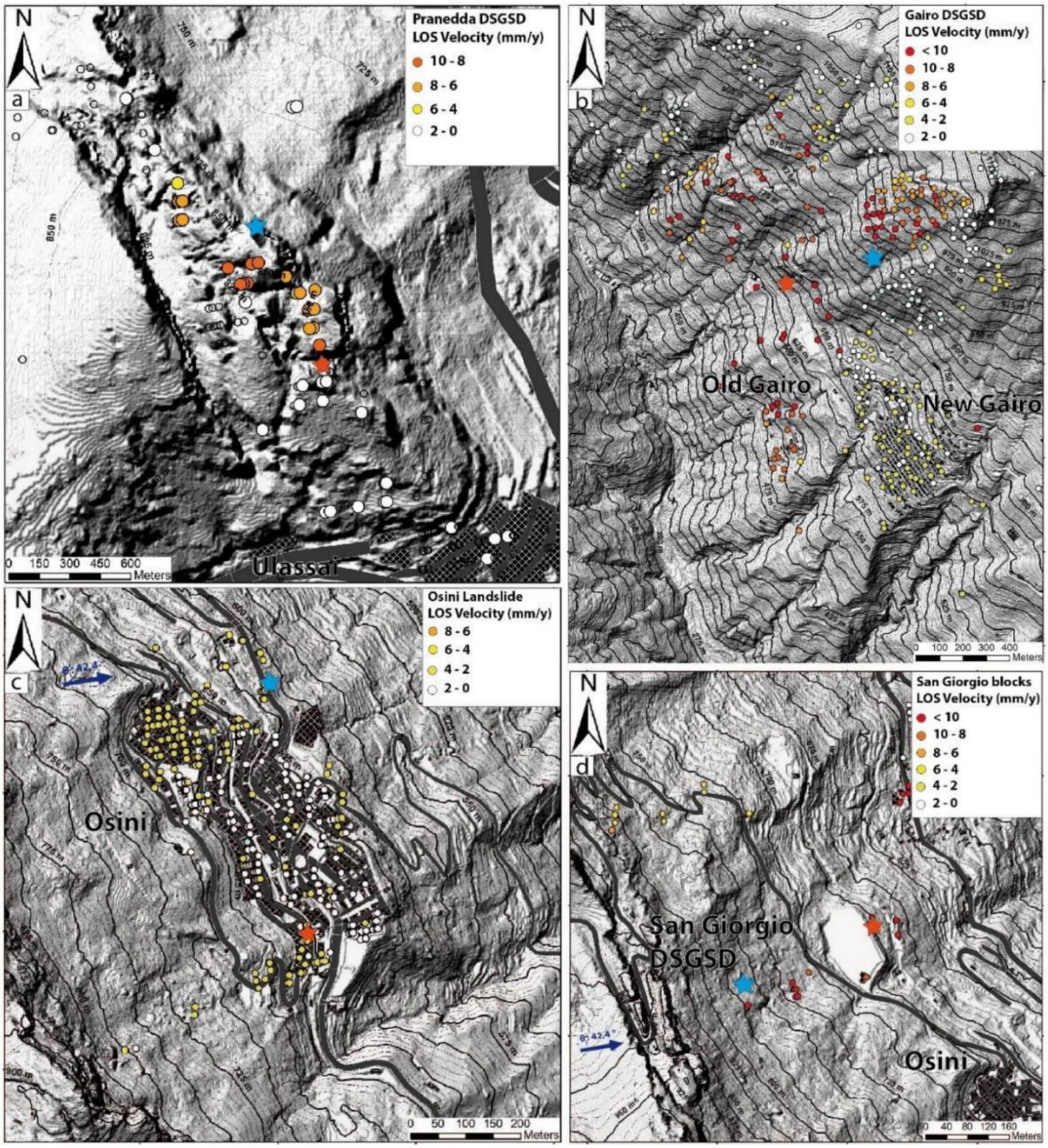

Figure 25 - Analysis of the focus areas with InSAR data. The points represent high-coherence permanent scatters located on buildings, rocky outcrops, and blocks of large rock avalanches. The stars represent the PSs used to analyze the time series shown in 26. (a) Bruncu Pranedda lateral spread. (b) Gairo DGSD. (c) Osini landslide. (d) San Giorgio paleo-rock avalanche.

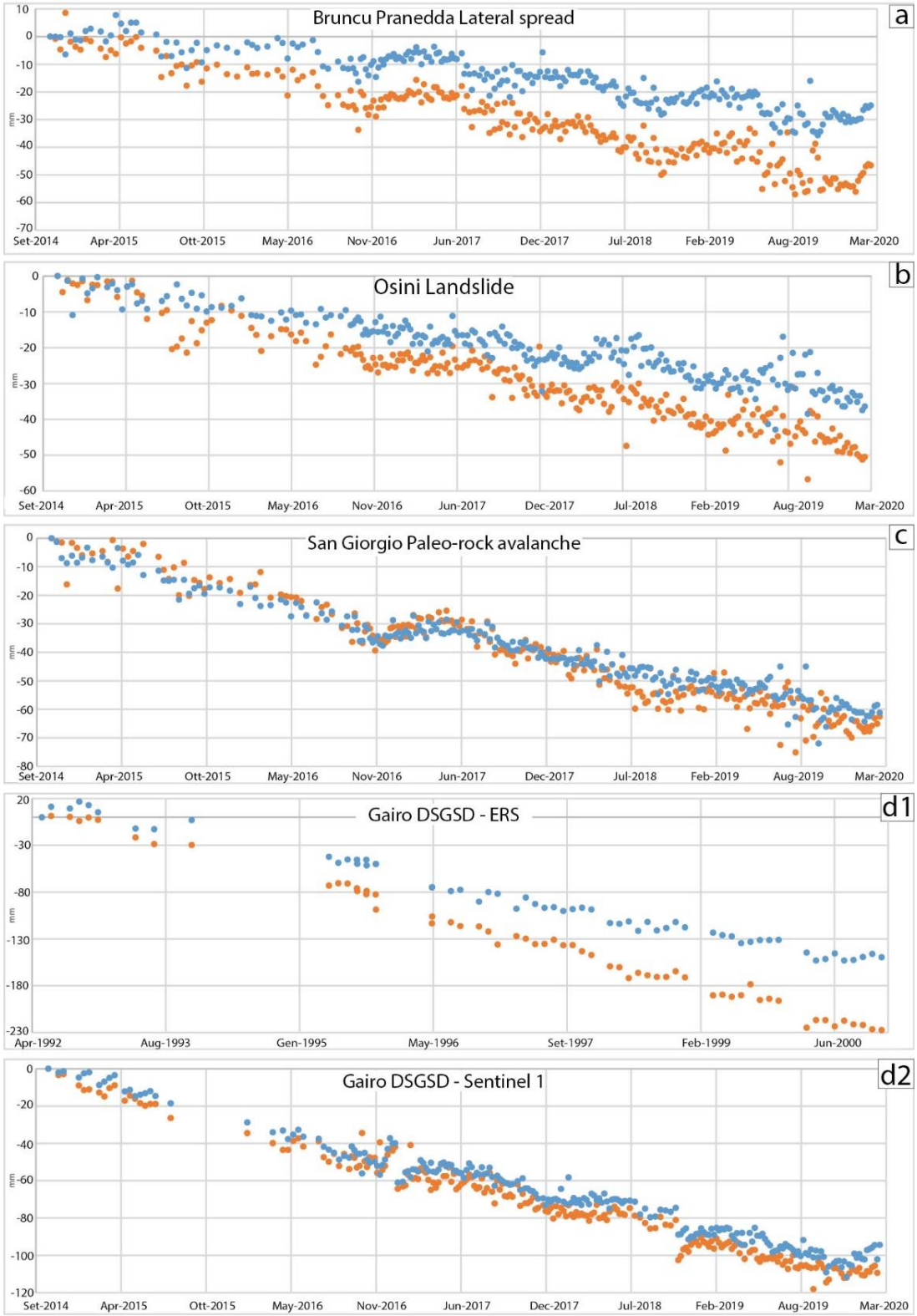

Figure 26 Time series extracted with the representative permanent scatters. The vertical axes represent the cumulative LOS displacement; the horizontal axes represent the time. (a) Bruncu Pranedda lateral spread—seasonal displacement trend, maximum displacement of 5 cm from 2014 to 2020; (b) Osini landslide—seasonal displacement trend, maximum displacement of 6 cm from 2014 to 2020; (c) San Giorgio paleo-rock avalanche—constant movement trend of the large blocks, maximum displacement of 6 cm from 2014 to 2020; (d) Gairo DGSD; (d1) the ERS data show a constant deformation trend, with a maximum displacement o f23 cm from 1992 to 2000; (d2) the Sentinel 1 data show a constant deformation trend that is correlated with the ERS data, with a maximum displacement of 10 cm from 2014 to 2020. The colors of the points agree with the colors of the stars that identifies the location of the PS in Figure 27.

In the Ulassai area, the PS analyses showed a stable surface in the urban area and on the west slope of the main extensional trench of Pranedda Canyon (Figure 25a and Figure 26a). However, in accordance with the geomorphological evidence, downstream from the main trench, the speeds of the PSs showed LOS displacements of up to 1 mm/y. In this sector, the PSs were located in rocky dolomitic outcrops on the top edge of the plateau, in the total absence of vegetation and in excellent exposure conditions. No movements were detected in the DGSD downstream from Bruncu Pranedda due to the low PS coherence due to dense vegetation. Using Sentinel data from 2014 to 2020, we measured a total of 5 cm (orange star in Figure 25). It was possible to observe seasonal deformation trends with an excellent correlation among all of the PSs analyzed. Generally, no movement was observed during the winter and spring, but an acceleration was observed during the summer and autumn.

In Osini, a cluster of PSs were well defined within the inhabited center, particularly in the northwest and southeast sectors, where there was a speed of between 4 and 6 mm/y, with a maximum of 8 mm/y (Figure 25c and Figure 26b) with a seasonal trend. Spotlights were located on the roofs of the buildings. In the surroundings of the inhabited center, the dense vegetation resulted in a low coherence of the PSs; therefore, they were not considered.

In the Gairo sector, the InSAR data showed a large area that was greater than 1 km2 with a high diffusion of PSs. Based on the high-resolution field surveys, the PSs are located on rocky metamorphic outcrops. The speeds were, on average, greater than 8 mm/y, with a maximum of 2 cm/y. The cluster identified a well-defined area with a circular shape that was delimited by PSs with zero or negligible speed (Figure 25b and Figure 26 d1,d2). The higher speeds were located in the central and basal part of the DGSD, while towards the top and lateral flanks, the speeds decreased. In the lateral and top parts, the DGSD was delimited by stable PSs (speeds of 0–2 mm/y), which allowed the deformed area to be circumscribed in detail. in the PSs on the foot slope with a low coherence due to the continuous movement of slope deposits and the vegetation were not considered. The deformation's progression was continuous and linear, and an excellent correlation was found between the Sentinel 1 and ERS data. In the southern part of the DGSD, a high concentration of PSs were located in the abandoned village of Old Gairo with speeds that were sometimes greater than 1 cm/y. The town of New Gairo, which was built after the 1951 catastrophe, showed displacements limited to 2–4 mm/y.

In the San Giorgio sector, scattered PSs were identified with speeds greater than 10 mm/y on the large blocks of the rock avalanche on the slope (Figure 25d and Figure 26c). These blocks, with dimensions of up to 30 m per side, were collateral landslides related to the collapsed DGSD located at the edge of the plateau above. All of the PSs showed a linear trend with a slowdown in the winter and spring

between 2016 and 2017. This slowdown, which was observed in all of the PSs, indicates that the causes of the movement are to be found in processes that involve a greater portion of the slope, and not only in the large blocks. The surrounding area did not allow a PS analysis due to the importance of the wooded vegetation, but evidence of deformation was visible in the road infrastructure.

4.6.2 Deep-Seated Gravitational Slope Deformation

Various areas affected by DGSDs and landslides that were located of the slopes of Pardu Valley and on the slope of Monte Arbu of Tertenia were identified (Table 2).

Table 2 Main characteristics of the DGSDs and landslides analyzed.

Location	Landslide	Geology	Landslide Kinematic	Displacement Speed mm/y	Displacement Trend	Area Km^2
North Ulassai	Bruncu Pranedda Lateral spread	Dolomitic limestone set on altered and fractured phillites	Lateral spread top slope; sackung middle slope	6–10 mm/y	Seasonal	0.2
South Ulassai	Monte Tisiddu Sackung	Dolomitic limestone set on altered and fractured phillites	Sackung	No movement	------	0.2
North Osini (San Giorgio)	San Giorgio Lateral spread	Dolomitic limestone set on altered and fractured phillites	Lateral spread	No movement	------	0.03
North Osini	San Giorgio paleo-rock avalanche	Megablock rock avalanche deposits set on paleo-rockfalls	Sliding	6–>10	Linear	≈0.1
Osini	Osini Landslide	Cemented paleo-rockfalls set on phillites	Sliding	4–8	Seasonal	≈0.3
Gairo	Gairo DGSD	Phillites on metavolcanites. Slope involved in Hercinical thrust	Sackung	6–20	Linear	1.2
South Tertenia	Tertenia DGSD	Dolomitic limestone set on altered and fractured phillites. Slope involved in Hercinical thrust	Sackung	No movement	------	1.5
North Tertenia	Paleo-DGSD	Dolomitic limestone set on altered and fractured phillites	Sackung	No movement Fossilized by Pleistocenic alluvium	------	1.5

On the east side of Tacco di Ulassai and Tisiddu Mountain, three DGSDs were analyzed (Figure 27). The main structures that indicated deep gravitational phenomena were large and deep extensional trenches that were evident in the dolomitic lithotypes. The extensional trenches had lengths of several hundreds of meters and a decametric opening and depth. This slope was characterized by the Mesozoic marine deposits resting on the Paleozoic metamorphites.

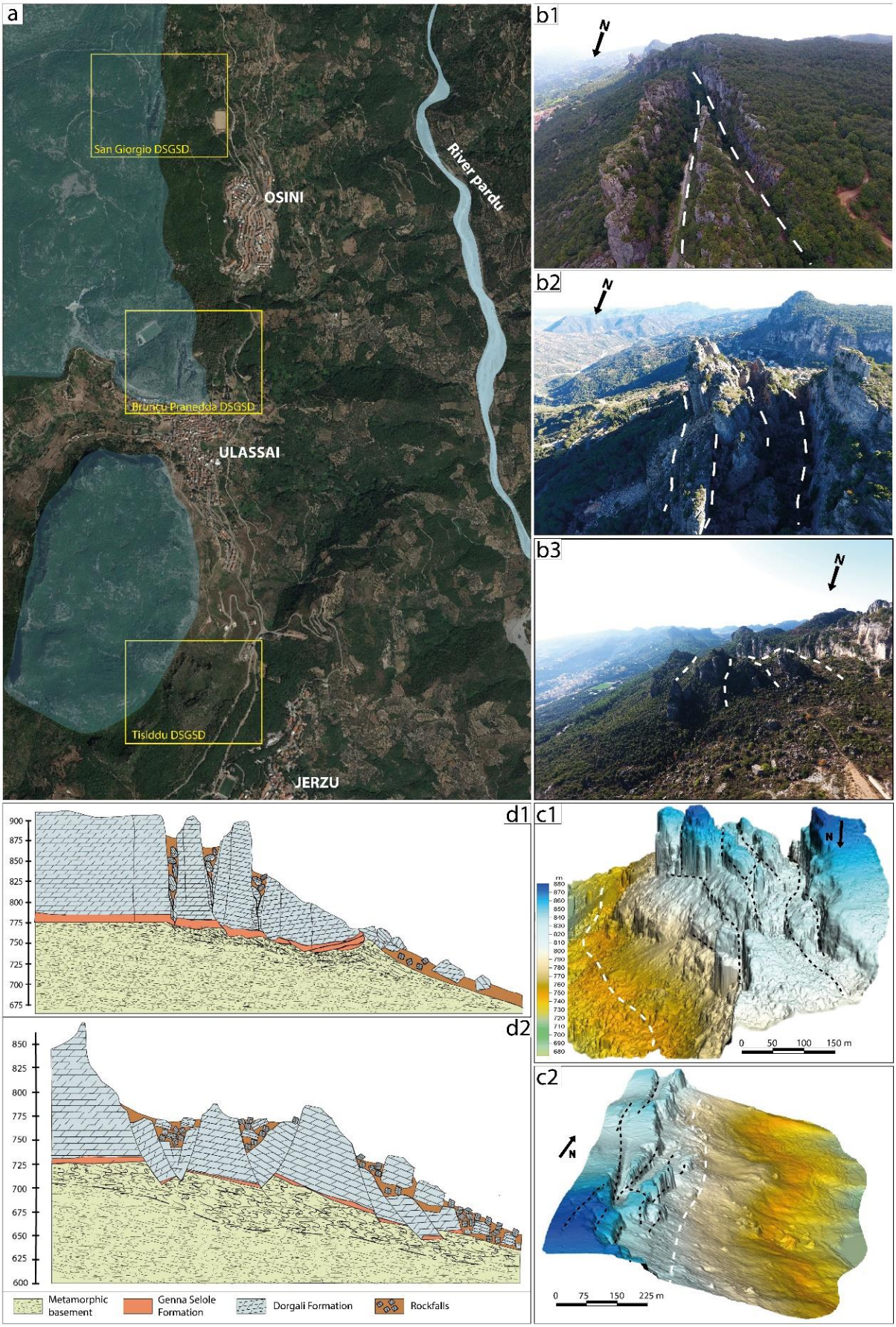

Figure 27 DGSD on the right slope of the Pardu River. (a) Orthophoto of the area of Ulassai, Osini, and Jerzu. The Jurassic dolostone plateaus on the metamorphic basement are shown in blue. The yellow square represents the analyzed

DGSD. (b) UAV images of the DGSD showing the major geomorphological and structural features. The white dashed lines represent the major extensional trenches. (b1) San Giorgio lateral spread, (b2) Bruncu Pranedda lateral spread, (b3) Monte Tisiddu sackung. (c) Three-dimensional LiDAR model of the DGSDs with a colored elevation scale. The black dashed lines represent the major extensional trenches. The white dashed lines represent the major stratigraphic discontinuity between the marine Mesozoic sequence and the metamorphic basement. (c1) Bruncu Pranedda lateral spread. (c2) San Giorgio lateral spread. (d) Interpretative geological cross-sections passing through the DGSD in the study area. The hypothetical basal shear zone is highlighted with black dotted lines. (d1) San Giorgio lateral spread. (d2) Monte Tisiddu sackung.

The Bruncu Pranedda DGSD (Figure 27b2,c1) is constituted by two regions with different settings located on the top and middle slopes. On the top slope, toward the east of the largest extensional trenches in the area called the Pranedda Canyon, the rock mass fracturing increased, and the attitude of the Dorgali Formation was toward the east, with a dip of up to 40°. In this area, both facies of the Dorgali Formation were visible, with the summit comprising dolomitic banks and the lower part being characterized by an alternation of well-stratified dolomites and marls. This subdivision was not observed in the middle slope, where basal marly levels did not appear on the surface. This indicates that the basal facies (approximately 30 m) were partially covered by slope deposits; however, they also sank a few meters inside the fractured and altered Paleozoic metamorphic basement. This could be correlated with the field observations at the same altitude, as well as with the basement and the massive facies of the Dorgali Formation (*Demurtas et al. 2021*).

The Scala San Giorgio DGSD (Figure 27b1,c2,d1) is located north of Osini Village and is characterized by two major extensional trenches that are parallel to the slope affecting the Dorgali Formation with a dip amount of up to 20°. All of the sequences of the Dorgali Formation are exposed; however, the Genna Selole Formation is covered by rockfall deposits.

The Tisiddu Mountain DGSD (Figure 27b3,d2) to the south of Ulassai Village is characterized by a highly fractured segment of the Dorgali Formation located tens of meters downstream. Only the tops of the massive banks of dolostones are visible. The basal level partially sank into the metamorphic basement.

In all cases, the shear zones are located in different geological units that represent structural weaknesses (Figure 27d1,d2). (I) The top of the metamorphites was affected by sub-horizontal foliation and advanced weathering, which was highlighted by the reddish or whitish color of the rocks. This type of alteration could be linked to the pre-transgressive Mesozoic period (*Marini C. 1984*). (II) The Genna Selole Formation was characterized by plastic clay layers; (III) basal levels of the Dorgali Formation were characterized by the alternation of marl and dolomite.

A large landslide that affected the town of Osini and the northernmost slope downstream of the San Giorgio DGSD was identified by using InSAR data. The inhabited center of Osini is built over an extensive cemented paleo-rockfall deposit that rests on the Paleozoic basement. Geomorphological evidence is difficult to observe due to the extensive vegetation around the village.

The left side of the Rio Pardu is characterized by a different geological and structural context compared to the opposite side (Figure 28a). There are metamorphic lithologies belonging to the formation of Monte Santa Vittoria and the Filladi del Gennargentu. The slope is affected by a dip-slope Hercynian thrust that brings the two formations belonging to two different tectonic units into contact. This structure plays a fundamental role in the deep gravitational processes, as it is marked by intense fracturing and alteration of the lithotypes. Based on the geomorphological evidence and the analysis of the InSAR data, a large landslide with a DGSD character was identified in the northwest sector with respect to the town of Gairo (Figure 28b–f). The DGSD extends from the top slope to the middle-lower part of the slope and is about 1 km wide. The crown is circular (Figure 28c,d) and joins laterally rectilinear structural flanks (Figure 28e). Analyzing the profile of the slope along the DGSD, the concave upstream part and the convex downstream part are clearly evident. The foot of the landslide is covered by landslide and slope deposits that reach the valley floor, where lateral erosion by the Rio Pardu is affected.

On the right side of the Rio Quirra, in correspondence with the Tacco di Tertenia, complex gravitational morphologies linked to paleo-DGSDs are evident (Figure 29). The morphology of Mount Arbu is also affected by the complex tectonic structure, which is characterized by a sub-horizontal thrust that brings the Pyllades del Gennargentu Formation into contact with the Metavolcanites of the Monte Santa Vittoria Formation (Figure 29a). The morphological analysis of the slope shows convexity and concavity linked to different DGSDs that are distributed at various altitudes of the slope. The DGSDs consist of portions of the Dorgali Formation, which is tilted up to 30–40° and is translated along the slope. The most complex and evolved movement was identified in the NE sector (Figure 29b,c1,c2). The area extends for a length of about 1800 m from the top of the plateau to the valley floor. The fan-shaped landslide body has a foot with a length of 2 km. The crown is located in the plateau edge, which is affected by faults and distension trenches. The latter delimit mega-blocks of the Dorgali Formation With a prismatic shape and inclination of up to 40°. The foot of the DGSD, which is represented by the Dorgali Formation, is marked by dolomitic outcrops with vertical heights of up to 40 m with sometimes sub-horizontal attitudes of the strata. On these walls, terraced alluvial deposits rest in onlap. Paleo-DGSDs are widespread in the upper part of the slope, with greater diffusion in the southern part of Mount Arbu, but they do not evolve until reaching the valley floor (Figure 29b,d).

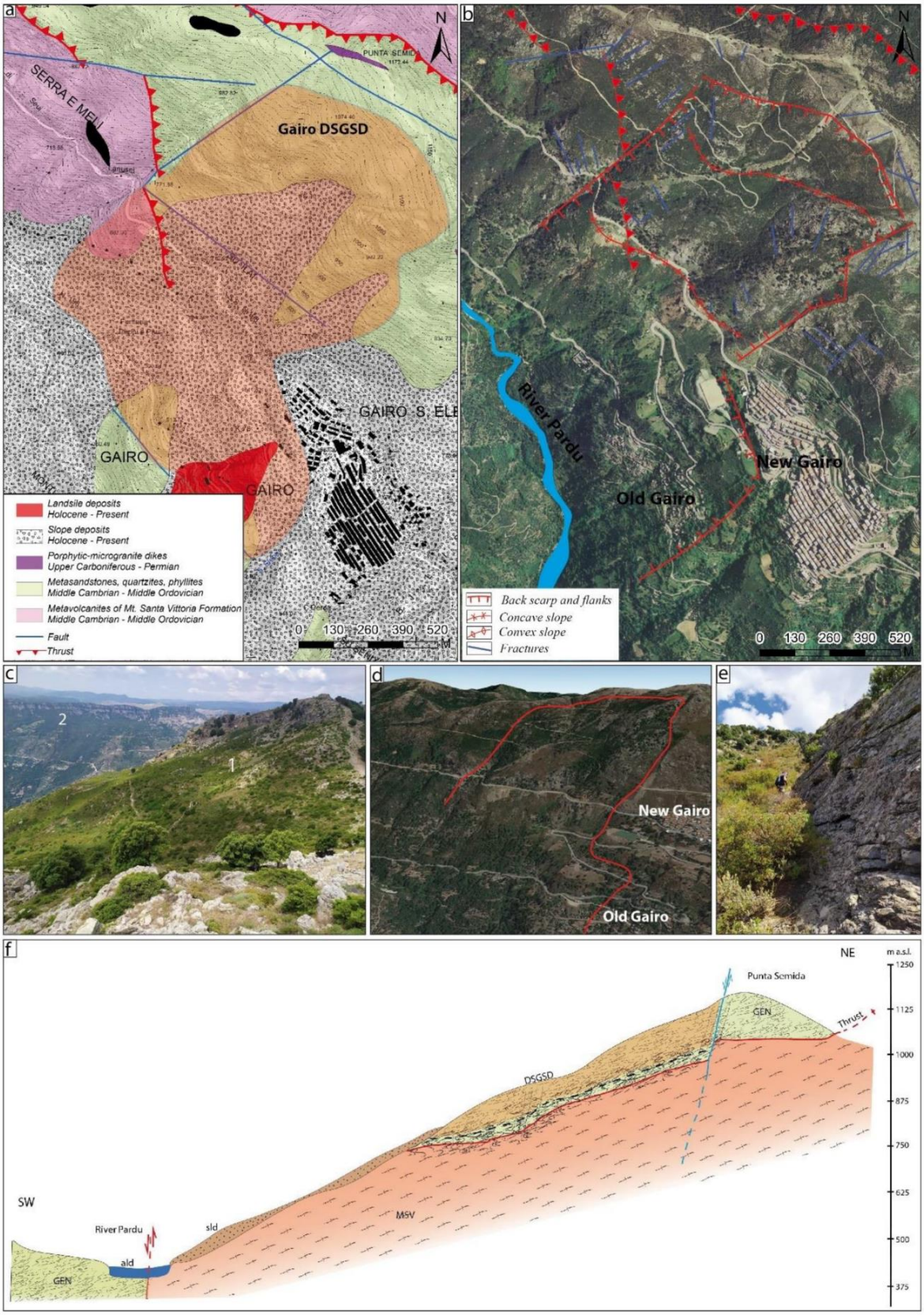

Figure 28 (a) Geological map of the Gairo slope with the DGSD localization. (b) Orthophoto with the main geomorphological feature of the DGSD. (c) Photo of the DGSD head. (1) Crown; (2) right slope of the Pardu River; (d) photo showing a 3D view with the DGSD border marked in red; (e) linear flank of the DGSD; (f) interpretative geological cross-section of the DGSD showing it (in transparent orange) sliding on the highly fractured rock due the underlying dip-slope Paleozoic thrust. Geolithological legend: MSV—Monte Santa Vittoria Formation; GEN—Filladi del Gennargentu Formation; ald—current alluvial deposits; sld—slope deposits.

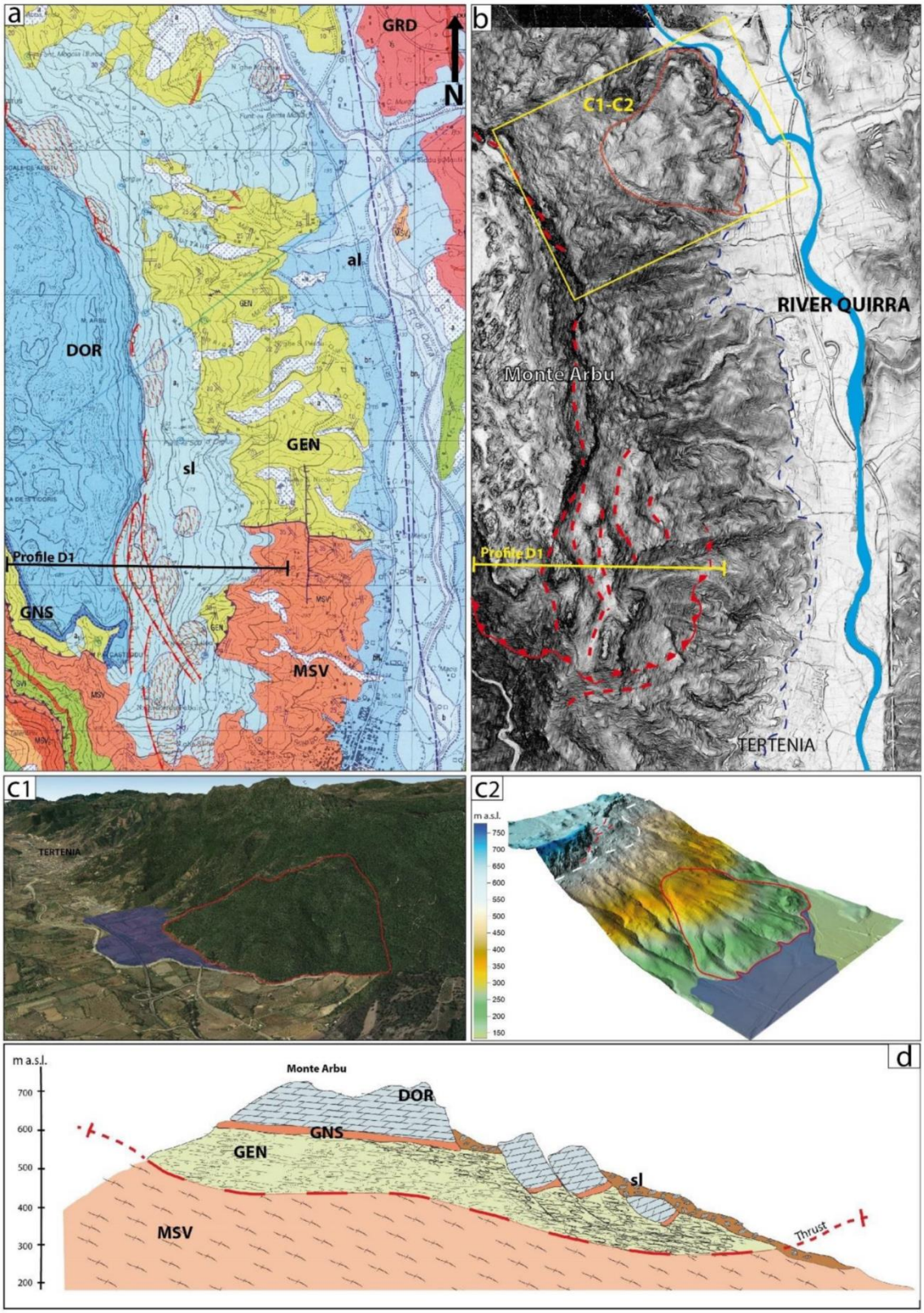

Figure 29 - (a) Geological map of the eastern slope of Monte Arbu (Tertenia). Geolithological legend: MSV—Monte Santa Vittoria Formation; GEN—Filladi Del Gennargentu Formation; GNS—Genna Selole Formation; DOR—Dorgali Formation; al—terraced and current alluvial deposits; sl—slope deposits. (Pertusati et al 2002). (b) LiDAR hillshade with the main geomorphological feature of the DGSD. (c1) Photographic 3D view with the DGSD border marked in red and the terraced alluvial deposit in blue. (c2) Three-dimensional LiDAR of the Tertenia paleo-DGSD with the border marked in red and the terraced alluvial deposit in blue. (d) Interpretative geological cross-section of the DGSD showing it sliding on highly fractured rock due the underlying Paleozoic thrust.

4.6.3 River Capture Analysis

The area has a deep cut made by the Rio Pardu Valley and Rio Quirra Valley, which extend in an NNW–SSE direction, following a major Tertiary fault. For most of the Pardu River's course, the talweg is set on rock, indicating its predominantly erosive nature. Downstream, the river is captured, turning in an eastward direction, and its name changes to Rio Pelau; then, it flows into the Tyrrhenian Sea. South of the capture, the abandoned Rio Pardu Valley continues southward as Rio Quirra. This valley is characterized by a bottom filled with Pleistocene and Holocene terraced alluvial deposits and slope deposits, which are currently undergoing erosion. It is clear that in the past, Rio Pardu was captured by Rio Pelau (Figure 30), causing a rapid incision upstream. Longitudinal profiles were constructed for Rio Pardu, Rio Quirra, and Rio Pelau. Rio Pardu flows up to 750 m below the dolostone near Ulassai, where the main active DGSDs are located. The evolutionary hypotheses are related to the Pliocene and Quaternary uplift, which led to an important erosive phase.

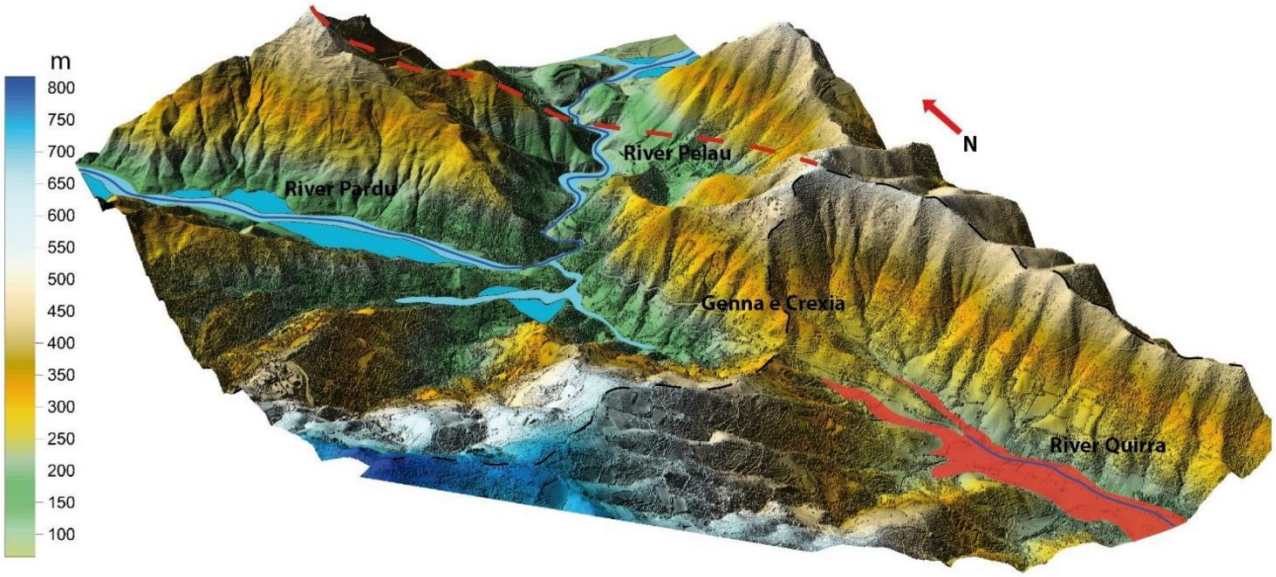

Figure 30 - Three-dimensional LiDAR model of the river capture sector. In the north, the Pardu River flows eastwards, taking the name of Rio Pelau. The blue and light blue show the Holocene alluvial deposit of the Pardu River. South of Genna and Crexia is the head of the Rio Quirra. In red is shown the paleo-slope and paleo-alluvial deposits of the Quirra River.

The triggering process can be justified in the following ways:

- An erosive increase caused by a generalized uplift that led to the retreat towards the inland by the head of the Rio Pelau until it connected with the Rio Pardu.
- Another hypothesis foresees the presence of a direct fault with an east–west course along which the Rio Pelau is set. In this case, the differential uplift of the block on which the Rio Quirra is currently set could justify the capture process as tectonogenic.

4.6.4 Fluvial Morphostratigraphic Analysis

A morphostratigraphic analysis was performed first on Rio Quirra and later on Rio Pardu, which isolated it following the capture (Table 3).

Table 3 Morphostratigraphic synthesis.

Deposits	Characteristic	Elevation from Talweg	Distribution
T0	Pebbles and clastosustained gravels with a scarce sandy matrix	0	Actual embrided riverbed
T1	Heterometric and polygenic pebbles with a scarce dark matrix	0.20/0.30–1.5	Pardu-Quirra
T2	The matrix is decidedly prevalent in the coarse fraction	2–5/6	Quirra
T3	Non-constant matrix–skeleton relationship. Reddish matrix (Fe oxides)	6/7–10	Quirra
Paleo-conoid C1	Clastosustained pebbles up to 40–50 cm in size. Scarce matrix	30	Pardu
Paleo-conoid C2	Reddish pebbles and gravels in sandy, silty, reddish matrix	15	Quirra
Paleo-slope deposits		20–40	Quirra

In the valley of the Rio Quirra, above the current riverbed, the following were identified (Figure 31):
T0—Actual flood surface consisting of pebbles and clastosustained gravels with a scarce sandy matrix (Holocene).
T1—Sub-current Holocene terrace with a maximum height on the riverbed of about 20–30 cm up to 1.5–2 m. The dark brown matrix is subordinate to the coarse fraction, which is represented by heterometric and polygenic pebbles. This terrace often forms alluvial islands in the upstream part of the river; they reach a good stability due to the dense vegetation that has settled there (Upper Pleistocene–Holocene).
T2—In this terrace, the matrix, which is decidedly prevalent in the coarse fraction, has a dark brown color. There is no evidence of prolonged chemical alterations due to climatic conditions other than the current ones. The pebbles are less varied: mainly quartz with, subordinately, granite and schistose. On average, the height of T1 with respect to the riverbed is about 2 m, with a maximum of 5–6 m and a minimum of 50 cm. The deposits that form this terrace show forms of erosion linked to secondary climatic pulsations (Upper Pleistocene).
T3—This is the oldest terrace, with an average height of 6–7 m and a maximum of 10 m (Figure 31c). The matrix–skeleton relationship is not constant. The depository is made up of alternations of fine and large sediments that testify to the variations in the river's energy.

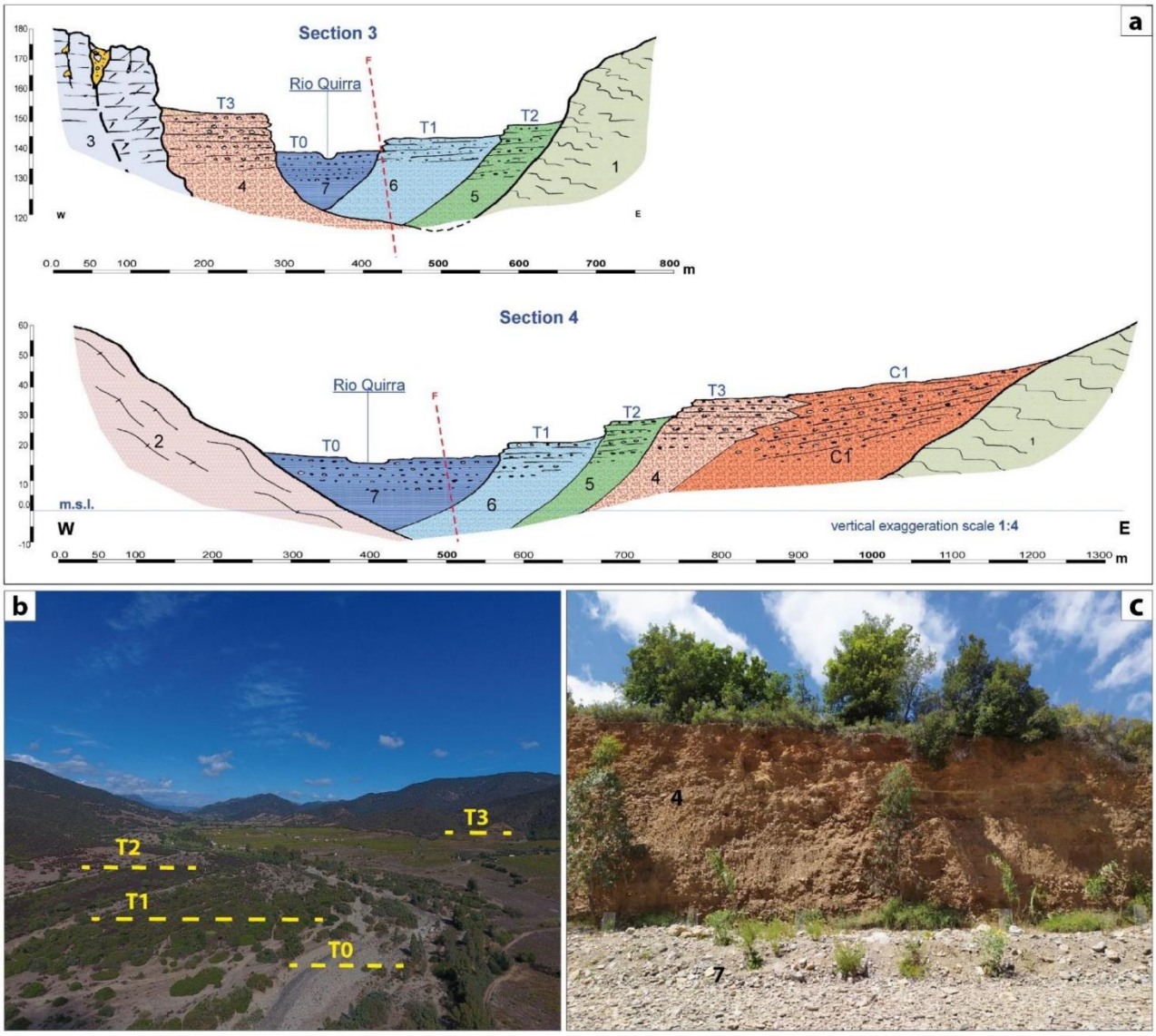

Figure 31 - (a) Morphostratigraphic profiles of the Quirra River. (b) UAV photo in the river alluvial plain. (c) Outcrop of Terrace T3. Lithological legend: (1) Filladi Grigie del Gennargentu Formation; (2) Monte Santa Vittoria Formation; (3) paleo-DGSD; (C1) paleo-conoid; (4) T3; (5) T2; (6) T1; (7) T0.

The matrix is red and sometimes whitish. In the first case, the color derives from Fe oxides, indicating a warm, humid climate typical of tropical and sub-tropical regions; in the second case, the oxides have been leached and for an eluviation horizon. The pebbly fraction does not have a varied lithological composition. It is mainly schistose and, subordinately, quartz. The deposit is well cemented. This terrace rests directly on the slope. The frame of erosion along the riverbed is clear, and the lower terraces rest on it (Middle Pleistocene).

In Rio Pardu, the alluvial deposits cover a valley floor characterized by a well-defined flood bed, which is limited by banks that are intensely affected by landslides. Two orders of alluvial terraces up to 2 m above the current level were detected (Figure 32). The maturity of the flood clasts is very low due to the continuous supply of material from the slopes, while the grain size distribution along the

longitudinal profile reflects the trend characterized by the high slope. By analyzing the longitudinal profile of the Rio Pardu, it can be observed that it is divided into two well-defined parts separated by the knickpoint in Ponti Mannu. In the initial part, near the steeply sloping trunk, there is the head of the valley, which continues until an area with a low slope where alluvial deposits appear. Downstream of the Ponte Mannu, after a section of the river in which the waters flow on the rock, the river becomes slightly sloped and establishes an alluvial plain with anastomotic channels and river islands.

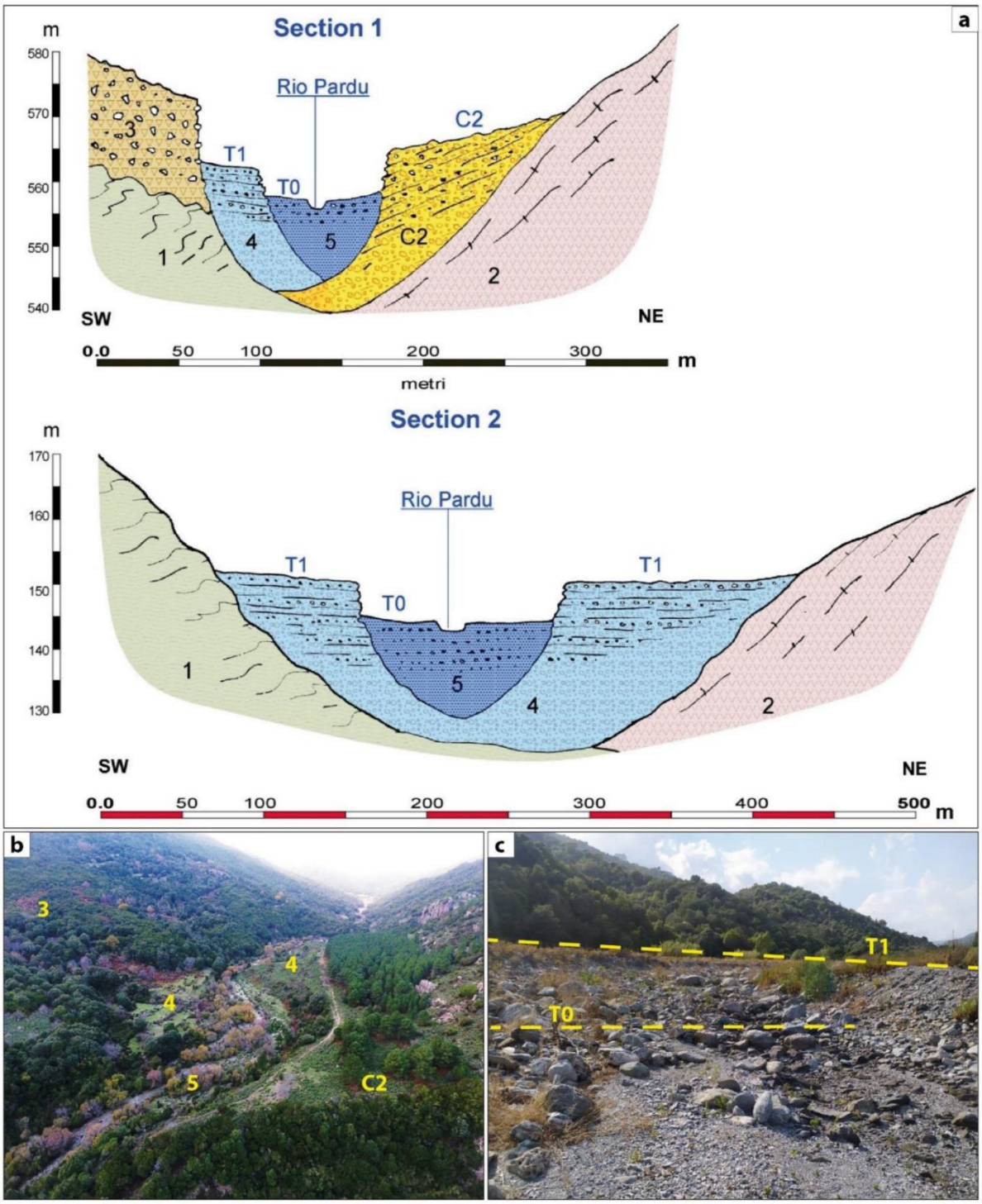

Figure 32 - (a) Morphostratigraphic profiles of the Pardu River. (b) UAV photo near the head of the Pardu River. (c) The bottom of the Pardu Valley near the capture elbow. Lithological legend: (1) Filladi Grigie del Gennargentu

Formation; (2) Monte Santa Vittoria Formation; (3) paleo-rockfall deposits; (C2) paleo-conoid; (4) Terrace T1; (5) Terrace T0.

Active and quiescent dejection cones are distributed over the Quirra and Pardu Valleys. The active conoids are well highlighted by the morphology, and they have a poorly elaborated clastic component and an uncemented dark brown matrix. In the terminal part of the Quirra, a terraced dejection cone (C1) assumes a certain importance due to its size and evolutionary stage (Inner–Middle Pleistocene). The often large pebbles are very elaborate and have blackish patinas of Mn oxides on their surfaces. Oxides also accumulate inside the matrix, which presents an intense redness. In the upper part of the Rio Pardu, a paleo-conoid (C2) with large pebbles and a brown matrix is currently engraved by the current course of the river (Upper Pleistocene and Holocene).

The paleo-slope deposits are characterized by coarse, elaborate, and sharp-edged components. The matrix is very abundant, strongly cemented, and bright red in color due to the accumulation of pockets of Mn oxides. These deposits are located at the same altitude as that of T3 or sometimes at higher altitudes, and they are connected to the base of the slope (Inner-Middle Pleistocene).

4.7 Discussion

4.7.1 River Analysis

The hydrographic network engraved by torrential watercourses possesses a tectonic control linked to the Cenozoic structural features. The main incisions that cross the basin of the Rio Pardu give rise to deep valleys with a mainly erosive and only locally depositional character. The Pardu Valley has a transverse “V” profile, which is more or less open depending on the evolutionary stage, the distance from the point of origin, and the competence of the lithotypes in which the river incision takes place. Sometimes, the profiles show marked asymmetries due to the different positions of the layers or the different exposure, which influences the vegetation. A lower steepness can be observed on the left side, which probably due to a lower vegetation cover, which favors erosion. The valley has developed in the formation of the Filladi grigie del Gennargentu. Only in the southeast is the formation of Monte Santa Vittoria affected.

As regards the evolutionary conditions of the Pardu Valley, considering the descriptive parameters, the geometric conditions, and the hypsometric curve, it is noted that was not able to develop to the point of acquiring characteristics that are attributable to a cycle of river erosion in an evolved phase, which suggests a relatively young age for engraving (*Maxia et al. 1973; Marini A. & Ulzega A., 1977; Ulzega A. & Marini A., 1973*).

The longitudinal profile of the Rio Quirra differs from the normal profile of a river; it has an initial concave part with a strong steepness within the first kilometer from the head and a regular decrease in the slope along the rest of the watercourse. The evolutionary stage of the Quirra appears to have

advanced; however, it must be considered that it represents the middle and final parts of the original Rio Pardu–Quirra, which are divided in two by the capture of the Rio Pelau. Currently, the Rio Quirra does not have a catchment basin at the head, and its feeding is mainly given by certain tributaries. The valley is oversized and over-flooded with respect to the current basin (Figure 33).

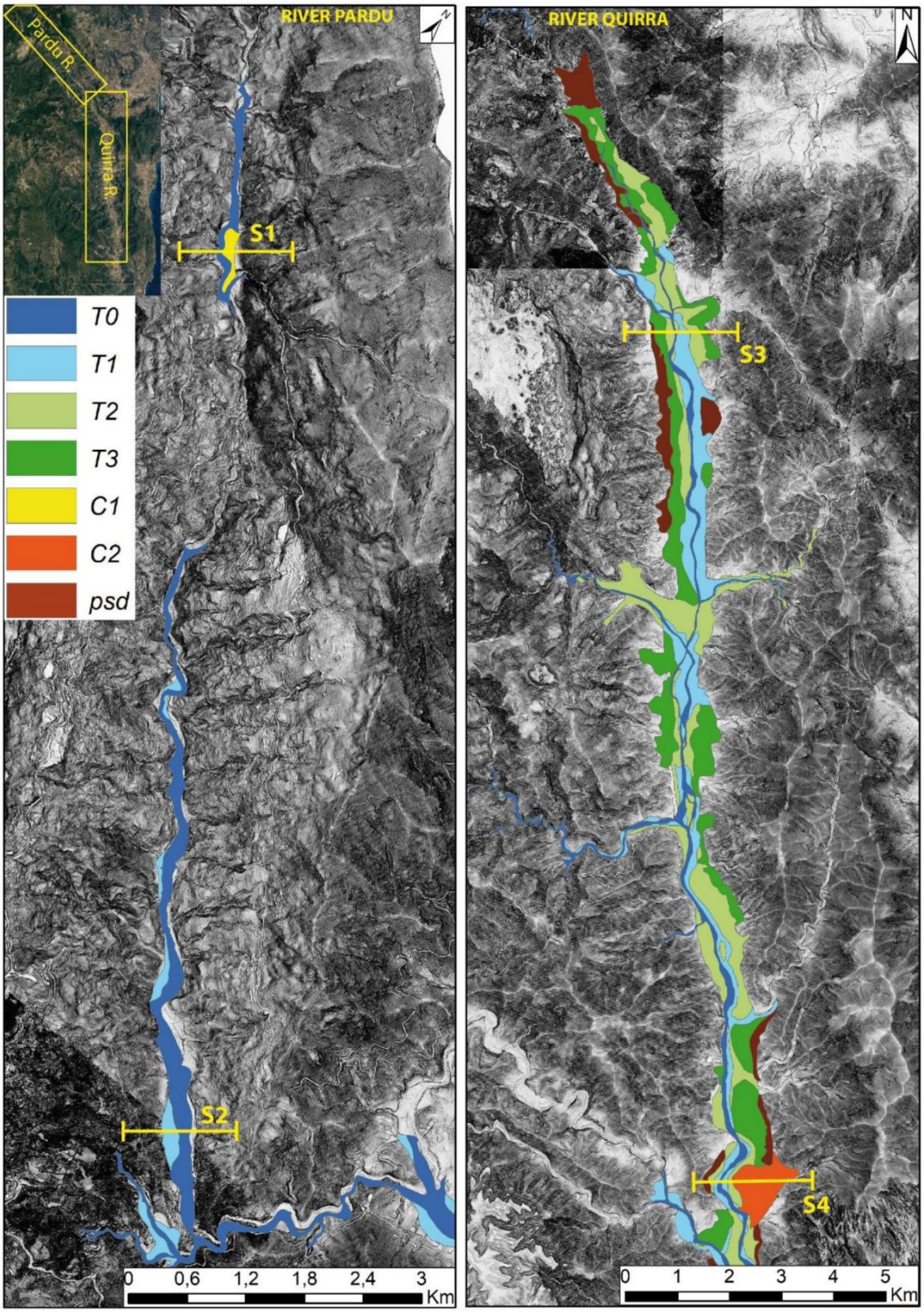

Figure 33 Map of the distribution of alluvial deposits in Rio Pardu and Rio Quirra.

4.7.2 DGSD Dynamics

The Rio Pardu and Quirra River represent two of the most susceptible areas to landslides in Sardinia, as well as to rockfalls and rainstorm-induced superficial landslides (*Maxia 1973; Ulzega & Marini 1973; Avi project*). This sector is also interesting due to the fact that extreme rainfall over the last centuries has led to the evacuation and reconstruction of the towns of Osini and Gairo (*De Waele 2012, Ulzega 77*). Recent studies have highlighted the presence of deep landslides with sackung-type kinematics and lateral spreads on the right side of the Rio Pardu (*Demurtas et al 2021*).

In this paper, by analyzing integrated geomorphological, geo-structural, high-resolution topography and InSAR displacement data, we identified diffuse DGSDs on both sides of the valleys of the Pardu River and Quirra River, which are characterized by different kinematics.

DGSDs are commonly found in orogenetic environments with high tectonic and seismic activity and in areas affected by slope decompression due to post-deglaciation. The present work aimed to contribute to the knowledge on the influence of evolution of valleys—in particular, with high incision—on the triggering of large landslides or DGSDs in relation the Quaternary uplift.

Lateral spreads were developed at the edge of the plateau in relation to the favorable stratigraphy (dolostone on clays and altered metamorphites). The slope deformation generates vertical fractures in the carbonate and a zone of ductile basal deformation that affects the Genna Selole Formation and the summit, which thus altered the metamorphites (Bruncu Pranedda and San Giorgio DGSD). DGSDs with a higher vertical shift represent a more advanced stage with sackung features (Tisiddu Mountain and Tertenia DGSDs). The latter evolves in relation to the thrust that affects the median part of the slope. A large part of the deformation affects the Paleozoic basement, which was evidenced by the sinking of the carbonate sequence into the metamorphites.

On the left side of Rio Pardu, Gairo's DGSD shows a different behavior in relation to the different stratigraphic and structural setup. The DGSD has sackung-type kinematics with an important translational component linked to the thrust.

From the structural viewpoint, the major faults in the NW–SE and NE–SW directions were in concordance with the main trenches and back-scarps in all sectors, indicating an important structural control. The secondary trenches and the joints did not exhibit a good correlation with the large-scale structures because they were associated with the features inside the deformation rock mass.

The Rio Pardu shows a straight valley with steep slopes, a valley bottom with a mainly erosive character, and two orders of terraces. This is linked to the intense erosive phase following the capture by the Rio Pelau. The valley of Rio Quirra shows a flat-bottomed valley with an actual riverbed of the braided channel type. The valley is over-sized and over-flooded with four orders of terraces, the result of an evolution prior to the capture of the Rio Pardu. The T3 terrace shows sedimentological

characteristics related to a sub-tropical climate, which is probably linked to the warm climatic phase of MIS 5. The InSAR and morphostratigraphic analyses made it possible to define the state of activity of the DGSDs in the two hydrographic basins. In the valley of Rio Pardu, various areas of the slope that are affected by movements that can be classified as active DGSDs were identified, with movements of up to 2 cm/y on the left slope and up to 1 cm/y on the right slope. However, in the Quirra River, paleo-DGSD bodies are fossilized by the alluvial deposits of the T3 terrace. This indicates that the river capture led to an intense erosive phase in the Rio Pardu, leading to the recent instability of the slopes, thus justifying the active DGSD (Figure 34).

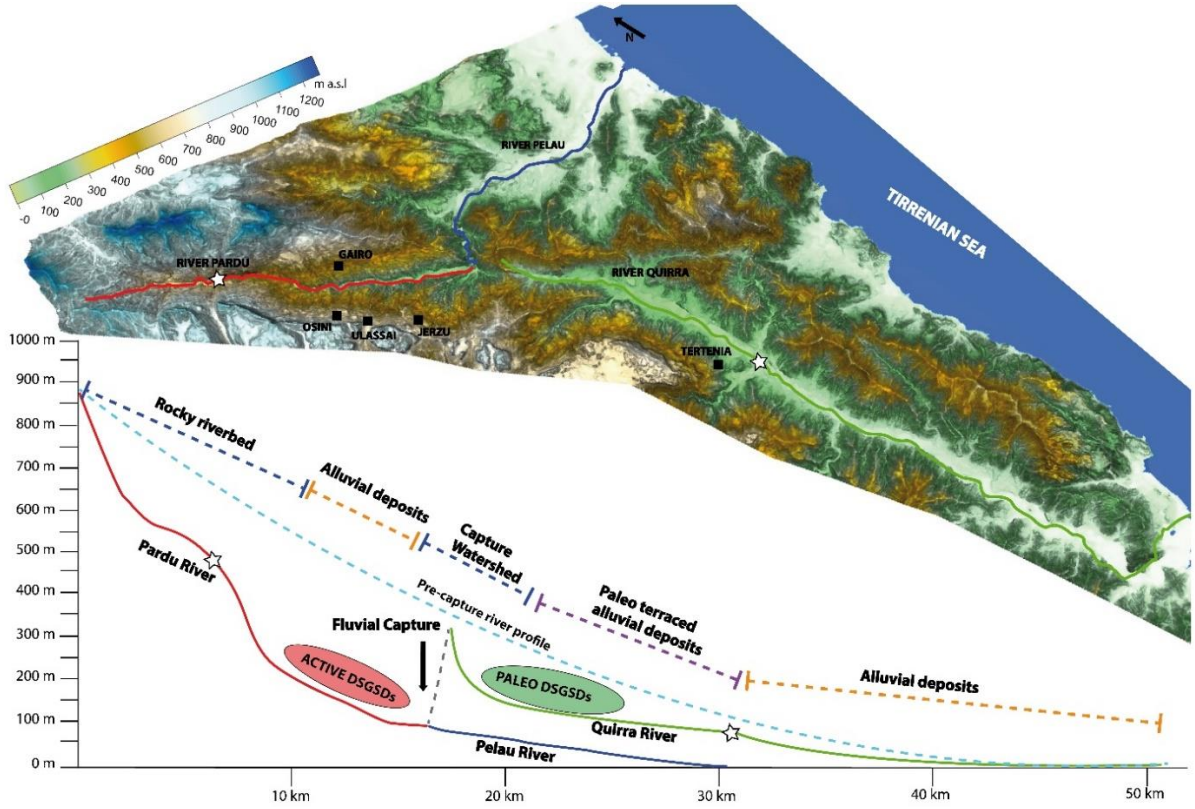

Figure 34 - Relation between DGSD activity and river parameters.

These DGSDs were associated with numerous large collateral rockfalls and toppling landslides that affected the slopes. Dolomitic blocks with sizes of up to 30 m on each side were identified; these moved up to 900 m away from the detachment points, which were linked to mega-rockfall events with rock avalanche features. We also identified paleo-DGSDs on the downslope that were associated with the collapsed slope side. Currently, a reactivation of quiescent DGSDs or an acceleration of movements can be triggered by extreme weather events or earthquakes.

Therefore, an acceleration of slope movements leading to a potential catastrophic failure poses a threat to communities, and the monitoring of these slopes is important for early warning and risk reduction. So, we studied the DGSDs and landslides in the inhabited areas of Pardu Valley in detail by using integrated remote sensing techniques, field mapping, and InSAR in order to understand the

temporal evolution. The historical InSAR deformation rate supports our model of rock slope deformation. However, for risk reduction in a populated area, a 24/7 monitoring system could become an essential component of an early-warning system that is aimed at preparing evacuation protocols (*Demurtas et al 2021b, Zhang et al 2011 ,Barla et al 2010 ,Intrieri et al 2012 , Naidu et al 2018 , Piciullo et al 2018 , Guzzetti et al 2020 , Xu et al 2020 ,Tzouvaras et al 2021*).

4.8 Conclusions

The connection between Plio-Pleistocenic tectonic activity and geomorphological evolution in the Pardu Valley and Quirra Valley (Ogliastra, East Sardinia) was studied. The evolutionary conditions of the Pardu Valley are associated with a cycle of undeveloped fluvial erosion, which suggests a relatively young age of the engraving in relation to the capture by the Rio Pelau and the isolation of the Rio Quirra. The intense post-capture erosion has given the Rio Pardu Valley morphometric features that are favorable for the evolution of DGSDs. However, the Rio Quirra Valley presents paleo-DGSDs that have been fossilized by pre-capture terraced alluvial deposits.

The DGSDs' movements are linked to the recent tectonic evolution (areal uplift). The two valleys analyzed are controlled by transcurrent faults that have recently recorded low-magnitude seismic events. Therefore, it is possible that the constant movement of the DGSDs (between about 1 and 2 cm/y) may be susceptible to accelerations due to seismic triggering, causing the partial collapse of the slopes.

In particular, this research highlighted the following:

- The geomorphological and structural setting of Ogliastra is closely linked to the genesis of the east Sardinian continental margin due the opening of the Tyrrhenian basin (Miocene–Pliocene)
- Distensive Pliocene tectonics accompanied by widespread volcanism resulted in a general uplift in Sardinia. The Quaternary uplift rebound manifested itself with an important erosive phase and variations in the hydrographic network. We have evidence of this phase in the Rio Quirra Valley, which is represented by paleo-DGSDs fossilized by pre-Tyrrhenian alluvial deposits (Lower Pleistocene).
- The river capture of Rio Pardu is associated with this important erosive phase and caused an erosive increase that led to a complete emptying of the valley (Upper-Middle Pleistocene).
- The post-capture decompression of the slopes of the Rio Pardu triggered DGSDs in both flanks in the current state of activity.
- Using InSAR data, it was possible to identify and assign displacement rates to the Ulassai, Osini, and Gairo DGSDs.

5 CHAPTER III

Preliminary results from active lateral spreads monitoring using Multi-source and multi-scale monitoring system in East-Central Sardinia

Abstract

In Italy, landslides are one of the main geological hazard. In particular, active landslides that are a danger to the population affect many urban centers. Sometimes such urban contexts are affected by Deep-seated gravitational slope deformations (DGSDs) can leading to a potential catastrophic failure trigger secondary collateral landslide end monitoring is important for early warning and risk reduction. In this study, we analysed DGSDs and landslides in the inhabited areas of Pardu Valley in eastern-central Sardinia using integrated field mapping, remote-sensing, and monitoring systems. Active Lateral spread processes and large toppling in an urban and tourist contest were highlighted. Starting from high resolution geostructural and geomorphological surveys of DGSDs at local scale and using high-resolution digital elevation models acquired by UAV (Uncrewed Aerial Vehicle), we created a geological 3D models of the slope deformations.To better understand the kinematics and temporal evolution of unstable slopes deformation, a conoscitive monitoring system, consisting of Space-borne Interferometric Synthetic Aperture Radar (InSAR), GNSS antenna, tiltmeter, and extensometer, has been installed along the DGSDs near urban areas.Sentinel-1 PS- InSAR analysis confirmed by GNSS periodic measurement identified downslope movement of up to 10 mm per year on the main DGSD. A continuous acquisition by extensometers and tiltmeters have been recording displacement in large block inclinations and opening and closing of fractures since 2021. Integrated data analysis will be essential to define threshold for a future 24/7 early-warning system.

Keywords*: UAV-DF*; Monitoring, InSAR; DGSDs, Early Warning System, Sardinia; Italy

5.1 Introduction

Landslides are extremely widespread phenomena on the Italian national territory and each year cause significant impacts on the population, on inhabited centers, on linear communication infrastructures and on the economic sector. Italy, with over 620,000 landslides recorded in the Inventory of Landslide Phenomena in Italy (*IFFI, Trigila et al., 2007*), is the country with the most landslides in Europe. In particular, Sardinia, with 22.5% of landslide hazard areas, is one of the regions of Italy with the greatest landslide risk (*Trigila et al., 2007, 2018*).

Every year much money are used for landslide risk mitigation using of direct structural interventions by building geoengineering works to make landslides safe. Sometimes the volumes affected by the landslide are too large to use this methods and monitoring is the only methodology for risk mitigation (*Wieczorek and Snyder 2009*). In particular Deep-seated gravitational slope deformation (DGSD, *Dramis & sorriso Valvo 1994*) is a complex type of rock slope failure characterized by large dimensions generated in stone rocks (*Dramis etal.,2002*). In particular, lateral spreading DGSD type (*Mateos et al., 2018, Cruden &Varnes,1996; Jahn, 1964; Pasuto & Soldati, 1996; Soldati et al., 2019; Devoto et al., 2021, Agnesi et al., 2015*) consisting of rock spreads often evolving in cathastrophic collapsed and trigger secondary landslide (*Demurtas et al. 2021a*). DGSDs are characterized by slow movements that can suddenly accelerate and cause catastrophic collapse of sections of the deformed slopes (*Radbruch-Hall, D. et al 1976, Agliardi, F. et al 2020, Crosta, G.B. et al. 2003, Nemčok, A, 1972 and Ostermann, M. & Sanders, D 2017*). Therefore, this phenomenon represents an important geo-hazard in relation to high magnitude secondary collateral landslides.

Monitoring is a fundamental tool for deepening the knowledge of landslides and evaluating deformation trends (*Palis E et al. 2017*). Iit also provides preliminary data for the design stabilization works and verifying their effectiveness over time. Monitoring represents a “non-structural” risk mitigation measure which is fundamental manage correctly the territory and activating procedures for alerting the population to safeguard human lives.

Monitoring landslides, in fact, is a complex and dynamic process, which requires continuous technological and managerial adjustments in order to obtain more and more detailed information on the phenomena and their evolution. The design of an effective monitoring network is based on technical, logistical and economic evaluations.

Landslide conoscitive monitoring purposes it is essential to install a definitive monitoring system for early warning system (EWS) (*Intrieri et al 2012*).

Several definitions of EWS can be found in the literature. *Medina-Cetina and Nadim (2008)* define them as “monitoring devices designed to avoid, or at least to minimize the impact imposed by a threat on humans, damage to property, the environment, or/and to more basic elements like livelihoods.”

According to United Nations International Strategy for Disaster Reduction (UNISDR, 2009) they are "the set of capacities needed to generate and disseminate timely and meaningful warning information to enable individuals, communities and organizations threatened by a hazard to prepare and to act appropriately and in sufficient time to reduce the possibility of harm or loss."

Even after an event, landslides are always characterized by significant residual instability related to possible reactivation of the entire landslide or, more frequently, parts of it.

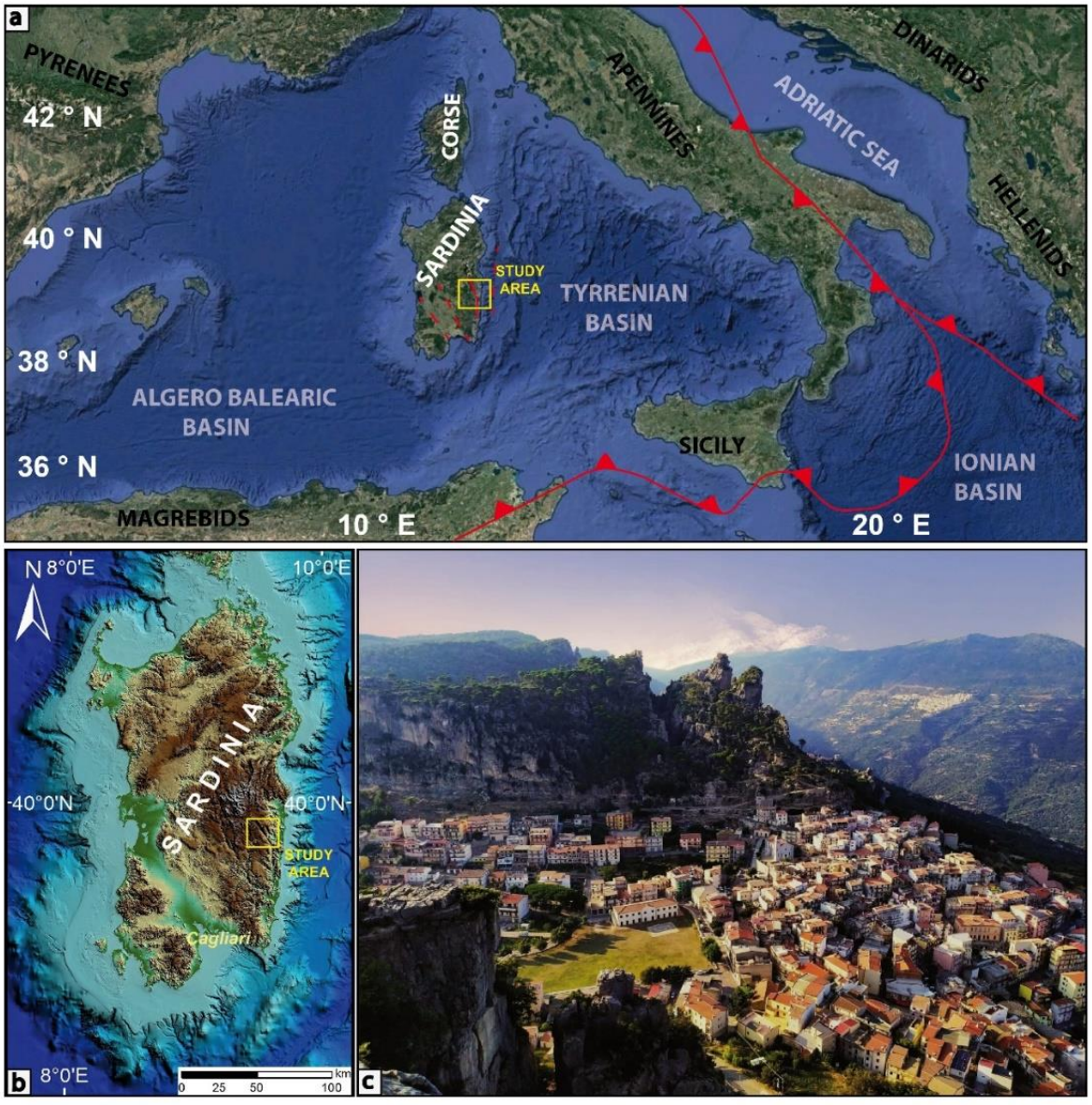

Figure 35 - a) Geographical location and structural features of the study area. b) Digital terrain model of Sardinia bloc comprising continental and marine area. c) Ulassai village under plateau edges.

Central East Sardinia is particulary susceptible to landslides because is characterized by steep slpes (*Maxia et al., 1973; Marini & Ulzega, 1977*). In this area DGSDs, rockfalls, rock avalanches and giant toppling represents high geological risk inserted in an urban context (*Demurtas et al. 2021*).

In fact, as is well known, different inhabited centers are continually threatened by disasters (*Demurtas et al 2021b*). Different types of interventions were carried out to protect inhabited centers and infrastructures, but they were carried out without a global study of the problem and, therefore, without real knowledge of the evolutionary modalities of the slopes and the real gravitational dynamics. We analyse in detail the area around the municipality of Ulassai (Figure 35). This village is located under the carbonate plateau walls edges and is affected by different gravitational processes that need to be mapped, characterized and monitor and design an early-warning system (*Demurtas v. et al 2021 a,b,c*) . Uncrewed aerial vehicle digital photogrammetry (UAV-DP), geological, geomorphological and structural field surveys, allowed an accurate mapping of the surface evidences and gravitational processes. Using a temporal series of InSAR data , the DGSDs under study can be classified as extremely slow and slow, in which movement is imperceptible without monitoring tools. The problem in this context is linked to extremely rapid collateral landslides with possible catastrophic scenarios. The type of monitoring is aimed at the acquisition of data to understand the kinematics of landslides (deformation speed, Direction).

Monitoring networks for early warning or alert purposes are aimed at identifying the variation and dynamics of landslides in real time and therefore require planning, construction and, in particular, more expensive and complex management than conoscitive monitoring systems. These peculiarities mean that, to date, in Italy monitoring networks for alerting purposes are less widespread. Understanding the kinematics and temporal behavior of DGSDs and landslides is important for designing monitoring systems based on strong process knowledge. In some cases, continuous monitoring is the only way to reduce risk (*Frigerio, S. et al 2014; Sestras et al. 2021; Zhang L. et al. 2021; Bianchini S et al 2021, Demurtas et al 2021c*).

The main aims of this paper can be summarized as follows:

- evaluation of all the dimensional and evolutionary parameters that contribute to defining the conceptual models of a specific type of landslide phenomenon;
- assessment of the evolution and state of activity of the landslide phenomenon, of the predisposing and triggering causes in order to correctly manage the risk;
- support for territorial planning (urban planning tools) and for the preparation of civil protection plans;
- support for the design of monitoring networks for alert purposes.

5.2 Geological setting

In East-central Sardinia (Italy) are widespread Jurassic dolomitic plateaus (Tacchi) overlying a metamorphic Palaeozoic basement, primarily comprising metasandstone, quartzites, and phyllites (*Demurtas et al 2021a; Carmignani et al., 2016; Pertusati et al., 2002*) (Figure 36). The area is characterised by the Pardu River Valley in the east and the Barigau River Valley in the south-west; the central and north-western sectors include extensive dolomitic plateau called Tacco of Ulassai. The geological basement comprises Palaeozoic metamorphites affected by complex plicative structures and regional low-grade metamorphism (*Carmignani et al., 2001, 1994; Elter et al., 2004, 2010*). The major Palaeozoic units are the Filladi Grigie del Gennargentu Formation constitute by metarenites, quartzites, shales (Middle Cambrian–Middle Ordovician) (*Meloni et al., 2017; Pertusati et al., 2002; Vai & Cocozza, 1974*). The metamorphic basement summit has suffered chemical alteration associated with a warm humid climate during the Permian and Triassic periods (*Costamagna & Barca, 2004; Marini, 1984*).

An angular unconformity of Mesozoic sedimentary succession rests on the metamorphic basement. Basal layers are primarily fluvial sediments of the Genna Selole Formation (Middle Jurassic), which are overlain by dolomitic limestones of the Dorgali Formation (Middle–Upper Jurassic). (*Costamagna et al., 2018; Costamagna & Barca, 2004; Pertusati et al., 2002*). These Mesozoic deposits are extensive and decipherable from their plateau morphology. The Genna Selole Formation (*Costamagna, 2015; Dieni et al., 1983*) represents a mixed succession of siliciclastic to siliciclastic–carbonate deposits. The Dorgali Formation is represented by dolomitic sequences with thickness up to tens of metres. The lower part, with a thickness of approximately 30 m, is affected by marl intercalations, whereas the upper part is typically massive. Mesozoic units are sub-horizontal strata with an attitude of approximately N90/0–5°, and the plateau edges can reach a dip amount of up to 40° and direction parallel to the slope owing to the DGSD (*Demurtas et al 2021 a,b*).

Quaternary covers are primarily represent by landslide deposits, including rockfalls, toppling, and collapsed DGSDs at the foot-slope of the Tacchi.

The rockfalls and toppling landslides have been characterised by different sedimentological features based on age. These deposits are associated with rockfalls affecting the plateau edge wall and the collapse of some parts of the DGSDs. We have focussed on the DGSD of Bruncu Pranedda an the “Torre dei venti (Sector 1)”, as they are important geological hazard in the urban area (Figure 37).

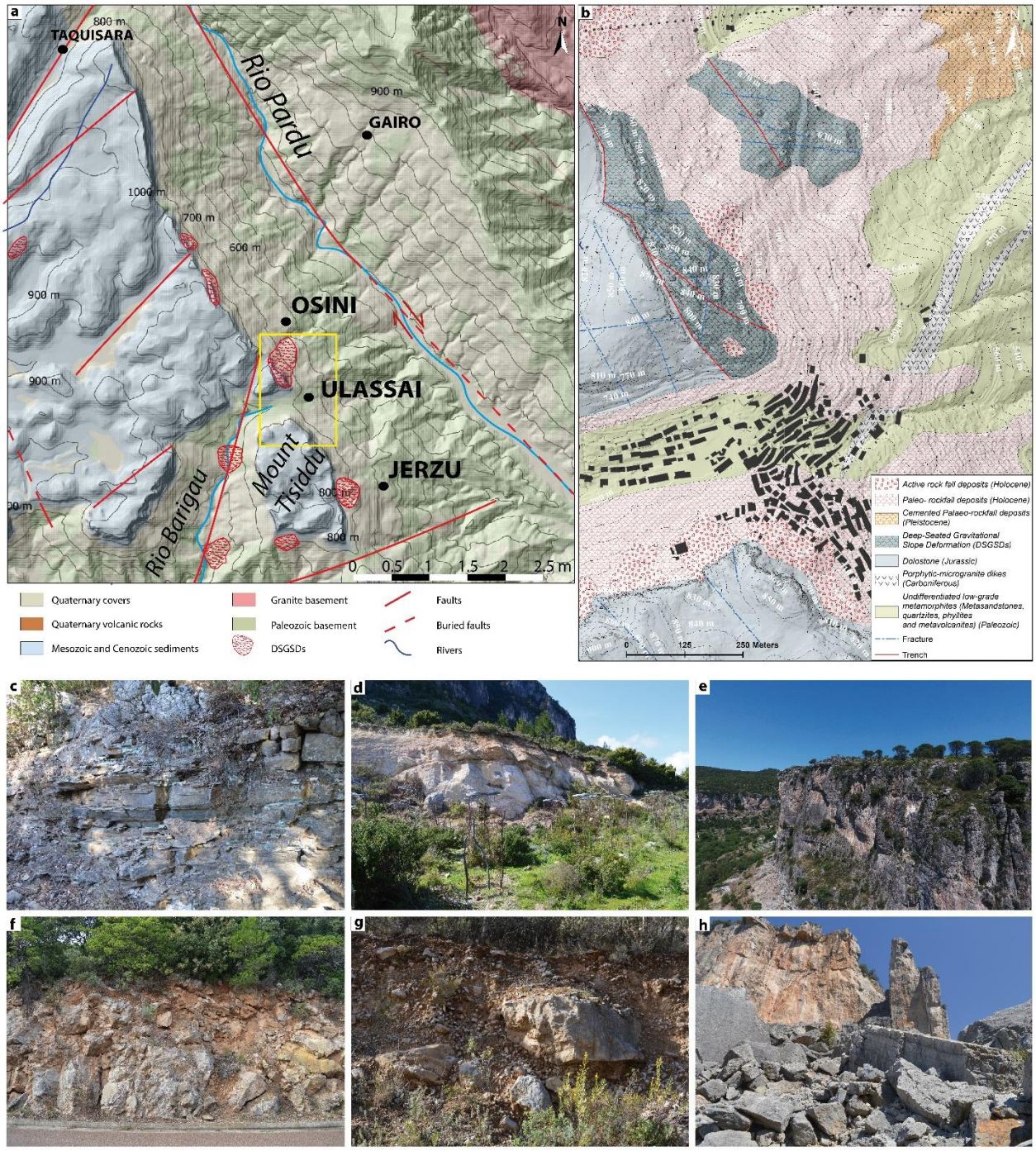

Figure 36 . a) Geolithological sketch map of the study area based on geological data of Autonomous Region of Sardinia. The Yellow box indicate the location the study area. b) detailed geological map modified from Demurtas et al. 2021. c *) Metamorphic basement, fractured metasand- stone and quartzites. Transitional and marine Mesozoic succession:(d) Genna Selole Formation (siliciclastic–carbonate deposits and clays);(e)Dolostone of massive Dorgali Formation. Rock-fall deposits: (f) Cemented; (g) Quiescent; (h) active.*

5.3 Tectonic and geodynamic setting

The geodynamic setting is associated with the collisional dynamics between the African and European plates. The structural setting is associated with the Alpine cycle, which first appeared with a strike-slip fault in the Oligo–Miocene and in the Pliocene and Quaternary with an extensional

component (*Carmignani etal.,2001, 2016; Carminati & Doglioni, 2005; Cherchi &Montadert,1982; Gattacceca etal., 2007; Gueguen etal.,1997; Oggiano etal.,2009; Ulzega etal.,2002*). Based on preliminary geodetic data from the Peri-Tyrrhenian Geodetic Array network, *Ferranti etal. (2008)* revealed the presence of low internal deformation in Sardinia. In Sardinia, seismicity is typically scattered and sporadic, except for the dozen tremors detected following the ML4.7 earthquake of 7 July 2011 in the Corsican Sea, which primarily characterises the edges of the continental lithosphere block. Significant seismic events also occurred in the eastern sector, in particular, three events with a magnitude >4 (26 April 2000, magnitude ML4.2 and 4.7, and 18 December 2004, magnitude ML 4.3) located in the central Tyrrhenian Sea approximately 60km east of Olbia in the Comino depression (Cimini etal.,2016). The most recent low-magnitude earthquake events were ML1.8 (Escalaplano, 4 April 2019) and ML1.6 (Perdasdefogu, 14 October 2020) (*INGV, 2021*).

5.4 Methodology

The proposed methodology is based on a preliminary conoscitive phase about geological and geomorphological context basic to project a DGSD monitoring system with early warning system (*Demurtas et al 2021 a & b*).

High detail geo-structural and geomorphological analysis of the area around Ulassai was carried out based on an integrated approach that incorporated a cartographic and morphometric analysis. In particular, detailed reconstruction of surface systems was performed, in order to guide the landslide kinematic interpretations.

The geomorphological analysis made it possible to identify the main risk factors in the sector, in particular the landslides at the Bruncu Pranedda DGSD and the possible collapse of large prismatic bodies of dolomitic with toppling kinematics.

Three sectors with high hazard have been identified in fiction of the type of process and proximity to populated areas. The sector north of Ulassai represented by the side of Bruncu Pranedda is affected by an extended DGSD with different evolutionary stages.

The top slope has an active lateral spread that triggers collateral landslides of rockfalls and toppling. The middle part of the slope consists of a paleo sackung with a residual hazard linked to possible large Toppling. (*Demurtas et al 2021*.) The other sector is socialized in the south of the country and has a dolomite premiere with evidence of an enormous overturning.

Bruncu Pranedda DGSD displacement and rate were evaluated using space-borne interferometric synthetic aperture radar (InSAR). Over the last 30 years, InSAR techniques have been widely used to investigate geological (e.g., volcano activity, earthquakes' ground effects, etc.) and geomorphological processes—in particular, DGSD. In different geological and climatic contexts, this technique allows

one to analyze extremely slow DGSDs and to identify displacements of about 1–2 mm in favorable conditions (*Devoto S. et al, 2020; Gaidi, S et al. 2021; Delgado, J. et al. 2011; Oliveira, S.C et al. 2015; Crosetto, M.;et al. 2016; Mantovani, M. et al 2016; Frattini, P. et al. 2018; Novellino, A. et al. 2021; Eker, R.; & Aydın, A 2021*. Based on these preliminary data, a monitoring based on periodic GNSS antenna mesures and real time monitoring system with geotechnical instrumentation was started and they also sell preliminary indications for risk management in terms of civil protection.
In the Table 4 we summarize the main method used to preliminary geomorphological characterization and monitoring.

Table 4 Methodology synthesis

Method	**Instrumentation**	**Data**	**information acquired**	**Spatial scale**
Field survey	Geological mapping	Geological and Geomorphological maps	Lithostratigraphic contacts, Structural setting, Landslide deposits, morphostratigraphy	Local scale 1:500
UAV DF	Phantom 4 Matrix 200 Methashape software	High resolution 3D models	High resolution DGSD topography 5cmX5cm cell size	Landslides and DGSD scale
LIDAR	Autonomous region of Sardinia LIDAR data	DEMs	High resolution topography 1m X 1m cell size	Slope scale
InSAR	Sentinel 1 radar data	LOS displacement	Slope displacement	Regional scale
GNSS	Trimble R8	Coordinates differences	Large block displacing	Rock mass
Geothecnical	Extensimeters Tiltmeters	Misuses of distances Tilting degree	Fracture opening and closing Block tilting	Fracture

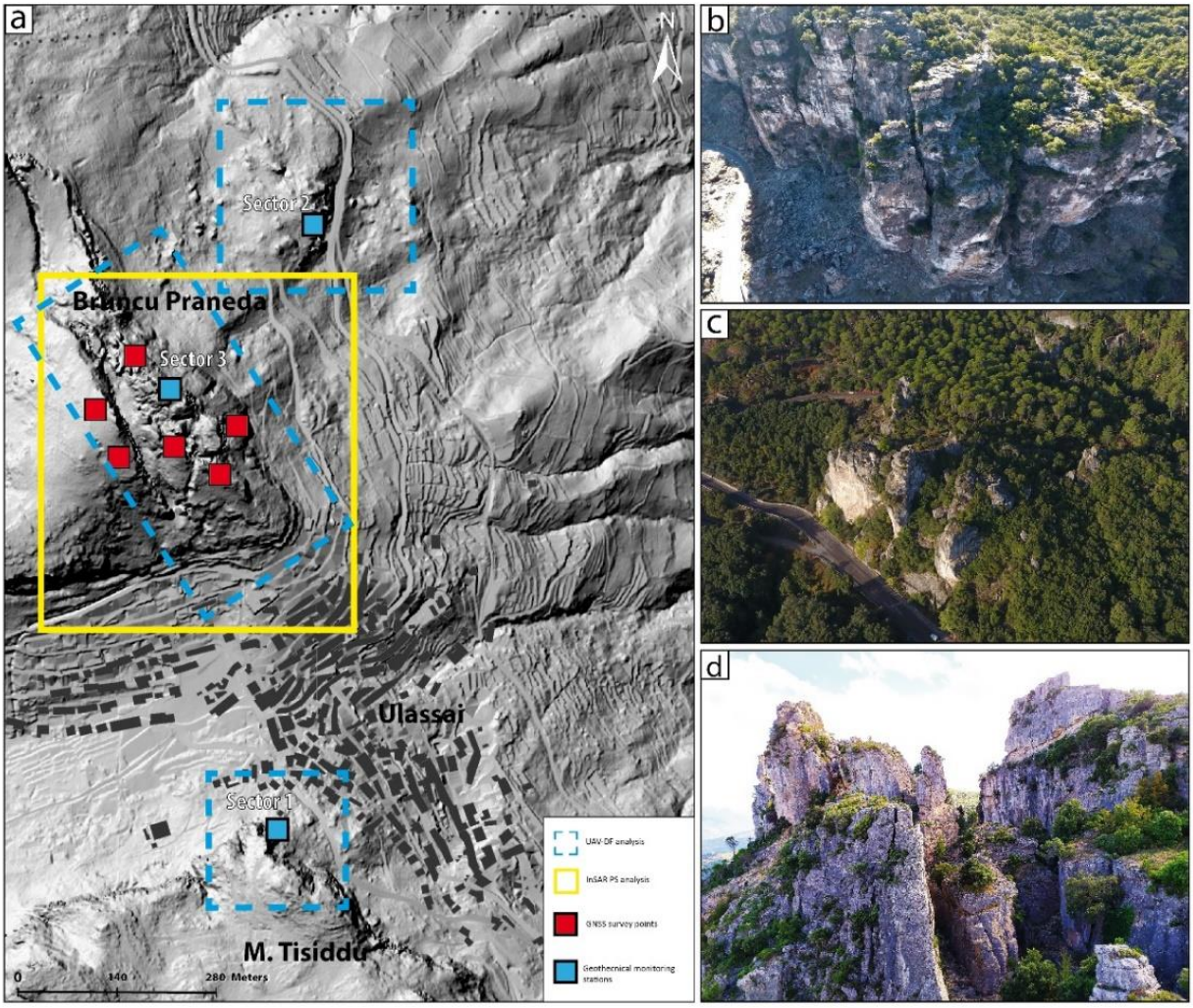

Figure 37 - Location of different monitoring stations and surveys. A) Hillshade 1x1 m cell size Lidar DTM of area around Ulassai whit highlighted the sector of different methodology used. In the area geological and geomorphological field surveys was performed. B) Monte tissiddu large toppling (Torre dei Venti). C)Middle slope sector of Pranedda DGSD whit sackung feature. D) Top slope of Bruncu Pranedda DGSD whit lateral spread features.

5.4.1 Geomorphological, Lidar and UAV analysis

Multi-scale remote sensing and field surveys were carried out to analyze the geological, structural and morphotectonic setting of the slopes in particular, the plateaus' edges. (*Guzzetti, F. et al, 1999; Dragićević, S et al. 2015; Shi, W et al. 2018; ISPRA & AIGEO 2018; Miccadei E. et al. 2018; Miccadei E. et al. 2021; Yi, Y et al 2020; Deiana, G. et al 2019; Melis, M.T et al 2020; Demurtas et al 2021 a*). Geological and geomorphological field mapping in the walls around Ulassai were performed on a scale of 1:500. Particular attention was paid to the study of morphologies related to DGSDs and collateral landslides.

The detailed analysis was carried out with the aim of understanding the interconnection between the surface systems and the tectonic fracturing network, stratigraphic discontinuity, families of junctions from biogenic or thermoclastic processes and decompression junctions.

Uncrewed aerial vehicle digital photogrammetry (UAV-DP) is a robust methodology for the investigation of DGSDs and large landslides. In particular, it was used for the recognition of large lateral spreads in Malta and Tunisia (*Devoto, S et al 2020; Gaidi, S et al 2021*). We used UAV-DF and light detection and ranging (LiDAR) to extract high-resolution topographic 3D DGSD models and perform detailed morphometric analyses. LiDAR and aerial photogrammetric data produced by the Autonomous Region of Sardinia were used to perform visual and morphometric analysis of DGSDs and plateau edges. A detailed orthophoto dating from 2016 was used together with LiDAR data with a cell size of 1 × 1 m and vertical resolution of 30 cm.

The aerial surveys were performed using UAVs (DJI Phantom 4 and DJI Matrix 200) flying at altitudes of 50–60 m above ground level. The acquired images were analyzed and processed using the photogrammetric Agisoft MetaShape software and constrained by 10–12 ground control points using GEODETIC LEICA GNSS for each area. The resulting orthorectified mosaic and DEM (WGS 84 datum and UTM 32N projection) had a cell size of 5 cm/pixel and were considered sufficiently precise to be used for the geomorphological analysis.

The 3D high-resolution UAV-DF models were used to develop interpretative superficial models by using geomorphological evidence and stratigraphic and structural data of the DGSDs.

The DTMs were used to analyze the morphometric parameters and visually identify the areas with the greatest risk of collateral landslides. Geological interpretative cross-sections of geologic features crossing the major DGSDs were also generated to define the movement kinematics, deformative style, and deep geometries of the DGSDs.

5.4.2 InSAR Analysis

Space-borne interferometric synthetic aperture radar (InSAR) data were used to analyze the slope deformation (*Ietto, F et al 2015; Mateos, R.M et al 2018; Moretto, S. et al 2021; Mondini, A.C et al 2021, Demurtas et al 2021*). Permanent scatters Differential Interferometric Synthetic Aperture Radar (PS-DInSAR) (*Ferretti 2000, Crossetto M et al 2016*) are used to investigate the temporal and spatial superficial slope deformation. This technique together with a correct identification of the ground reflectors is widely used to better comprehension of the geomorphological evolution of extremely slow mass movements (*Mantovani 2016*).

The aim of PS-DInSAR techniques is the analysis of backscattering signals (in terms of phase and amplitude) detected during multiple passages of a survey satellite over the same area (*Rosen et al., 2000*). In particular, PS-DInSAR focuses on the evaluation of phase difference ($\Delta\phi$ for each pixel, also said interferometric phase difference), from successive SAR images (*Goldstein et al., 1993, Massonnet et al., 1993*) (Figure 38). Such $\Delta\phi$ are used to perform interferograms, which can

be related to the change in radar signal path length and, finally, to the displacement (Δϕdispl). Basically, Δϕ is the sum of different factors which can be described as follows (*Hanssen, 2001*):

$$(1) \quad \Delta\phi = \Delta\phi_{flat} + \Delta\phi_{topo} + \Delta\phi_{atm} + \Delta\phi_{noise} + \Delta\phi_{displ}$$

where Δϕflat is due to the different positions assumed by the satellite during the acquisition, Δϕtopo is the topographic contribution, Δϕatm is due to the atmospheric variations during the acquisitions and finally Δϕnoise is induced by temporal decorrelation (variation of the scatters), spatial decorrelation (variation of the incidence angle) and volumetric scattering (different paths of the incident signal inside the cell resolution).

The Persistent Scatterers are targets that keep the electromagnetic signature (ie their reflection characteristics) unaltered in all the images, depending on the acquisition geometry and climatic conditions; therefore they preserve the wave amplitude information over time.

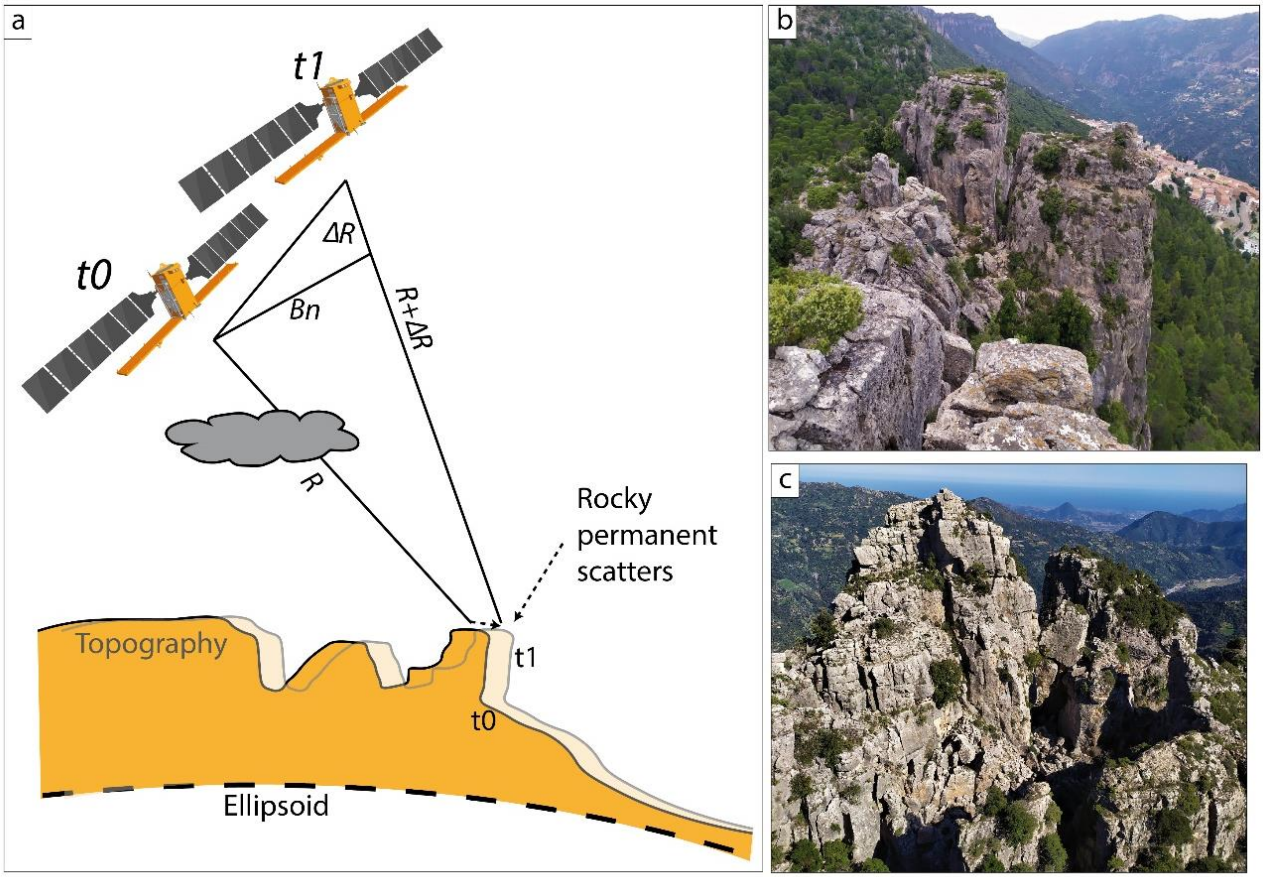

Figure 38 Simplified sketch showing InSAR monitoring DGSD. T0 time of first acquisition. T1-tn time of successive acquisition. R distance ground surface and the satellite.

Permanent diffusers are commonly parts of buildings, metal structures, exposed rocks, while the vegetation that continuously changes its electromagnetic characteristics, does not constitute a strong diffuser. The PS technique is very simple as it identifies these permanent speakers within the SAR images.

As a final result of applying the PS technique, we obtain:

- a map of the DPs identified in the images and their spatial coordinates;
- the average speed of movement of each single PS along LOS (mm / year);
- the travel data of each PS in the analyzed time frame (time archive of the movements);

The advantages of the PS technique concern the estimation and removal of atmospheric disturbance, the very high resolution of the results and the estimation of speeds with accuracies of mm / year over long periods. The limits of its applicability are represented by the availability of at least 20 SAR acquisitions, by the assumption of a linear trend of displacement and by the presence of vegetated areas.

We used the Sentinel-1 data and took into account the line-of-sight (LOS) velocities. We used a dataset from 2014 to 2020 in ascending geometry. The processed data were provided, by the Geological Survey of Norway.

To detect ground displacement, we used only high-PS coherence (0.6–1) located on built dolomitic blocks and the metamorphic rock outcrops. Low-coherence PSs, which are not useful, are located on rockfall deposits and in vegetated areas.

5.4.3 GNSS monitoring

Global Navigation Satellite System is a system of global positioning based on the use of the satellite system (*Krüger, R. et al 1994*) .Topographic monitoring systems such as GNSS surveys measurements have been more commonly used in landslides monitoring (*Gili J. A. et al., 2000, Malet, J.-P., et al 2002, Coe, J.A., et al 2003; Peyret, M. et al 2008, Wang, G.Q., 2012, Agnesi et al. 2015*).

The monitoring of a landslide area using the GNSS methodology in differential mode, consists in measuring the position of one or more stations within the landslide area (monitoring stations) with respect to one or more reference stations (Master or Base) positioned in stable areas and determining the displacement vector (baseline) as an expression of the coordinate difference.

In the top slope of Bruncu Pranedda based on geomorphological and InSAR data, a network of topographic nails was built to measure the displacement by Static mode GNSS techniques).

The transmission of the satellite signal is independent of weather conditions and does not require intervisibility between the individual GNSS stations, but it is however disturbed by the presence of

obstacles (plants, foliage, anthropogenic structures, etc.). Therefore the measuring stations were installed at the top of the rocky peaks of the DGSD.

The aim is to measure the movements of coherent blocks of rock mass separated from the trenches in order to understand the differential movements. Topographic survey points with brass support have been created to mount the GNSS antenna and reduce the positioning error to fractions of mm (Figure 39).

GNSS surveys points was installed in 2021, and measurements have been realised with intervals of 4 months. Three GNSS data acquisition surveys were carried out in 2021. During each campaign, two measurements were made for each point on different close days in order to correctly estimate the error associated with the measurement. These two acquisitions are called the first acquisition measure and the second (performed the following day in the same time) calibration measure. The acquisitions are performed with Trimble R8 GNSS in static mode with an acquisition of 1 hour and 30 min with recording rate of 5s. The acquisition parameters (frequency and duration) were chosen in order to make the best compromise between the quality of the acquired data and the times used. Five acquisition points were installed, in each surveys the acquisition duration was 15h to be added to the displacement within the landslide area. The travel and repositioning times are 1 hour for each point due to the accidental terrain. In general, each acquisition campaign lasted 4 days.

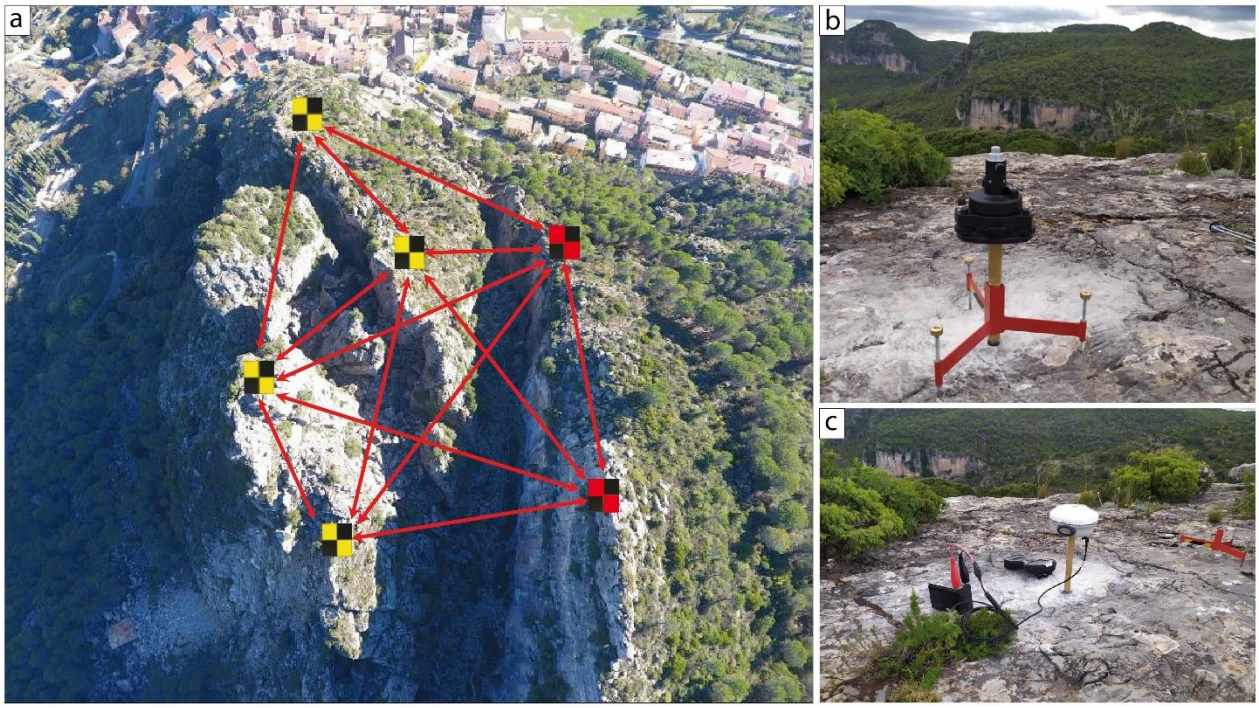

Figure 39 a) network of GNSS survey points, Black-Yellow monitoring points in instable are. Black-Red references stations. b) System for the vertical positioning of topographic nails. c) GNSS data acquisition phase in static mode.

In the GNSS monitoring system, 4 phases can be identified:

- Pre-data acquisition phase (choice of equipment, choice of sites);
- Data acquisition phase;
- Data quality control (pre-processing);
- Processing and anterpretation;

To achieve the maximum precision possible, the data were processed in post-acquisition using the RINEX files of the SARNET network recorded by the antenna (TERNENIA) at 14.6 km from the acquisition points in the study area. The data was processed with the TRIMBLE BUSINESS CENTER software.

5.4.4 Geotechnical monitoring

A geotechnical monitoring network, consisting by 6 extensimeters and 2 tiltmeters, in extension fractures was designed in 3 sites to validate InSAR and GNSS displacement data. (Figure 40). The sensors installed are Extensimeters GEFRAN GSF1800 and Tiltmeters MEMS Earth System.

Extensometers were used to quantitatively evaluate the opening/closing of cracks in rock/soil with sub-millimeter precision. They consist of a measurement sensor (protected inside a stainless steel box) and a wire, made of a material with a low coefficient of thermal expansion, held in tension by a spring system. To obtain a maximum representativeness of the data, the extensometric lines were installed parallel to the vector of maximum expected displacement of the DGSDs evaluated through geomorphological evidence. Since the measurement can be conditioned by environmental variables (eg snow on the wire, wind, the passage of animals, etc.) the wires have been protected with external aluminum pipes.

Tiltmeters were installed to monitor changes of large block inclination, related to rotational downslope movement of the rockmass that is evident in the strata attitude of the Dorgali formation. The tiltmeters consists of a dual axis inclinometer sensor which measure in two directions orthogonal to each other with an accuracy of 0.1° mounted in the rock sourface. The two tilt meters were connected to a data logger recording tilt angles.

The monitoring system is powered by batteries recharged from a photovoltaic panel. The data with continuous acquisition are managed by Campbell scientific CR1000X control unit with Sierra Wireless RV50X remote data transmission system.

The data are managed through the HMS-WED online platform created by Hortus srl.

Figure 40 a)Geothecnical station trumentations b) Extensimeter C)Tiltmeter T1; d) Extensimeter Ext 1; e) Extensimeter Ext3; f) Sensor installed in the station 3.

5.4.5 Weather station

In the monitoring station 1 a weather station was installed to measuring, humidity, precipitation and temperature. The data were recorded and stored using the same data logger as for recording the tiltmeter readings. A larger centriline was used to manage a greater amount of data. Precipitation is measured using a rain gauge, a high-precision sensor designed to measure the cumulative and intensity of precipitation.

5.5 Results

5.5.1 DGSD and large toppling analysis

The surveys made possible to map and characterize the gravitational processes affecting the inhabited center of Ulassai (Figure 41). In particular were identified:

• Widespread processes of rock fall in the walls projecting the inhabited center;

• Marginal sectors of the plateau affected by the toppling of dolomitic giant prismatic block;

• The north side of Ulassai slope (Bruncu Pranedda) affected by DGSD.

The Bruncu Pranedda DGSD is represented by two sectors located in the top and middle slopes that have different features.

In the top slope a large extensional trenches with NNW-SSE direction, called Pranedda Canyon, is present. Eastward the rock mass show high fracturing and the strata attitude of the Dorgali Formation is toward the east, with a dip up to 40°. The shear basal surface located in the marls and clay between the dolomitic plateau and the metamorphic basement. This setting indicates a deformation kinematics type lateral spread (*Cruden & Varnes, 1996, Demurtas et al 2021*).

This sector is located in the upper part of the country and constitutes a geomorphosite of great interest for environmental tourism activities and for moving climbs. This anthropogenic presence increases the risk associated with the presence of collateral rockfalls and toppling landslides of small and large magnitude. The DGSD led to an important and widespread fracturing, therefore source areas for surface landslides often triggered by the creep movement of the lateral spread. Widespread mega block deposits sometimes with dimensions up to 30/40 m per side are present at the base of the lateral spreads. These deposits are linked to the collapse phase of DGSD parts. In fact, rock avalanche deposits have been found to exhibit sedimentological and geomorphological characteristics of a very recent event. The evidence of current activity is demonstrated by the detachment of a rock avalanche which occurred in November 2014, involving a total volume of rock more than 1500m3.

Figure 41 a) main landslides distribution around Ulassai Village. B) UAV-DF acqusition and output. b1) Groung control poins acquired by GNSS. b2)Phantom 4; b3) DJI Matrix 200; b4) textured 3D model of bruncu pranedda.b)5 particular of b5. C1)Bruncu Pranedda Lateral spread. C2) particular of c1. Large instable block inside an extensional trenche. D) Monte Tisiddu large toppling on urban area. e) middle slope bruncu Pranedda sackung affected by large toppling.

A more evolution stage with partial sinking of Dorgali Fm. in the altered and fractured metamorphites, were identify in the middle slope. The basal shear surface involves the top of the metamorphites with high fracturing and chemical alteration. The kinematic deformation of this area is Sackung type (*Zichinsky, 1966, Demurtas et al 2021*). Here three large vertical prismatic blocks of dolostone show evidence of toppling. Between these rocky pillars there are partially cemented paleo landslides with evident fractures in the matrix. This indicates that the paleo deposit is in motion and undergoes compressive stresses or deconfinement due to the movement of the parts of the paleio sackung.
In the Tisiddu sector, a rock pillar with a size of about 40,000 cubic meters is completely separated from the plateau by an important fracture with an opening of up to 5 meters.
This coherent block with dimensions of about 25 x 20 per side and 80 m thick rests on the of Genna Selole Fm. and on the altered metamorphites. This block slides over these last units in a similar way to the lateral spread of Bruncu Pranedda. At the base of the slope, paleo-deposits of large collateral landslides with large blocks privy of vegetation were identified, indicating a recent age of the event. Most of the accumulation area of these past events is currently urbanized by the town of Ulassai.

5.5.2 InSar analisys

Space-borne Interferometric Synthetic Aperture Radar (InSAR) data have been used to analyse the slope deformation in Bruncu Pranedda area. According with the geomorphological evidences PS-InSAR analysis showed that most PSs were located inside the Bruncu Pranedda Lateral spread. The data on the period 2014–2020 allowed the recognition of active lateral spread and the measurement of their movement rates, which turned out to be extremely slow, ranging from 4 to 10 mm/year (Figure 42). We used only high PS (Permanent scatters) coherence (0.6 – 1) located in the rocky outcrops. Low coherence points are located on rockfall deposits and in vegetate areas.
It was possible to observe seasonal deformation trends with an excellent correlation among all of the PSs analyzed. Generally, no movement was observed during the winter and spring, but an acceleration was observed during the summer and autumn.
No movement was individuated in urban area, in the middle slope of Bruncu Pranedda paleo DGSD and in the Tisiddu large toppling.

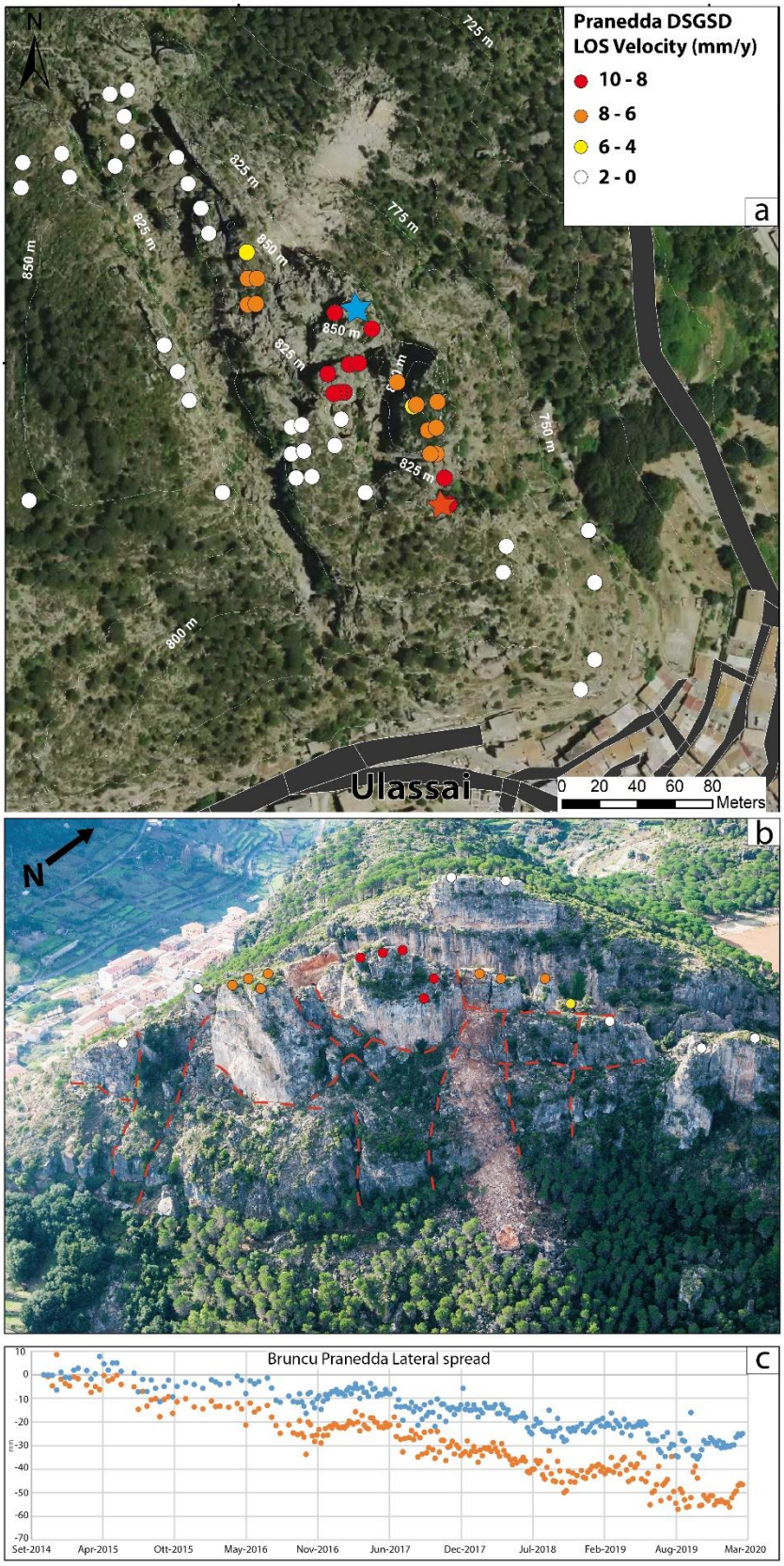

Figure 42 Analysis of the InSAR data. The points represent high-coherence permanent scatters located on rocky outcrops. The stars in a represent the PSs used to analyze the time series shown in c. (a) Bruncu Pranedda lateral spread., b) UAV photo with localization of the permanent scatters. C) Time series extracted with the representative permanent scatters. The vertical axes represent the cumulative LOS displacement; the horizontal axes represent the time. (a) Bruncu Pranedda lateral spread—seasonal displacement trend, maximum displacement of 5 cm from 2014 to 2020;

5.5.3 GNSS movement vectors

The GNSS survey carried out in 3 acquisitions from January 2021 to November 2021 in the lateral spread of Bruncu Pranedda showed data consistent with the geomorphological evidence and the InSar data (Figure 43). There is a need to acquire the data for a longer period in order to have more representative data of the kinematics in progress.

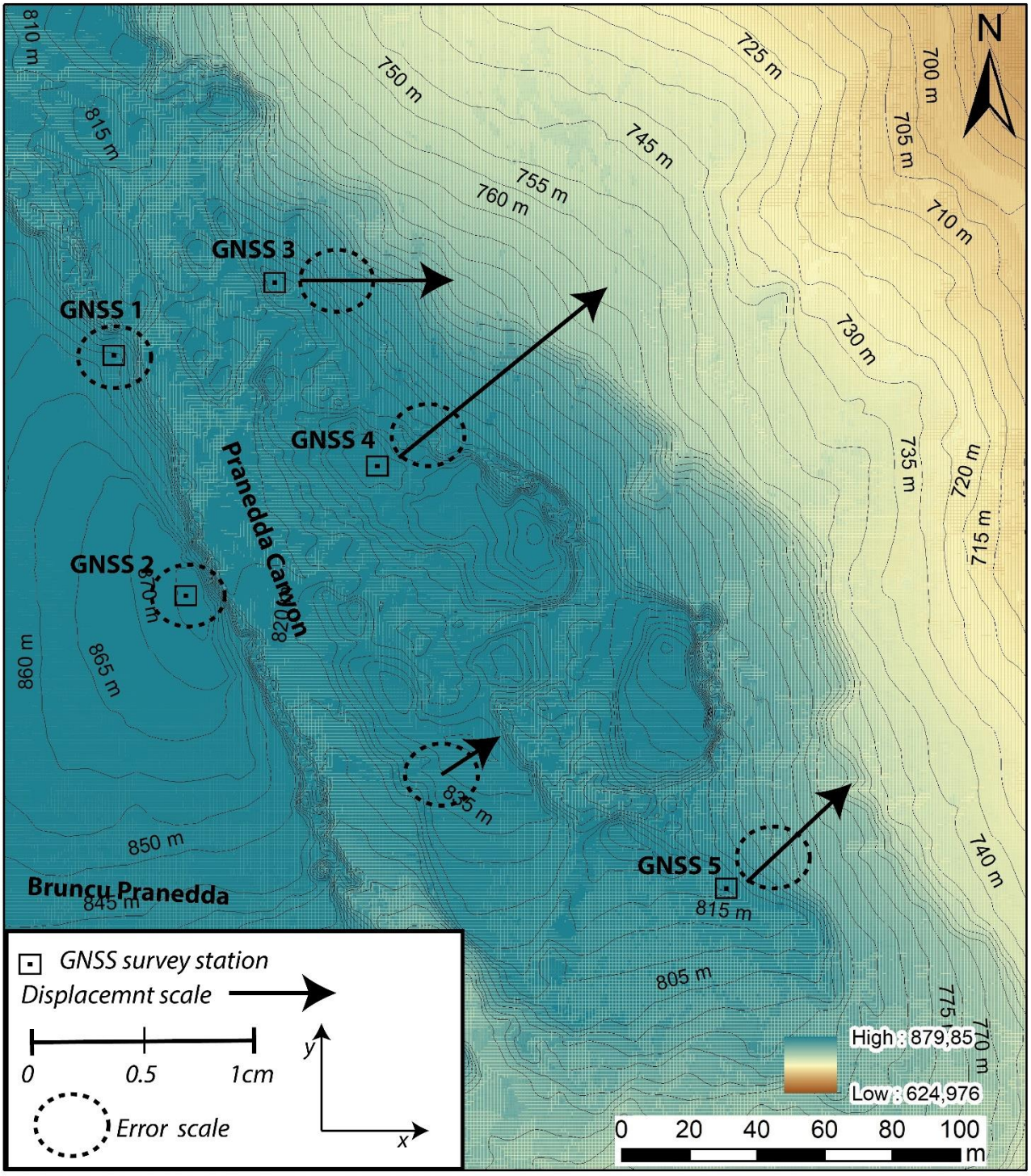

Figure 43 - GNSS Displacement of Bruncu Pranedda Lateral Spread. Black arrow represent the direction and the speed of the measured points.

The movement data are representative of the large Dolomite blocks with diferential displacements that modulate a larger-scale shift of the entire portion of the slope. It is necessary to take into account that the movements measured with GNSS are representative of the top of the rocky reliefs on which the measurement was acquired and could be different in depth due to tilting movements that may have affected the block. The processing showed error values of approximately +- 3mm per acquisition. To validate the error, the acquisitions were performed with a distance of 24 h. The analysis of the data of the acquisition measurement and of the calibration measurement showed a correlation between the error identified by the software and the measured error. In accordance with the geomorphological and insar data, the survey points G1 and G2 located on stable sector did not show any movement. Difference between coordinates are always less than 3 mm within the instrumental accuracy of +-3 mm. While the three points measured in the deformation sector showed comparable values with the radar displacement rates between 7 and 12 mm during the acquisitions. These data will be used for a future design and installation of a real time GNSS detection system for alert purposes.

5.5.4 Geotecnical data

The data acquired in continuous by the data logger whit a sensor sampling interval of 30 s and an automatic data transmission to HMS-WEB platfor of 5 min. The data has been continuously acquired since installation, there were some interruptions of some nights caused by persistent conditions of high cloudiness that did not allow to recharge the batteries. This problem will be compensated by increasing the photovoltaic panel and modifying the setting of the acquisition parameters on the basis of the warning thresholds that will be defined. Preliminary data analysis acquired since January 2021 to Decembre 2021 show very low velocity deformation (Table 2) (Figure 44)in the Extensimeters and tiltmeters movements. In particular the extensimeters show a total closing movement between 0.6 and 1.2 mm. Only the E 4 Show a stable condition in during the entire year. The tiltmeter 1 show a Tilting through SSW indicating a rotational movement of the Block of 1.2°. While the tiltmeter 2 show toppling type movement through NE of 2.4°.

Table 5- Geotechnical monitoring data synthesis

MONITORING STATION	**sensor**	**Max openin (mm)**	**Max Closing (mm)**	**Max Excursion (mm)**	**Total Movement (mm)**
Extensimeters					
1 Mt Tisiddu	EXT E1	+1.2	-2.2	2.2	-0.6
	EXT E2	+1.8	-2.2	2.2	-0.8
2 Bruncu Pranadda East	ETX E3	+4.6	-5.6	5.6	-1
	EXT E4	+0.4	-0.2	0.4	+0.2
3 Bruncu Pranadda west	EXT E5	+1.1	-2.4	2.4	-0.7
	EXT E6	+0.5	-1.1	1.1	-1.2

Tilitimeters			
MONITORING STATION	sensor	Max degree	Direction
1 Mt Tisiddu	TLT 1x	0.1	WNW
	TLT 1Y	1.2	SSW
3 Bruncu Pranadda west	TLT 2X	0.4	SSW
	TLT 2Y	2.4	NE

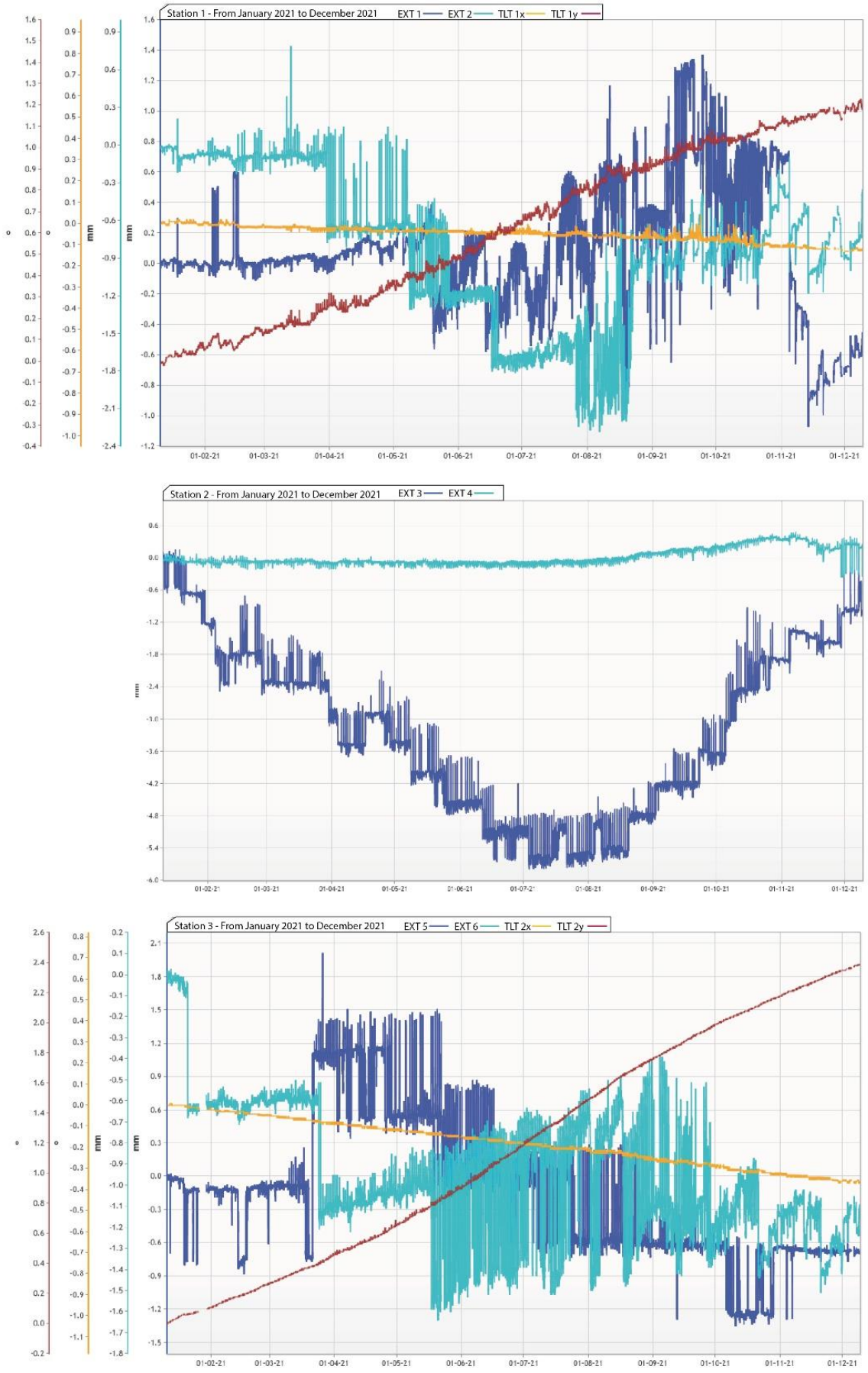

Figure 44 Extensimeters and tiltmeters movements

5.6 Discussion

5.6.1 Landslide hazard

Analysis of the geological and geomorphological setting of plateau edge in Ulassai using UAV photogrammetry and high resolution field surveys allowed to identify different gravitational geological hazard. Landslides with different kinematic and magnitude has been identified: DGSDs with sackung and lateral spread kinematic, giant toppling and widespread rockfalls.

Using InSAR, GNSS, Geotechnical data allows us to understand the kinematic and rates of movement of Ulassai DGSD and Large collateral landslides. These data allowed us to estimate the landslide's future behavior.

The DGSDs is associated with numerous large collateral rockfalls and toppling landslides that affected in the past the area were is located the village. Dolomitic blocks with sizes of up to 30 m on each side were identified widespread linked to mega-rockfall events with rock avalanche features. Currently, a reactivation of quiescent parts of the DGSDs or an acceleration of movements can be triggered by extreme weather events or earthquakes.

Therefore, an acceleration of slope movements leading to a potential catastrophic failure poses a threat to communities, and the monitoring of these slopes is important for early warning and risk reduction.

InSAR data indicate in the lateral spread of Bruncu Pranedda a large slope side affected by a deformation about 1 cm/y downslope in the last 6 years.

The DGSD body of Bruncu Pranedda is composed of several kinematic domains with different speeds. The total collapse of the landslide could partially destroy the northern part of the inhabited center of Ulassai or compromise the provincial road below. The most probable hazard is the partial collapse of the most marginal sectors or the triggering of secondary collateral landslides linked to the deep movements. Evidence of collateral landslides is reported in historical memory with the most recent event of 2014 which led to tremors in the center inhabited.

The InSAR historical series show a trend of seasonal accelerations linked to the may precipitation which leads to an increase in the plasticity of Genna Selole Fm and altered metamorphites.

The availability of an integrated monitoring system made it possible to correlate the displacements measured with the insar technique with data acquired on the ground. Since January 2021, the ground monitoring network using geotechnical instrumentation and GNSS has provided important information on surface displacements. Generally speaking, strain gage instruments recorded a non-linear displacement velocity, with displacement rates that of fractions of mm per month. This depends on the fact that the two ends of the fracture do not show diferenzile displacements but move in a manner consistent with the slope.

In this area we stared a geodetic monitoring system to validate and calibrate satellite data and to understand the differential movement under deformation slope.

The initiation of rapid catastrophic processes such as rock avalanche is associated with the accelerations of DGSDs. These accelerations are linked to seismic activities and extreme rainfall events. The latter cause the hydration of the rocks in the shear zones, decreasing the geomechanical characteristics. In this sector, the geotechnical instrumentation was installed in two orthogonal fractures to each other and within the deformation mass. In this area, tiltmeter show a tendency to close fractures up to 1.2mm. The major component of the closing movement is towards the East in accordance with the direction of movement of the lateral spread.

The tiltimeter shows a tilting of the block up to 2.4 ° in accordance with the lay of the stratification. This inclination value turns out to be quite high for such a short time span of acquisition. The future acquisition will clarify whether the tilting movements are of a linear or oscillatory nature related to the movements of the lateral spread.

In the paleo-DGSD with sackung characteristics there are no InSAR data due to a quiescent state of the deformation. In this contest, the geological hazard is linked to the overturning of large dolomitic pillars separated by paleotrenches and landslides. These are filled with collapse deposits and internal movement can trigger secondary landslides. In this context, monitoring is necessary both in anticipation of the toppling of the great Dolomite bodies and for secondary landslides. The extensimeters sensors installed made it possible to measure internal movements of the paleo DGSD in particular, the extensimeter E3 showed a closure trend of 5mm and reopening of 5mm during the year, this linked to movement linked to basal variations in the stratigraphic contact between the formation. of Dorgali and the formation of Genna Selole and the altered base. The E4 extensimeter did not show any movement, identifying a momentary stability condition.

In the Monte Tisiddu sector, the rock pillar is monitored with two extensimeters and a tilt meter. The fracture separates it from the planking up to 5 m indicates a prevalent kinematics of distension with a slightly larger opening in the upper part. This indicates a slight tilting component downstream of the block. The data from the geotechnical instrumentation indicate a cumulative deformation in closure up to 0.8 mm and a tilting of the block up to 1.2 ° upstream, indicating a sliding movement of the foot downstream.

It should be emphasized that these data are preliminary and fundamental as they are for cognitive monitoring purposes. The monitoring system will be integrated and appropriately sized on the basis of the information acquired, this does not affect the use of an early warning system in the cognitive phase.

In general, the main deformation context is linked to dynamics associated with the lateral spread at various scales. The rigid formation of the Dorgali dolomites slides with a speed of up to 1 cm per year on the formation of genna Selole and on the altered metamorphites. This process is observable on a lower scale in the paleo-Sackung of bruncu Pranedda and in Mount Tisiddu. This process is dominated by predisposing factors related to the tectonic and stratigraphic context well described in previous works (*Demurtas et al. 2021*). Extreme meteorological events linked to precitypitation and earthquakes can trigger an acceleration in the deformation process and cause collateral landslides or the collapse of parts of the DGSD. The collateral landslides are of two types:

- large toppling related to the collapse of marginal parts of the slope or similar isolated cases and large toppling of Mount Tisiddu
- collapse landslides (decompression landslides) with source area in extensional trenches and open fractures. These are filled with deposits of collapse caused by the movement of the walls causing the landslide.

5.6.2 Early warning system

In order to mitigate the geomorphological risk and guarantee safety conditions for the inhabitants of the municipality of Ulassai and for the users of the tourist activities, it is necessary to set up a real-time monitoring system with the aim of early warning (Figure 45)**Errore. L'origine riferimento non è stata trovata.**Based on the typology and volumes involved by the DGSD and the large toppling, it is not possible to build engineering works to counteract the state of activity of the processes in place. The simplicity of the early warning system management system is a fundamental component for the correct functioning of the system. It is therefore necessary to propose a management system that is editable by the population. In emergency conditions, the action to be taken must be clear and rapid. Predicting the imminent failure of a landslide and alerting people is a very complicated task and the parameters to be taken into consideration are the following:

- Type and kinematics of the process.
- Evidence of historical landslides
- Evolutionary trend based on the PS-InSAR time series validated by ground data using GNSS
- Constant monitoring of geotechnical data and validation of alert thresholds.

The early warning system will be based on the measurements of the geotechnical instrumentation, in particular by continuously monitoring the opening or closing of fractures with extensimeters and the inclination of large blocks with tiltmeters, and whit widespread GNSS antenna that acquired in continuous to monitor the differential displacement of the blocks

The next step consists in the selection of appropriate thresholds. The choice of reliable values depends on both scientific and social considerations. In fact lower and more conservative thresholds are more likely to produce false alarms that may have strong impacts on the society.

Conversely, higher values result in a shorter time left for taking action or, in the worst case, in missing events. In other words the thresholds can only vary within a range between two boundaries defined by tolerability of false alarms and acceptable risk criteria. Based on InSAR displacement rates which correspond to about 10 mm/y The alert thresholds provisional have been defined. The thresholds are 2.5 mm/h and 5 mm/day for extensimeters and 0.3 °/h and 0.5 °/day for tiltmeters. These thresholds will be calibrated through the analysis of the movements recorded by the sensors over the course of a years. The alert measures proposed are based on information actions such as visual and audible alarms by siren and evacuation of the areas affected by mega-toppling processes.

a

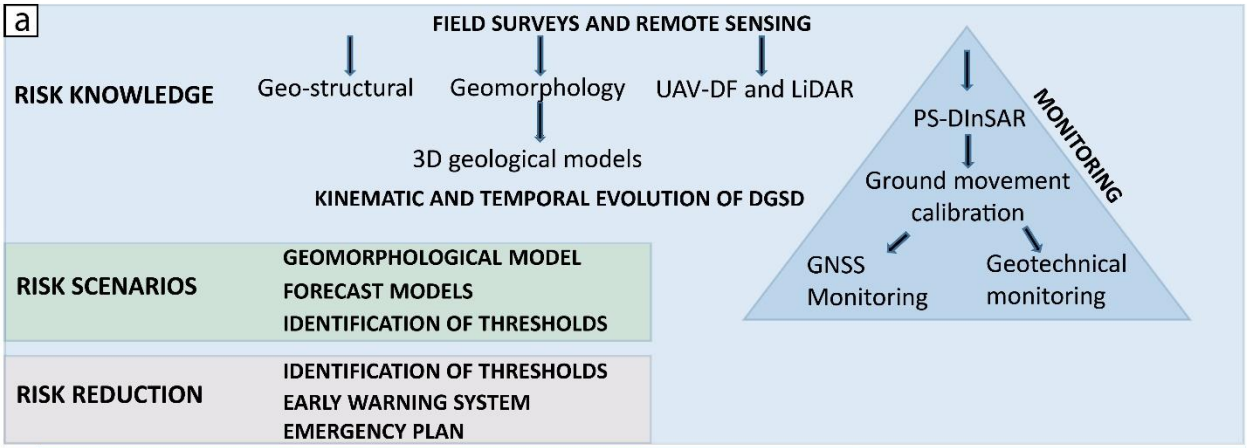

b

WARNING LEVEL	TRIGGER	DEFINITION	RESPONSE
ORDINARY LEVEL	Default level	Normal activity encompassing to some degree, seasonal variation	Data are checked daily. Half yearly monitoring bulletin
ATTENTION LEVEL	Acceleration of movement below the threshold	Increased activity possibility due to prolonged rainfalls. Seismic event of interest. Potentially dangerous events.	Data are checked more frequently. Daily monitoring bulletin. Evaluation of false alarms. H24 personnel from each stakeholder are alerted. Preparing for alarm.
ALARM LEVEL	Exceeding the thresholds. Forecast evaluation by experts	Accelerating trend far beyond any seasonal fluctuation. Collapse is expected	Data are checked even more frequently. evaluation of false alarms. Two monitoring bulletins per day. partial evacuation of areas at greatest risk.

c

Figure 45 –A) Conceptual model of the work. B) Alarm levels. C) Monitoring station 1 whit weather station the siren.

6 CHAPTER V

6.1 Correlation with different geodynamic and climatic context

In Sardinia, the DGSDs were analyzed for the first time in this thesis with particular reference to the cases described above. Correlations with different scenarios present in the literature have been performed. DGSDs and large landslides have been analyzed in the emerged and submerged area of southern Sardinia. During the abroad research period, DGSD in artic environmental of the Svalbard archipelagos ware carry out. Starting from bibliographic analysis, a different DGSD cases around the world were studied. DGSDs are present in different geological, geodynamic and climatic context how report in the the map produced by *Pánek & Klimeš (2016)* (Figure 46)

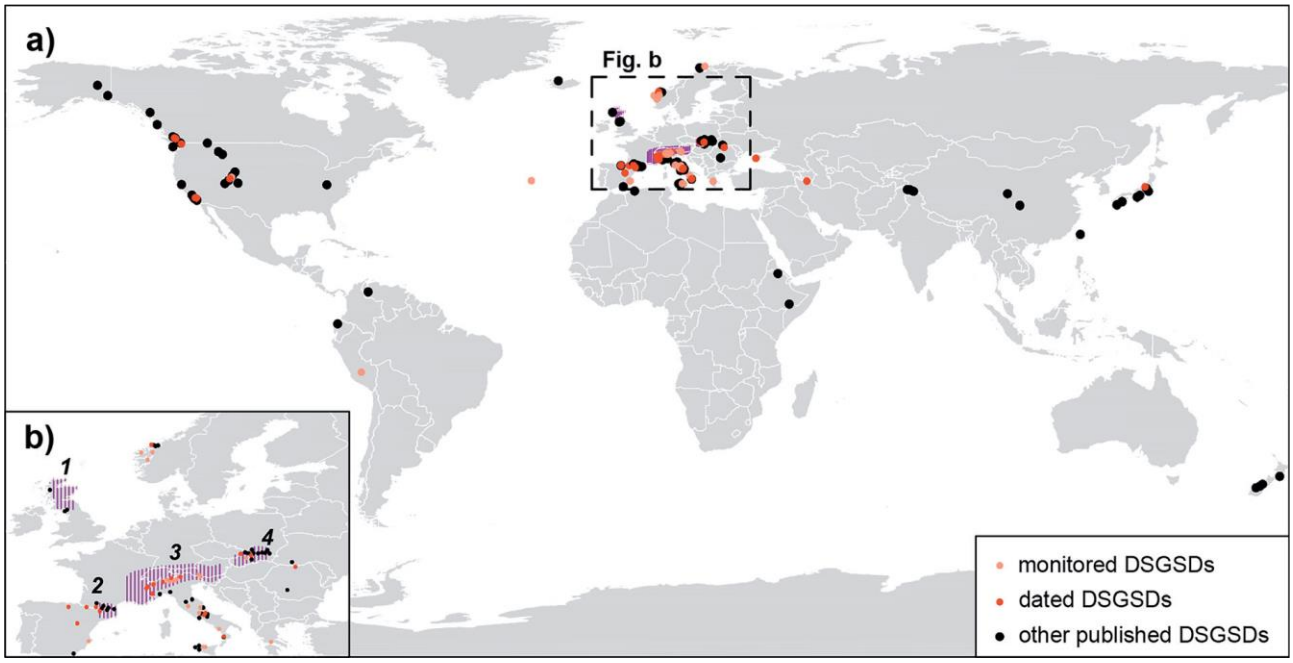

Figure 46 Distribution of key DGSDs in the world, especially cases from studies published since 1990s (redrawn from Pánek & Klimeš, 2016): a) worldwide context; b) detailed view of Europe. The numbered hatched regions contain published databases of DGSDs from: 1) Scottish Highland (Jarman, 2006); 2) Eastern Pyrenees (Jarman et al., 2014); 3) European Alps (Crosta et al., 2013); 4) Western Carpathians (Nemčok, 1982; Alexandrowicz & Alexandrowicz, 1988)

The main bibliographic cases present in bibliography can by summarize into different context.

In mountain chains: Andes (*Vilímek et al., 2007; Audemard et al., 2010; García-Delgado, 2020*), Carpathians (*Hradecký & Pánek, 2008; Pánek et al., 2011*), Himalaya (*Thuro et al., 2004*), Japanese Alps (*Chigira, 2009; Chigira et al., 2013a*) Rocky Mountains (*Varnes et al., 1990; McCalpin & Irvine 1995*), In glacial and periglacial environment: Alaska (*McCalpin et al., 2011; Newman, 2013*), Iceland (*Coquin et al., 2015*). The European Alps are certainly among the most studied places: many cases have been studied in Italy (*Discenza e Esposito 2021*)

6.2 DGSDs in south-west Sardinia

Extracted from: Deiana, G.; Lecca, L.; Melis, R.T.; Soldati, M.; Demurtas, V.; Orrù, P.E. Submarine Geomorphology of the Southwestern Sardinian Continental Shelf (Mediterranean Sea): Insights into the Last Glacial Maximum Sea-Level Changes and Related Environments. *Water* 2021, *13*, 155. https://doi.org/10.3390/w13020155

The paper shows the results of a high-resolution survey on the continental shelf off San Pietro Island (southwestern Sardinia) (Figure 47). Multisensor and multiscale data obtained by means of seismic sparker, sub-bottom profiler chirp, multibeam, side scan sonar, diving, and uncrewed aerial vehicles made it possible to reconstruct the morphological features shaped during the LGM at depths between 125 and 135 m. In particular, for the topic of this thesis, tectonic controlled palaeo-cliffs affected by landslide were detected.

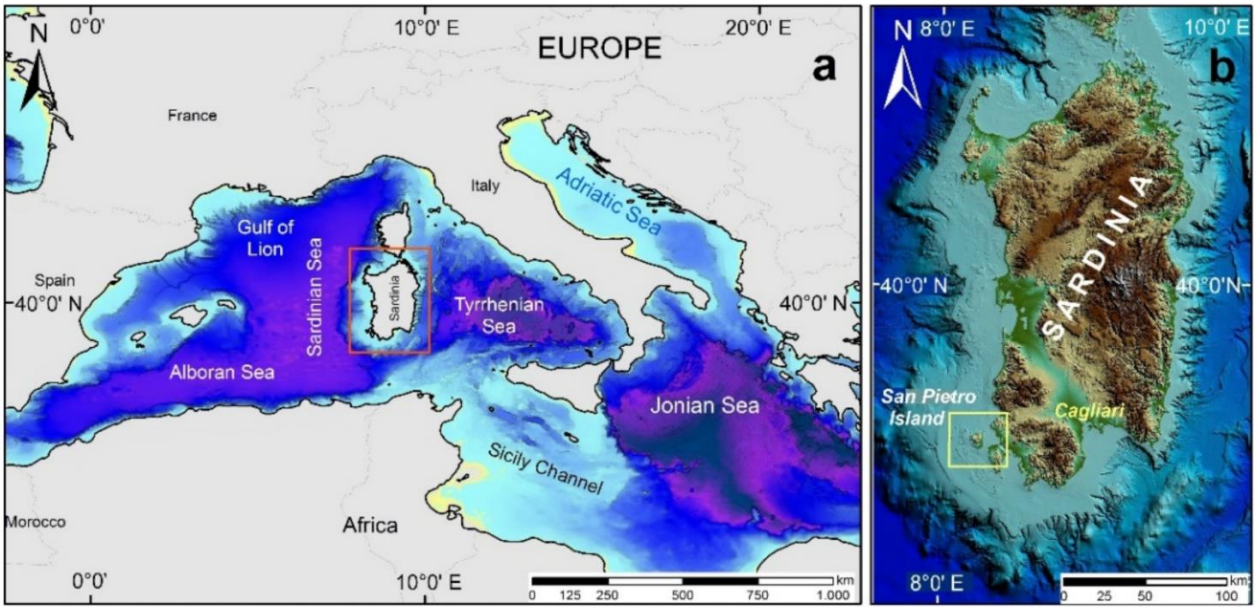

Figure 47 Geographic location and structural setting of the study area: (a) Sardinia Island within the Mediterranean Sea; (b) San Pietro Island on the SW side of Sardinia.

The submerged palaeo-cliff base is predominantly located at the shore platforms and is often affected by iso-oriented shallow erosive channels in line with the main tectonic lineaments. The basal abrasion platform has an irregular shape and is frequently covered by large sub-angular blocks of multi-decametric dimensions or by rockfall deposits. Some large blocks were found hundreds of metres from the detachment areas and recalled the evolutionary model of the block slides diagnosed in other submerged areas, such as the continental sector of the Gulf of Cagliari (*Deiana et al. 2016*), the southern Apulian margin off the coast of Santa Maria di Leuca (*Savini & Corselli, 2010*), and the Malta continental shelf (*Prampolini et al. 2017,2018, 2019 , Soldati et al. 2018*).The palaeo-cliff surfaces are often sub-vertical and are affected by sub-vertical fracture systems, which run parallel to the main tectonic lineaments. In some areas, sub-orthogonal joints are present and probably represent

columnar cooling fracturing, similar to that in the southern coastal sector of Sardinia. The cliff summit edges are developed at depths of 80–90 m, exhibiting a palaeo-cliff system 30–50 m high, on average. In some palaeo-cliff sectors, double ridges can be observed, pinpointing to the extensional trenches with counter-slope flanks. They were interpreted as distensional landforms and correlated with mass movement involving rotational kinematics (Figure 48b and Figure 49).

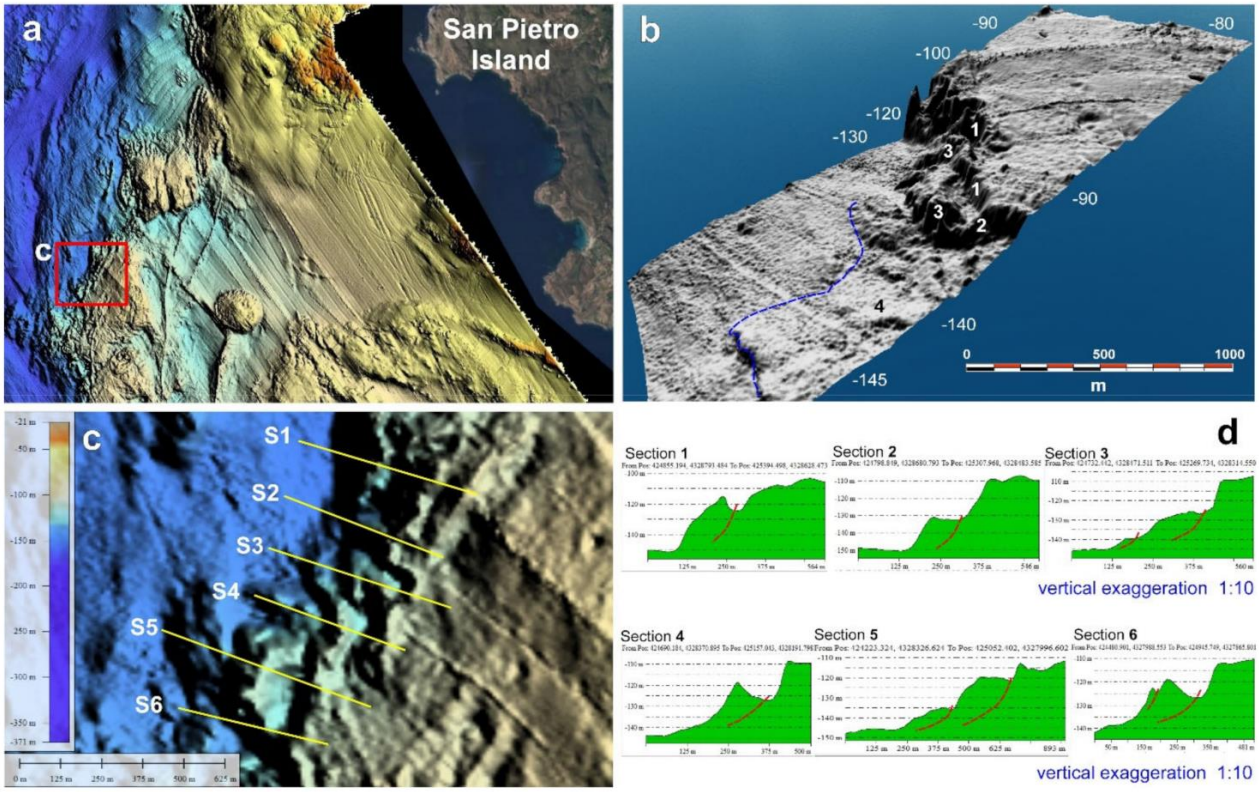

Figure 48 DTM from MBES data showing the Last Glacial Maximum (LGM) palaeo-cliffs. (b) DTM 3D from MBES data showing some landslides affecting the submerged palaeo-cliffs: 1-main scarp; 2-distensional trench; 3-landslide bodies; LGM palaeo-sea-level (blue line). (c) detail of tectonic controlled palaeo-cliffs with localization of morphometric profiles. (d) Morphometric sections and hypothesized sliding surfaces (red lines).

The interpretation of the kinematics of these drowned-landslides was based on the geomorphological surveys of similar palaeo-landslides located along the coast between Capo Altano and Porto Paglia. In this sector, large landslides with rotational kinematics were systematically observed (*Castedo et al 2017*). The first landslide is located 500 m north of Altano Cape, while the second landslide has been recently found to the south of Porto Paglia (Figure 49A). Both palaeo-landslides have their foot fossilised by regression eolianites (MIS 4, MIS 3). Therefore, their movement likely occurred at a high sea-level stand during the last interglacial period (MIS 5) (*Orrù & Ulzega 1986*) (Figure 49D). From a morphological point of view, the first palaeo-landslide is distinguished by a complex detachment niche and is organized in two scarps. A wide trench and a counter-slope terrace are considerably lowered and are partially covered by colluvial deposits. This landslide shows the evidence of recent reactivation. The second palaeo-landslide has a detachment niche with a single

scarp, a counter-slope terrace at the base of the niche, and a trench partially buried by collapsed blocks (Figure 49C,D).

In order to correlate the shapes of the submerged palaeo-cliffs with the modern (subaerial) cliffs and relate them to the landforms associated with rock falling and toppling, we carried out proximity remote sensing surveys by UAVs on some modern cliffs engraved in the same volcanic lithologies on Sant'Antioco Island and Altano Cape.

The ROV surveys allowed us to explore the palaeo-cliff morphology, particularly, the extensional trenches.

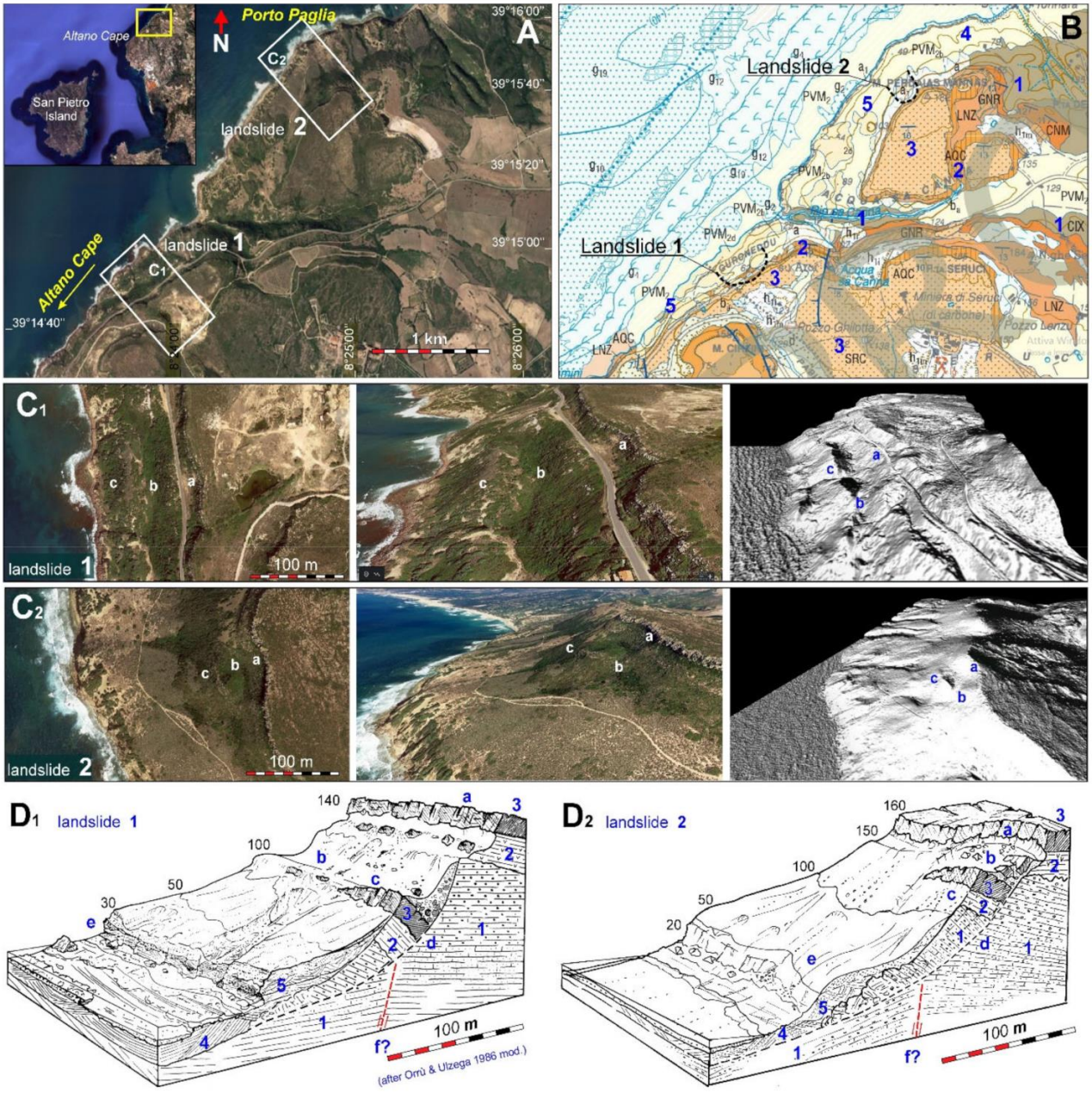

Figure 49 (A) Location of the studied coastal palaeo-landslides; (B) Excerpt of Geological Map of Italy—scale 1:50,000 Sheet 555 "Iglesias" (Pasci et al., 2015 [33]), with landslides location; (C) Aerial photo, photo 3D view and Lidar DTM 3D of landslide 1 (C1) and landslide 2 (C2); (D) Palaeo-landslide 1 3D interpretive models (D1) and Palaeo-landslide 2 (D2), showing rotational kinematics, probably due to the basal erosion during the high-stand MIS 5.5 and the subsequent foot fossilization by continental deposits of the Upper Pleistocene (MIS 4,3,2). Geolithological

legend: (1) sandstones and conglomerates, Cixerri Formation—CIX (Eocene-Oligocene); (2) ignimbrites, tuffs—AQC (Middle Miocene); (3) ignimbrites, lavas—SRC (Middle Miocene); (4) eolianites (Upper Pleistocene—MIS 4-3?); (5) eolianites and colluvia—PVM (Upper Pleistocene—MIS2). Morphological legend: (a) detachment niche; (b) trench; (c) counter-slope terrace; (d) rotational sliding surface; (f) cliff engraved in the Pleistocene aeolian deposits that fossilize the landslide foot.

The comparison between the geomorphological features of the subaerial coastal palaeo-landslides (Figure 49) and the identified submerged palaeo-landslides (Figure 48) has shown that both types of landslides were affected by rotational kinematics. However, the submerged palaeo-landslides have low-angle sliding surfaces, and their landslide bodies are stacked, dissimilar to the present-day landslides. These differences can be linked to instability after drowning, in wave energy conditions probably very different from the present ones (*Sunamura 1977; Kageyama et al 1999*). To better understand the coastal landslides kinematics in this area, it is important underline that the waves currently interacting on the coasts of western Sardinia are the most energetic in the entire Mediterranean basin. In fact, the waves measured in Alghero (northwestern Sardinia) during extreme meteorological events have a maximum height of over 10 m (*Atzeni 2003; Sulis & Annis 2014*).

6.3 Evidence of Deep-seated Gravitational Slope Deformation on Nordenskiold Land (Western Svalbard)

During the research period carried out in Trondheim in Norway, in collaboration with the Norwegian Geological Survey (NGU) and the University Center in Svalbard, the DGSDs in the Svalbard Islands were studied as part of the "Mapping of deep seated gravitational slope deformations (DGSDs) on Svalbard (Svalbard-dgsds)" project. The first results are summarized in the paper "Evidence of Deep-seated Gravitational Slope Deformation on Nordenskjold Land (Western Svalbard)" ***In prep. paper****. The work is based on remote sensing mapping and database creation of the geomorphological elements related to potential DGSDs in the Svalbard Islands. The survey and the geomorphological description/mapping is carried out through DEM and aerial photographs together. The work allowed the identification of large areas affected by DGSDs in the slopes of glacial valleys and in the coasts of the fjords in a sector of the archipelago.*

In Western Svalbard Islands morphotectonic evidences and deep-seated gravitational slope deformations (DGSDs) are studied. They have so far not been extensively described or analysed in relation to arctic environments. We analysed geomorphological setting and DGSDs located on the coastal fiord and U-Shaped valleys slope on Nordenskiold land. On Svalbard Island the last Uplift phase and active erosion of the last glacial stage leads high slope topography. Mesozoic and cenozoic, by marine to continental facies sedimentary rocks affected by compressional to transpressional tectonism are presented. This litho-structural structural setting is prone to the development of DGSDs. In this context, we investigated a large-scale DGSDs distribution and the control factors linked to litostructural and geomorphyc setting. The data show correlations between DGSDs dynamics and the geomorphological evolution of the area closely linked with uplift rebound. A compound landslides with lateral spreading and rock slide features which involves mainly clastic sediments rocks and shales are analysed. Based on a detailed remote sensing surveys and bibliographic data, we studied geological, structural, geomorphological setting, the kinematics and temporal behavior of the main DGSDs. The use of high resolution aerial photogrammetry DTM allowed a depth morphometric analysis and the creation of interpretative 3d models.

Different morphological feature are individuated linked to slopes instability such as trenches, scarps, tilted blocks and abnormal slope profiles. This features show a different evolutionary stages of DSSD that we related whit morphotectonic and glacio-fluvial deposits of the area. A multidisciplinary and multiscale approach allowed the formulation of new hypotheses about geo-structural setting, evolution and kinematics of deep landslides.

6.3.1 Introduction

In west-central Svalbard Island different morphological features such as trenches, scarps, tilted blocks and abnormal slope profiles linked to deep-slopes instabilities have been identified. DGSDs have so far not been extensively described or analysed in arctic environments. We analyse the geomorphological setting of identified DGSDs located in the coastal fjord- and U-shaped valleys in Nordenskiold land. The last tectonic phase and the glacial erosion of the last glacial stage lead to a steep slope topography. Mesozoic and Cenozoic marine to continental facies sedimentary rocks that have been affected by compressional to transpressional tectonism are present in the peninsula. This litho-structural structural setting is known to be prone to the development of DGSDs. Deep-seated gravitational slope deformation (DGSD, *Dramis & Sorriso-Valvo, 1994*) is a complex type of rock slope failure characterised by large dimensions generated in stone rocks (*Dramis et al., 2002*). DGSDs are characterised by slow movements that can suddenly accelerate and cause catastrophic collapse of sections of the deformed slopes (*Agliardi et al., 2020; Crosta & Agliardi, 2003; Nemčok, 1972; Ostermann et al., 2017; Radbruch-Hall, 1978*). Therefore, this phenomenon represents an important geo-hazard in relation to the deformation of large infrastructures and secondary landslides. Although DGSDs represent an important geological hazard, information about them was scarce for a long time (*Soldati, 2013*). Recent technologies for both remote sensing (satellite data, space-borne interferometric synthetic aperture radar, etc.) (*Mantovani et al., 2016; Frattini et al., 2018; Novellino et al., 2021*) and proximal sensing (unmanned aerial vehicle (UAV) (*Devoto et al. 2020; Eker & Aydin, 2021, Deiana et al.2021*), light detection and ranging (LiDAR), etc.) have enabled a better understanding of these processes. They are characterised by very slow deformation rates (*Cruden & Varnes, 1996*), landform assemblages (as double-crested ridges, trenches, synthetic and antithetic (uphill-facing) scarps, tension cracks, convex (bulged toes), and deep basal shear zones (*Agliardi et al., 2001, Chigira, 1992; Crosta et al., 2013; Mariani & Zerboni, 2020; Panek et al., 2016*). Shear zones present characteristics of cataclastic breccias with abundant fine matrix (*Crosta & Zanchi, 2000*) and thicknesses up to tens of metres (*Ostermann et al., 2017*).

In this study, we present for the first time a DGSD inventory in Svalbard archipelago. The study area is located in Nordenskiold land (Figure 50). The area is characterised, in the Eastern sector, by plateaus separated by deep glacial valley and in the western alpine type mountain in relation to the different lithologies.

Main evidence of DGSD in U-shape valleys and Fjord coast vary along the slope. A set of ridge-top trenches and back scarps with lengths of hundreds of metres are present in the top slope. Hummocky

slopes, scarps and tilted bedrock blocks characterize the middle slopes. In the foot slope landsforms are constituted by fluvio-glacial deposits

Nordenskiöld Land in Central Spitsbergenof Svalbard is characterized as a high latitude, high relief periglacial landscape with permafrost occurring both in mountains and lowlands

We have investigated the large-scale distribution of DGSDs and the potential control factors linked to litostructural and geomorphic setting. Compound DGSDs with lateral spreading and rock-slide features involving mainly clastic sedimentary rocks and shales are analysed. Based on detailed remote sensing surveys and bibliographic data, we studied the kinematics and temporal behavior of the main mapped DGSDs. The use of high-resolution aerial photogrammetry DTM enabled in-depth morphometric analysis and the creation of interpretative 3D models. Various marine terraces of late Pleistocene and Holocene ages are present in the coastal fjords and down slope of the glacial valleys. These deposits are located at different elevations above sea level due to the post-glacial glacio-eustatic uplift. Morphostratigraphic studies were made to attempt a correlation between Quaternary paleo-coastlines and the DGSDs processes. The morphological features show the same evolutionary stages of DGSD that we relate to morphotectonics and marine/glacio-fluvial deposits of the area. A multidisciplinary and multiscale approach allowed the formulation of new hypotheses about geo-structural setting, evolution, and kinematics of deep landslides in the arctic valley/fjord landscape. The data indicates, through correlations between DGSDs dynamics and the geomorphological evolution of the area, that DGSD activity is closely linked to uplift rebound.

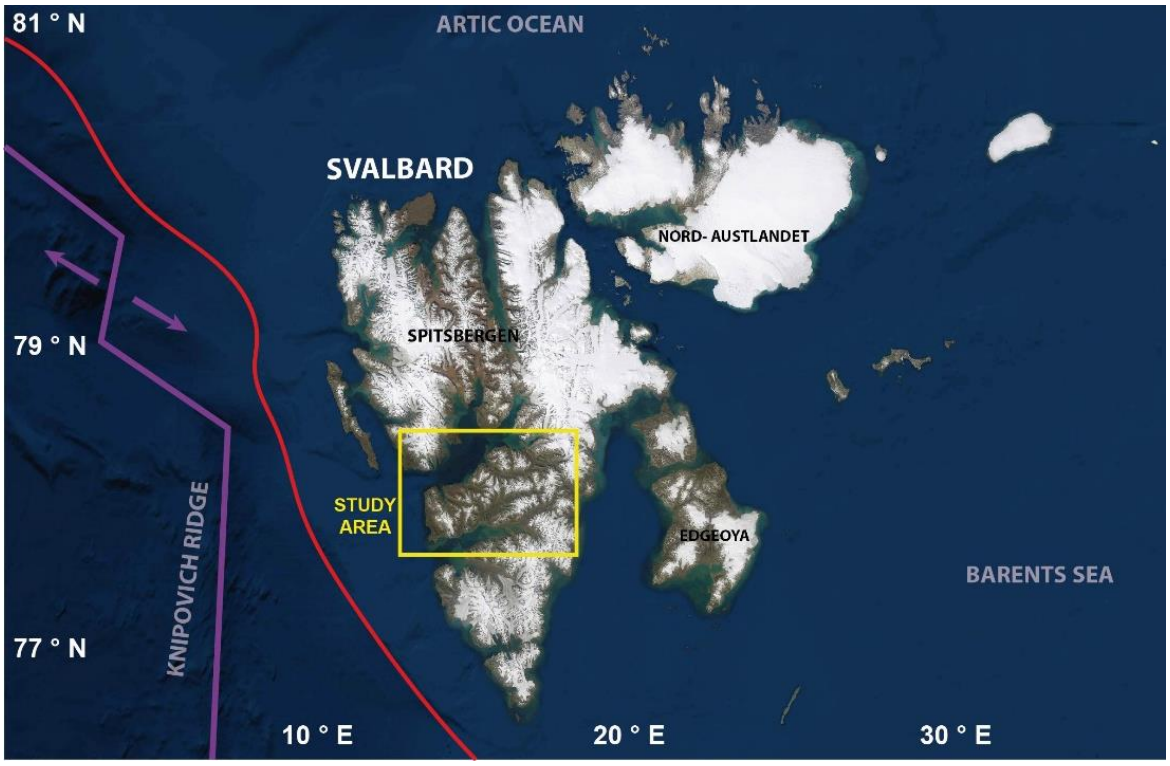

Figure 50 Geographical location and structural features of the study area: red line represent the continental crust; Violet line are the oceanic rift; In yellow the study area.

6.3.2 Geological and geomorphological setting

The study area encompasses the land area in central Spitsbergen called Nordenskiöld Land. This forms a kind of large-peninsula delineated by Isfjorden and Sassenfjorden to the north and by Van Mijenfjorden in the south.

The landscape is dominated by mountain plateaus with a sub-horizontal stratification of sedimentary bedrock (*Dallmann et al., 2001; Major et al., 2000*). Glacial and periglacial processes are the main superficial agents that modified the landscape after the regional deglaciation (*Gilbert et al., 2018; Härtel and Christiansen, 2014; Sørbel et al., 2001*).

The geology of Svalbard is varied and complex and covers all the geological periods (*Humlum et al. 2003*). The bedrock geology and fault system controls most of the landscape. The highest mountains (> 1000 m a.s.l.) are located in the central part of Nordenskiöld Land, with the highest altitude being at Gustavfjellet mountain (1235 m a.s.l), located north of the mining settlement of Svea. Bedrock is exposed mainly on rock noses in the upper steep part of the slopes composed of the resistant Tertiary sediments (*Dallmann et al., 2001; Major et al., 2001*).

Nordenskiöld Land geology is characterize by 3 main tectonic control contexts. In the western sector there are the oldest geological units in a complex geostructural contest with ages from the Precambrian to the Permian. The sector is made up of EW and SW-NE main folds and NS faults. The oldest units are mainly made up of low and medium grade metamorphic lithologies.

The central and eastern part is made up of Jurassic and Cretaceous and Paleogenic and Neogenic units and units. The latter settled in a grabben valley called the central tertiary basin. While the paleogenic units consist of sandstone, siltstone and shale and the Mesozoic units from bituninus shales. The plateaus are covered by extensive block fields. The lower and central parts of Adventdalen and the neighboring valleys are characterized by fluvial, alluvial and eolian (loess) deposits with typical permafrost-related landforms, such as ice-wedge polygons and pingos (*Sørbel et al., 2001*).

The valley slopes are covered by allochthonous weathered material, colluvium and alluvial fans, that have been further reworked by mass-wasting processes, such as by debris-flows (*André, 1995*), solifluction (*Harris et al., 2011*), snow avalanche activity (*Eckerstorfer et al., 2013*), and talus-derived rock glaciers (*Humlum, 2000*).

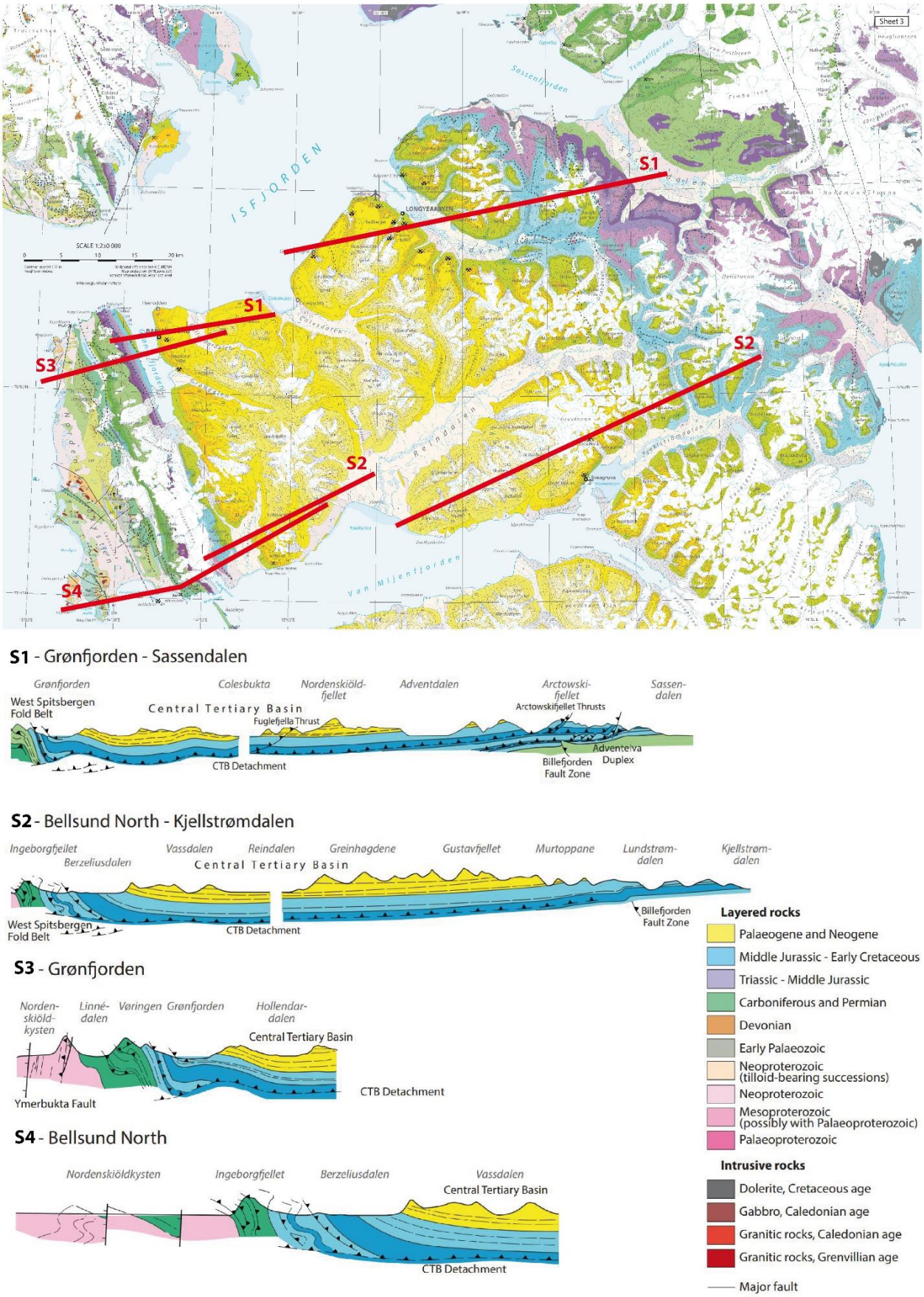

Figure 51 - Geolithological sketch map of the study area based from Geoscience Atlas of Svalbard (Dallmann et al. 2014). Red line indicate the geological cross sections.

6.3.3 Methods

The present paper aim to produce a DGSDs distribution map using of GIS and remote sensing tools in artic enviroment. A geomorphological approach was applied to mapping surficial evidences of the DGSD in the U-shaped valleys and coastal fjords at 1:10.000 scale and were then reduced to 1:250.000 for mapping purposes for about 3.500 km square area

The DGSD distribution map was created using the ESRI ArcGIS/ArcMap using the hillshade from 50x50m cell size from Norwegian polar institute. We analysed in detail two areas with specifically interesting DGSD process: Arktowskifjellet and Hiortfjellet.

To analyse the DGSDs at the local scale, we used high-resolution digital elevation models (DEMs) acquired via aerial digital photogrammetry and LiDAR at scale 2,5x2,5 m cell size and 1x1m cell size. The main evidences linked to rock slope failures are back scarps, extensional trenches, morphological depression, convex slopes (*Agliardi et al 2001*).

Geodatabase into a GIS using the WGS_1984_UTM_Zone_33N reference system was created. A morphotectonic analysis of the peninsula was carried out based on an integrated approach that incorporated a cartographic and morphometric analysis. The rock slope failures evidences was related with geological and geomorphic parameters included geology, tectonic structures, slope, aspect and relief.

3D high-resolution models were used to develop interpretative superficial models using geomorphological evidence and stratigraphic and structural data of the DGSDs.

6.3.4 Results

6.3.4.1 DGSDs inventory and mapping

A detailed landslide inventory map in Nordenskiöld Land first show the distribution and characteristic of DGSD. Also the data allowed to identify the main control factors analysing the relation whit bedrock geology, slope, aspect and geomorphological processes.

The main evidences linked to rockslope faillures are back scarps parallel to contourline with a length of hundreds of meters up to kilometers. Second scarp along the slope evidences a fragmentescion of rockmass due the landslide. Close depressions filled by slope deposits re widespread probably set on extensional trenches. From DEM slope, aspect and elevation topographic attributes s have been derived. These parameters are important to describe the landforms and slope processes. The slope was divided in a scale from 0 to 60°. The aspect is divide in eight classes. The elevation is between 0 and 1217 m a.s.l.

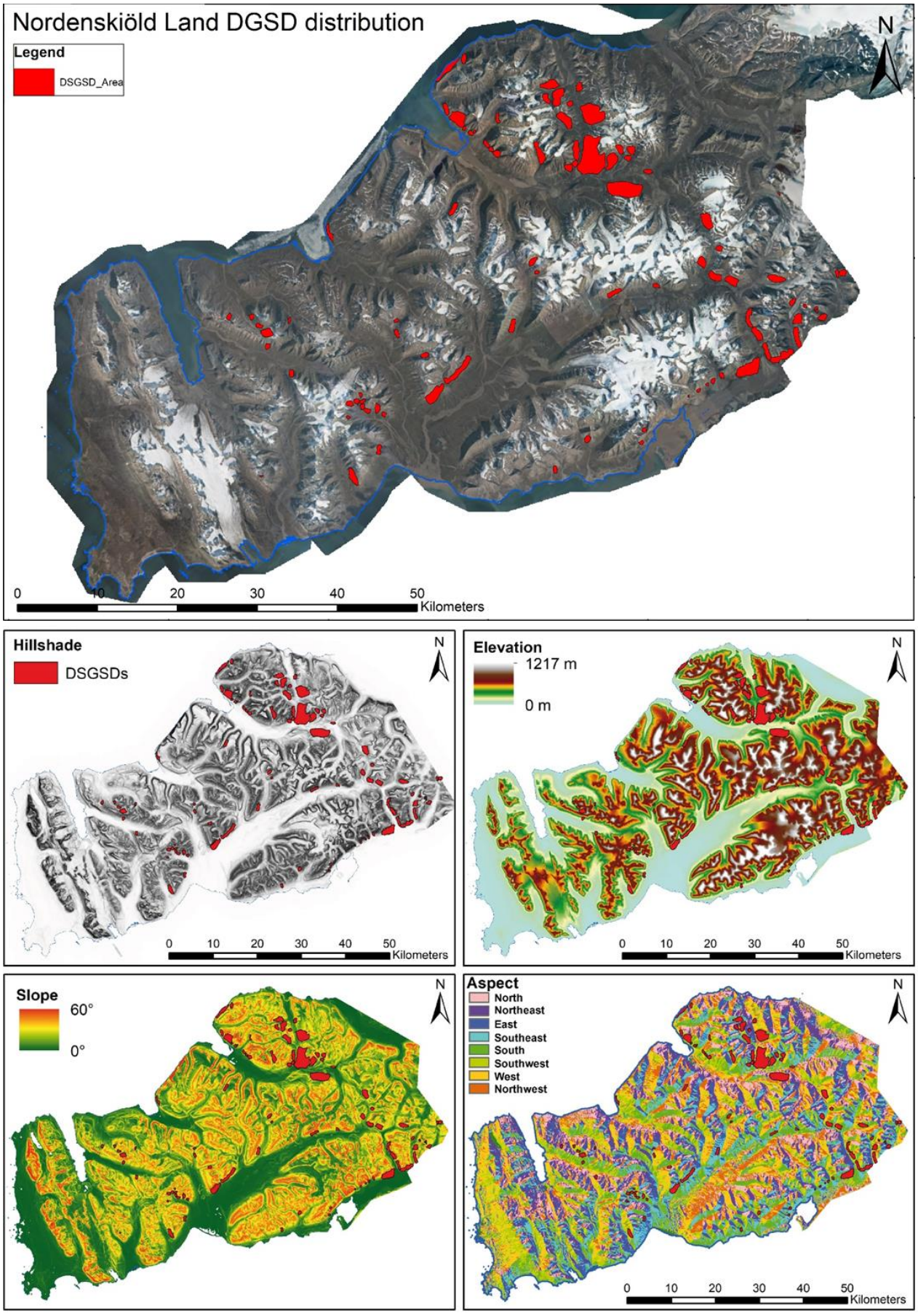

Figure 52 Nordenskiöld Land DGSDs inventory; DEMs geomorphological analysis

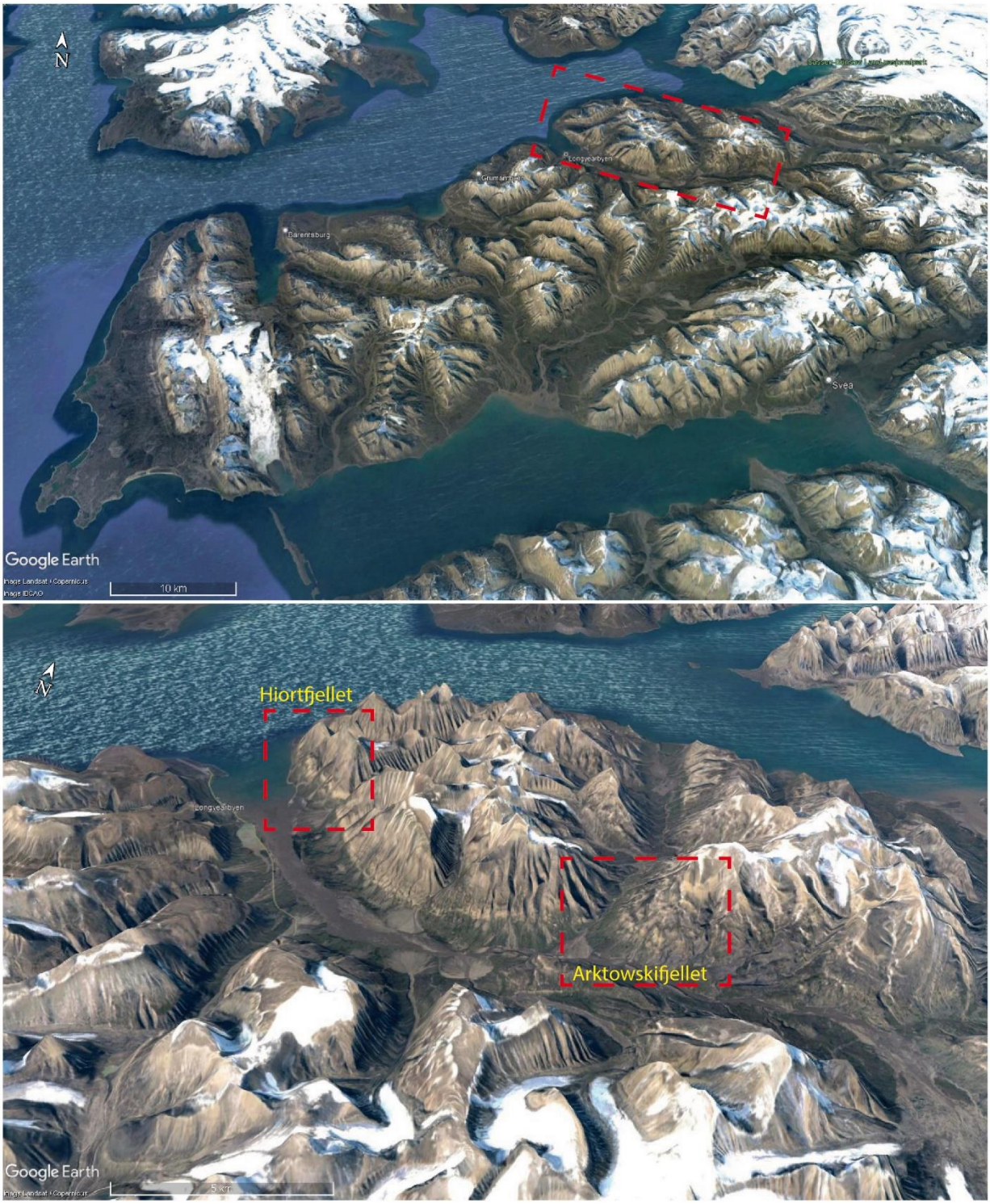

Figure 53 - Google Earth 3d models- In red the location of the two focus areas.

6.3.4.2 Arktowskifjellet

The arktowskifjelle DGSD is located in the right slope of Adventelva valley at elevations of between 100 and 700 m a.s.l.

The slope is characterized by erosional features of both glacial, fluvial and gravitational origin. In particular, the south-west facing slope is represented by marked hummocky morgologies linked to gravitational processes. The tops of the hummocky are represented by rocky outcrops while the

concave parts are covered with glacial deposits and slope deposits. The slope joins the flat bottom valley filled by glacio-fluvial sediments. Black shale and siltstones belonging (late Jurassic) are found in the basal part of the slope on which the dark shale, siltstone and sanstone rest. The sequence ends with a sequence of sandstone, shale, conglomerates affected by coal levels. The structural setting is linked to a fault with immersion at West that plays an important role in the evolution of gravitational processes by weakening the rock mass a few tens of meters from the surface. Helvetiafjellet formation is commonly located at about 600 m of altitude but along the slope there are outcrops up to the valley floor. The thickness of the shear zone ranges from a few meters to tens of meters and is located in the top of Rurikfjellet formation (Figure 54).

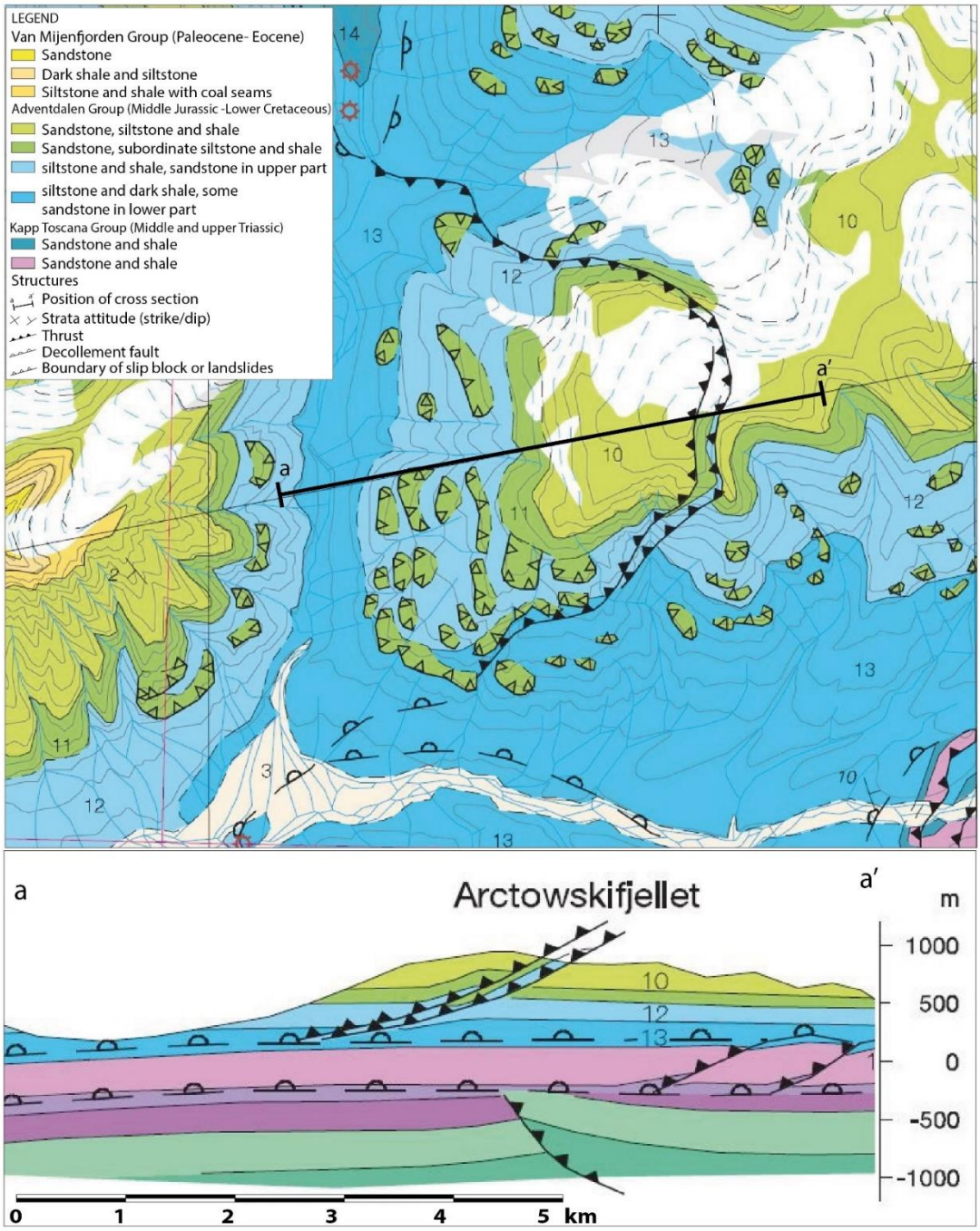

Figure 54 - Arctowskifjellet geological map. From Geoscience Atlas of Svalbard (Dallmann et al. 2014).

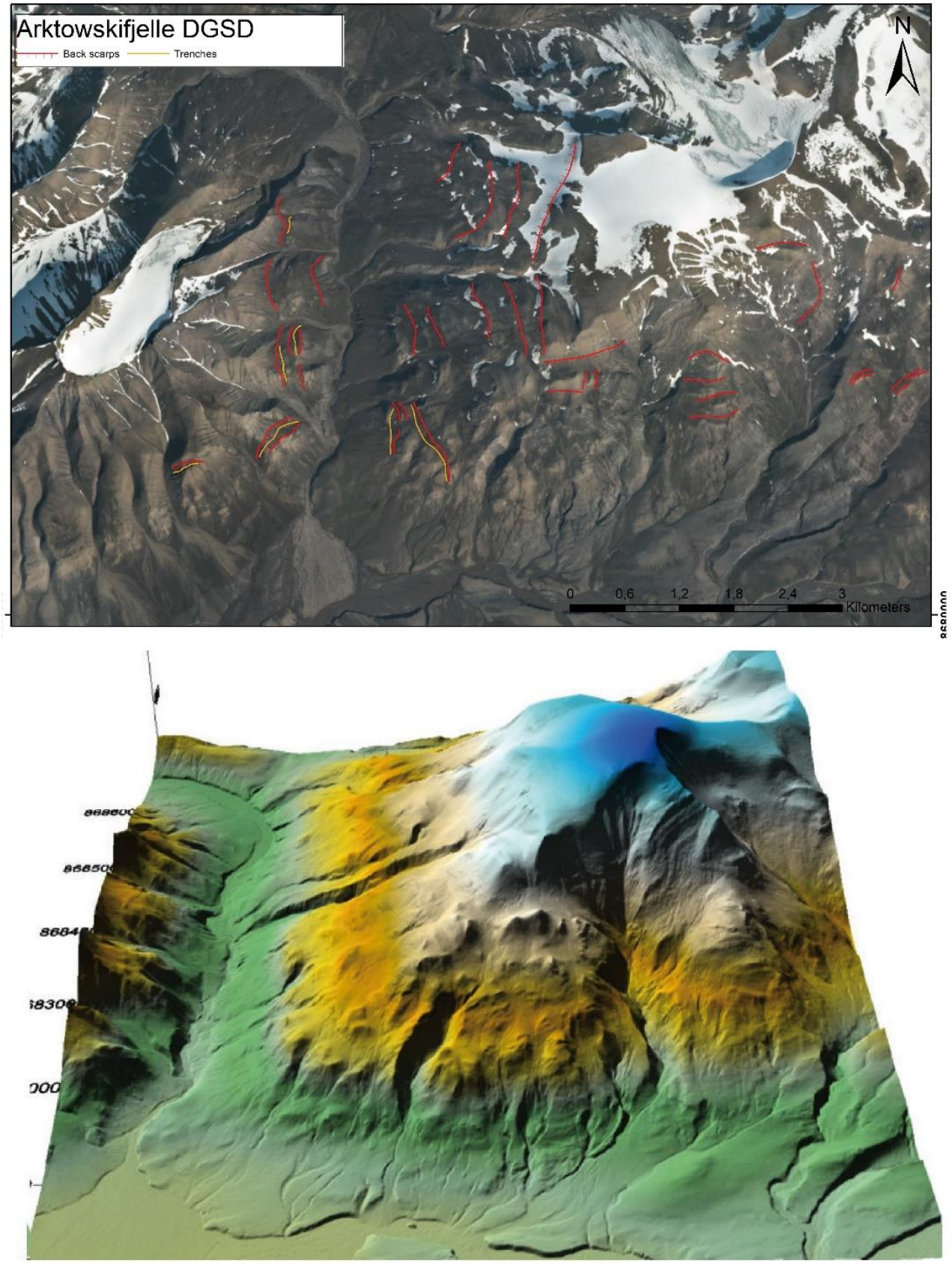

Figure 55 - A) DGSD superficial geomorphological evidences. b) 3D high resilution model.

6.3.4.3 *Hortfjellet*

The Hiortfjellet DGSD is located in the right slope of Adventalen valley at elevations of between 100 and 800 m a.s.l. The slope with evident morphologies linked to gravitational instability is located in the opposite slope of the coast with respect to the city of Longyearbyen.

The slope is characterized by erosional features of both glacial, fluvial and gravitational origin.

In particular, the rectilinear slope with W-SW exposure is represented by escarpments and counter-escarpments, giving the slope a stepped morphology. The slope is represented by elongated NW-SE rocky outcrops alternating with slope deposits in the gravitational depressions. The stratigraphic structure is made up of a sub-horizontal sequence of sandstone siltstones and shale, in the lower part fine-grained lithologies are prevalent. There are no important tectonic structures, there are rectilinear structural features that guided the setting of the valleys. One of these with NW-SE direction on which the Adventalen valley is set.

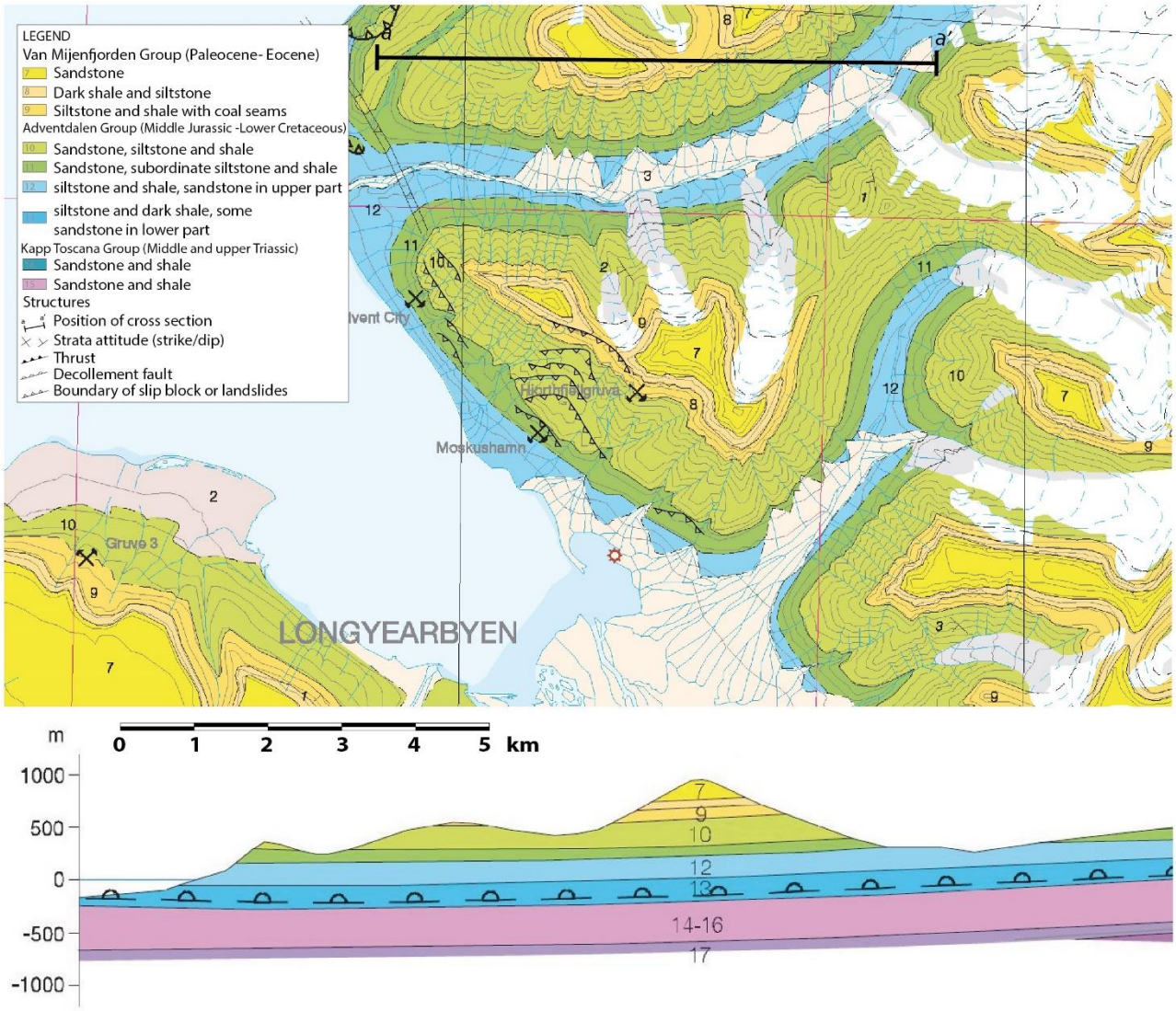

Figure 56 Hiortfjellet geological map. From Geoscience Atlas of Svalbard (Dallmann et al. 2014)

Parallel to this structural line, the main gravitational structures were set up. In the lower part of the slope there are marine terraces that rest in on-lap on the bedrock. Marine terraces, also known as raised beaches, which reflect millennial-scale isotactic rebound after the end of the Last Glacial Maximum. The slope in the lower middle part is affected by glacial erosive morphologies that have affected the bedrock. These can be observed up to an altitude of 200-250m a.s.l. They can be used as marks to analyze the slope deformation as they are sometimes deformed or transposed by the DGSD.

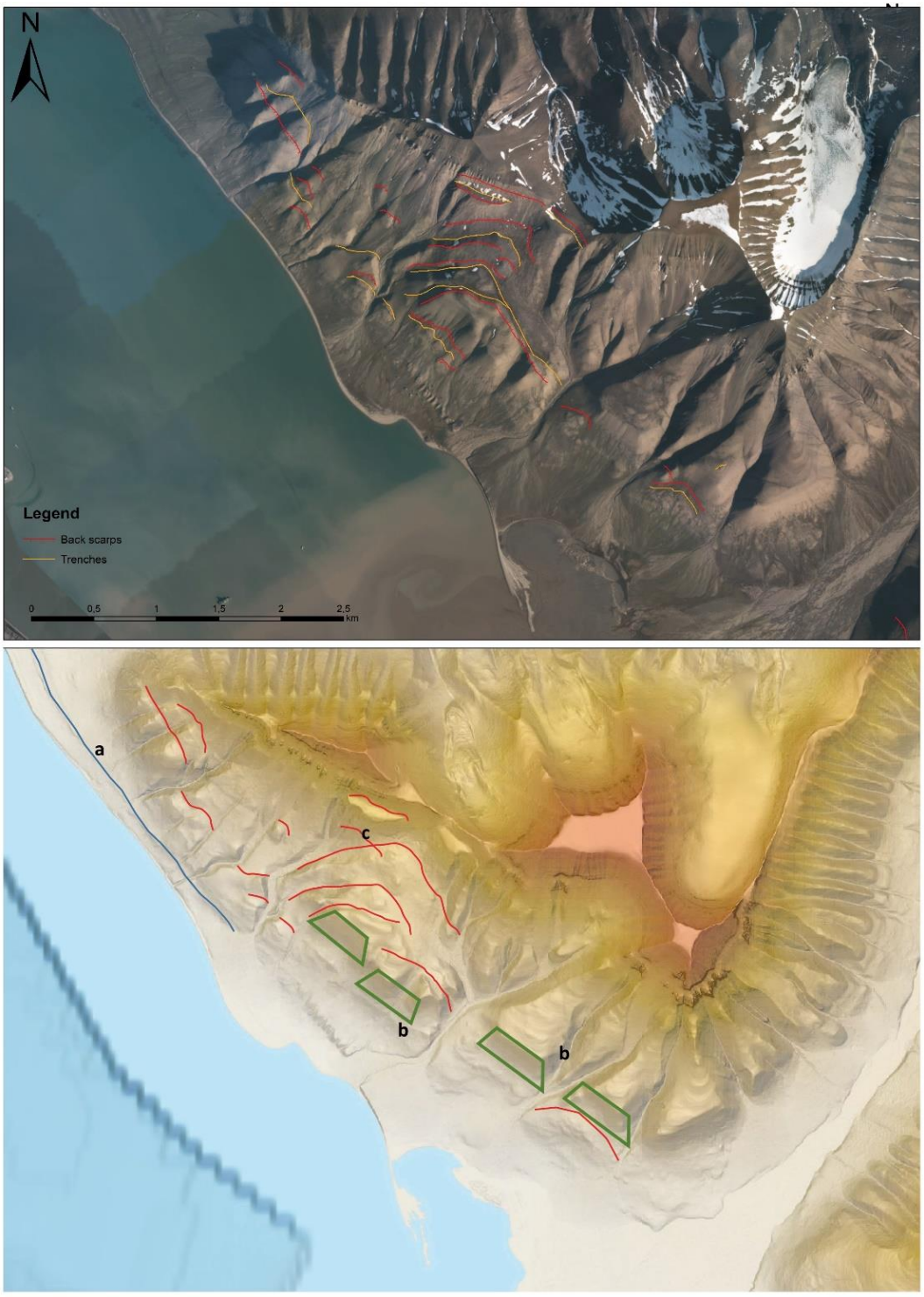

Figure 57 Ortophoto and 3D model of Adventtoppen-Hiorthfjellet DGSD. a) Glacio-eustatic uplifted marine terraces. b) Glacial erosive surfaces. c) DGSD scarps.

6.3.5 Discussions and conclusions

Geomorphological data regarding the DGSD of Nordenskiöld Land were used to generate geological sections for reconstructing a hypothetical surface of basal rupture and deep geometries.

Geological and geomorphological analyses using high-resolution topographic data enabled the identification of different DGSD kinematic.

The Arktowskifjelle DGSD is characterised by lateral spread type kinematics (*Delgado et al., 2011; Dramis & Sorriso-Valvo, 1994; Fioraso, 2017; Gutiérrez-Santolalla et al., 2005; Pánek & Klimeš, 2016; Taramelli & Melelli, 2008*), with the sliding of rigid lithologies over the black shales which, also due to the high fracture caused by thrust, behaves in a plastic way.

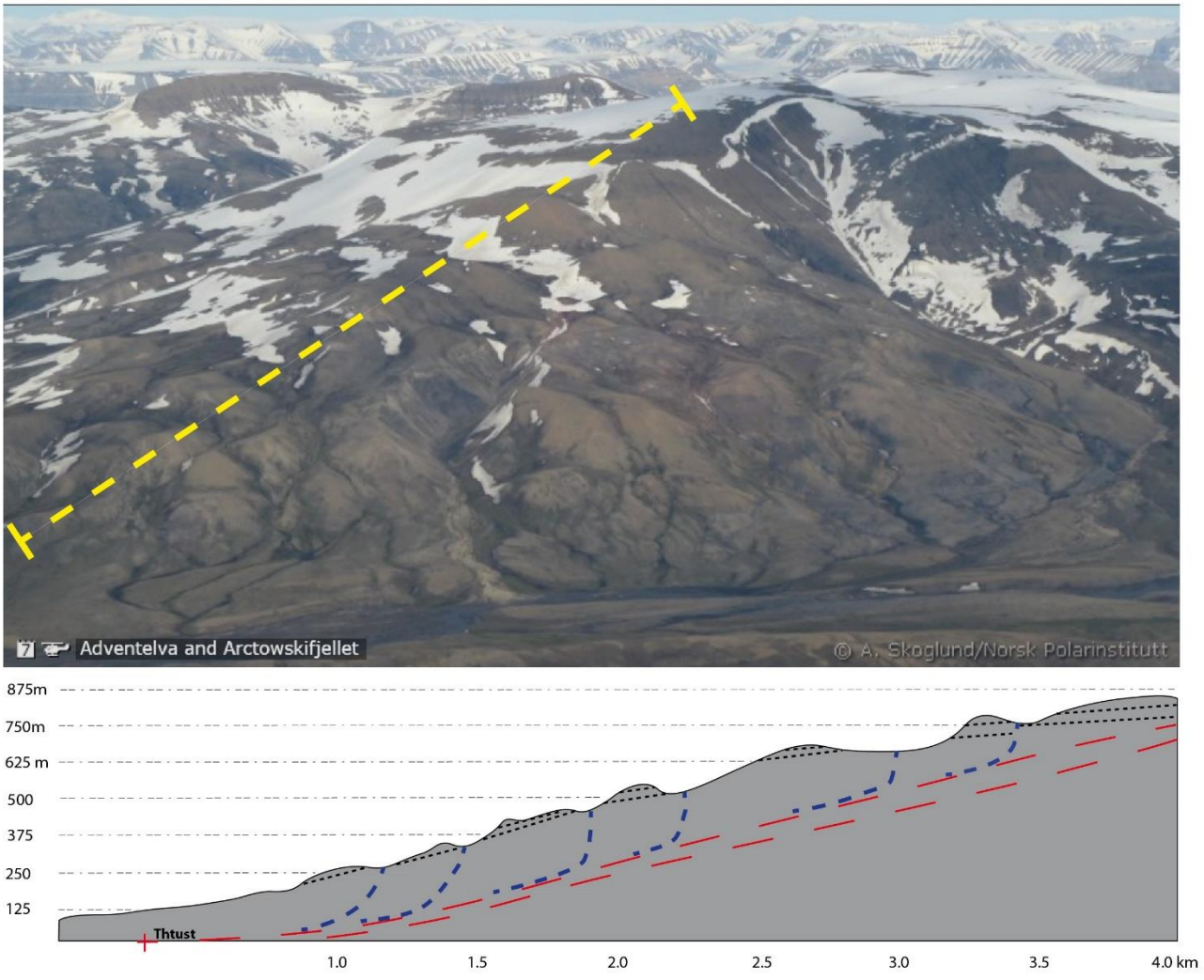

Figure 58 Interpretative geological cross section of Arctowskigjellet DGSD. Red line is the basal shear surface set on the thrust. Blu lines the extensional trenches.

The stratigraphic sequence is characterized by sub-horizontal layers and by analyzing the stratigraphic relationships and the topography we can identify the sliding surface guided mainly by the thrust. Superficially the trench slopes with a main relaxing character are evident. The distances

between the rocky outcrops are of the order of tens of meters. This behavior can be associated with an important translational component of the deformation kinematics.

The hiortfjellet DGSD is associated with the deformation pattern of the sackung type (*Ambrosi & Crosta, 2006, 2011; Audemard et al., 2010; Bovis & Evans, 1996; Coquin et al., 2015; McCalpin & Irvine, 1995; Oppikofer et al., 2017; Soldati et al., 2004*), with a sliding surface not guided by pre-existing structures.

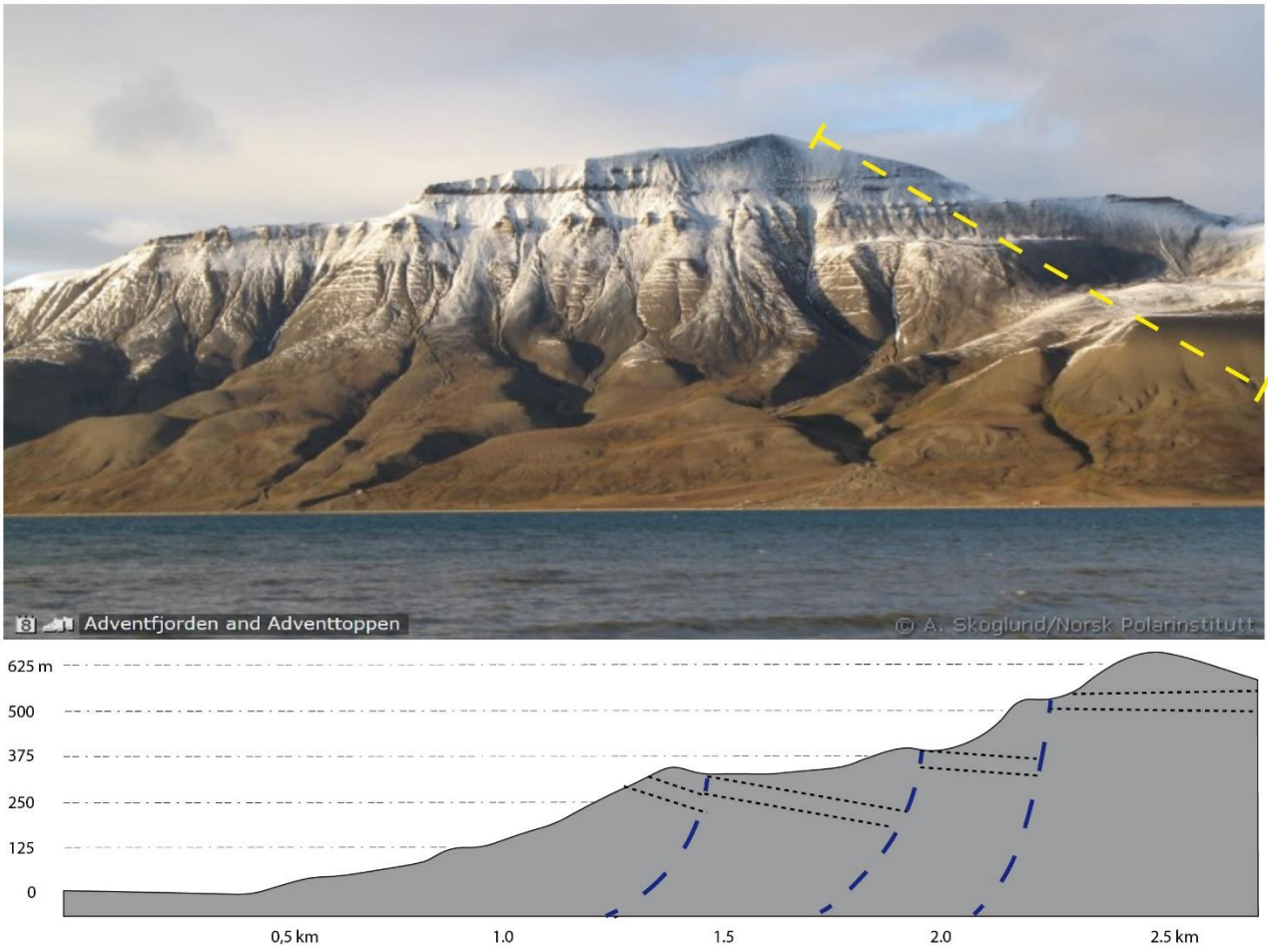

Figure 59 Interpretative geological cross section of Hiortfjellet DGSD. Blu lines main shear surfaces.

This type of DGSD is the most widespread among those analyzed and is distributed throughout the sector of the central tertiary basin where Paleocene and Neogenic sedimentary lithologies prevail. Gravitational shear structures with a high slope appear on the surface as back scarps, giving the slopes a stepped morphology

While the Arktowskifjelle DGSD is driven by the presence of a thrust as a sliding surface, the deformation of Hiortfjellet DGSD is caused by the post glacial deconfinement stresses In general the two DGSD describer are characterised by the fragmentation of the sliding mass into separate blocks.

7 CONCLUSIONS

Deep-Seated Gravitational Slope Deformations are phenomena of great importance from a scientific point of view, both for the role they play in the evolution of relief and for the significant social impact should they occur in proximity to peoples and infrastructures (*Záruba & Mencl, 1969; Dramis & Sorriso-Valvo, 1994; Pánek & Klimeš, 2016; Martino et alii, 2020, Discenza & Esposito 2021*). Large landslides with rapid kinematics were recognized in many parts of the world in association with DGSD phenomena (*Hungr & Evans, 2004; Pánek & Klimeš, 201*6), both in historical and recent times.

A kinematic model and geomorphological evolution characteristics of DGSDs in Sardinia were described for the first time in this study. This thesis proposes the study of these dynamics in central Sardinia, framing them under different aspects:

- Correlating them into the complex geodynamic setting of the Western Mediterranean in particular with the Uplift processes;
- Analyzing the relationships with the river slope evolutionary system complicated by a river capture;
- Identification of the various DGSD evolutionary stages through the use of morphostratigraphy;
- Use of technologies such as UAV-DF, InSAR, LiDAR, GNSS for detection and monitoring;
- A monitoring hypothesis is also proposed for the Early Warning System in the urban contest of Ulassai.
- Correlations were made with different geological, geodynamic and climatic contexts, in particular with Southern Sardinia and the Svalbard Islands;
- A geomorphological map was created, where a comprehensive mapping of structural, karst, fluvial, and slope morphologies in Pardu and Ulassai valleys is presented.

Methology

Multi-scale geological and geomorphological analyzes using remote sensing and field surveys tecniques was performed. The field surveys made it possible to map both the lithological units and the geomorphological processes in the valley of the Rio Quirra and the Rio Pardu. A morphotectonic approach was used to correlate the morphologies with the evolution of the study area and to correlate it with the geodynamic evolution of the western Mediterranean. The morphostrattigraphy of

gravitational deposits and alluvial deposits made it possible to correlate the evolution of the DGSD with the fluvial evolution in particular with capture.

Using UAV-DF and Lidar data it was possible to perform detailed morphometric analyzes of the DGSDs. Using InSAR data it was possible to understand the temporal evolution, the state of activity and the rates of displacement of the DGSDs. GNSS monitoring and geo-technical monitoring made it possible to calibrate and validate the displacement data of the DGSDs in the Ulassai sector. These data will be used to design an Early warning system.

Morphotectonic Implications

The study highlighted an extremely young territory conformation of the Eastern Sardinia, associated with the Neogene and Quaternary geodynamic events, implying a series of problems related to the slope process.The connection between Plio-Pleistocenic tectonic activity and geomorphological evolution in the Pardu Valley and Quirra Valley (Ogliastra, East Sardinia) was studied. The evolutionary conditions of the Pardu Valley are associated with a cycle of undeveloped fluvial erosion, which suggests a relatively young age of the engraving in relation to the capture by the Rio Pelau and the isolation of the Rio Quirra.

- The geomorphological and structural setting of Ogliastra is closely linked to the genesis of the east Sardinian continental margin due the opening of the Tyrrhenian basin (Miocene–Pliocene)
- Distensive Pliocene tectonics accompanied by widespread volcanism resulted in a general uplift in Sardinia. The Quaternary uplift rebound manifested itself with an important erosive phase and variations in the hydrographic network. We have evidence of this phase in the Rio Quirra Valley, which is represented by paleo-DGSDs fossilized by pre-Tyrrhenian alluvial deposits (Lower Pleistocene).
- The river capture of Rio Pardu is associated with this important erosive phase and caused an erosive increase that led to a complete emptying of the valley (Upper-Middle Pleistocene).
- The post-capture decompression of the slopes of the Rio Pardu triggered DGSDs in both flanks in the current state of activity.

DGSD

The causes of the DGSDs are associated with the structural characteristics of the area and the Neogene and Quaternary geomorphological evolution of the river valley associated with the recent uplift.The intense post-capture erosion has given the Rio Pardu Valley morphometric features that are favorable

for the evolution of DGSDs. However, the Rio Quirra Valley presents paleo-DGSDs that have been fossilized by pre-capture terraced alluvial deposits.

The two valleys analyzed are controlled by transcurrent faults that have recently recorded low-magnitude seismic events. Therefore, it is possible that the constant movement of the DGSDs (between about 1 and 2 cm/y) may be susceptible to accelerations due to seismic triggering, causing the partial collapse of the slopes.

Using InSAR data, it was possible to identify and assign displacement rates to the Ulassai, Osini, and Gairo DGSDs.

The initiation of rapid catastrophic processes such as rock avalanche is associated with the accelerations of DGSDs. These accelerations are linked to seismic activities and extreme rainfall events. The latter cause the hydration of the rocks in the shear zones, thereby decreasing the geomechanical characteristics.

The predisposing factors of DGSDs can be identified in the following points:

- The tectonic history of the slope with a passive influence has been caused by a major uplift associated with the Neogene and Quaternary geodynamic events. The upliftment has increased the erosion rates, thereby leading to the deepening of the valleys and detente of the slopes. The energy of the relief of the slopes is the decisive morphological element which initiates the DGSDs; in the cases studied, it is higher than 650 m.
- Cenozoic tectonics have also conferred the structural conditions that predisposed the development of DGSD, particularly in the Dorgali Formation. In fact, the major DGSD trenches are evidently parallel to the major faults and primarily parallel to that of Pardu Valley in the NW–SE direction, on which the slope is also set
- The lithostratigraphic conditions are represented by the Mesozoic units on the foliated and altered metamorphic basement.

Ulassai Landslide hazard

Particular interest was given to the gravitational processes in the municipality of Ulassai. Analysis of the geological and geomorphological setting of plateau edge in Ulassai using UAV photogrammetry and high resolution field surveys allowed to identify different gravitational geological hazard. Landslides with different kinematic and magnitude has been identified: DGSDs with sackung and lateral spread kinematic, giant toppling and widespread rockfalls. Different techniques aiming to understand the temporal evolution of DGSD and giant toppling and future dynamics have been applied in three areas in Ulassai. InSAR data indicate in the lateral spread of Bruncu Pranedda a large

slope side affected by a deformation about 1 cm/y downslope in the last 6 years. In this area we stared a geodetic monitoring system to validate and calibrate satellite data and to understand the differential movement under deformation slope.

To analyse the deformation at fracture scale three geotechnical monitoring stations were installed with continuous acquisition in order to project an early-warning system. In conclusion, based on high resolution geomorphological model of the gravitational process affecting Ulassai, we build multi-source and multi-scale monitoring system.

8 REFERENCES

1. Agliardi F., Crosta G.B. & Frattini P. (2012) - Slow rock-slope deformation. In: Clague J.J. & Stead D. (Eds.), Landslides: Types, Mechanisms and Modeling. Cambridge University Press, Cambridge, 207-221.
2. Agliardi F., Crosta G.B., Zanchi A. & Ravazzi C. (2009) - Onset and timing of deep-seated gravitational slope deformations in the eastern Alps, Italy. Geomorphology, 103 (1): 113-129.
3. Agliardi F., Riva F., Barbarano M., Zanchetta S., Scotti R. & Zanchi A. (2019) - Effects of tectonic structures and long-term seismicity on paraglacial giant slope deformations: Piz Dora (Switzerland). Engineering Geology, 263: 105353
4. Agliardi, F., Crosta, G., & Zanchi, A. (**2001**). Structural constraints on deepseated slope deformation kinematics. Engineering Geology, 59(1–2), 83 102.
5. Agliardi, F., Scuderi, M. M., Fusi, N., & Cristiano, C. (2020). Slow-to-fast transition of giant creeping rockslides modulated by undrained loading in basal shear zones. Nature Communications, 11(1), 1352.
6. Agnesi, V., Macaluso, T., Monteleone, S. & Pipitone, G. (1978) Espansioni laterali (Lateral Spreads) nella Sicilia occidentale. Geologia Applicata e Idrogeologia, 13, 319-326.
7. Agnesi, V., Rotigliano, E., Tammaro, U., Cappadonia, C., Conoscenti, C., Obrizzo, F., Di Maggio, C., Luzio, D., Pingue, F., 2015. GPS monitoring of the Scopello (Sicily, Italy) DGSD phenomenon: relationships between surficial and deep-seated morphodynamics. In: Lollino, G., Giordan, D., Crosta, G.B., Corominas, J., Azzam, R., Wasowski, J., Sciarra, N. (Eds.), Engineering Geology for Society and Territory, 2. Springer, Cham, pp. 1321–1325.
8. Alvarez W., 1972. Rotation of the Corsica-Sardinia microplate. Nature, 235, 103-105.
9. Amadesi E., Cantelli C., Carloni G.C. & RabbI E. (1960) – Ricerche geologiche sui terreni sedimentari del foglio 208 Dorgali. Giorn. Geol., 2 (28), 59-87.
10. Ambrosi, C., & Crosta, G. B. (2006). Large sackung along major tectonic features in the central Italian Alps. Engineering Geology, 83(1–3), 183–200.
11. Ambrosi, C., & Crosta, G. B. (2011). Valley shape influence on deformation mechanisms of rock slopes. Geological Society, London, Special Publications, 351(1), 215233.
12. Amodio-Morelli, L., Bonardi, G., Colonna, V., Dietrich, D., Giunta, G., Ippolito, F., et al. (1976). L'Arco Calabro-Peloritano nell'Orogene Appenninico-Maghrebide. Mem. Soc. Geol. It., 17, 1–60.
13. André, M.F., 1995. Holocene climate fluctuations and geomorphic impact of extreme events in Svalbard. Geografiska Annaler: Series A, Physical Geography 77 (4), 241–250. https://doi.org/10.1080/04353676.1995.11880444.
14. Antón, L.; De Vicente, G.; Munoz-Martin, A.; Stokes, M. Using river long profiles and geomorphic indices to evaluate the geomorphological signature of continental scale drainage capture, Duero basin (NW Iberia). Geomorphology 2014, 206, 250–261.
15. APAT (2007) Trigila A. (ed.) Rapporto sulle frane in Italia – Il Progetto : Metodologia, risultati e rapporti regionali. Rapporti 78/2007.
16. Apuani T., Masetti M. & Rossi M. (2007) - Stress-strain-time numerical modelling of a deep-seated gravitational slope deformation. Preliminary results. Quaternary International, 171: 80-89.
17. Ardau F., Bianco L., De Waele J. & Vernier A. (1993) - Studio dell'idrogeologia e caratterizzazione idrochimica delle acque del Tacco di Ulàssai (Sardegna centro-orientale) - Atti 3° Congr. Naz. dei Giov. Ric. di Geol. Appl., Potenza 28-30 ottobre 1993, Geologia Applicata e Idrogeologia, 27, pp. 27-34.
18. Aslan, A.; Hood, W.C.; Karlstrom, K.E.; Kirby, E.; Granger, D.E.; Kelley, S.; Asmerom, Y. Abandonment of Unaweep Canyon (1.4–0.8 Ma), western Colorado: Effects of stream capture and anomalously rapid Pleistocene river incision. Geosphere 2014, 10, 428–446.

19. Assorgia A., Barca S., Spano C., (1997). A synthesis on the Cenozoic stratigraphic, tectonic and volcanic evolution in Sardinia (Italy). Boll. Soc. Geol. It., 116, 407-420.
20. Audemard, F., Beck, C., & Carrillo, E. (2010). Deep-seated gravitational slope deformations along the active Boconó Fault in the central portion of the Mérida Andes, western Venezuela. Geomorphology, 124(3–4), 164–177.
21. Barla G. (2009). Grandi movimenti di versante in ambiente alpino. Acc. Sc. Torino. Quad. 18, Merc. XIV.
22. Barla, G.; Antolini, F.; Barla, M.; Mensi, E.; Piovano, G. Monitoring of the Beauregard landslide (Aosta Valley, Italy) using advanced and conventional techniques. Eng. Geol. 2010, 116, 218–235.
23. Baroň I., Kernstocková M., Faridi M., Bubík M., Milovský R., Melichar R., Sabouri J. & Babůrek J. (2013) - Paleostress analysis of a gigantic gravitational mass movement in active tectonic setting: The Qoshadagh slope failure, Ahar, NW Iran. Tectonophysics, 605: 70-87.
24. BECK, A.C. (1968) Gravity faulting as a mechanism of topographic adjustment. New Zealand Journal of Geology Geophysics, 11 (1), 191-199.
25. Bianchini, S.; Solari, L.; Bertolo, D.; Thuegaz, P.; Catani, F. Integration of satellite interferometric data in civil protection strategies for landslide studies at a regional scale. Remote Sens. 2021, 13, 1881. https://doi.org/10.3390/rs13101881.
26. Bigi G., Bonardini G., Catalano R., Cosentino D., Lentini F., Parlotto M., Sartori R., Scandone P., Turco E., 1992. Structural Model of Italy, 1:500.000. Consiglio Nazionale delle Ricerche, Rome.
27. Bisci, C., Dramis, F., & Sorriso-Valvo, M. (1996). Rock flow (sackung). In R. Dikau, D. Brunsden, L. Schrott, & M.-L. Ibsen (Eds.), Landslide Recognition: Identification, movement and causes (pp. 150–160). John Wiley & Sons.
28. Bishop, P. Drainage rearrangement by river capture, beheading and diversion. Prog. Phys. Geogr. 1995, 19, 449–473.
29. Blikra, L.H., Christiansen, H.H., 2014. A field-based model of permafrost-controlled rockslide deformation in northern Norway. Geomorphology 208, 34–49. https://doi.org/10.1016/j.geomorph.2013.11.014.
30. Boccaletti M., Nicolich R., Tortorici L., 1990. New data and hypothesis on the development of the Tyrrhenian basin. Paleogeogr. Palaeoclim. Palaeoecol., v. 77, 115-740.
31. Bois T., Bouissou S. & Guglielmi y. (2008) - Influence of major inherited faults zones on gravitational slope deformation: A two-dimensional physical modelling of the La Clapière area (Southern French Alps). Earth and Planetary Science Letters, 272 (3-4): 709-719.
32. Boschi E., Guidoboni E., Ferrari G., MAriotti D., Valensise G. E Gasperini P. (Eds.), 2000. Catalogne Of Strong Italian Earthquakes from 461 B.C. to 1980. Ann. Geofis., 43 (4), 609-868.
33. Bosellini A. & Ogniben G. (1968) - Ricoprimenti ercinici nella Sardegna centrale. Ann. Univ. Ferrara: 1, 1-15, Ferrara.
34. Bovis, M.J. (1982) Uphill facing (antislope) scarps in the Coast Mountains, southwest British Columbia. Geological Society of America Bulletin, 93, 804- 812.
35. Bovis, M. J., & Evans, S. G. (1996). Extensive deformations of rock slopes in southern coast mountains, southwest British Columbia, Canada. Engineering Geology, 44(1-4), 163–182.
36. Bracciali, L.; Najman, Y.; Parrish, R.R.; Akhter, S.H.; Millar, I. The Brahmaputra tale of tectonics and erosion: Early Miocene river capture in the Eastern Himalaya. Earth Planet. Sci. Lett. 2015, 415, 25–37.
37. Carabella, C.; Buccolini, M.; Galli, L.; Miccadei, E.; Paglia, G.; Piacentini, T. Geomorphological analysis of drainage changes in the NE Apennines piedmont area: The case of the middle Tavo River bend (Abruzzo, central Italy). J. Maps 2020, 16, 222–235.

38. Carmignani L., (Coordinatore) 1996. Carta geologica della Sardegna (scala 1:200.000). A cura del Servizio Geologico Nazionale, Regione Autonoma della Sardegna. Litografia Artistica Cartografica (L. A. C.), Firenze.
39. Carmignani, L., Carosi, R., Di Pisa, A., Gattiglio, G., Musumeci, G., Oggiano, G., & Pertusati, P. C. (1994). The Hercynian chain in Sardinia (Italy). Geodinamica Acta, 7(1), 31–47.
40. Carmignani, L., Oggiano, G., Barca, S., Conti, P., Salvadori, I., Eltrudis, A., Funedda, A., & Pasci, S. (2001). Geologia della Sardegna; Note Illustrative della Carta Geologica della Sardegna in scala 1:200.000. Memorie Descrittive della Carta Geologica d'Italia (Vol. 60, 283pp). Servizio Geologico d'Italia.
41. Carmignani, L., Oggiano, G., Funedda, A., Conti, P., & Pasci, S. (2016). The geological map of Sardinia (Italy) at 1:250,000 scale. Journal of Maps, 12(5), 826–835.
42. Carminati, E., & Doglioni, C. (2005). Mediterranean tectonics. In R. Selley, R. Cocks, & I. Plimer (Eds.), Encyclopedia of geology (pp. 135–146). Elsevier
43. Carosi R., Musumeci G. & Pertusati P.C. (1991) – Differences in the structural evolution of tectonics units in central-southern Sardinia. Boll. Soc. Geol. It.: 110, 543-551, Roma.
44. Carraro, F., Dramis, F. & Pieruccini, U. (1979) Large-scale landslides connected with neotectonic activity in the alpine and appennine ranges. In: Proceedings of the XV meeting "Geomorphological Survey and Mapping", Modena.
45. Castedo, R.; Paredes, C.; De la Vega-Panizo, R.; Santos, A.P. The Modelling of Coastal Cliffs and Future Trends; Hydro-Geomorphology-Models and Trends; InTech: Houston, TX, USA, 2017.
46. Casula, G., Cherchi, A., Montadert, L., Murru, M., & Sarria, E. (2001). The cenozoic graben system of Sardinia (Italy): Geodynamic evolution from new seismic and field data. Marine and Petroleum Geology, 18(7), 863–888.
47. Cavallin A., Crescenti U., Dramis F., Prestinizi A. E Sorriso-Valvo M. (1987) Tipologia e diffusione delle deformazioni gravitative profonde di versante in Italia. Atti Conv. Soc. Geol. It. "Le scienze della Terra nella Pianificazione Territoriale", Chieti, 7/8 Maggio 1987. Mem Soc. Geol. It.
48. Cavinato A. & Charrier G. & Zucchetti S. (1976). Foglio n. 207-Nuoro della Carta geologica d'Italia a scala 1:100.000.
49. Cherchi, A., & Montadert, L. (1982). Oligo-Miocene rift of Sardinia and the early history of the Western Mediterranean Basin. Nature, 298(5876), 736–739.
50. Chigira M. (1985) Minor structures formed by gravitational mass rock creep. In: Proceedings of the 4th International Conference and Field Workshop on Landslides, Tokyo, 419-428.
51. Chigira, M. (1992). Long-term gravitational deformation of rocks by mass rock creep. Engineering Geology, 32(3), 157–184.
52. Chiocci, F.L.; Budillon, F.; Ceramicola, S.; Gamberi, F.; Orrù, P. A Tlante dei Lineamenti di Pericolosità Geologica dei Mari Italiani-Risultati del Progetto MaGIC; CNR Edizioni: Rome, Italy, 2021.
53. Cimini, G. B., Marchetti, A., & Silvestri, M. (2016). L'esperimento Sardinia passive array (spa): acquisizione dati sismici per lo studio della geodinamica e della sismotettonica dell'area mediterranea. INGV (Istituto Nazionale di Geofisica e Vulcanologia, Centro Nazionale Terremoti).
54. Clapuyt, F., Vanacker, V., & Oost, K. V. (2016). Reproducibility of UAV-based earth topography reconstructions based on structure-from-motion algorithms. Geomorphology, 260, 4–15.
55. Cocozza T., Jacobacci A., Nardi R. & Salvadori I. (1974) - Schema stratigrafico-strutturale del Massiccio Sardo-Corso e minerogenesi della Sardegna. Mem. Soc. Geol. It.: 13, 85 186, Roma.
56. Coe, J.A., Ellis, W.L., Godt, J.W., Savage, W.Z., Savage, J.E., Michael, J.A., Kibler, J.D., Powers, P.S., Lidke, D.J., Debray, S., 2003. Seasonal movement of the Slumgullion landslide determined from Global Positioning System surveys and field instrumentation, July 1998-March 2002. Eng. Geol. 68, 67–101. https://doi.org/ 10.1016/S0013-7952(02)00199-0.

57. Coltorti M., Dramis F., Gentili B., Pambianchi G., Crescenti U. and Sorriso-Valvo M. (1984) The december 1982 Ancona landslide: a case of deep-seated gravitational slope deformation evolving at unsteady rate. Zeitschrift fur Geomorphologie, N.F., 29 (3), 335-345.
58. Comerci, V., D'Agostino, N., Fubelli, G., Molin, P., Piacentini, T., Eds.; APAT: Rome, Italy, 2002; Volume 21, pp. 17–30.
59. Coquin, J., Mercier, D., Bourgeois, O., Cossart, E., & Decaulne, A. (2015). Gravitational spreading of mountain ridges coeval with late Weichselian deglaciation: Impact on glacial landscapes in Tröllaskagi, northern Iceland. Quaternary Science Reviews, 107, 197–213.
60. Costamagna L.G. & Barca S. (2004) - Stratigrafia, analisi di facies, paleogeografia ed inquadramento regionale del Giurassico dell'area dei Tacchi (Sardegna centro-orientale). Boll. Soc. Geol. It., 123, 477-495.
61. Costamagna L.G. & Lecca L. (2002) - Preliminary facies analysis and evidence of aggradation/progradation in the drowning Jurassic of Eastern Sardinia. 6° International Symposium on the Jurassic System, Palermo, 12-22/09/2002, Abstract-book, 41-42.
62. Costamagna, L. G. (2015). Middle Jurassic continental to marine transition in an extensional tectonics context: The Genna Selole Fm depositional system in the Tacchi area (central sardinia. Italy). Geological Journal, 51(5), 722–736.
63. Costamagna, L. G., & Barca, S. (2004). Stratigraphy, facies analysis, paleogeography and regional framework of the Jurssic succession of the "tacchi" area (Middle-Eastern Sardinia). Bollettino della Societa Geologica Italiana, 123(3), 477–495.
64. Costamagna, L. G., Kustatscher, E., Scanu, G. G., Del Rio, M., Pittau, P., & Van Konijnenburg-van Cittert, J. H. A. (2018). A palaeoenvironmental reconstruction of the Middle Jurassic of Sardinia (Italy) based on integrated palaeobotanical, palynological and lithofacies data assessment. Palaeobiodiversity and Palaeoenvironments, 98(1), 111–138.
65. Crescenti U., Dramis F., Gentili B. E Praturlon A. (1983) The Bisaccia landslide: a case of deep-seated gravitational movement reactived by earthquakes. Actes Coll. "Ground Movements de terrains". 11, Caen, Doc. B.R.G.M., 83, 15-21.
66. Crosetto,M; Oriol Monserrat, María Cuevas-González, Núria Devanthéry, Bruno Crippa, Persistent Scatterer Interferometry: A review, ISPRS Journal of Photogrammetry and Remote Sensing, Volume 115, 2016, Pages 78-89, ISSN 0924-2716,
67. Crosta, G. B., & Agliardi, F. (2003). Failure forescast for large rock slides by surface displacement measurements. Canadian Geotechnical Journal, 40(1), 176–191.
68. Crosta, G. B., & Zanchi, A. (2000). Deep-seated slope deformations. Huge, extraordinary, enigmatic phenomena. In E. Bromhead, N. Dixon, & M. Ibsen (Eds.), Landslides in research, theory and practice (pp. 351–358). Thomas Telford.
69. Crosta, G. B., Frattini, P., & Agliardi, F. (2013). Deep seated gravitational slope deformations in the European Alps. Tectonophysics, 605, 13–33.
70. Cruden, D. M., & Varnes, D. J. (1996). Landslide Types and Processes. Transportation Research Board, U.S. National Academy of Sciences, Special Report (Vol. 247, pp. 36–75).
71. Dallmann, W.K., Kjaernet, T. & Nottvedt, A. 2001: Geological map of Svalbard 1:100,000, Sheet C9G Adventdalen, Norsk Polarinstitutt.
72. De Waele, J., Di Gregorio, F., Follesa, R., & Piras, G. (2005). Geosites and landscape evolution of the "tacchi": an example from central-east Sardinia. Il Quaternario, 18(1), 211–220.
73. De Waele, J., Ferrarese, F., Granger, D., & Sauro, F. (2012). Landscape evolution in the Tacchi area (central-east Sardinia, Italy) based on karst and fluvial morphology and age of cave sediments. Geografia Fisica e Dinamica Quaternaria, 35, 119–127.
74. Deganutti, A.M. (2008) The hypermobility of Rock Avalanches. Ph.D. Thesis, Università di Padova, Padova, Italia, 106 pp.

75. Deiana, G.; Meleddu, A.; Paliaga, E.; Todde, S.; Orrù, P. Continental slope geomorphology: Landslides and pockforms of Southern Sardinian margin (italy). Geogr. Fis. Dinam. Quat. 2016, 39, 129–136.
76. Deiana, G.; Melis, M.T.; Funedda, A.; Da Pelo, S.; Meloni, M.; Naitza, L.; Orrù, P.; Salvini, R.; Sulis, A. Integrating remote sensing data for the assessments of coastal cliffs hazard: MAREGOT project. Earth Obs. Adv. Chang. World 2019, 1, 176–181.
77. Deiana, G., Lecca, L., Melis, R. T., Soldati, M., Demurtas, V., & Orrù, P. E. (2021). Submarine Geomorphology of the southwestern Sardinian continental shelf (Mediterranean Sea): Insights into the last glacial maximum sea-level changes and related environments. Water, 13(2), 155.
78. Del Rio M. (1977) - Analisi palinologica del Giurese della Sardegna centrale. Boll. Soc. Geol. It.: 95, 619-631, Roma.
79. Del Rio M. (1985) - Palynology of Middle Jurassic black organic shales of "Tacco di Laconi", Central Sardinia, Italy. Boll. Soc. Paleont. It.: 23, 325-342, Modena.
80. Delchiaro M., Della Seta M., Martino S., Dehbozorgi M. & Nozaem R. (2019) - Reconstruction of river valley evolution before and after the emplacement of the giant Seymareh rock avalanche (Zagros Mts., Iran). Earth Surface Dynamics, 7: 929-947.
81. Delgado, J.; Vicente, F.; García-Tortosa, F.; Alfaro, P.; Estévez, A.; Lopez-Sanchez, J.M.; Tomás, R.; Mallorquí, J.J. A deep seated compound rotational rock slide and rock spread in SE Spain: Structural control and DInSAR monitoring. Geomorphology 2011, 129, 252–262.
82. Delgado, J., Vicente, F., García-Tortosa, F., Alfaro, P., Estévez, A., Lopez-Sanchez, J. M., Tomás, R., & Mallorquí, J. J. (2011). A deep seated compound rotational rock slide and rock spread in SE Spain: Structural control and DInSAR monitoring. Geomorphology, 129(3–4), 252–262.
83. Della Seta M., Esposito C., Marmoni G.M., Martino S., Scarascia Mugnozza G. & Troiani F. (2017) - Morpho-structural evolution of the valley-slope systems and related implications on slope-scale gravitational processes: New results from the Mt. Genzana case history (Central Apennines, Italy). Geomorphology, 289: 60-77.
84. Demurtas, V.; Orrù, P.; Deiana, G. Multi-source and multi-scale monitoring system of deep-seated gravitational slope deformation in east-central sardinia. Planet Care Space 2021, 2, 28–32. https://doi.org/10.978.88944687/00.
85. Demurtas, V.; Orrù, P.E.; Deiana, G. Evolution of Deep-Seated Gravitational Slope Deformations in Relation with Uplift and Fluvial Capture Processes in Central Eastern Sardinia (Italy). Land 2021, 10, 1193. https://doi.org/10.3390/land10111193
86. Demurtas. V.; Orrù, P.E.; Deiana, G. Deep-seated gravitational slope deformations in central Sardinia: Insights into the geomorphological evolution. J. Maps 2021, 17, 594–607.
87. Dessau G., Duchi G., Moretti A. & OggianO G. (1982) – Geologia della zona del Valico di Correboi (Sardegna centro-orientale). Rilevamento, tettonica e giacimenti minerari. Boll. Soc. Geol. It.: 101, 497-522, Roma.
88. Devoto, S., Hastewell, L.J., Prampolini, M., Furlani, S., 2021. Dataset of gravity-induced landforms and sinkholes of the Northeast Coast of Malta (Central Mediterranean Sea). Data 6, 81.
89. Devoto, S., Macovaz, V., Mantovani, M., Soldati, M., & Furlani, S. (2020). Advantages of using UAV digital photogrammetry in the study of slow-moving coastal landslides. Remote Sensing, 12(21), 3566.
90. Dewey J.F., Helman M.L., Turco E., Hutton D.H.W., Knott S.D., 1989. Kinematics of the Western Mediterranean. In: Coward M.P., 181 Dietrich D. & Park R.G. Eds., Alpine Tectonics, 265-284. Geol. Soc. London Spec. Publ., 45.
91. Di Maggio C., Madonia G. & Vattano M. (2014) - Deep-seated gravitational slope deformations in western Sicily: Controlling factors, triggering mechanisms, and morphoevolutionary models. Geomorphology, 208: 173-189.

92. Dieni, I., Fischer, J. C., Massari, F., Salard-Cheboldaeff, M., & Vozenin-Serra, C. (1983). La succession de Genna Selole (Baunei) dans le cadre de la paléogéographie mésojurassique de la Sardaigne orientale. Memorie della Società Geologica Italiana, 36, 117–148.
93. Discenza M.E., Esposito C., Martino S., Petitta M., Prestininzi A. & Scarascia Mugnozza G. (2011) - The gravitational slope deformation of
94. Discenza M.E., Martino S., Bretschneider A. & Scarascia Mugnozza G. (2020) - Influence of joints on creep processes involving rock masses: Results from physical-analogue laboratory tests. International Journal of Rock Mechanics and Mining Sciences, 128: 104261.
95. Discenza, M.E.; Esposito E. (2021) State-of-art and remarks on some open questions about DSGSDs: Hints from a review of the scientific literature on related topics. Italian Journal of Engineering Geology and Environment 21 (1), 31-59
96. Dragićević, S.; Lai, T.; Balram, S. GIS-based multicriteria evaluation with multiscale analysis to characterize urban landslide susceptibility in data-scarce environments. Habitat Int. 2015, 45, 114–125.
97. Dramis, F. (1984) Aspetti geomorfologici e fattori genetici delle deformazioni gravitative profonde di versante. Bollettino della Società Geologica Italiana, 103, 681-687.
98. Dramis, F., & Sorriso-Valvo, M. (1994). Deep-seated gravitational slope deformations, related landslides and tectonics. Engineering Geology, 38(3–4), 231–243.
99. Dramis, F., Farabollini, P., Gentili, B., & Pambianchi, G. (2002, September 21–27). Neotectonics and large scale gravitational phenomena in the Umbria –Marche Apennines, Italy. In V. Comerci, N. D'Agostino, G. Fubelli, P. Molin, & T. Piacentini (Eds.), Seismically induced ground ruptures and large scale mass movements, Field excursion and Meeting Atti APAT 4/2002 (Vol. 21, pp. 17–30).
100. Drouillas Y., Lebourg T., Zerathe S., Hippolyte J.C., Chochon R., Vidal M. & Besso R. (2020) - Alpine deep-seated gravitational slope deformation and the Messinian Salinity Crisis. Landslides, 18 (2): 539-549.
101. Eckerstorfer, M., Christiansen, H.H., Vogel, S., Rubensdotter, L., 2013. Snow cornice dynamics as a control on plateau edge erosion in central Svalbard. Earth Surf.Process. Landf. 38 (5), 466–476. https://doi.org/10.1002/esp.3292.
102. Eker, R., & Aydın, A. (2021). Long-term retrospective investigation of a large, deep-seated, and slow-moving landslide using InSAR time series, historical aerial photographs, and UAV data: The case of Devrek landslide (NW Turkey). Catena, 196.
103. Elter, F. M., Corsi, B., Cricca, P., & Muzio, G. (2004). The south-western Alpine foreland: Correlation between two sectors of the Variscan chain belonging to "stable Europe": Sardinia (Italy) Corsica and Maures Massif (South-Eastern France). Geodinamica Acta, 17(1), 31–40.
104. Elter, F. M., Padovano, M., & Kraus, R. K. (2010). The emplacement of Variscan HTmetamorphic rocks linked to the interaction between Gondwana and Laurussia: Structural constraints in NE Sardinia (Italy). Terra Nova, 22(5), 369–377.
105. Engelen, G.B. (1963) Gravity tectonics in the North-Western Dolomites (North Italy). Geologica Ultraiectina, 13, 1-92.
106. Esposito C., Martino S. & Scarascia Mugnozza G. (2007) - Mountain slope deformations along thrust fronts in jointed limestone: An equivalent continuum modelling approach. Geomorphology, 90 (1-2): 55-72.
107. Faccenna C., Becker T.W., Lucente F.P., Jolivet L., Rossetti F., 2001. History of subduction and back-arc extension in the Central Mediterranean. Geophys. J. Int. 145, 809–820.
108. Fan, N.; Chu, Z.; Jiang, L. Abrupt drainage basin reorganization following a Pleistocene river capture. Nat. Commun. 2018, 9, 3756.

109. Farabollini P., Folchi Vici D'Arcevia C., Gentili B., Luzi L., Panbianchi C. E Viglioni F. (1995) La morfogenesi gravitativa nelle deformazioni litoidi dell'Appennino Centrale. Mem. Soc. Geol. It., L, 123-136.
110. Ferranti, L., Oldow, J.S., D'Argenio, B., Catalano, R., Lewis, D., Marsella, E., Avellone, G., Maschio, L., Pappone, G., Pepe, F., & Sulli, A. (2008). Active deformation in Southern Italy, Sicily and southern Sardinia from GPS velocities of the Peri-Tyrrhenian Geodetic Array (PTGA). Bollettino della Società Geologica Italiana, 127(2), 299–316.
111. Ferretti, A.; Prati, C.; Rocca, F. Analysis of permanent scatterers in SAR interferometry. In Proceedings of the IGARSS 2000. IEEE 2000 International Geoscience and Remote Sensing Symposium. Taking the Pulse of the Planet: The Role of Remote Sensing in Managing the Environment. Proceedings (Cat. No.00CH37120), Honolulu, HI, USA, 24-28 July 2000; Volume 2, pp. 761–763.
112. Fioraso, G. (2017). Impact of massive deep-seated rock slope failures on mountain valley morphology in the northern Cottian Alps (NW Italy). Journal of Maps, 13(2), 575–587.
113. Fleurant, C., Tucker, G. E., & Viles, H. A. (2008). A model of cockpit karst landscape, Jamaica. In Géomorphologie: relief, processus, environnement, Groupe français de géomorphologie (GFG) (pp. 3–14).
114. Franceschelli, M., Puxeddu, M., Cruciani, G., 2005. Variscan metamorphism in Sardinia, Italy: review and discussion. Journal of Virtual Explorer 19 (2)
115. Francioni M., Calamita F., Coggan J., De Nardis A., Eyre M., Miccadei E., Piacentini T., Stead D. & Sciarra N. (2019) - A multi-disciplinary approach to the study of large rock avalanches combining remote sensing, GIS and field surveys: The case of the Scanno landslide, Italy. Remote Sensing, 11 (13): 1570.
116. Frattini, P., Crosta, G. B., Rossini, M., & Allievi, J. (2018). Activity and kinematic behaviour of deep-seated landslides from PS-InSAR displacement rate measurements. Landslides, 15(6), 1053–1070.
117. Frigerio, S.; Schenato, L.; Bossi, G.; Cavalli, M.; Mantovani, M.; Marcato, G.; Pasuto, A. A web-based platform for automatic and continuous landslide monitoring: The Rotolon (Eastern Italian Alps) case study. Comput. Geosci. 2014, 63, 96–105.
118. Gaidi, S.; Galve, J.P.; Melki, F.; Ruano, P.; Reyes-Carmona, C.; Marzougui, W.; Devoto, S.; Pérez-Peña, J.V.; Azañón, J.M.; Chouaieb, H.; et al. Analysis of the geological controls and kinematics of the chgega landslide (Mateur, Tunisia) exploiting photogrammetry and InSAR technologies. Remote Sens. 2021, 13, 4048. https://doi.org/ 10.3390/rs13204048.
119. Galvani A. (2009) Phd Tesi. Indagini geodetiche e geomorfologiche in Appennino Centrale per la caratterizzazione della tettonica attiva. UNIVERSITA' DEGLI STUDI "ROMA TRE
120. Gamberi, F.; Leidi, E.; Dalla Valle, G.; Rovere, M.; Marani, M.; Mercorella, A. Foglio 57 Arbatax. In A Tlante dei Lineamenti di Pericolosità Geologica dei Mari Italiani-Risultati del Progetto MaGIC; Chiocci, F.L., Budillon, F., Ceramicola, S., Gamberi, F., Orrù, P., Eds.; CNR Edizioni: Rome, Italy, 2021.
121. Gattacceca, J., Deino, A., Rizzo, R., Jones, D. S., Henry, B., Beaudoin, B., & Vadeboin, F. (2007). Miocene rotation of Sardinia: New paleomagnetic and geochronological constraints and geodynamic implications. Earth and Planetary Science Letters, 258(3-4), 359–377.
122. Genevois R. & Prestininzi A. (1979) - Time dependent behaviour of granitic rocks related to their alteration grade. In: Proceedings of the 4th International Congress on Rock Mechanics, Montreaux, 153-159 pp.
123. Genevois, R. & Perstininzi, A. (1979) Time-dependent behaviour of granitic rocks related to their alteration grade. In: Proceedings of the 4th International Congress on Rock Mechanics, Montreux, 153-159.
124. Genevois, R. & Tecca, P.R. (1984) Alcune considerazioni sulle "deformazioni gravitative profonde" in argille sovraconsolidate. Bollettino della Società Geologica Italiana, 103, 717-729.

125. Gentili, B.; Pambianchi, G. Gravitational morphogenesis of the Apennine chain in Central Italy. In Proceedings of the 7th
126. Ghirotti M., Martin S. & Genevois R. (2011) - The Celentino deep-seated gravitational slope deformation (DSGSD): Structural and geomechanical analyses (Peio Valley, NE Italy). Geological Society, London, Special Publications, 351 (1): 235-251.
127. Gilbert, G. L., O'neill, H. B., Nemec, W., Thiel, C., Christiansen, H. H., and Buylaert, J. P.: Late Quaternary sedimentation and permafrost development in a Svalbard fjord-valley, Norwegian high Arctic, Sedimentology, 65, 2531-2558, 2018.
128. Gili, J.A., Corominas, J., Rius, J., 2000. Using global positioning system techniques in landslide monitoring. Eng. Geol. 55 (3), 167–192. https://doi.org/10.1016/s0013- 7952(99)00127-1.
129. Glueer F., Loew S., Manconi A. & Aaron J. (2019) - From Toppling to Sliding: Progressive Evolution of the Moosfluh Landslide, Switzerland. Journal of Geophysical Research: Earth Surface, 124 (12): 2899-2919.
130. GNGFG. (1994). Proposta di legenda geomorfologica ad indirizzo applicativo. Geografia Fisica e Dinamica Quaternaria, 16(2), 129–152.
131. Goldstein RM, Engelhardt H, Kamb B and Frolich RM (1993) Satellite radar interferometry for monitoring ice sheet motion: application to an Antarctic ice stream. Science 262(5139): 1525–1530.
132. Gueguen E., Doglioni C., Fernandez M., 1998. On the post-25 Ma geodynamic evolution of the western Mediterranean. Tectonophysics 298, 259–269.
133. Gueguen, E., Doglioni, C., & Fernandez, M. (1997). Lithospheric boudinage in the Western Mediterranean back-arc basin. Terra Nova, 9(4), 184–187.
134. Guerricchio A. E Melidoro G. (1979) Deformazioni gravitative profonde del tipo Sackung nei Monti di Maratea. Geol. Appl. Idrogeol., 14, 13-22
135. Gutiérrez F., Ortuño M., Lucha P., Guerrero J., Acosta E., Coratza P., Piacentini D. & Soldati M. (2008) - Late Quaternary episodic displacement on a sackung scarp in the central Spanish Pyrenees. Secondary paleoseismic evidence?. Geodinamica Acta, 21 (4): 187-202.
136. Gutiérrez-Santolalla, F., Acosta, E., Ríos, S., Guerrero, J., & Lucha, P. (2005). Geomorphology and geochronology of sackung features (uphill-facing scarps) in the central spanish pyrenees. Geomorphology, 69(1–4), 298–314.
137. Guzzetti, F.; Carrara, A.; Cardinali, M.; Reichenbach, P. Landslide hazard evaluation: A review of current techniques and their application in a multi-scale study, central Italy. Geomorphology 1999, 31, 181–216.
138. Guzzetti, F.; Gariano, S.L.; Peruccacci, S.; Brunetti, M.T.; Marchesini, I.; Rossi, M.; Melillo, M. Geographical landslide early warning systems. Earth-Sci. Rev. 2020, 200, 102973. [CrossRef]
139. Haines A. J., Holt W. E., 1993. A procedure for obtaining the complete horizontal motions within zones of distributed deformation from the inversion of strain rate data. J. Geophys. Res., 98, 12,057–12,082.
140. Hanssen, Ramon F. Radar interferometry: data interpretation and error analysis. Vol. 2. Springer Science & Business Media, 2001.
141. Harris, C., Kern-Lütschg, M.A., Christiansen, H.H., Smith, F., 2011. The role of interannual climate variability in controlling solifluction processes, Endalen, Svalbard.
142. Heim, A. (1932) Bergsturz und Menschenleben. Fretz und Wasmuth, Zürich, 218 p.
143. Humlum, O., Instanes, A. & Sollid, J.L. 2003: Permafrost in Svalbard: a review of research history, climatic background and engineering challenges. Polar Research 22, 191–215. https://doi.org/10.1111/j.1751-8369.2003.tb00107.x.
144. Hungr O. & Evans S.G. (2004) - Entrainment of debris in rock avalanches: An analysis of a long run-out mechanism. Geological Society of America Bulletin, 116 (9-10): 1240-1252.

145. Hungr O., Leroueil S. & Picarelli L. (2014) - The Varnes classification of landslide types, an update. Landslides, 11 (2): 167-194.
146. Hürlimann M., Ledesma A., Corominas J. & Prat P.C. (2006) - The deep-seated slope deformation at Encampadana, Andorra: Representation of morphologic features by numerical modelling. Engineering Geology, 83 (4): 343-357.
147. Hutchinson, J.N. (1988) General Report: morphological and geotechnical parameters of landslides in relation to geology and hydrogeology. In: Proceedings of the 5th International Symposium on Landslides, Lausanne, A.A. Balkema, 1, 3-35.
148. Ietto, F.; Perri, F.; Fortunato, G. Lateral spreading phenomena and weathering processes from the Tropea area (Calabria, southern Italy). Environ. Earth Sci. 2015, 73, 4595–4608.
149. INGV. INGV Special, the Earthquakes of 2020 in Italy. 2021. Available online: http://terremoti.ingv.it/ (accessed on
150. International Congress International Association of Engineering Geology, Lisboa, Portugal, 5–9 September 1994; Volume 3, pp. 1177–1186.
151. Intrieri E., Giovanni Gigli, Francesco Mugnai, Riccardo Fanti, Nicola Casagli, Design and implementation of a landslide early warning system,Engineering Geology,Volumes 147–148,2012,Pages 124-136,ISSN 0013-7952,https://doi.org/10.1016/j.enggeo.2012.07.017.
152. Iovine, G.; Tansi, C. Gravity-accommodated 'structural wedges' along thrust ramps: A kinematic scheme of gravitational evolution. Nat. Hazards 1998, 17, 195–224.
153. ISPRA & AIGEO. (2018). Aggiornamento ed integrazione delle linee guida della Carta Geomorfologica d'Italia in scala 1:50,000. Quaderni Serie III del Servizio Geologico Nazionale.
154. ISPRA. (2007). Guida alla rappresentazione cartografica della Carta Geomorfologica d'Italia in scala 1:50,000. Quaderni Serie III del Servizio Geologico Nazionale.
155. Jaboyedoff M., Crosta G.B. & Stead D. (2011) - Slope tectonics: A short introduction. Geological Society, London, Special Publications, 351 (1): 1-10.
156. Jaboyedoff M., Penna I., Pedrazzini A., Baroň I. & Crosta G.B. (2013) - An introductory review on gravitational-deformation induced structures, fabrics and modeling. Tectonophysics, 605: 1-12.
157. Jahn, A. (1964). Slope morphological feature resulting from gravitation. Zeitschrift für Geomorphologie(Suppl. 5), 59–72.
158. Jarman D. & Harrison S. (2019) - Rock slope failure in the British mountains. Geomorphology, 340: 202-233.
159. Jarman D. (2006) - Large rock slope failures in the Highlands of Scotland: Characterisation, causes and spatial distribution. Engineering Geology, 83 (1-3): 161-182.
160. Jibson R.W., Harp E.L., Schulz W. & Keefer D.K. (2004) - Landslides triggered by the 2002 Denali fault, Alaska, earthquake and the inferred nature of the strong shaking. Earthquake Spectra, 20 (3): 669-691.
161. Kastens K., Mascle J. & OtherS (1988) - ODP Leg 107 in the Tyrrhenian Sea: insights into passive margin and back-arc basin evolution. Geol. Soc. Am. Bull.: 100, 1140-1156, Boulder.
162. Kojan, E. & Hutchinson, J.N. (1978)Mayunmarca rockslide and debris flow. In: Voight, B. (ed.) Rockslides and Avalanches - Natural Phenomena. evelopment in Geotechnical Engineering, 14, 25-35.
163. Krüger, R. Springer, W. Lechner, Global Navigation Satellite Systems (GNSS), Computers and Electronics in Agriculture, Volume 11, Issue 1, 1994, Pages 3-21, ISSN 0168-1699, https://doi.org/10.1016/0168-1699(94)90049-3.
164. Lentini F., Carbone S., Guarnieri P., 2006. Collisional and postcollisional tectonics of the Apenninic-Maghrebian Orogen (Southern Italy). In: Y. DILEK & S. PAVLIDES (Eds.), "Post-collisional Tectonics and Magmatism in the Eastern Mediterranean Region". Geological Society of America, Special Paper 409, 57-81.

165. Lentini F., Catalano S., Carbone S., 1996. The External Thrust System in Southern Italy: a target for petroleum exploration. Petroleum Geoscience, 2, 333-342.
166. Liang, F., & Xu, B. (2014). Discrimination of tower-, cockpit-, and non-karst landforms in Guilin, Southern China, based on morphometric characteristics. Geomorphology, 204, 42–48.
167. Lustrino, M., Melluso, L., & Morra, V. (2007). The geochemical peculiarity of Plio-Quaternary volcanic rocks of Sardinia in the circum-Mediterranean area. Geological Society of America, 418, 277–301.
168. Madritsch H. & Millen B.M.J. (2007) - Hydrogeologic evidence for a continuous basal shear zone within a deep-seated gravitational slope deformation (Eastern Alps, Tyrol, Austria). Landslides, 4 (2): 149-162.
169. Mahr T. & Nemčok A. (1977) - Deep-seated creep deformations in the crystalline cores of the Tatry Mts. Bulletin of the International Association of Engineering Geology, 16 (1): 104-106.
170. Mahr, T. (1977) Deep-reaching gravitational deformations of high mountain slopes. IAEG Bulletin, 19, 121-127.
171. Major H., Haremo P., Dallmann W.K., Andresen A. and Salvigsen O. 2000. Geological map of Svalbard 1:100 000, sheet C9G Adventdalen. Norsk Polarinstitutt Temakart 31. With map description by Dallmann W.K., Kjarnet T. and Nottvedt A. 2001. Norsk Polarinstitutt Temakart 31/32.
172. Malet, J.-P., Maquaire, O., Calais, E., 2002. The use of Global Positioning System techniques for the continuous monitoring of landslides: application to the Super- Suaze earthflow (Alpes-de-Haute-Provence, France). Geomorphology 43, 33–54. https://doi.org/10.1016/S0169-555X(01)00098-8.
173. Malinverno A., Ryan W.B.F., 1986. Extension in the Tyrrhenian Sea and shortening in the Apennines as result of arc migration driven by sinking of the lithosphere. Tectonics 5, 227-245.
174. Mantovani, M., Devoto, S., Piacentini, D., Prampolini, M., Soldati, M., & Pasuto, A. (2016). Advanced SAR interferometric analysis to support geomorphological interpretation of slow-moving coastal landslides (Malta, Mediterranean Sea). Remote Sensing, 8(6), 443.
175. Marani, M.; Gamberi, F. Structural framework of the Tyrrhenian Sea unveiled by seafloor morphology. In From Seafloor to Deep Mantle: Architecture of the Tyrrhenian Backarc Basin; Memorie Descrittive della Carta Geolologica d'Italia; Marani, M., Gamberi, F., Bonatti, E., Eds.; ISPRA: Rome, Italy, 2004; Volume 44, pp. 97–108.
176. Mariani, G. S., & Zerboni, A. (2020). Surface geomorphological features of deep-seated gravitational slope deformations: A look to the role of lithostructure (N Apennines, Italy). Geosciences, 10(9), 334.
177. Marini, A.; Murru, M. Movimenti tettonici in Sardegna fra il Miocene Superiore ed il Pleistocene. Geografia Fisica e Dinamica Quaternaria 1983, 6, 39–42.
178. Marini, A., & Ulzega, A. (1977). Osservazioni geomorfologiche sul tacco di ulassai. Rendiconti Seminario Facoltà Scienze Università di Cagliari, 47(1–2), 192–208.
179. Marini, C. (1984). Le concentrazioni residuali post-erciniche di Fe dell'Ogliastra (Sardegna orientale): contesto geologico e dati mineralogici. Rendiconti della Societa Italiana di Mineralogia e Petrologia, 39, 229–238.
180. Martino S., Cercato M., Della Seta M., Esposito C., Hailemikael S., Iannucci R., Martini G., Paciello A., Scarascia Mugnozza G., Seneca D. & Troiani F. (2020) - Relevance of rock slope deformations in local seismic response and microzonation: Insights from the Accumoli case-study (central Apennines, Italy). Engineering Geology, 266: 105427.
181. Martino S., Della Seta M. & Esposito C. (2017) - Back-analysis of rock landslides to infer rheological parameters. In: Feng X.T. (Ed.), Rock Mechanics and Engineering, Analysis, Modeling and Design. Taylor and Francis, London, vol. 3, 237-268 pp.

182. Martino S., Prestininzi A. & Scarascia Mugnozza G. (2004) - Geological-evolutionary model of a gravity-induced slope deformation in the carbonate Central Apennines (Italy). Quarterly Journal of Engineering Geology and Hydrogeology, 37 (1): 31-47.
183. Martinotti G., Giordan D., Giardino M. & Ratto S. (2011) - Controlling factors for deep-seated gravitational slope deformation (DSGSD) in the Aosta Valley (NW Alps, Italy). Geological Society, London, Special Publications, 351 (1): 113-131.
184. MassironI, M., Bistacchi, A., Dal Piaz, G.V., Monopoli, B. & Schiavo, A. (2003) Structural control on mass-movement evolution: a case study from the Vizze Valley, Italian Eastern Alps. Eclogae Geologicae Helvetiae, 96, 85-98.
185. Massironi, M., Genevois, R., Floris, M. & Stefani, M. (2010) Influence of the antiformal setting on the kinematics of a large mass movement: the Passo Vallaccia, eastern Italian Alps. Bulletin of Engineering Geology and the Environment, 70, 497-506.
186. Massonnet D, Rossi M, Carmona C, Adragna F, Peltzer G, Feigl K, Rabaute T (1993) The displacement field of the landers earthquake mapped by radar interferometry. Nature 364(6433):138
187. Mateos, R.M., Ezquerro, P., Aza˜n´on, J.M., Gelabert, B., Herrera, G., Fern´andez- Merodo, J.A., Spizzichino, D., Sarro, R., Garcia-Moreno, I., Bejar-Pizarro, M., 2018. Coastal lateral spreading in the world heritage site of the Tramuntana Range (Majorca, Spain). The use of PSInSAR monitoring to identify vulnerability. Landslides 15, 797–809. https://doi.org/10.1007/s10346-018-0949-5.
188. Maxia, C., Ulzega, A., & Marini, C. (1973). Studio idrogeologico dei dissesti nel bacino del rio Pardu (Sardegna centro-orientale). Pubblicazione dell'Istituto di Geologia, Paleontologia e Geografia Fisica, 121(12), 9.
189. Mazzella M.E.; Ferranti L.; Palano M.; Mattia M.; Oldow J.S.; Catalano R.; D'Argenio B.; Gueguen E.; Marsella E.; Monaco C.; Orru' P.E.; Avellone G.; Gasparo Morticelli M.; Maschio L.; Santoro E.; Spampinato C.R.; Scicchitano G. – 2010 -Active deformation in southern Italy from GNNS velocity: updated results of the PTGA network
190. Mazzella Marina Enrica (2010) - Tettonica attiva nel settore peri-tirrenico meridionale tramite integrazione di dati geodetici e geologici. [Tesi di dottorato]
191. McCalpin, J., & Irvine, J. R. (1995). Sackungen at the Aspen Highlands Ski area, Pitkin County, Colorado. Environmental & Engineering Geoscience, I(3), 277–290.
192. Mckenzie D., 1972. Active tectonics of the Mediterranean Region. Geophysical Journal of the Royal Astronomical Society; 30:109-185.
193. Melis, M.T.; Da Pelo, S.; Erbì, I.; Loche, M.; Deiana, G.; Demurtas, V.; Meloni, M.A.; Dessì, F.; Funedda, A.; Scaioni, M.; et al. Thermal remote sensing from UAVs: A review on methods in coastal cliffs prone to landslides. Remote Sens. 2020, 12, 1971.
194. Meloni, M. A., Oggiano, G., Funedda, A., Pistis, M., & Linnemann, U. (2017). Tectonics, ore bodies, and gamma-ray logging of the Variscan basement, southern Gennargentu massif (central Sardinia, Italy). Journal of Maps, 13(2), 196–206.
195. Mencl, V. (1968) Plastizitatslehre und das wirkliche Verhalten von Gebirgsmassen. Felsmech. U. Ing. Geol., Suppl. IV, 1-8.
196. Miccadei, E.; Carabella, C.; Paglia, G. Morphoneotectonics of the Abruzzo Periadriatic area (central Italy): Morphometric analysis and morphological evidence of tectonics features. Geosciences 2021, 11, 397. https://doi.org/10.3390/geosciences11090397.
197. Miccadei, E.; Carabella, C.; Paglia, G.; Piacentini, T. Paleo-drainage network, morphotectonics, and fluvial terraces: Clues from the verde stream in the Middle Sangro River (central Italy). Geosciences 2018, 8, 337. https://doi.org/10.3390/geosciences8090337.
198. Miccadei, E., Orrù, P., Piacentini, T., Mascioli, F., & Puliga, G. (2012). Geomorphological map of the Tremiti Islands (Puglia, Southern Adriatic Sea, Italy), scale 1:15,000. Journal of Maps, 8(1), 74–87.

199. Mondini, A.C.; Guzzetti, F.; Chang, K.-T.; Monserrat, O.; Martha, T.R.; Manconi, A. Landslide failures detection and mapping using synthetic aperture radar: Past, present and future. Earth-Sci. Rev. 2021, 216, 103574.
200. Montigny R., Edel J.B. & Thuizat R. (1981) - Oligo-Miocene rotation of Sardinia: K-Ar ages and paleomagnetic data of Tertiary volcanics. Earth Planet. Sci. Lett.: 54, 261-271, Amsterdam.
201. Moretti, A. Sui movimenti franosi degli abitati di Osini e di Gairo (Nuoro). Bollettino del Servizio Geologico d'Italia 1953, 75, 2.
202. Moretto, S.; Bozzano, F.; Mazzanti, P. The role of satellite InSAR for landslide forecasting: Limitations and openings. Remote Sens. 2021, 13, 3735. https://doi.org/10.3390/rs13183735.
203. Mortara, G. & Sorzana, P.F. (1987) Fenomeni di deformazione gravitativa profonda nell'arco alpino occidentale italiano. Considerazioni lito-strutturali e morfologiche Bollettino della Società Geologica Italiana, 106, 303-314.
204. Mt. Rocchetta ridge (central Apennines, Italy): Geological-evolutionary model and numerical analysis. Bulletin of Engineering Geology and the Environment, 70 (4): 559–575.
205. Müller, L. (1968) New consideration on the Vajont slide. Felsmechanik Ingegnieur geologie, 6 (1), 1-91.
206. Naidu, S.; Sajinkumar, K.S.; Oommen, T.; Anuja, V.J.; Samuel, R.A.; Muraleedharan, C. Early warning system for shallow landslides using rainfall threshold and slope stability analysis. Geosci. Front. 2018, 9, 1871–1882.
207. Nemčok, A. (1972) Svahove deformacie v karpatskem flysi. Sborník Geologických Věd, Hydrogeologie Inženýrská Geologie, R. HIG, (in ceco con riassunto in inglese), 11, 99-124.
208. Nemčok, A. (1982) Zosuvy v Slovenskych Karpatoch. Veda, Bratislava, 319 pp.
209. Nemčok, A. (1972). Gravitational slope deformation in high mountains. In Proceedings of the 24th International Geology Congress, Montreal, Sect. 13 (pp. 132–141).
210. Nichol S.L., Hungr O. & Evans S.G. (2002) - Large-scale brittle and ductile toppling of rock slopes. Canadian Geotechnical Journal, 39 (4): 773-788.
211. Novellino, A., Cesarano, M., Cappelletti, P., Di Martire, D., Di Napoli, M., Ramondini, M., Sowter, A., & Calcaterra, D. (2021). Slow-moving landslide risk assessment combining machine learning and InSAR techniques. Catena, 203.
212. Oggiano, G., Funedda, A., Carmignani, L., & Pasci, S. (2009). The Sardinia-Corsica microplate and its role in the northern Apennine geodynamics: New insights from the tertiary intraplate strike-slip tectonics of Sardinia. Italian Journal of Geosciences, 128(2), 527–541.
213. Oldow J. S., Ferranti L., Lewis D. S., Campbell J. K., D'Argenio B., Catalano R., Pappone G., Carmignani L., Conti P., Aiken C.L.V., 2002. Active fragmentation of Adria, the north African promontory, central Mediterranean orogen. Geology; 30:779-782.
214. Oliveira, S.C.; Zêzere, J.L.; Catalão, J.; Nico, G. The contribution of PSInSAR interferometry to landslide hazard in weak rockdominated areas. Landslides 2015, 12, 703–719. https://doi.org/10.1007/s10346-014-0522-9.
215. Onida, M. (2001) Deformazioni gravitative profonde di versante: stato delle conoscenze e progresso della ricerca in Italia. In: PASQUARÈ, G. (ed.) Tettonica recente e instabilità di versante nelle Alpi Centrali. CNR – Istituto per la Dinamica dei Processi Ambientali, Fondazione Cariplo, Milano, Italy, 35-74.
216. Oppikofer, T., Saintot, A., Hermanns, R., Böhme, M., Scheiber, T., Gosse, J., & Dreiås, G. (2017). From incipient slope instability through slope deformation to catastrophic failure—Different stages of failure development on the Ivasnasen and Vollan rock slopes (western Norway). Geomorphology, 289, 96–116.
217. Orrù, P.; Ulzega, A. Geomorfologia costiera e sottomarina della baia di Funtanamare (Sardegna sud-occidentale). Geogr. Fis. Din. Quat. 1986, 9, 59–67.

218. Ostermann, M., & Sanders, D. (2017). The Benner pass rock avalanche cluster suggests a close relation between long-term slope deformation (DSGSDs and translational rock slides) and catastrophic failure. Geomorphology, 289, 44–59.
219. Palis, E., Lebourg, T., Tric, E., Malet, J.-P., Vidal, M., 2017. Long-term monitoring of a large deep-seated landslide (La Clapiere, South-East French Alps): initial study. Landslides 14, 155–170. https://doi.org/10.1007/s10346-016-0705-7.
220. Palomba, M., & Ulzega, A. (1984). Geomorfologia dei depositi quaternari del Rio Quirra e della piattaforma continentale antistante (Sardegna Orientale). Rendiconti Saminario Facoltà Scienze. Università Cagliari, 54(2).
221. Pánek T. & Klimeš J. (2016) - Temporal behavior of deep-seated gravitational slope deformations: A review. Earth-Science Reviews, 156: 14-38.
222. Panek, T., Hradecky, J., Minar, J., Hungr, O. & Dusek, R. (2009) Late Holocene catastrophic slope collapse affected by deep-seated gravitational deformation in flysch: Ropice Mountain, Czech Republic. Geomorphology, 103, 414-429.
223. Pánek, T.; Šilhán, K.; Tábo˘rík, P.; Hradecký, J.; Smolková, V.; Lenart, J.; Pazdur, A. Catastrophic slope failure and its origins: Case of the May 2010 Girová Mountain long-runout rockslide (Czech Republic). Geomorphology 2011, 130, 352–364.
224. Pánek, T., & Klimeš, J. (2016). Temporal behavior of deep-seated gravitational slope deformations: A review. Earth-Science Reviews, 156, 14–38.
225. Panizza, M. (1973) Glacio-pressure implications in the production of landslides in the dolomitic area. Geologia Applicata e Idrogeologia, 8, I, 289-297.
226. Pasuto, A., & Soldati, M. (1996). Lateral spreading. In R. Dikau, D. Brunsden, L. Schrott, & M.-L. Ibsen (Eds.), Landslide recognition: Identification, movement and causes (pp. 122–136). Wiley.
227. Patacca E., Sartori R., Scandone P., 1990. Tyrrhenian Basin and Apenninic Arcs: kinematic relations since Late Tortonian times. Mem. Soc. Geol. Ital. 45, 425451.
228. Patton, F.D. & Hendron, JR. A.J. (1974) General report on mass movements. In: Proceedings of the 2nd International Congress IAEG, São Paulo, Volume 5, GR1-GR57
229. Permafr. Periglac. Process. 22 (3), 239–253. https://doi.org/10.1002/ppp.727.
230. Pertusati, P. C., Sarria, E., Cherchi, G.
P., Carmignani, L., Barca, S., Benedetti, M., Chighine, G., Cincotti, E., & Oggiano, G. (continental area). Ulzega, A., Orrù, P.E., & Pintus, C. (marine area) (2002). Geological Map of Italty. Scale 1:50.000. Scheet 541 “Jerzu” – ISPRA- Servizio Geologico Nazionale.
231. Peternal, T., Kumelj, S., Ostir, K., & Komac, M. (2017). Monitoring the Potoška planina landslide (NW Slovenia) using UAV photogrammetry and tachymetric measurements. Landslides, 14(1), 395–406.
232. Peyret, M., Djamour, Y., Rizza, M., Ritz, J.-F., Hurtrez, J.-E., Goudarzi, M.A., Nankali, H., Ch´ery, J., Le Dortz, K., Uri, F., 2008. Monitoring of the large slow Kahrod landslide in Alborz mountain range (Iran) by GPS and SAR interferometry. Eng. Geol. 100, 131–141.
233. Piciullo, L.; Calvello, M.; Cepeda, J.M. Territorial early warning systems for rainfall-induced landslides. Earth-Sci. Rev. 2018, 179, 228–247.
234. Prampolini, M.; Foglini, F.; Biolchi, S.; Devoto, S.; Angelini, S.; Soldati, M. Geomorphological mapping of terrestrial and marine areas, northern Malta and Comino (central Mediterranean Sea). J. Maps 2017, 13, 457–469.
235. Prampolini, M.; Foglini, F.; Micallef, A.; Soldati, M.; Taviani, M. Malta’s submerged landscapes and landforms. In Landscapes and Landforms of the Maltese Islands. World Geomorphological Landscapes; Gauci, R., Schembri, J.A., Eds.; Springer: Cham, Switzerland, 2019; pp. 117–128.
236. Prampolini, M.; Gauci, C.; Micallef, A.S.; Selmi, L.; Vandelli, V.; Soldati, M. Geomorphology of the north-eastern coast of Gozo (Malta, Mediterranean Sea). J. Maps 2018, 14, 402–410.

237. Prince, P.S.; Spotila, J.A.; Henika,W.S. Stream capture as driver of transient landscape evolution in a tectonically quiescent setting.Geology 2011, 39, 823–826.
238. Proggetto AVI Aree Vulnerate Italiane. Available online: http://avi.gndci.cnr.it/ (accessed on 1 September 2020).
239. Quesada-Román, A. Landslide risk index map at the municipal scale for Costa Rica. Int. J. Disaster Risk Reduct. 2021, 56, 102144.
240. Quesada-Román, A.; Fallas-López, B.; Hernández-Espinoza, K.; Stoffel, M.; Ballesteros-Cánovas, J.A. Relationships between earthquakes, hurricanes, and landslides in Costa Rica. Landslides 2019, 16, 1539–1550.
241. Radbruch-Hall, D., Varnes, D.J. & Colton, R.B. (1977) Gravitational spreading of steep-sided ridges ("Sackung"). Colorado Journal of Research of the U.S. Geological Survey, 5 (3), 359-363.
242. Radbruch-Hall, D. (1978). Gravitational creep of rock masses on slopes. In B. Voight (Ed.), Rockslides and avalanches – Natural phenomena: Developments in geotechnical engineering (Vol. 14, pp. 607–658). Elsevier.
243. Radbruch-Hall, D., Varnes, D. J., & Savage, W. Z. (1976). Gravitational spreading of steep-sided ridges ("sackung") in western United States. IAEG Bulletin, 14, 23–35.
244. Rosen PA, Hensley S, Joughin I, Li FK, Madsen SN, Rodriguez E and Goldstein RM (2000) Synthetic aperture radar interferometry. Proceedings of the IEEE 88(3): 333–382, 10.1109/5.838084
245. Sartori R. (1989) - Evoluzione neogenico-recente del bacino tirrenico e suoi rapporti con la geologia delle aree circostanti. Giorn. di Geol.: 51, 1-39, Bologna.
246. Savage, W.Z. & Varnes, D.J. (1987) Mechanics of gravitational spreading of steep-sided ridges ("Sackung"). Bulletin of the International Association of Engineering Geology, 35, 31-36.
247. Savini, A.; Corselli, C. High-resolution bathymetry and acoustic geophysical data from Santa Maria di Leuca Cold Water Coral province (Northern Ionian Sea—Apulian continental slope). Deep Sea Res. Part II Top. Stud. Oceanogr. 2010, 57, 326–344.
248. Sestras, P.; Bilașco, Ș.; Roșca, S.; Dudic, B.; Hysa, A.; Spalević, V. Geodetic and UAV monitoring in the sustainable management of shallow landslides and erosion of a susceptible urban environment. Remote Sens. 2021, 13, 385.
249. Shi, W.; Deng, S.; Xu, W. Extraction of multi-scale landslide morphological features based on local Gi* using airborne LiDARderived DEM. Geomorphology 2018, 303, 229–242.
250. Shou, K.J.; Chen, J. On the rainfall induced deep-seated and shallow landslide hazard in Taiwan. Eng. Geol. 2021, 288, 106156.
251. Shugar, D.; Clague, J.; Best, J.; Schoof, C.;Willis, M.; Copland, L.; Roe, G. River piracy and drainage basin reorganization led by climate-driven glacier retreat. Nat. Geosci. 2017, 10, 370–375.
252. Smith, M. J., Paron, P., & Griffiths, J. (2011). Geomorphological mapping, methods and applications: Vol. 15. Developments in earth surface processes. Elsevier Science
253. Soldati, M., Devoto, S., Prampolini, M., Pasuto, A., 2019. The Spectacular Landslide- Controlled Landscape of the Northwestern Coast of Malta. In: Gauci, R., Schembri, J. (Eds.), Landscapes and Landforms of the Maltese Islands. World Geomorphological Landscapes. Springer, Cham, pp. 167–178. https://doi.org/10.1007/978-3-030- 15456-1_14.
254. Soldati, M.; Barrows, T.T.; Prampolini, M.; Fifield, K.L. Cosmogenic exposure dating constraints for coastal landslide evolution on the Island of Malta (Mediterranean Sea). J. Coast. Conserv. 2018, 22, 831.
255. Soldati, M. (2013). Deep-seated gravitational slope deformation. In P. T. Bobrowsky (Ed.), Encyclopedia of natural hazards. Encyclopedia of earth sciences series. Springer.
256. Soldati, M., Corsini, A., & Pasuto, A. (2004). Landslides and climate change in the Italian dolomites since the late glacial. Catena, 55(2), 141–161.

257. Solonenko, V.P. (1977) Landslides and collapses in seismic zones and their prediction. IAEG Bulletin, 15, 4-8.
258. Solonenko, V.P. (1979) Mapping the after-effects of disastrous earthquakes and estimation of hazard for engineering constructions. IAEG Bulletin, 19, 138- 142.
259. Sorbel L., Tolgensbakk J., Hagen J.O. and Hogvard K. 2001. Geomorphological and Quaternary Geological Map 1:100 000, sheet C9Q Adventdalen. With map description. Norsk Polarinstitutt Temakart 32.
260. Sorriso-Valvo M. (1988) Studi sulle deformazioni gravitative profonde di versante in Italia. Relazione introduttiva alla tavola rotonda "Deformazioni gravitative profonde di versante". Memorie della Società Geologica Italiana, 41, 877-888.
261. Sorriso-Valvo, M. (1979) Trench features on steep-sided ridges of Aspromonte, Calabria, Italy. In: Proceedings of the Polish-Italian Seminar "Superficial mass movements in mountain regions", Warszawa, p. 98-109.
262. Starkel, L. (1976) The role of extreme (catastrophic) meteorological events in contemporary evolution of slopes. In: Derbyshire, E. (Ed.) Geomorphology and climate, John Wiley & Sons, 203-246.
263. Suhail, H.A.; Yang, R.; Chen, H.; Rao, G. The impact of river capture on the landscape development of the Dadu River drainage basin, eastern Tibetan plateau. J. Asian Earth Sci. 2020, 198, 1367–9120.
264. Sweeting, M. M. (1972): Karst Landforms. XCI, 362 pp. London: Macmillan.
265. Tabor, R.W. (1971) Origin of ridge-top depressions by large scale creep in the Olimpic Mountains. Geological Society of America Bulletin, 82, 1811-1822.;
266. Taramelli, A., & Melelli, L. (2008). Map of deep seated gravitational slope deformations susceptibility in central Italy derived from SRTM DEM and spectral mixing analysis of the landsat ETM+ data. International Journal of Remote Sensing, 30(2), 357–387
267. Ter-Stepanian, G. (1966) Type of depth creep of slopes in rock masses. Problems of Geomechanics, 3, 49-69.
268. Terzaghi, K. (1962) Stability of steep slopes on hard unweathered rock. Gèotechnique, 12, 251-270. (Hutchinson, 1988)
269. Thuro K., Eberhardt E. & Gasparini M. (2004) - Deep seated creep and its influence on a 1.5 GW hydroelectric power plant in the Himalayas. Felsbau, 22 (2): 60-66.
270. Tibaldi A., Corazzato C., Rust D., Bonali F.L., Pasquarè Mariotto F.A., Korzhenkov A.M., Oppizzi P. & Bonzanigo L. (2015) - Tectonic and gravity-induced deformation along the active Talas-Fergana Fault, Tien Shan, Kyrgyzstan. Tectonophysics, 657: 38-62.
271. Trigila A., Iadanza C., Bussettini M., Lastoria B. (2018)Dissesto idrogeologico in Italia: pericolosità e indicatoridi rischio. Rapporto 2018. ISPRA, Rapporti 287/2018.
272. Tzouvaras, M. Statistical time-series analysis of interferometric coherence from sentinel-1 sensors for landslide detection and early warning. Sensors 2021, 21, 6799. [CrossRef]
273. Ulzega, A., & Marini, A. (1973). L'évolution des versants dans la vallée du Rio Pardu (Sardaigne centre-orientale). Zeitschrift fur Geomorphologie, 21(4), 466–474.
274. Ulzega, A., Orrù, P. E., & Pintus, C. (marine area). Pertusati, P. C., Sarria, E., Cherchi, G. P., Carmignani, L., Barca, S., Benedetti, M., Chighine, G., Cincotti, E., & Oggiano, G. (continental area). (2002). Geological Map of Italty. Scale 1:50.000. Scheet 541 "Jerzu" – ISPRA- Servizio Geologico Nazionale.
275. UNISDR (United Nations International Strategy for Disaster Reduction) Terminology on Disaster Risk http://www.unisdr.org (2009)
276. Vai, G. B., & Cocozza, T. (1974). Il "postgotlandiano" sardo, unità sinorogenica ercinica. Bollettino della Società geologica italiana, 93, 61–72.

277. Valkaniotis, S., Papathanassiou, G., & Ganas, A. (2018). Mapping an earthquake-induced landslide based on UAV imagery; case study of the 2015 Okeanos landslide, Lefkada, Greece. Engineering Geology, 245, 141–152.
278. Varnes D.J. (1978) Slope movements. Types and processes. In: Shuster & Krizker (eds) "Landslides: analysis and control". Spec. Rep. 176, Transp. Res. Board. Nat. Ac. of Sc., Washington.
279. Varnes D.J., Radbruch-Hall D.H., Varnes K.L., Smith W.K. & Savage W.Z. (1990) - Measurement of ridge-spreading movements (Sackungen) at Bald Eagle Mountain, Lake County, Colorado, 1975–1989. US Geological Survey, Open File Report, Denver, 90-543 pp.
280. Varnes, D.J., Radbruch-Hall, D. & Savage, W.Z. (1989) Topographic and structural conditions in area of gravitational spreading of ridges in the Western United States. U.S. Geological Survey Professional Paper, Volume 1496, Washington, 1-28.
281. Vick L.M., Böhme M., Rouyet L., Bergh S.G., Corner G.D. & Lauknes T.R. (2020) - Structurally controlled rock slope deformation in northern Norway. Landslides, 17: 1745-1776.
282. Vigliotti L., Langenheim V.E., 1995. When did Sardinia stop rotating? New paleomagnetic results. Terra Nova, 7, 424-435.
283. Vilímek V., Zvelebil J., Klimeš J., Patzelt Z., Astete F., Kachlík V. & Hartvich F. (2007) - Geomorphological research of large-scale slope instability at Machu Picchu, Peru. Geomorphology, 89 (3-4): 241-257.
284. Voight B. (1973) - The mechanics of retrogressive block-gliding, with emphasis on the evolution of the Turnagain Heights landslide, Anchorage, Alaska. In: De Jong K.A. & Scholten R. (Eds.), Gravity and Tectonics. John Wiley and Sons, New York, 97-257.
285. Volpe, E.; Ciabatta, L.; Salciarini, D.; Camici, S.; Cattoni, E.; Brocca, L. The impact of probability density functions assessment on model performance for slope stability analysis. Geosciences 2021, 11, 322.
286. Waltham, T. (2008). Fengcong, fenglin, cone karst and tower karst Cave and Karst. Science, 35(3), 77–88.
287. Wang, G.Q., 2012. Kinematics of the Cerca del Cielo, Puerto Rico landslide derived from GPS observations. Landslides 9, 117–130. https://doi.org/10.1007/s10346-011- 0277-5.
288. Whipple, K.X.; Forte, A.M.; Di Biase, R.A. Timescales of landscape response to divide migration and drainage capture: Implications for the role of divide mobility in landscape evolution. J. Geophys. Res. Earth Surf. 2017, 122, 248–273.
289. Wieczorek, G.F., & Snyder, J.B. (2009). Monitoring slope movements. In R. Young & L. Norby (Eds.), Geological Society of America (pp. 245–271). Boulder, CO: Geological Monitoring. doi:10.1130/2009
290. Willett, S.D.; McCoy, S.W.; Perron, J.T.; Goren, L.; Chen, C.Y. Dynamic reorganization of river basins. Science 2014, 343, 1117.
291. Xu, Q.; Peng, D.; Zhang, S.; Zhu, X.; He, C.; Qi, X.; Zhao, K.; Xiu, D.; Ju, N. Successful implementations of a real-time and intelligent early warning system for loess landslides on the Heifangtai terrace, China. Eng. Geol. 2020, 278, 105817.
292. Yi, Y.; Zhang, Z.; Zhang, W.; Jia, H.; Zhang, J. Landslide susceptibility mapping using multiscale sampling strategy and convolutional neural network: A case study in Jiuzhaigou region. Catena 2020, 195, 104851.
293. Z. Medina-Cetina, F. Nadim Stochastic design of an early warning system Georisk: Assessment and Management of Risk for Engineered Systems and Geohazards, 2 (2008), pp. 223-236
294. Zaruba Q. AND Mencl V. (1969) Landslide and their control. I ed., Elsevier Amsterdam. Academia Praha, cap. 10, 174-193.
295. Zaruba, Q., & Mencl, V. (1982). Landslides and their control: Development in geotechnical engineering. Elsevier, 324p.

296. Zhang, L.; Wang, X.; Xia, T.; Yang, B.; Yu, B. Deformation characteristics of Tianjiaba landslide induced by surcharge. ISPRS Int. J. Geo-Inf. 2021, 10, 221.
297. Zhang, Y.; Li, H.; Sheng, Q.;Wu, K.; Chen, G. Real time remote monitoring and pre-warning system for highway landslide in mountain area. J. Environ. Sci. China 2011, 23, S100–S105.
298. Ziegler P. A., 1988. Evolution of the Arctic–North Atlantic and the western Tethys. American Association of Petroleum Geologists Memoir 43, 198 p.
299. Zischinsky U. (1966) On the deformation of high slopes. Proc. 1st Conf. Int. Soc.Rock. Mec., Lisbon, Sect 2, 179-185.
300. Zischinsky, U. (1966). On the deformation of high slopes. In Proceedings of the 1st Conference International Society for Rock Mechanics, Lisbon, Sect 2 (pp. 179–185).
301. ZischinskY, U. (1969). Über Sackungen. Rock Mechanics, 1(1), 30–52.